Attachment 2

WCAP-17116-NP-A
Revision 0

Westinghouse BWR ECCS Evaluation Model: Supplement 5 – Application to the ABWR

Westinghouse Non-Proprietary Class 3

WCAP-17116-NP-A
Revision 0

May 2014

Westinghouse BWR ECCS Evaluation Model: Supplement 5 – Application to the ABWR

WCAP-17116-NP-A
Revision 0

Westinghouse BWR ECCS Evaluation Model: Supplement 5 – Application to the ABWR

J. Blaisdell*
Transient and LOCA Analysis

May 2014

Reviewer: P. Kottas*
Transient and LOCA Analysis

Approved: J. Ghergurovich*
Transient and LOCA Analysis

*Electronically approved records are authenticated in the electronic document management system.

Westinghouse Electric Company LLC
1000 Westinghouse Drive
Cranberry Township, PA 16066

February 3, 2013

Mr. Scott Head, Manager
Regulatory Affairs
South Texas Project Units 3 and 4
Nuclear Innovation North America, LLC
122 West Way, Suite 405
Lake Jackson, TX 77566

SUBJECT: FINAL SAFETY EVALUATION FOR SOUTH TEXAS PROJECT WCAP-17116-P, "WESTINGHOUSE BWR ECCS EVALUATION MODEL: SUPPLEMENT 5 – APPLICATION TO ABWR"

Dear Mr. Head:

By letter dated September 30, 2009 (Agencywide Documents Access and Management System (ADAMS) Accession Number ML092810247), South Texas Project (STP) Units 3 and 4 submitted to the U.S. Nuclear Regulatory Commission (NRC) staff Topical Report (TR) WCAP-17116-P, "Westinghouse BWR ECCS Evaluation Model: Supplement 5 – Application to ABWR," as part of a series of advanced boiling-water reactor (ABWR) fuel-related topical reports that will support a future license amendment for STP Units 3 and 4. By email dated January 10, 2013 (ML13308B996), an NRC draft safety evaluation (SE) regarding approval of TR WCAP-17116-P was provided for your proprietary review and verification of factual accuracy. By an email dated January 21, 2013 (ML13308B989), NINA provided feedback on the draft SE. A summary of the NINA's comments on the draft SE and NRC's disposition are included in Enclosure (3) to this letter.

The NRC staff has found that TR WCAP-17116-P is acceptable for referencing in licensing applications for STP Units 3 and 4 designed ABWR reactors to the extent specified and under the limitations and conditions delineated in the TR and in the enclosed final SE. The final SE defines the basis for our acceptance of the TR.

Our acceptance applies only to material provided in the subject TR. We do not intend to repeat our review of the acceptable material described in the TR. When the TR appears as a reference in license applications, our review will ensure that the material presented applies to the specific plant involved. License amendment requests that deviate from this TR will be subject to a plant-specific review in accordance with applicable review standards.

In accordance with the guidance provided on the NRC website, we request that Westinghouse publish accepted proprietary and non-proprietary versions of this TR within three months of receipt of this letter. The accepted versions shall incorporate this letter and the enclosed final SE after the title page. Also, they must contain historical review information, including NRC's requests for additional information (RAI) and your responses. The accepted versions shall include an "-A" (designating accepted) following the TR identification symbol.

Document transmitted herewith contains sensitive unclassified information. When separated from the enclosure, this document is "DECONTROLLED."

As an alternative to including the RAIs and RAI responses behind the title page, if changes to the TR were provided to the NRC staff to support the resolution of RAI responses, and the NRC staff reviewed and approved those changes as described in the RAI responses, there are two ways that the accepted version can capture the RAIs:

1. The RAIs and RAI responses can be included as an Appendix to the accepted version.

2. The RAIs and RAI responses can be captured in the form of a table (inserted after the final SE) which summarizes the changes as shown in the approved version of the TR. The table should reference the specific RAIs and RAI responses which resulted in any changes, as shown in the accepted version of the TR.

If future changes to the NRC's regulatory requirements affect the acceptability of this TR, Westinghouse and/or licensees referencing it will be expected to revise the TR appropriately, or justify its continued applicability for subsequent referencing.

Sincerely,

/RA/

Frank Akstulewicz, Director
Division of New Reactor Licensing
Office of New Reactors

Project No.: 0772

Enclosures:
1. Final SE to TR WCAP-17116-P (non-proprietary version)
2. Final SE to TR WCAP-17116-P (proprietary version)
3. Summary of Comments and Resolution

As an alternative to including the RAIs and RAI responses behind the title page, if changes to the TR were provided to the NRC staff to support the resolution of RAI responses, and the NRC staff reviewed and approved those changes as described in the RAI responses, there are two ways that the accepted version can capture the RAIs:

3. The RAIs and RAI responses can be included as an Appendix to the accepted version.

4. The RAIs and RAI responses can be captured in the form of a table (inserted after the final SE) which summarizes the changes as shown in the approved version of the TR. The table should reference the specific RAIs and RAI responses which resulted in any changes, as shown in the accepted version of the TR.

If future changes to the NRC's regulatory requirements affect the acceptability of this TR, Westinghouse and/or licensees referencing it will be expected to revise the TR appropriately, or justify its continued applicability for subsequent referencing.

Sincerely,
/RA/

Frank Akstulewicz, Director
Division of New Reactor Licensing
Office of New Reactors

Project No.: 0772

Enclosures:
1. Final SE to TR WCAP-17116-P (non-proprietary version)
2. Final SE to TR WCAP-17116-P (proprietary version)
3. Summary of Comments and Resolution

DISTRIBUTION:

PUBLIC	RidsOgcMailCenter	JGilmer, NRO
NON-PUBLIC	RidsAcrsAcnwMailCenter	RidsNroDseaSrsb
RidsNroOd	TTai,NRO	
RidsNroDnrlLB3	SGreen, NRO	

ADAMS ACCESSION NOS.: ML13311A784*see previous concurrence via-email

OFFICE	DNRL/LB3/PM	DNRL/LB3/LA	DSRA/SRSB	DSRA/SRSB:BC	DNRL/LB3:BC	DNRL:DD
NAME	TTai*	SGreen*	JGilmer*	JDonoghue	RJenkins	FAkstulewicz
DATE	12/03/13	12/03/13	12/04/13	01/14/14	01/22/14	02/03/14

OFFICIAL RECORD COPY

SAFETY EVALUATION BY THE OFFICE OF NEW REACTORS
LICENSING TOPICAL REPORT WCAP-17116-P
"WESTINGHOUSE BWR ECCS EVALUATION MODEL:
SUPPLEMENT 5 - APPLICATION TO THE ABWR"
PROJECT NO. 0772

1.0 INTRODUCTION

South Texas Project Nuclear Operating Company submitted WCAP-17116-P, "Westinghouse BWR ECCS Evaluation Model: Supplement 5 – Application to the ABWR" (hereafter referred to as Supplement 5) for U.S. Nuclear Regulatory Commission (NRC) review and approval by letter dated September 30, 2009 (Ref. 1). Supplement 5 is an extension of the Westinghouse boiling-water reactor (BWR) emergency core cooling system (ECCS) evaluation model (EM) to the advanced boiling-water Reactor (ABWR) loss-of-coolant accident (LOCA) analysis. The Westinghouse ABWR ECCS EM, as described in Supplement 5, is identified as USA7. It consists of the GOBLIN and CHACHA-3D proprietary computer codes, as well as the parameters and input required to select features and enable the use of the desired models. GOBLIN is a one-dimensional, two-phase thermal-hydraulic code, and CHACHA-3D is a one-dimensional code that performs detailed temperature calculations at a particular axial level within a fuel assembly.

GOBLIN analyzes the time-dependent thermal-hydraulic response of the reactor coolant system during the blowdown and the re-flood phases of loss of coolant accidents (LOCAs), including the interactions with various control and safety systems. GOBLIN calculates the pressure and enthalpy at the core inlet and outlet, using the core power generation, system geometry, ECCS performance, and the break specification. The GOBLIN code calculations are performed by modeling the reactor core with two parallel flowpaths, with one flowpath representing the hot assembly, and the other flowpath representing the remaining assemblies. CHACHA-3D performs detailed temperature calculations at a specified axial level within the hot assembly previously analyzed by the GOBLIN code. All necessary fluid boundary conditions are obtained from the GOBLIN calculation. CHACHA-3D determines the temperature distribution of each rod throughout the accident and ultimately determines the peak cladding temperature (PCT) and cladding oxidation at the axial plane under investigation. CHACHA-3D also provides input for the calculation of total hydrogen generation by supplying the local oxidation at various axial and radial core locations.

BACKGROUND

The staff first approved the Westinghouse BWR ECCS EM, incorporating the then-current versions of GOBLIN/DRAGON and CHACHA codes, in 1989. The initial version of the Westinghouse BWR ECCS EM was identified as USA1 (Refs. 2, 3).

DRAGON is a mode or option within GOBLIN that uses the GOBLIN results (i.e., the plenum to plenum flow boundary conditions), to analyze the response of hot channel. The DRAGON option determines the response of the hot channel to the LOCA event (e.g., boiling transition, dryout, and refill). Since in USA7 the GOBLIN code calculations are performed by modeling the reactor core with two parallel flowpaths, the DRAGON option of GOBLIN is not exercised for ABWR applications.

ASEA Brown Boveri (ABB)/ Combustion Engineering (ABB/CE) supplemented the original BWR ECCS licensing topical report (LTR) with CENPD-293-P, "BWR ECCS Evaluation Model: Supplement 1 to Code Description and Qualification," for staff review in 1994. Approval for Supplement 1 to the EM (known as USA2) was granted in 1996 (Ref. 4). The purpose of CENPD-293-P-A was to update the EM to enable analysis of cores containing SVEA-96 fuel.

Westinghouse Electric Company (Westinghouse) submitted WCAP-15682-P, "Westinghouse BWR ECCS Evaluation Model: Supplement 2 to Code Description, Qualification and Application," for NRC review in 2002.

The purpose of Supplement 2 was to introduce improved fuel cladding rupture criteria and provide qualification bases for the improvement while maintaining the overall conservatism of the previously approved versions of the EM. The staff approved Supplement 2 to the EM (known as USA4) in 2003 (Ref. 5).

In 2003, Westinghouse submitted WCAP-16078-P, "Westinghouse BWR ECCS Evaluation Model: Supplement 3 to Code Description, Qualification and Application to SVEA-96 Optima2 Fuel," for NRC review. The purpose of Supplement 3 was to update the EM to enable analysis of cores containing SVEA-96 Optima 2 fuel design. The staff approved Supplement 3 in 2004, with the EM identified as USA5 (Ref. 6).

Westinghouse submitted WCAP-16865-P, "Westinghouse BWR ECCS Evaluation Model Updates: Supplement 4 to Code Description, Qualification and Application," for NRC review in 2007. The updates to the EM in Supplement 4 included a change to determine the end of lower plenum flashing calculations for small- and large-break LOCA analysis. The staff approved Supplement 4, with the EM identified as USA6 in 2011 (Ref. 7).

The previously approved BWR ECCS evaluation models were developed for application to BWR/2 to BWR/6 designs. The design of the ABWR is quite different to that of BWR/2 to BWR/6. The differences include the presence of internal recirculation pumps in the ABWR and the lack of any external recirculation piping. Therefore, the response of the ABWR system to a LOCA event is quite different than for a BWR with external recirculation pumps. In ABWR, the core flow rate decreases quickly because of the rapid coastdown of the reactor internal pumps (RIPs) following pump trip (if the loss of offsite power is assumed). Also the elevations of large pipe breaks are above, not below, the top of active fuel. As a result, different features of the evaluation model become more important and require additional qualification.

The stated objective of Supplement 5 is to provide a basis for extending the applicability of the EM to the ABWR.

2.0 REGULATORY EVALUATION

The staff used the review guidance provided in Standard Review Plan (SRP) Section 15.0.2, "Review of Transient and Accident Analysis Methods," (SRP 15.0.2, Ref. 8) in the conduct of its review of Supplement 5. The review covered the areas of: (1) documentation, (2) evaluation model, (3) accident scenario identification process, (4) code assessment, (5) uncertainty analysis, and (6) quality assurance plan. SRP 15.0.2 incorporates the requirements expressed in Title 10 of the *Code of Federal Regulations* (10 CFR) 50.46, "Acceptance Criteria for Emergency Core Cooling Systems for Light-Water Nuclear Power Reactors" and those in 10 CFR Part 50, "Domestic Licensing of Production and Utilization Facilities," Appendix K, "ECCS Evaluation Models" (Ref. 9).

10 CFR 50.46

A LOCA, as defined in 10 CFR 50.46, is a postulated accident to determine the design acceptance criteria for a plant's ECCS (Ref. 9). The calculated maximum fuel element cladding temperature shall not exceed 1,204 degrees Celsius (C) (2,200 degrees Fahrenheit (F) or 1,477 degrees Kelvin (K)).

To establish that the ECCS design performance satisfies the aforementioned criteria, SRP 15.0.2 (Ref. 8) and 10 CFR 50.46 (Ref. 9) provide guidance to ensure that the ECCS analyses is performed using an acceptable ECCS EM. Regulations in 10 CFR 50.46 state that the EM must identify and account for uncertainties in the analysis method and inputs such that there is a high level of probability that the acceptance criteria are not exceeded. Alternatively, the EM may be conservatively developed in conformance with the required and acceptable features of 10 CFR Part 50, Appendix K. Supplement 5 states that USA7 is compliant with the regulatory requirements of 10 CFR 50.46.

10 CFR Part 50, Appendix K

Appendix K to 10 CFR Part 50 specifies the required and acceptable features for ECCS evaluation models. The Appendix K requirements and features that are relevant to the present review are listed below:

Section I.A: Sources of heat during the LOCA

Section I.A.1: The initial stored energy in the fuel

Section I.A.2: Fission heat

Section I.A.3: Decay of actinides

Section 1.A.4: Fission product decay

Section 1.A.5: Metal-water reaction rate

Section I.A.6: Reactor internals heat transfer

Section I.A.7: Pressurized water reactor primary-to-secondary heat transfer (applies only to PWR)

Section I.B: Swelling and rupture of the cladding and fuel rod thermal parameters

Section I.C.1.a: Break characteristics and flow

Section I.C.1.b: Discharge model

Section I.C.1.c: End of blowdown (applies only to PWR)

Section I.C.1.d: Noding near the break and the ECCS injection points

Section I.C.2: Frictional pressure drops

Section I.C.3: Momentum equation

Section I.C.4.(a–e): Critical heat flux

Section I.C.5.(a and b): Post-CHF heat transfer correlations

Section I.C.6: Pump modeling

Section I.C.7: Core flow distribution during blowdown (applies only to PWR)

Section I.D.1: Single failure criterion

Section I.D.2: Containment pressure

Section I.D.3: Calculation of reflood rate for pressurized water reactors (applies only to PWR)

Section I.D.4: Steam interaction with emergency core cooling water in pressurized water reactors (applies only to PWR)

Section I.D.5: Refill and reflood heat transfer for pressurized water reactors (applies only to PWR)

Section I.D.6: Convective heat transfer coefficients for boiling water reactor fuel rods under spray cooling (in ABWR, the core flooding is used rather than spray cooling; this requirement, therefore, does not apply to ABWR)

Section II (1.a, 3, and 4): Required documentation

3.0 TECHNICAL EVALUATION

The staff performed its review of Supplement 5 to the Westinghouse BWR ECCS EM as reported in WCAP-17116-P under a technical assistance contract with Energy Research, Inc. (ERI). Detailed descriptions of the evaluation and findings of the review are described in the ERI technical evaluation report (TER).

A key element of this review is to recognize that SRP 15.0.2 (Ref. 8) provides an evaluation methodology that may be used to determine if a change to an EM should be subjected to a graded or a full review. The SRP recommends judging the submittal against the following criteria: (1) novelty, (2) complexity, (3) degree of conservatism in the evaluation model, and (4) extent of plant or operational changes requiring reanalysis. With respect to this guidance, the staff makes the following observations:

- Novelty: The changes to the EM in Supplement 5 are not particularly novel. They consist primarily of changes to noding and structure commensurate with ABWR component dimensions, elevations, and descriptions. The staff believes that consideration of this aspect does not indicate that a full review of the EM is required.

- Complexity: There are no significant changes to the complexity of the EM resulting from Supplement 5 changes. The staff believes that consideration of this aspect does not indicate that a full review of the EM is required.

- Degree of conservatism in the EM: This consideration is not applicable as the conservatism is addressed fully by using the 10 CFR Part 50, Appendix K requirements.

- Extent of changes requiring reanalysis: Since ABWR has not yet been licensed, it is not necessary to consider the issue of reanalysis.

On the basis of the evaluation above, the staff believes that a graded review is appropriate for Supplement 5, and the staff conducted its review in this manner. The criteria used for this focused review are the same as for a full review. The EM elements reviewed, however, are limited to those introduced by the LTR for which approval is sought or to those elements that are related because of their importance to ABWR analysis but not specifically discussed in sufficient detail to allow the staff to conclude that they are equally applicable to BWR/2 through BWR/6.

To accomplish the required review objectives, the staff issued several requests for additional information (RAIs 1 to 33). RAIs were answered in a series of seven responses. In addition, the staff conducted an audit in February 2011, during which several RAIs were discussed in considerable detail (Ref. 25).

3.1 Documentation

The staff reviewed Supplement 5 to determine the adequacy of the documentation relative to the review guidance provided in SRP 15.0.2.

The documentation in Supplement 5 and that was submitted in response to the staff's questions included the following in accordance with the requirements stated in SRP 15.0.2:

- an overview of the evaluation model
- a complete description of the accident scenario
- a complete description of the code assessment
- a determination of the code uncertainty
- a quality assurance plan

The staff finds the submitted documentation to be acceptable. Based on the review of Supplement 5, responses to RAIs and questions during the audit, the staff determined that the graded review did not require inspection of the theory and user manuals. The staff concluded that the previously reviewed versions of these documents are acceptable.

3.2 Evaluation Model

USA7 is the ECCS evaluation model based on 10 CFR Part 50, Appendix K. Therefore, the review in this section is focused on assessing the conformance of USA7 to the requirements of 10 CFR Part 50, Appendix K. The applicability of USA7 to ABWR is determined based on the review of Supplement 5 and the evaluation of responses to RAIs and discussions during the audit. Section 3.2.1 presents discussion of important elements of the USA7 model. The conformance of USA7 to each applicable item of the requirements established in 10 CFR Part 50, Appendix K is evaluated in Section 3.2.2.

3.2.1 Assessment of USA7 Model Elements

Table 1 shows various elements of USA7 as documented in Table A-1 of Supplement 5 and the relevant Appendix K criteria. Since the basic thermal-hydraulic phenomena are the same for the ABWR and the operating BWRs, many elements of USA7 that were found to be applicable for the BWR/2 through BWR/6 are still applicable for the ABWR. Therefore, only those aspects of USA7 that are unique for the ABWR analysis are addressed here. These include the following:

- nodalization
- use of the two-phase level tracking model
- ECCS injection flow
- break flow and ADS flow models
- conservative model assumptions

The relevant USA7 model elements that are addressed in this SER are highlighted in Table 1. Table 1 also shows the associated RAIs and sections of this SER.

Table 1 - Applicability of USA7 to ABWR

EM Element	Appendix K Criteria	Applicability to ABWR		
		Y/N	Basis*	SER Sections and RAI
Thermal-Hydraulic Models in GOBLIN				
Mass Conservation Equations	-	Y	A1	-
Energy Conservation Equations	-	Y	A1	-
Momentum Conservation Equations	I.C.3	Y	A1, A2	Section 3.2.2
Fluid Properties	-	Y	A1	-
Equation of State	-	Y	A1	-
Two-Phase Energy Flow Model	-	Y	A1	-
Two-Phase Level Tracking	-	Y	A1, A3	-
Frictional Pressure Drop Correlations	I.C.2	Y	A1, A2	Section 3.2.2
Injection Flow – Fluid Interaction	I.C.1.d	Y	A1, A2, A3	Section 3.2.2, RAI-13 -14, -24
Critical Flow Model	I.C.1.b	Y	A1, A2, A3	Section 3.2.2, RAI-7, -8, -15
Recirculation Pump Model	I.C.6	Y	A2, A3	Section 3.2.2, RAI-5, 6, -10, -11, -12
Jet Pump Model	I.C.6	N	A4	Section 3.2.2
Separator and Dryer Model	-	Y	A1	-
Feedwater and Steam line Systems	-	Y	A1, A3	RAI-2
Reactor Measurement and Protection Systems	-	Y	A1, A3	RAI-18
Heat Transfer Regimes	I.A.6	Y	A1, A2, A3	Section 3.2.2, RAI-26
Convective Heat Transfer Coefficients	I.A.6	Y	A1, A2, A3	Section 3.2.2, RAI-26
Critical Power Ratio Correlation	I.C.4.c	Y	A1, A2, A3	Section 3.2.2, RAI-20, -21
Transition Boiling	I.C.5	Y	A1, A3, A2	Section 3.2.2, RAI-20
Radiation Heat Transfer	I.A.6	Y	A1, A2	Section 3.2.2
Fuel Rod Conduction Model	I.A.1	Y	A1, A2	Section 3.2.2
Plate Conduction Model	I.A.6	Y	A1, A3, A2	Section 3.2.2, RAI-16, -23
Material Properties	I.A.1 I.A.6, & I.B	Y	A1, A2	Section 3.2.2
Point Kinetics Model	I.A.2	Y	A1, A2	Section 3.2.2

EM Element	Appendix K Criteria	Applicability to ABWR		
		Y/N	Basis*	SER Sections and RAI
Metal-Water Reaction Model	I.A.5	Y	A1, A2, A3	Section 3.2.2, RAI-29
Point Kinetics Solution	I.A.2 & I.A.3	Y	A1, A2	Section 3.2.2
Hydraulic Model Solution	-	Y	A1	-
Heat Conduction and Transfer Solution	I.A.6	Y	A1, A2	Section 3.2.2
Nodalization	I.C.1.d	Y	A2, A3	Section 3.2.2, RAI-1, -13, -14, -24, -30
Rod Heat-up Models in CHACHA				
Fuel Rod Conduction Model	I.A.1 & I.B	Y	A1, A2	Section 3.2.2
Channel Temperature Model	-	Y	A1	-
Heat Generation Model	I.A	Y	A1, A2	Section 3.2.2
Metal-Water Reaction Model	I.A.5	Y	A1, A2, A3	RAI-29
Thermal Radiation Model	-	Y	A1	-
Gas Plenum Temperature and Pressure Model	I.A.1	Y	A1, A2	Section 3.2.2
Channel Rewet Model	I.D.7	Y	A1, A2	Section 3.2.2
Pellet-Cladding Gap Heat Transfer Model	I.B	Y	A1, A2	Section 3.2.2
Cladding Strain and Rupture Model	I.B	Y	A1, A2	Section 3.2.2
Fuel Bundle Material Properties	I.A and I.B	Y	A1, A2	Section 3.2.2

* A1: Fundamental phenomenon remains the same for ABWR. A2: In conformance with the 10 CFR Part 50, Appendix K requirements. A3: Based on the information in the LTR and applicant's responses to RAIs. A4: Not Applicable to the ABWR design.

3.2.1.1 Nodalization

The nodalization of the ABWR model used for USA7 is different from that used in previous submittals because of the differences in the design between the ABWR and BWR/2 through BWR/6. As compared to the previous Westinghouse BWR EM, the major change in the ABWR model is the increased number of nodes to represent the active core region. The core region is modeled using multiple parallel control volumes representing the average core and the hot channel. Section 4.3.1.1 of Supplement 5 indicates that 25 axial nodes are used to model the ABWR active core, as compared to 6 nodes that were used in the GOBLIN nodalization for BWR (Ref. 2). The steam dome is represented by a single control volume in USA7. The upper and lower downcomer regions are represented by nine one-dimensional control volumes (i.e., there is no azimuthal or radial nodalization). Feedwater, as well as reactor core isolation cooling (RCIC) and low pressure flooder (LPFL) injection are directed into the downcomer at the appropriate elevations. The break flow paths for the feedwater line break (FWLB) and the residual heat removal system (RHR) suction and discharge line breaks also are connected

directly to the downcomer control volumes. [[ ]] The High Pressure Core Flooder (HPCF) injection is directed into the upper plenum. The noding near the break in the ABWR LOCA analysis is similar to that used in the BWR/2 through BWR/6 LOCA models (Ref. 2).

Based on the review of Supplement 5, the staff raised the following issues regarding the nodalization used in USA7:

- The nodalization sensitivity studies that result in the choice of 25 axial nodes for modeling the ABWR core in GOBLIN are not present in Supplement 5. Therefore, the justification for the use of 25 nodes, as required by Section II.3 of Appendix K to 10 CFR Part 50, is not evident. (RAI-1).

- The one-dimensional nodalization of the upper plenum and downcomer can lead to the prediction of incorrect thermal-hydraulic behavior. Because of the nodalization of the upper plenum, the mass inflow from the HPCF would be automatically distributed uniformly throughout the upper plenum node volume. The HPCF mass flow also would immediately reach thermal equilibrium. Furthermore, if the HPCF flow is available from only one sparger, the resulting asymmetric effects on core cooling would not be accounted for by the one-dimensional nodalization. Similarly, there is a potential for nonuniform delivery of LPFL flow in the downcomer. The one-dimensional downcomer nodalization may not be appropriate for possible imperfect mixing. There also is a potential for ECCS injection exiting through a line break without providing any cooling (e.g., FWLB). The justification for the use of one-dimensional nodalization for the downcomer and upper plenum regions, as required by Section II.3 of Appendix K to 10 CFR Part 50, is not provided.

- Supplement 5 states that noding near the break in the ABWR LOCA analysis is similar to that used in the BWR/2 through BWR/6 LOCA models. However, the BWR/2 through BWR/6 break location noding sensitivity studies were performed for a break in the recirculation line piping, which is not present in the ABWR. As noted in Supplement 5, the maximum ABWR line break size is only approximately 15 percent of the size of the double-ended recirculation line in a BWR. For the ABWR design, the effects of break location noding on break flow and system inventory may be different than for BWR/2 through BWR/6 designs. As required by Section 1.C.1.d of Appendix K, justification for the selected break location noding is necessary to determine its adequacy. Section 1.C.1.d of Appendix K also requires justification for the noding in the vicinity of ECCS injection point. Therefore, additional sensitivity studies are required to assess the effect of noding near the ECCS injection points and breaks in the upper plenum and in the downcomer (RAI-24).

In response to RAI-1, Westinghouse provided results from GOBLIN simulations of FRIGG tests using 15, 25, and 50 axial nodes. The predicted dryout times were similar for the 25- and 50-node cases, while the 15-node case showed slight over-prediction for some tests. Since FRIGG has similar scaling as the ABWR for a single bundle, the selected core noding is considered acceptable for the evaluation of an ABWR LOCA.

The drift flux model, as implemented in USA7, is a one-dimensional mixture model. It cannot resolve the exact location of the mixture level within a given nodal region. Consequently, if the node (or computational control volume) containing a mixture level is large, the calculated

mixture void fraction (and quality) for the node would be different from the actual void fraction (and quality) below and above the mixture level. Therefore, the finer nodalization is essential to provide better estimation of the nodal void fraction and steam quality.

There is a mixture level tracking option available in USA7 that can be activated to calculate the actual position of the mixture level in a given node. Supplement 5 notes that the two-phase level tracking feature can be introduced when it is impractical to reduce the node size below a certain limit. However, this model cannot be activated in the core region. In the absence of the level tracking model in the core region, the finer nodalization is essential to improve the prediction of local void fraction and quality, which can also improve the prediction of boiling transition (dryout). Therefore, the finer nodalization selected in USA7 based on the FRIGG experiments also is considered to be acceptable for prediction of boiling transition under ABWR LOCA conditions.

In response to RAIs 13 and 14, Westinghouse noted that since the HPCF flow mixes with the upward flow from the reactor core and overflows into the downcomer via the steam separators, details of how the HPCF flow is distributed in the upper plenum are not important. Furthermore, the HPCF is not a core spray system and, therefore, the radial distribution of HPCF flow in the upper plenum is not important for safety analysis. The staff finds this explanation to be acceptable only if the flow at the core exit is in upward direction during the HPCF injection period under all LOCA conditions. If, in future applications of USA7, downward flow into the core is predicted during the HPCF injection period, the assumption of one-dimensional upper plenum nodalization should be reconsidered. Therefore, this imposes a limitation on the use of USA7 to restrict the one-dimensional nodalization in the upper plenum to conditions where the flow is always from the core to the upper plenum region during the HPCF injection period.

Westinghouse also stated that at the time of the initiation of LPFL injection, the LPFL fluid must fall through approximately 2 meters of a saturated steam environment in the downcomer. This provides ample opportunity to interact with and condense the steam. Consequently, the LPFL fluid is expected to be saturated upon mixing with the downcomer fluid. If subcooled LPFL flow is able to penetrate the steam environment and reach the downcomer mixture level, interaction and mixing in the downcomer region is expected to result in thermal equilibrium. Westinghouse also performed a conservative analytic calculation demonstrating that flow rates in the downcomer region are insufficient to entrain LPFL fluid out to the break and bypass core cooling by failing to reach the downcomer mixture level. The staff finds the justifications and explanations provided by Westinghouse to be acceptable. Consequently, the one-dimensional nodalization downcomer is considered acceptable for the ABWR LOCA analysis.

To justify the noding near the break, Westinghouse presented the results of nodalization sensitivity studies performed for the RHR suction line break and the main steam line break (MSLB) scenarios. In both sensitivity studies, the results showed no significant effect on calculated peak cladding temperature. Westinghouse also presented the results of a sensitivity study for more detailed noding in the upper plenum for the HPCF line break case. The upper node [[ ]] For the sensitivity case, the break flow, system mass, and downcomer water level were virtually identical to the base case. The staff finds the results of the sensitivity studies and, consequently, the noding in the vicinity of the break and the ECCS injection points as used in USA7 acceptable.

Westinghouse also clarified that the use of multiple parallel control volumes in GOBLIN representing the average core and the hot channel eliminated the need to use the DRAGON option (RAI-28). The DRAGON option has been used in previous LOCA analysis

(for BWR/2 through BWR/6) to provide hot channel predictions based on boundary conditions determined from the GOBLIN simulation. Since the DRAGON option has not been reviewed for ABWR LOCA analysis, the staff imposes a restriction that before there is any use of the DRAGON option in GOBLIN in conjunction with the USA7 EM, appropriate prior approval shall be sought by the applicant from the NRC.

3.2.1.2 Two-Phase Level Tracking Model

As noted earlier, the one-dimensional drift flux model as implemented in USA7 cannot resolve the exact location of the mixture level within a given nodal region. Therefore, finer nodalization is essential to provide better estimation of the nodal void fraction and steam quality near the expected mixture level. Alternately, the two-phase level tracking option that is available in USA7 can be activated to calculate the location of a distinctive mixture level where an abrupt void fraction distribution occurs within a control volume containing a two-phase mixture. The intent of the level tracking model is to capture the time-dependent interaction of the mixture level with flow paths or with ECCS injection within coarse mesh control volumes (Ref. 6).

The GOBLIN code has the capability to specify a series of control volumes in which a two-phase level is calculated and tracked. Supplement 5 states that the two-phase mixture level tracking model is activated throughout the downcomer. The use of the two-phase level tracking model was questioned by the staff:

- To assess the adequacy of two-phase level tracking in USA7, justification is necessary regarding its inclusion or exclusion at various locations (RAI-17).

- Feedwater flow, as well as RCIC and the LPFL injection, is directed into the lower downcomer control volumes in which the two-phase mixture level tracking model is active. From the discussion provided in WCAP-11284-P-A (Ref. 2), it appears that the two-phase level tracking model assumes saturated conditions below the two-phase mixture level interface. However, after the break initiation and before ECCS injection, the downcomer fluid below the mixture level is expected to be subcooled. The mixture level and the interfacial mass and energy exchange calculations under such conditions are not clear (RAI-17S01).

In response to the above concerns, Westinghouse clarified that the two-phase mixture level tracking model is not activated in the lower plenum, core, upper plenum, and steam dome. It was explained that the position of the two-phase mixture level in the downcomer is important since it affects the break flow and system depressurization for both the FWLB and MSLB LOCAs. Furthermore, the results of a sensitivity study showing the effect of activating the two-phase level tracking in the upper plenum on a HPCF line break LOCA also were provided. The results show that the activation of two-phase tracking in the upper plenum results in reduced break flow rate and less inventory loss. These studies indicated some effect on calculated inventory loss. However, no impact was observed on the peak cladding temperature (PCT).

The ABWR model in USA7 uses the same nodalization in the downcomer as previous BWR models. Westinghouse explained that in the two-phase level tracking model, the nodal boundaries change depending upon the elevation of the mixture level. When the mixture level decreases below the bottom of a node, the volume of the vapor region from the lower node is added to the volume of the node above, and the volume of the lower node is decreased to include only the liquid. Westinghouse indicated that in this situation, there is no energy

exchange between the steam above the interface and the liquid below the interface. Any water injection above the interface results in homogenization with the two-phase mixture above the interface, with mass and energy transfer addressed through the solution of the conservation equations.

Westinghouse also noted that the mixture level tracking model is not capable of calculating the two-phase mixture level within the core. As a result, the determination of core uncovery is based upon nodal void fractions. However, the nodal void fraction defining whether or not the node is assumed to be uncovered was not provided. During the audit, Westinghouse clarified that the core uncovery is assumed to occur when the nodal void fraction in the first unheated node above the core increases to unity. Using this void fraction criterion, Westinghouse showed a comparison of the GOBLIN predictions to a two-loop test apparatus (TLTA) boil-off test. The mixture level calculated using this criterion was compared against the experimental data. The comparison showed satisfactory prediction of the mixture level.

The staff finds the use of the two-phase level tracking model as it exists in USA7 to be acceptable. The staff also notes that the determination of core uncovery in not essential for the calculation of boiling transition (dryout) and, subsequently, cladding heat-up in USA7. Therefore, core uncovery in USA7 has only qualitative significance. To use a drift flux model to precisely calculate core uncovery in the absence of two-phase level tracking, it is necessary to use finer noding near the top of the core. However, in response to RAI-1, Westinghouse showed that increasing the number of core nodes to more than 25 does not result in better prediction of dryout time in using the FRIGG test data. Therefore, the staff concluded that the modeling of the core region in USA7 is adequate for the proper prediction of PCT in the ABWR.

3.2.1.3 ECCS Injection Flow

The ABWR ECCS is comprised of the RCIC, HPCF system, and LPFL mode of RHR system. The HPCF delivers coolant to the upper plenum. The RCIC and the LPFL inject coolant to the downcomer. The calculation of mixing of ECCS injection flow and the amount of steam condensation caused by ECCS injection are important. The issues related to the nodalization and mixing of the ECCS injection flows are addressed in this safety evaluation report (SER). The injection flow–fluid interaction model is a special model available in GOBLIN to calculate the steam condensation caused by ECCS injection flow. Since Supplement 5 lacks detailed discussion on modeling of ECCS injection flow; the staff requested additional information in RAI-13 and RAI-14.

In response, Westinghouse clarified that since the two-phase tracking model is not active in the upper plenum region of USA7, the injection flow–fluid interaction model cannot be used for HPCF injection flow. [[ ]] This modeling approach was justified by noting that there is always upward flow from the reactor core to upper plenum. However, the staff finds this explanation acceptable only if the flow at the core exit is in upward direction during the HPCF injection period. If in the future applications of USA7 it is observed that the flow at core exit is in downward direction during the HPCF injection period, the assumptions of one-dimensional nodalization, no two-phase level tracking, and no use of "injection flow–fluid interaction model for the HPCF injection in the upper plenum should be reconsidered. Therefore, the staff imposes limitation on the use of one-dimensional nodalization in upper-plenum without the activation two-phase level tracking and injection flow-fluid interaction model, unless it is demonstrated that the flow at core exit is in upward direction during the HPCF injection period.

Westinghouse also clarified that the injection flow–fluid interaction model is not activated for the LPFL injection in the downcomer.

It was noted that at the time of the initiation of LPFL injection, the LPFL fluid must fall through approximately 2 meters of a saturated steam environment, providing ample opportunity to realistically interact with the steam environment and condense steam. Consequently, LPFL fluid is expected to saturate upon mixing with the downcomer fluid. If subcooled LPFL flow is able to penetrate the steam environment and reach the downcomer mixture level, interaction and mixing in the downcomer region is expected to result in thermal equilibrium. The staff finds the justifications and explanations provided by Westinghouse to be acceptable.

3.2.1.4 Break Flow and ADS Flow Models

The calculation of break flow discharge is essential for the LOCA analysis. Based on the review of the break flow and ADS flow models used in USA7, the staff raised the following reservations:

- Additional details and sensitivity calculations regarding the modeling and effect of longitudinal split type breaks were necessary to determine the compliance with Section 1.C.1.a of Appendix K (RAI-8).

- Activation of the ADS is typically one of the most important features for the recovery from a hypothetical LOCA event. Therefore, the conditions at the ADS valve choke point and the model used to represent the flow through the ADS valves are important. Additional details regarding the model used to determine ADS flow were necessary (RAI-15).

In response to the above concerns, Westinghouse clarified that GOBLIN cannot simulate the characteristic effects of entrainment or vapor-pull-through in a longitudinal split break. One might expect longitudinal split and double-ended guillotine breaks to behave similarly in cases of single phase steam flow (for example, main steam line break). However, if the break location were to contain liquid and gas phases in close proximity (e.g., feedwater line break), then entrainment of one phase into the other could result in different break flow characteristics (also dependent upon whether the break is in the top, bottom, or side of the pipe). Westinghouse stated that since the feedwater sparger nozzles have a diameter of only 1.75 inches (0.0445 meters), the characteristic effects of entrainment or vapor-pull-through in a longitudinal split break are not expected to have a significant effect on the analysis results assuming the flow choking occurs at the nozzles on the feedwater spargers.

To further clarify this issue, Westinghouse presented the results of FWLB sensitivity calculations using GOBLIN for a break location downstream of the feedwater sparger nozzle. The noding was revised to represent the feedwater lines [[ ]], and the break was modeled in the feedwater line node connected to the downcomer fluid node. It was shown that when the break area is smaller than 50 percent of the feedwater line flow area, choking would occur at the break rather than at the feedwater sparger nozzles. Therefore, the staff restricts the use of USA7 for modeling of longitudinal FWLB, unless it can be demonstrated that the break area is greater than 50 percent of the feedwater line flow area.

In response to questions about the ADS modeling, Westinghouse clarified that the flow area is determined based on the safety valve design flow conditions using a homogeneous equilibrium model (HEM) for critical flow. Upon ADS actuation, flow through the valve is based on the

upstream (steam line) stagnation pressure, stagnation enthalpy, ADS flow area, and the HEM critical flow model.

According to 10 CFR Part 50, Appendix K (Ref. 10), the Moody model is to be used after the discharging fluid through the postulated break has been calculated to be two-phase. It is worth noting that since the flow through the ADS valves will be choked in the same manner as the flow through the postulated break in a LOCA, the ADS flow calculated using the HEM critical flow model would be different than that calculated using the Moody critical flow model if two-phase discharge occurs through the ADS. Westinghouse provided a comparison between the HEM and the Moody critical flow to show that the two models show very similar results, with HEM predicting a slightly lower flow as compared with Moody's critical flow model (which is conservative in terms of ADS flow). Also, Westinghouse informed the staff that validation studies for HEM using FIX-II data have been performed. The use of HEM results in a slightly lower discharge flow through the ADS valves, which would result in a slightly slower depressurization rate.

The staff finds the break flow and ADS flow modeling in USA7 to be acceptable with the following restriction:

- GOBLIN cannot simulate the characteristic effects of entrainment or vapor-pull-through in a longitudinal split break. Consequently, GOBLIN is not applicable for modeling longitudinal breaks. Therefore, the modeling of longitudinal feedwater line breaks is restricted to a break area demonstrated to be greater than 50 percent of the feedwater line flow area.

3.2.1.5 Other Conservative Assumptions in USA7

Certain modeling assumptions used in USA7— including feedwater flow isolation, reactor internal pump (RIP) operation, reactor power, and power profile—were evaluated by the staff. The staff expressed the following concerns regarding these assumptions in USA7:

- The feedwater flow is assumed to terminate in 1 second after the initiation of a break (because of loss of offsite power (LOOP) coincident with the LOCA), even though the pump coastdown may take longer because of their inertia. However, sensitivity analyses were not presented to demonstrate that the assumption for feedwater flow termination time is conservative from the standpoint of PCT. Maintaining the design feedwater flow will result in lower enthalpy fluid entering the core until isolation occurs. PCT in ABWR is a function of very early formation and collapse of voids in the reactor coolant rather than long-term coolant inventory makeup. The fast isolation of feedwater may not lead to a conservative estimation of PCT (RAI-2).

- For most of the break spectrum cases documented in Supplement 5, the initial core flow rate showed the greatest impact on PCT. This is because of the effect of the flow rate on early occurrence of boiling transition. The low (90 percent) core flow rate usually yields the highest PCT. However, no justification or sensitivity studies were provided in Supplement 5 for the selected core flow rates (i.e., 90 percent and 111 percent) (RAI-5).

- The ABWR LOCA analysis assumes a LOOP in combination with failure of one emergency diesel generator (EDG). Furthermore, all RIPs were assumed to coastdown rapidly as a result of the LOOP. The rapid reduction in core flow leads to boiling transition and excursion of the fuel cladding temperature. Supplement 5 states that the

assumptions of LOOP and RIP trip coincident with the LOCA are conservative. However, sensitivity analyses or justification supporting this assumption are not provided. In the event the RIPs are not immediately tripped, their operation would keep fluid in much of the reactor coolant system homogeneously distributed following a LOCA. This would enhance decay heat removal, but the turbulent mixing of the fluid may result in low quality fluid at the break location for a longer period of time, which may result in lower system inventory. Thereafter, inopportune tripping of the RIPs at this lower system inventory may result in more severe consequences (RAI-10).

- The chopped cosine power distribution is used for the ABWR LOCA analyses. However, since the PCT for ABWR LOCA results from the early power to flow mismatch, it is not unreasonable to expect that a top peaked power distribution may provide a higher PCT (RAI-19).

Westinghouse performed various sensitivity studies in response to the above concerns. Three sensitivity calculations consider feedwater coastdown times of 0.01, 10, and 20 seconds, respectively. The results demonstrate that there is no change in PCT in either case. Therefore, the assumed coastdown time of 1 second for feedwater flow following the initiation of a LOCA is conservative and acceptable.

To justify the initial core flow assumption, the Westinghouse response supplies a power flow operating map for ABWR showing that 102 percent power is designed to be sustainable only in the range of 90 percent to 111 percent core flow. Operation outside of this flow range could be sustained by adjustment of control rods. This response justifies the selected initial core flow values and is acceptable.

Westinghouse performed LOCA analyses for the MSLB, FWLB, and HPCF line break in which RIP operation was continued for 5 seconds and 20 seconds following the initiation of the LOCA, after which the RIPs were tripped. The results of these sensitivity studies showed that, assuming a trip of all RIPs coincident with the LOCA, LOOP coincidence provides conservative results. Any decrease in total system inventory because of continued operation of RIPs is more than compensated for by makeup flow (e.g., feedwater, ECCS). Therefore, continued operation of the RIPs is conservatively bounded by assuming that the RIPs are tripped at the same time as the initiation of the break.

Sensitivity calculations also were performed by Westinghouse for a bottom-skewed and top-skewed power distribution for a typical fuel cycle. The results indicated that the chopped cosine resulted in the highest PCT. The assumption of a chopped cosine axial power distribution is acceptable.

3.2.1.6 Reactor Internal Pump (RIP) Model

The GOBLIN pump model uses the angular momentum conservation equation. The coolant momentum equations and the pump angular momentum equation are coupled in GOBLIN through the four-quadrant pump homologous curves. This pump model is the same as the one previously approved by the NRC. Supplement 5 provides the method for calculating the hydraulic and frictional torque for the RIP model based on the pump design parameters. The frictional torque used in the pump model is a function of the pump speed and is set to a constant value below a specific speed threshold. The pump inertia is adjusted to match the minimum

safety analysis limit for the pump coastdown time constant. In Supplement 5, the behavior of the RIP model was compared against the Okiluoto 1 plant startup test data, and it demonstrated acceptable agreement.

In response to a staff question on the effect of the coastdown time on the PCT (RAI-6), Westinghouse performed a sensitivity study using higher pump inertia for the FWLB. The results show that the PCT is slightly lower for the sensitivity case because of the longer coastdown time. The result of the sensitivity is used to show that the model is conservative because of the conservative selection of the minimum coastdown time. Moreover, in the base and sensitivity case, the PCT is predicted to occur before pump speed reaching the value below which a constant frictional torque is applied. Therefore, the value of the constant frictional torque is not expected to affect the PCT. In response to the staff's concerns regarding the pump model behavior for reverse flow conditions and the loss coefficient used for reverse flow through a locked rotor (RAI-6), Westinghouse clarified that the RIP homologous curves that are implemented in USA7 (i.e., GOBLIN) include conditions representing head versus flow characteristics corresponding to a locked rotor (i.e., zero rotor speed). Westinghouse also presented information that indicated that the pump homologous curves were developed based on pump data that included forward and reverse flow through a locked rotor (zero speed). It was also shown that at low flows (less than 25 percent of rated), the absolute value of the pump head was virtually the same for flow in the positive and negative directions, indicating that there would be little resistance for flow reversal through the pumps.

The staff finds that the RIP model in USA7 is acceptable for use in ECCS analysis.

3.2.1.7 Boiling Transition Model

The onset of the boiling transition in GOBLIN is calculated using a boiling length based critical power ratio (CPR) correlation that was developed for the SVEA-96 Optima2 fuel used in the ABWR design. The CPR correlation is developed from steady-state test data collected from the FRIGG loop and includes corrections because of the sub-bundle to full-bundle effect, the double-peaked axial power profile correction, and the R-factor correction. These corrections are documented in WCAP-16081-P-A (Ref. 22).

To demonstrate the ability of GOBLIN to conservatively predict the occurrence of boiling transition, GOBLIN simulations are compared against test data from the FRIGG loop. Eighty five of the 253 FRIGG transient tests are used to validate the GOBLIN dryout prediction capability. The selected test cases include a variety of axial power shapes and power and flow transients, including flow coastdowns as are expected to occur during a LOCA event in the ABWR.

Comparisons of the measured versus predicted dryout times show that GOBLIN predictions are typically conservative as compared to the measurements. All of the flow transient tests were predicted conservatively by the boiling transition model in USA7.

The NRC SER for the previous CPR correlation, which forms the basis of the current one, recommended the use of different uncertainties based on the system pressure (i.e., 3.15 percent below 45 bar and 2.32 percent above 45 bar). However, a single value of the uncertainty is used for the current CPR correlation in GOBLIN. Westinghouse justifies this based on the occurrence of PCT very early in the transient before significant changes in pressure. Moreover, based on the requirements in Section I.C.4.c of 10 CFR Part 50,

Appendix K (Ref. 10), it is not required to use multiple uncertainties since the CPR correlation is based on steady-state experimental data (RAI-20).

Based on the review of the boiling transition model in USA7 and Westinghouse's responses to the staff's concerns, the staff finds the EM to be conservative and acceptable for prediction of boiling transition.

3.2.2 Conformance of USA7 to 10 CFR Part 50, Appendix K

Section I.A. Sources of Heat during the LOCA

Core thermal power assumed for the ABWR LOCA analysis presented in Supplement 5 is 102 percent of the rated thermal power (see Table B-1 of Supplement 5). This assumption is in compliance with the requirement of Appendix K. However, in Section 6.1 of Supplement 5, the applicant also indicated that lower power level may be used in future analyses if it is demonstrated that the uncertainty in power measurement instrumentation is less than 2 percent. The applicant assured that, as required by Appendix K, the power level less than the demonstrated uncertainty would not be used.

The chopped cosine power distribution is used for the ABWR LOCA analyses in Supplement 5. The applicant performed sensitivity studies to determine the effect of power distributions on the PCT. Calculations were performed for a bottom-skewed power distribution and a top-skewed power distribution based on typical fuel cycle burnup. The results indicated that the chopped cosine resulted in the highest PCT (see RAI-19). This satisfies the requirement of Appendix K.

Section I.A.1. The Initial Stored Energy in Fuel

The fuel thermal conductivity model in USA7 accounts for the effects of burnup and temperature and is consistent with the NRC approved methodology (i.e., STAV7.2 code thermo-mechanical fuel rod design code). The fuel data inputs for USA7 describing the initial fuel conditions (e.g., gap size, gap gas compositions, and gap volume) are generated by the STAV7.2 code in a bounding manner, which minimizes gap conductance for the entire burnup range. These considerations result in compliance with Appendix K requirement.

Section I.A.2. Fission Heat

The point kinetic model is used for the calculation of fission power in USA7. The calculations account for the feedback effect from voiding, Doppler broadening, moderator temperature, and control rod. The point kinetics model input parameters (e.g., delayed neutron fraction, void and Doppler feedback coefficient) are conservatively estimated from the NRC-approved methodology (PHOENIX code fuel bundle designs, 2-D transport code).

Section I.A.3. Decay of Actinides

The actinide decay power in USA7 is determined from the decay rate equations described in the American Nuclear Society (ANS) Standard 5.1. The energy release from isotopes uranium-239 and neptunium-239 is accounted for. As required by Appendix K, the actinide production rate was chosen to yield the highest actinide decay power throughout the fuel life.

Section I.A.4. Fission Product Decay

The decay heat in USA7 is calculated by accounting for the decay of 11 groups of fission products. The calculated decay heat is in agreement with the Appendix K proposed 1971 ANS standard. Furthermore, as prescribed by Appendix K, the decay heat multiplier 1.2 is used. The fraction of the locally generated gamma energy that is assumed to be deposited fuel and cladding is justified.

Section I.A.5. Metal-Water Reaction Rate

As proposed in Appendix K, the Baker-Just equation is used to calculate the rates of energy release, hydrogen generation, and zirconium oxidation.

Section I.A.6. Reactor Internal Heat Transfer

USA7 accounts for heat transfer from the piping, vessel walls, and non-fuel internal hardware, which is in compliance with the requirement of Appendix K (see RAI-23).

Section I.B. Swelling and Rupture of the Cladding and Fuel Rod Thermal Parameters

The previously approved mechanistic model for calculation of cladding swelling and rupture is used in USA7 [5]. This model has been compared against the applicable data in Reference [4].

Section I.C.1.a. Break Characteristics and Flow

Supplement 5 presented the results of break spectrum sensitivity studies. These sensitivity studies considered double-ended breaks in feedwater line, main steam line, RHR suction and injection lines, HPCF line, and drain line. However, USA7 cannot simulate the characteristic effects of entrainment or vapor-pull-through in a longitudinal split break.

Modeling of a longitudinal break is particularly important if the two-phase flow is expected at the break location (e.g., FWLB and RHR line break). However, as discussed in response to RAI-7, in most break cases the break flow would be choked at the feedwater sparger nozzles. Therefore, the characteristic effects of entrainment or vapor-pull-through in a longitudinal split break would not be expected to have a significant effect on the analysis.

However, additional analysis by the applicant showed that if the break area is smaller than 50 percent of the area of a feedwater line, choking would occur at the break rather than at the feedwater sparger nozzles. Consequently, the reviewers indicated that the SER will impose a restriction on modeling of longitudinal FWLB in GOBLIN, unless it can be demonstrated that the break area is greater than 50 percent of the feedwater line flow area.

Section I.C.1.b. Discharge Model

As required by Appendix K, the Moody model is used in USA7 to calculate the break flow. The break sizes considered in Supplement 5 cover a range from 50 percent to 100 percent. A sufficient range of break sizes is equivalent to use of different break discharge coefficients. The range of break size considered in Supplement 5 more than covers the required range of discharge coefficients from 0.6 to 1.0 (See RAI-8).

Section I.C.1.d. Noding near the Break and the ECCS Injection Points

As discussed in Section 3.2.1.1, the applicant performed several break location and ECCS injection point noding sensitivity studies. The results of these sensitivity studies are discussed in detail in response to RAI-24. Consequently, the noding in the vicinity of break and ECCS injection points as used in USA7 is acceptable.

Section I.C.2. Frictional Pressure Drops

As required by Appendix K, the frictional pressure losses are calculated using models that include a realistic variation of the friction factor with Reynolds number and realistic two-phase friction multipliers that are based on acceptable open literature correlations and test data.

Section I.C.3. Momentum Equation

The momentum equation used in USA7 accounts for all terms specified in Appendix K requirement.

Section I.C.4. Critical Heat Flux

The onset of the boiling transition in USA7 is calculated using a boiling length based critical power ratio (CPR) correlation that was developed for the SVEA-96 Optima2 fuel. This correlation, called D4.1.2, was developed from steady-state test data collected from the FRIGG loop and documented in Reference 1. The correlation has been reviewed and approved by the NRC. See the response to RAI-20 for additional information on this correlation. As discussed in Section 3.2.1.7, that correlation has been benchmarked against the experimental data.

In response RAI-26, the applicant also confirmed that the USA7 has an input option that prevents the reestablishment of nucleate boiling after the first boiling transition occurs. The applicant confirmed that, as required by Appendix K, this option is exercised for the analysis presented in Supplement 5.

Section I.C.5. Post-CHF Heat Transfer Correlations

Post-CHF heat transfer correlations used in USA7 include the Groeneveld flow film boiling correlation specified in Appendix K, the NRC approved Westinghouse upper-head injection correlation, and the Bromley film boiling correlation. The lower limit to the heat transfer coefficient is calculated using the modified Bromley correlation, which is based on zero flow. The modified Bromley correlation has been demonstrated to be a conservative lower limit when compared to a wide range of tests (Ref. 1).

Section I.C.6. Pump Modeling

The pump behavior in USA7 is modeled using the angular momentum conservation equation. The coolant momentum equations and the pump angular momentum equation are coupled in through the four-quadrant pump homologous curves. Further discussion on the pump model is provided in Section 3.2.1.6. In response to RAI-6, the applicant confirmed that the pump model is the same model that was used in earlier approved submittals, and in earlier applications, such as RELAP4. The two-phase Semiscale test homologous pump data was used as input.

Section I.D.1. Single Failure Criterion

As required by Appendix K, the analyses in Supplement 5 have been performed assuming the single active component failure that results in the most severe consequences. Since no single active failure of ECCS equipment results in an extended uncovery of the ABWR core, the limiting single failure is determined as the one that results in the least transient system inventory.

Section I.D.2. Containment Pressure

USA7 analysis conservatively assumes atmospheric pressure in containment throughout the LOCA. This assumption is in compliance with Appendix K requirements.

Section II. Required Documentation

The reviewers confirmed that Supplement 5, responses to RAIs and questions during the audit and the previously approved model documentation provided sufficient details to permit the technical review of the analytical approach used in USA7. The documentation also provided appropriate sensitivity studies comparisons against the experimental data.

3.3 Accident Scenario Identification Process

A postulated LOCA may be initiated by a break in connecting piping of a wide range of sizes and locations. According to 10 CFR Part 50, Appendix K (Ref. 10), conservative LOCA analysis requires that the worst possible single failure of the ECCS be assumed when demonstrating ECCS performance. A spectrum of pipe breaks sizes, locations, and single failures is necessary in the evaluation of an ECCS performance.

The staff finds that the accident scenarios considered in the ECCS analysis follow the requirements in 10 CFR Part 50, Appendix K (Ref. 10) and are acceptable.

3.4 Code Assessment

The staff performed a detailed review of the ABWR LOCA results that are presented in Supplement 5. The staff also requested additional information on the event sequence timings and the transient plots for several important parameters for the scenarios in Supplement 5 (RAI-32). The review of the information in Supplement 5 and that was provided by Westinghouse in response to staff requests resulted in several important findings, which are summarized here.

High Amplitude Flow Oscillations in the Downcomer

The staff noted unrealistically high amplitude oscillations in the downcomer flow near the feedwater injection node for one of the LOCA scenarios (MSLB6a). Westinghouse explained that when the downcomer wide range (WR) level decreases to the low water level-1 (LWL-1) setpoint, LPFL flow is delivered to the upper downcomer at the feedwater inlet elevation. Injection of LPFL flow into a volume containing vapor or two-phase mixture results in the immediate condensation of vapor and saturation of the LPFL fluid. Under some conditions, injection of the LPFL fluid into a downcomer node may drive the node to a fully saturated liquid or even a subcooled liquid condition. When this occurs, it is possible to trigger high amplitude flow oscillations.

During the audit, Westinghouse stated that this behavior was an artifact of the thermal equilibrium formulation of GOBLIN code. Westinghouse presented additional plots for MSLB6a scenario showing that the flow conditions in the nodes surrounding the LPFL injection node do not propagate to the downcomer exit flow paths (i.e., flow from downcomer to lower plenum do not show these oscillations). Therefore, the staff concludes that the observed condensation induced flow oscillations do not impact the ECCS analysis.

Compensation Factor for Mixture Level Calculation

In examining the mixture level in the downcomer for the drain line break (DLB) analysis, the staff notes that the calculated mixture level is lower than the range available on the WR-level plant instrumentation. Similar behavior also is observed in the FWLB, the MSLB, and the RHR suction and injection line break simulations.

Since the WR-level represents the collapsed liquid level between the reference leg elevation and the WR-level lower tap elevation, the reason for the mixture level to be lower than the WR-level is expected to be because of a compensation factor on the WR-level that was not explained in Supplement 5.

Westinghouse acknowledged that such a compensation factor is indeed used to account for the effect of pressure on measurement of the WR-level. However, the compensation factor is not properly used in the Supplement 5 analyses. As a result of this, the WR-level is calculated to be lower than the mixture level under some low pressure conditions. Westinghouse stated that the ECCS activation is affected by this code input error, but the overall effect on PCT and minimum inventory is not significant. Westinghouse agrees to use the correct compensation factor in future analyses.

The staff finds the explanation provided by Westinghouse acceptable. The use of the correct compensation factor will be verified by the staff in future analyses using USA7.

Void Fraction "Sandwiching" in Plena

In the ABWR design, HPCF flow is delivered to the upper plenum. In USA7, the upper and lower plenums are represented by a series of one-dimensional nodes. The two-phase level tracking model is not activated in these volumes as noted in Section 3.2.1.2 of this SER. The review of responses to RAI-32 revealed that in virtually all of the LOCA cases in Supplement 5, the lowest void fraction node is "sandwiched" between two higher void fraction nodes in the upper and lower plenums.

Responding to the staff's question about the void fraction "sandwiching" behavior in the upper plenum noted in the LOCA analysis results, Westinghouse performed additional calculations (Ref. 21). The calculations demonstrated that the void distribution "sandwiching" in the upper plenum was because of the different flow path areas for the different regions in the upper plenum. The lower void fraction in the middle node of the upper plenum was because of a larger flow area for this node. The larger flow area results in relatively lower superficial vapor velocities and lower void fraction.

Responding to the staff's question about the void fraction "sandwiching" observed in the lower plenum, Westinghouse explained that this was caused by the negative flow through the bypass region that was deposited in the "sandwiched" node.

The staff considers the explanation of the void fraction "sandwiching" in the upper and lower plenums to be acceptable.

3.5 Uncertainty Analyses

Requirements in 10 CFR Part 50, Appendix K (Ref. 10) provide for a conservative analysis that prevents the need for an uncertainty analysis of the type discussed in the SRP (Ref. 8). Westinghouse has chosen to follow the approach outlined in 10 CFR Part 50, Appendix K (Ref. 10).

The staff has confirmed that the methodology used by Westinghouse includes appropriate conservatism in accordance with the requirements in 10 CFR Part 50, Appendix K (Ref. 10). Therefore, Westinghouse is not required to perform an uncertainty analysis.

3.6 Confirmatory Analyses

In support of the staff review of Topical Report WCAP-17116-P, "Westinghouse BWR ECCS Evaluation Model" (Ref. 1), the staff requested the Office of Nuclear Regulatory Research to perform the specific confirmatory analyses using TRAC/RELAP Advanced Computational Engine (TRACE) Simulations of Toshiba Advanced Boiling Water Reactor (ABWR) Loss of Coolant Accident (LOCA) analyses. The specific LOCA events considered were 1) feedwater line break, and 2) high pressure core flooder injection line break. The results of the TRACE calculations (Ref. 24) indicated that the ABWR meets all pertinent regulatory requirements. In all cases, the analyses provided in the ABWR topical report (Ref. 1) bound the TRACE calculation results.

3.7 Quality Assurance Plan

The staff audited the quality assurance (QA) plan in February 2011 (Ref. 25). Subsequent to this audit, the staff concluded that the QA procedures used by the applicant were acceptable.

The staff also has concluded that any changes to GOBLIN are restricted by the methodology (Ref. 1) and that changes to the models in Reference 1 may not be made without NRC review and approval. Changes in numerical methods to improve code convergence or code enhancements or error corrections must be tested, and auditable records must be kept in accordance with Appendix B, "Quality Assurance Criteria for Nuclear Power Plants and Fuel Reprocessing Plants," to 10 CFR Part 50.

4.0 CONDITIONS AND LIMITATIONS

The staff finds that Westinghouse has adequately demonstrated the compliance of USA7 to the requirements of 10 CFR Part 50, Appendix K. However, the approval of USA7 is subject to the following limitations:

- The modeling of longitudinal feedwater line breaks using USA7 shall be restricted to break areas that are demonstrated to be greater than 50 percent of the cross-sectional flow area of a feedwater line.

- The DRAGON option shall not be used for hot channel analysis using USA7 without prior review and approval by the NRC. LOCA analysis using USA7 will use multiple parallel channels in GOBLIN to represent the average core and hot channel.

- The compensation factor, which accounts for the effect of pressure on measurement of WR-level, should be used in all future analyses using USA7.

- In future analyses using USA7, if downward flow from the upper plenum into core region is predicted during the HPCF injection period, the assumptions one-dimensional nodalization and no two-phase level tracking and injection flow–fluid Interaction models in the upper plenum should be reconsidered. This SER restricts the use of one-dimensional nodalization of upper plenum without the activation two-phase level tracking and injection flow–fluid interaction code option, unless it is demonstrated that the flow at the core exit is in upward direction during the HPCF injection period.

- Changes in numerical methods (see Section 3.7 of this SER) to improve code convergence or code enhancements or error corrections must be tested, and auditable records must be kept in accordance with Appendix B to 10 CFR Part 50.

5.0 CONCLUSION

The applicant submitted Supplement 5 to the Westinghouse BWR ECCS EM (USA7) requesting approval to use the GOBLIN and CHACHA-3D codes for ABWR ECCS analysis. Supplement 5 and the information provided by the applicant in response to RAIs and during the audit were reviewed to determine the compliance of USA7 to the requirements of 10 CFR Part 50, Appendix K.

Since the basic thermal-hydraulic phenomena in ABWR and BWR/2 through BWR/6 are the same, many elements of USA7 which were previously reviewed by the NRC and were found to be applicable for BWR/2 through BWR/6, also are applicable to the ABWR. Therefore, only those aspects of USA7 that are unique for the ABWR or found to be inadequately addressed in Supplement 5 and the previously reviewed model documentation for BWRs were reviewed in this SER. This SER applies to the Toshiba ABWR only.

Principal Contributors: George Thomas, James Gilmer, and Fred Forsaty
Date: January 2013

6.0 REFERENCES

1. WCAP-17116-P, "Westinghouse BWR ECCS Evaluation Model: Supplement 5 Application to ABWR," September 2009 (Agencywide Documents Access and Management System (ADAMS) Accession No. ML092810301).
2. WCAP-11284-P-A, "Westinghouse Boiling Water Reactor Emergency Core Cooling System Evaluation Model: Code Description and Qualification," October 1989 (ADAMS Accession No. ML070890510).
3. WCAP-11427-P-A, "Westinghouse Boiling Water Reactor Emergency Core Cooling System Evaluation Model: Code Sensitivity," June 1987 (ADAMS Accession No. ML100840374).
4. CENPD-293-P-A, "BWR ECCS Evaluation Model: Supplement 1 to Code Description and Qualification," July 1996 (ADAMS Accession No. ML100150989).
5. WCAP-15682-P-A, "Westinghouse BWR ECCS Evaluation Model: Supplement 2 to Code Description, Qualification and Application," April 2003 (ADAMS Accession No. ML031540696).
6. WCAP-16078-P-A, "Westinghouse BWR ECCS Evaluation Model: Supplement 3 to Code Description, Qualification and Application to SVEA-96 Optima2 Fuel," November 2004 (ADAMS Accession No.ML050390440).
7. WCAP-16865-P-A, "Westinghouse BWR ECCS Evaluation Model Updates: Supplement 4 to Code Description, Qualification and Application," October 2011 (ADAMS Accession No. ML11308A065).
8. NUREG–0800, "Standard Review Plan for the Review of Safety Analysis Reports for Nuclear Power Plants," June 1996.
9. Title 10 of the Code of Federal Regulations (10 CFR) 50.46, "Acceptance Criteria for Emergency Core Cooling Systems for Light-Water Nuclear Power Reactors," 68 *Federal Register* 54142, September 16, 2003.
10. 10 CFR Part 50, "Domestic Licensing of Production and Utilization Facilities, Appendix K, "ECCS Evaluation Models."
11. P. Sawant, et al., "Technical Evaluation Report of the Westinghouse BWR ECCS Evaluation Model: Supplement 5 – Application to ABWR," Energy Research, Inc. (ERI)/U.S. Nuclear Regulatory Commission (NRC) 11-207, March 2012 (ADAMS Accession No. ML12353A627).
12. Letter from T. Govan to M. McBurnett, "Request for Additional Information Re: South Texas Project Nuclear Operating Company Topical Report (TR) WCAP-17116-P, Revision 0, Supplement 5 – Application to the Advanced Boiling Water Reactor," (TAC No. RG0012), June 7, 2010 (ADAMS Accession No. ML101580249).
13. Letter from T. Govan to M. McBurnett, "Request for Additional Information Re: South Texas Project Nuclear Operating Company Topical Report (TR) WCAP-17116- P, Revision 0, Supplement 5 – Application to the Advanced Boiling Water Reactor," (TAC No. R00007), August 24, 2010 (ADAMS Accession No. ML102360520).
14. Letter from S. Head to the NRC Document Control Desk, "South Texas Project Units 3 and 4 Docket No. PROJ0772 Responses to Request for Additional Information," U7-C-STP-NRC-100155, July 7, 2010. (ADAMS Accession No. ML101930158).

15. Letter from M. McBurnett to the NRC Document Control Desk, "South Texas Project Units 3 and 4 Docket No. PROJ0772 Responses to Request for Additional Information," U7-C-STP-NRC-100186, August 4, 2010 (ADAMS Accession No. ML102210131).

16. Letter from M. McBurnett to the NRC Document Control Desk, "South Texas Project Units 3 and 4 Docket No. PROJ0772 Responses to Request for Additional Information," U7-C-STP-NRC-100199, September 7, 2010 (ADAMS Accession No. ML102530167.)

17. Letter from S. Head to the NRC Document Control Desk, "South Texas Project Units 3 and 4 Docket No. PROJ0772 Responses to Request for Additional Information," U7-C-STP-NRC-100204, September 13, 2010.

18. Letter from M. McBurnett to the NRC Document Control Desk, "South Texas Project Units 3 and 4 Docket No. PROJ0772 Responses to Request for Additional Information," U7-C-STP-NRC-100 227, October 14, 2010 (ADAMS Accession Nos. ML102910347, ML102910343).

19. Letter from S. Head to the NRC Document Control Desk, "South Texas Project Units 3 and 4 Docket No. PROJ0772 Responses to Request for Additional Information," U7-C-STP-NRC-100233, October 25, 2010 (ADAMS Accession No. ML102910232).

20. Letter from S. Head to the NRC Document Control Desk, "South Texas Project Units 3 and 4 Docket No. PROJ0772 Responses to Request for Additional Information," U7-C-STP-NRC-100256, November 23, 2010 (ADAMS Accession No. ML103370089).

21. Letter from S. Head to the NRC Document Control Desk, "South Texas Project Units 3 and 4 Docket No. PROJ0772 Supplemental Responses to RAI Questions," U7-C-NINA-NRC-110052, April 18, 2011.

22. WCAP-16081-P-A, "10x10 SVEA Fuel Critical Power Experiments and CPR Correlation: SVEA-96 Optima2," May 2003.

23. Letter from S. Head to the NRC Document Control Desk, "South Texas Project Units 3 and 4 Docket No. PROJ0772 Responses to Supplemental Request for Additional Information," U7-C-NINA-NRC-110130, November 3, 2011.

24. Memo from K. Gibson to C. Ader, Transmittal of Deliverables 1(a) and 1(b) Associated with Response to User Need (NRO-2011-002) (ADAMS Accession No. ML12240A058 and ML12240A063).

25. Summary Report for February 15-17, 2011 Audit, Licensing Topical Report WCAP-17116-P, Westinghouse Boiling Water Reactor Emergency Core Cooling System Evaluation Model: Supplement 5- Application to the Advanced Boiling-Water Reactor, (ADAMS Accession No. ML111810561).

TABLE OF CONTENTS

LIST OF TABLES

LIST OF FIGURES

ACRONYMS AND ABBREVIATIONS

ADS	automatic depressurization system
ASD	adjustable speed drive
BAF	bottom of active fuel
CPR	critical power ratio
CTG	combustion turbine generator
EDG	emergency diesel generator
HPCF	high pressure core flooder
LHGR	linear heat generation rate
LPFL	low pressure flooder
LTR	licensing topical report
LWL	low water level
MAPLHGR	maximum average planar linear heat generation rate
MOV	motor operated valve
OL1	Okiluoto 1
PCT	peak cladding temperature
PLR	part-length rod
RIP	reactor internal pump
RWCU	reactor water clean-up
TCV	turbine control valve
TMOL	thermal mechanical operating limit
TSV	turbine stop valve
TVO	Teollisuuden Voima Oy

1 OBJECTIVE

The Safety Evaluation Report (SER) for the Westinghouse boiling water reactor (BWR) emergency core cooling system (ECCS) Evaluation Model, which is contained in RPB 90-93-P-A (Reference 1), concludes that the Evaluation Model is acceptable for large and small break applications involving BWR/2 through BWR/6 plants. The objective of this Licensing Topical Report (LTR) is to provide a basis for extending the applicability of the Evaluation Model to the Advanced Boiling Water Reactor (ABWR).

Because the response of the ABWR to a LOCA event is quite different than for a BWR with external recirculation pumps, different features of the Evaluation Model take on more importance and require additional qualification.

For example, the speed of internal recirculation pumps responds to a loss of power more quickly than external recirculation pumps. This results in boiling transition in the coolant channel in the first few seconds of the LOCA transient. Also, the absence of external recirculation piping connecting to the reactor vessel significantly reduces the loss of inventory due to postulated breaks in the attached piping. As a result, the phenomena of extended clad heat-up associated with core uncovery is absent in the ABWR design. The only significant cladding heatup predicted is due to early boiling transition in the hot channels as a result of the rapid decrease in core flow, which is independent of the ECCS equipment.

[

]^{a,c}

The LTR provides additional qualification of the internal pump model and benchmarks the system performance code GOBLIN to a series of dryout tests.

1.1 BACKGROUND

The licensing of the Westinghouse BWR reload safety analysis methodology for U.S. applications was begun by Westinghouse Electric Corporation in 1982 with the submittal of various LTRs. These reports describe codes and methodology developed by Westinghouse Atom AB, formerly known as ABB Atom (and ASEA Atom) of Sweden. Appendix A of this report provides a roadmap showing where various features of the Evaluation Model are described or revised.

In 1988, ABB Atom continued the licensing of the BWR reload methodology that was started by Westinghouse in 1982. The transfer of the licensing effort was formally facilitated by ABB's re-submittal of NRC-approved LTRs under ABB ownership.

After the acquisition of Combustion Engineering by the parent company of ABB Atom, the U.S. operations of ABB Atom were consolidated within ABB Combustion Engineering, which became the cognizant organization for BWR reload fuel application in the U.S. CENPD-300-P-A (Reference 2) describes the ABB BWR reload methodology that is currently used for U.S. reload applications.

ABB nuclear businesses were acquired by Westinghouse Electric Company LLC (the successor company of the Westinghouse Electric Corporation nuclear business) in April 2000.

The Westinghouse BWR ECCS Evaluation Model was originally approved by the NRC in 1989 and is described in RPB 90-93-P-A (Reference 2) and RPB 90-94-P-A (Reference 3). This methodology was first revised in 1996 to extend its application to SVEA-96 fuel. These revisions are described in CENPD-283-P-A (Reference 4) and CENPD-293-P-A (Reference 5). Two other revisions were made to the methodology in 2003 and 2004, primarily to improve the fuel rod cladding rupture model and to extend the application to SVEA-96 Optima2 fuel. These changes are described in WCAP-15682-P-A (Reference 6) and WCAP-16078-P-A (Reference 7) respectively.

It is noted that there is a difference in the total number of pages between the NRC-accepted proprietary and non-proprietary versions of this report (WCAP-17116-P-A and WCAP-17116-NP-A). This is due to a difference in the number of pages of the public and non-public versions of the NRC SER, and a difference in the number of pages of the proprietary and non-proprietary versions of two of the RAI responses in Appendix D (RAI 17 Supplement 1 and RAI 32 Supplement 2).

2 SUMMARY AND CONCLUSIONS

The ABWR LOCA transient assumed to occur coincident with a loss of offsite power is different than a typical BWR LOCA transient in two important ways:

- The core flow rate decreases quickly due to the rapid coastdown of the reactor internal pumps (RIPs) following the loss of power[1].
- The elevations of potential large pipe break sites are above the top of the active core.

The first difference results in early boiling transition before the reactor scram occurs. The reduction in heat transfer results in an increase in cladding temperature. The decrease in core power caused by increased voiding and reactor scram results in a rapid reduction in cladding temperature. As a result, the cladding temperature excursion is short-lived. The second difference, in conjunction with the actuation of the robust ECCS, results in nearly continuous two-phase cooling of the core. The typical extended core uncovery phase of the BWR loss of coolant accident (LOCA) transient does not occur in the ABWR. As a result, the peak cladding temperature (PCT) occurs before ECCS actuation and is independent of ECCS performance.

This LTR provides the basis for extending the Westinghouse BWR ECCS Evaluation Model to the ABWR. This version of the Evaluation Model is identified as USA7.

As discussed in Section 3, the methodology makes use of two computer codes, GOBLIN and CHACHA. These are the same codes used in the Westinghouse BWR ECCS performance analysis and no coding changes are necessary to apply these codes to the ABWR.

Section 4 describes the differences in the methodology with respect to typical BWR applications. In summary, the differences are:

- The nodalization for the system/hot assembly thermal-hydraulic response analysis is modified to account for the differences in design between BWRs and ABWRs. Most notably is the replacement of BWR external recirculation loops with ABWR internal recirculation pumps.
- [ ]^{a,c}
- [ ]^{a,c}

Section 4 presents a sample break spectrum analysis for a typical ABWR. The results of this sample break spectrum analysis show that the PCT occurs in the first few seconds and that the hot assembly is

1. A rapid coastdown of all RIPs is assumed, which ignores the effect that the 6 RIPs connected to the MG sets would coast down more slowly.

cooled by a two-phase mixture throughout the event. The case with the highest PCT, as predicted by the system/hot channel analysis, was further analyzed in a lattice heatup calculation using the CHACHA code to determine the MAPLHGR. As shown, the MAPLHGR [

]^{a,c}.

Section 5 of the topical report presents additional qualification for the GOBLIN code. A detailed description of the recirculation pump model is provided with emphasis on how the pump model is biased to ensure that a conservatively fast pump coastdown is predicted. A comparison of a predicted ABWR pump coastdown to a pump coastdown time constant specification (minimum safety analysis limit) is presented.

Section 5 also presents a comparison of GOBLIN test predictions of FRIGG loop transient dryout experiments. The predictions included comparisons to experiments with three different axial power shapes, decreasing flow rates, and increasing test section powers. The comparisons showed that GOBLIN predicted the time of boiling transition conservatively for all relevant test data.

Section 6 describes how the ABWR ECCS Evaluation Model complies with the requirements of 10 CFR 50 Appendix K and Section 7.

Appendix A provides an overview of the Westinghouse BWR/ABWR ECCS Evaluation Model methodology. A roadmap is provided to indicate what changes have been made to the methodology over the years and where the changes are described.

Appendix B provides a table of input parameters that were used to develop the GOBLIN system/hot channel analysis model. The data in the table is representative of an ABWR, but should not be assumed to be applicable to any particular plant.

Appendix C provides the changes that have been made to the approved version of this report as a result of NRC review and subsequent RAI responses.

Appendix D provides the NRC Requests for Additional Information (RAIs) and Responses.

3 OVERVIEW OF THE BWR/ABWR LOCA METHODOLOGY

The methodology and computer codes used for the ABWR are essentially the same as for the BWRs and are being applied in a manner that is generally consistent with the NRC approval for the BWR. The specific differences are described in Section 4.

The GOBLIN series of computer codes uses one-dimensional assumptions and solution techniques to calculate the ABWR transient response to both large- and small-break LOCAs. The series is comprised of two major computer codes, GOBLIN and CHACHA-3D. The flow of information between these codes is shown in Figure 3-1.

3.1 GOBLIN

GOBLIN performs the analysis of the LOCA blowdown and reflood thermal-hydraulic transient for the entire reactor, including the interaction with various control and safety systems. The GOBLIN code has what is referred to as the 'DRAGON' option that can be driven by boundary conditions supplied by the GOBLIN system analysis calculation. This option may be used to analyze the hot assembly in a series fashion rather than in parallel with the system response analysis. The parallel-channel calculation is accomplished by running GOBLIN with two or more parallel channels where one of the channels represents the hot assembly and the other(s) represents the remainder of the core. The latter approach is used in the examples presented in this report.

3.2 CHACHA-3D

The CHACHA-3D code performs detailed fuel rod mechanical and thermal response calculations at a specified axial level within the hot assembly previously analyzed by DRAGON or the multi-channel GOBLIN model. All necessary fluid boundary conditions are obtained from the hot channel calculation. CHACHA-3D determines the temperature distribution of each rod at a specified axial plane throughout the transient. These results are used to determine the PCT and cladding oxidation at the axial plane under investigation. CHACHA-3D also provides input for the calculation of total hydrogen generation.

The flow of information between these codes is shown in Figure 3-1. Reference 2 provides a detailed description of these codes. References 4, ,5 and 7 describe updates to the various components of the computer codes.

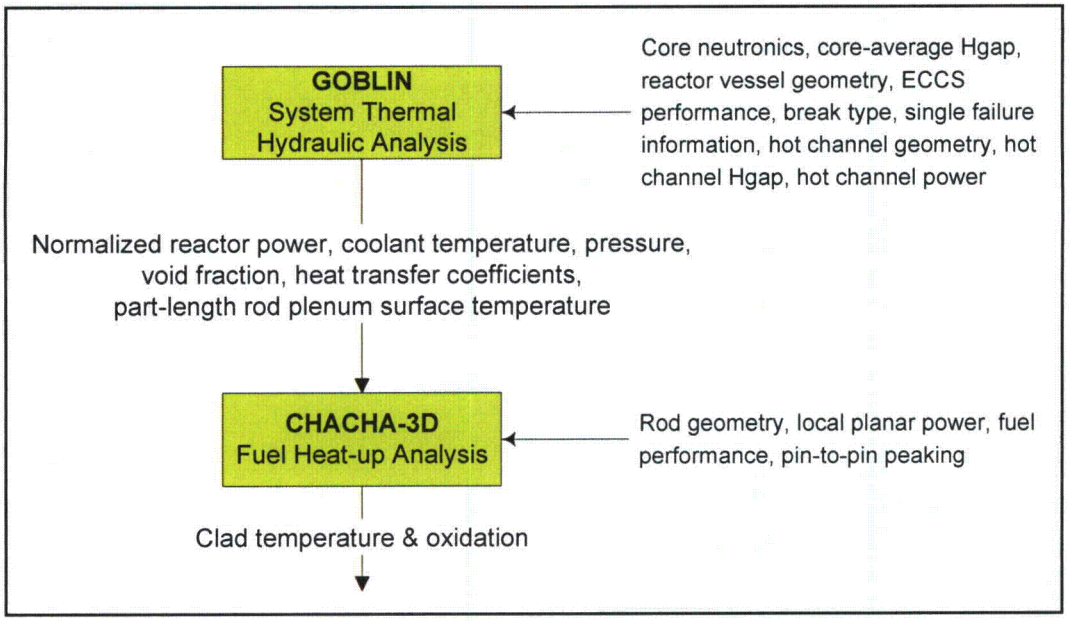

Figure 3-1 Flow of Information Between Computer Codes (parallel channel mode)

4 ABWR EVALUATION MODEL

4.1 DESCRIPTION OF THE ABWR

Figure 4-1 shows a cross section of the ABWR reactor vessel. The internals are similar to the BWR/3 to BWR/6 except that there are no jet pumps and no recirculation line nozzles connected to the lower part of the downcomer. The lack of large piping connecting to the lower part of the annulus, plus the capacity of the ECCS, significantly reduces the potential loss of inventory due to a postulated break in connecting piping. However, the low inertia of the impellers in the 10 variable speed reactor internal pumps (RIPs) cause them to coast down much faster than the larger external recirculation loops. The rapid reduction in core flow rate results in an early departure from nucleate boiling following the loss of offsite power that is assumed coincident with the LOCA.

During normal operation, the 10 RIPs provide forced circulation of reactor coolant through the lower plenum of the reactor and up through the lower grid, the reactor core, steam separators, and back down the downcomer annulus. By regulating the flow rate, the reactor power output can be regulated over an approximate range from 70% to 100% without moving control rods. The RIPs are mounted vertically with their drive shafts penetrating the RPV through nozzles arranged in an equally-spaced ring pattern on the bottom head. Adjustable speed drives (ASDs) provide power to the induction motors driving the RIPs. The RIPs are powered from two separate non-safety electrical load groups, each load group supplying 5 RIPs. Within each group, the RIPs are further divided between two 13.8 kV buses. Three RIPs connect via a motor/generator (M/G) set from one bus, and two, not connected to an M/G set, from another bus. On a single failure of a single power distribution component, two RIPs will trip simultaneously and three RIPs will continue to receive power as the M/G set coasts down. A maximum of three RIPs will trip simultaneously on a single failure of a 13.8 kV power system component (i.e., the M/G set). On a complete loss of alternating current (AC) power, the six RIPs connected to the M/G sets will continue to receive power as the M/G sets coast down. Although this system would significantly delay the early departure from nucleate boiling following a LOCA, the system is not credited for the analysis of LOCA coincident with loss of offsite power.

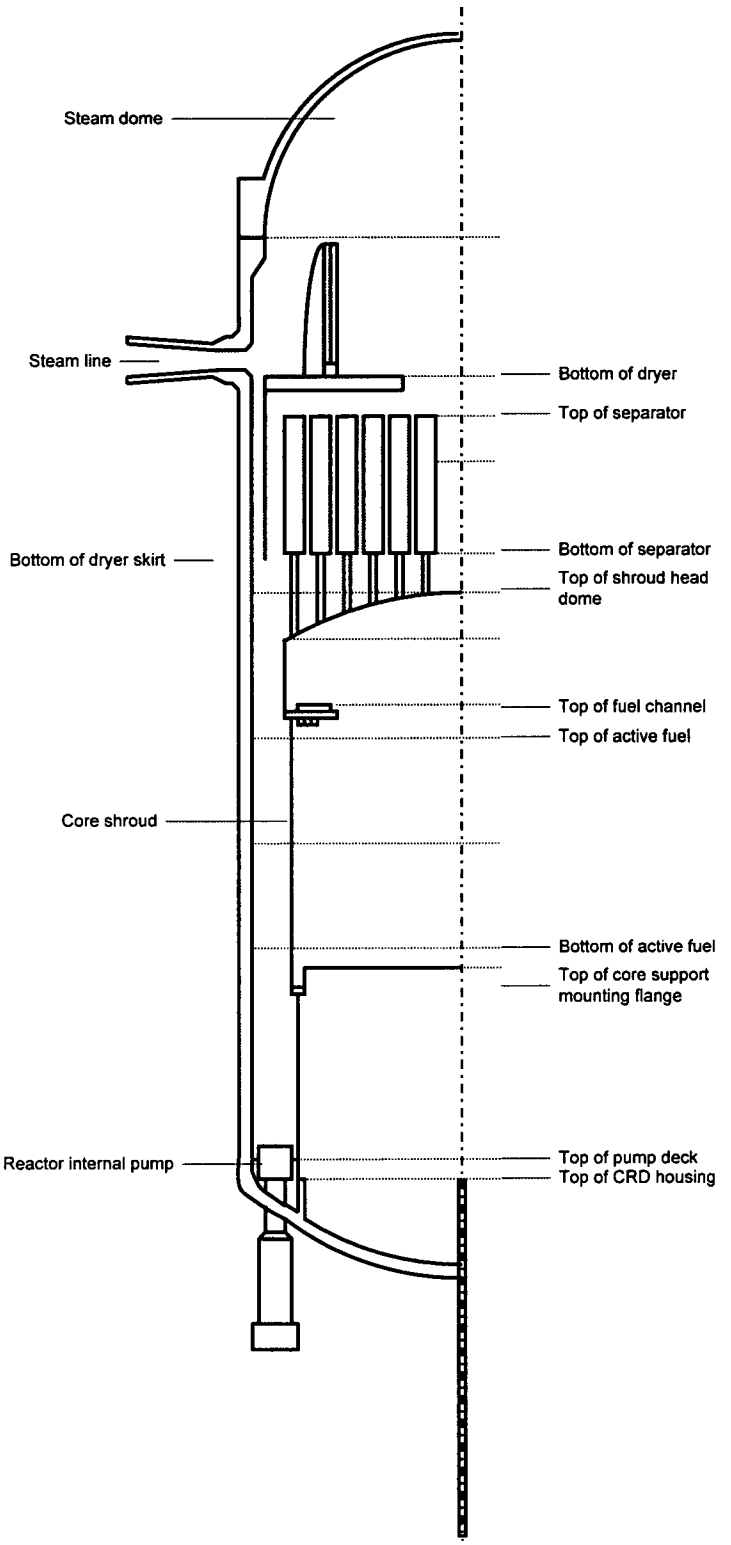

Figure 4-1 Schematic of ABWR Reactor Vessel Internals

4.2 DESCRIPTION OF ABWR ECCS

The ECCS is comprised of a reactor core isolation cooling (RCIC) system, a high pressure core flooder (HPCF) system, a residual heat removal (RHR) system, and an automatic depressurization system (ADS).

4.2.1 Reactor Core Isolation Cooling (RCIC)

The RCIC system consists of a single steam-driven turbine that drives a pump. The RCIC turbine steam supply is taken from one of the main steam lines upstream of the first MSIV. The turbine exhausts to the suppression pool. The RCIC pump discharges makeup water to one of the two main feedwater lines. The RCIC pump takes suction from the condensate storage tank (CST) or the suppression pool with the preferred source being the CST.

The RCIC system is initiated automatically when either a high drywell pressure signal or a low water level signal (LWL-2) signal is generated. The RCIC system is designed to deliver water to the RPV while the system is fully pressurized.

4.2.2 High Pressure Core Flooder (HPCF)

The HPCF is made up of two loops that deliver water to the RPV via two independent spargers above the core. The system is capable of injecting water into the reactor vessel over the entire operating pressure range. Both divisions take primary suction from the CST and secondary suction from the suppression pool. In the event the CST water level falls below a predetermined setpoint, the pump suction transfers automatically to the suppression pool.

The HPCF system is initiated automatically when either a high drywell pressure signal or a LWL-1.5 signal is generated.

4.2.3 Residual Heat Removal (RHR)

The RHR system consists of three independent loops that inject water into the RPV and/or remove heat from the reactor core or containment. In the low pressure flooder (LPFL) mode, each loop draws water from the suppression pool and injects water into the RPV outside of the core shroud via one of the feedwater lines on one loop and via the core cooling subsystem discharge return line on two loops.

The LPFL mode of RHR is initiated automatically when either a high drywell pressure signal or a LWL-1 signal is generated. Because the piping system is not designed for high system pressure, the injection valves require that the system pressure be below a pressure permissive setpoint before they will open.

4.2.4 Automatic Depressurization System (ADS)

If the RCIC and HPCF systems cannot maintain the RPV water level, the ADS, which is independent of any other ECCS, reduces RPV pressure so that flow from the RHR system operating in the LPFL mode enters the RPV in time to cool the core and limit fuel cladding temperature. The ADS is comprised of eight safety relief valves (SRVs). Each of the selected SRVs is equipped with an air accumulator and

check valve that ensures that the valves can be held open following failure of the air supply to the accumulators.

The system is designed so that a single active or passive component failure including power buses, electrical and mechanical parts, cabinets, and wiring will not disable ADS. A timer in the ADS is initiated when a high drywell pressure signal and a LWL-1 are present. If these conditions persist when the time delay expires, the ADS valves will open and steam will be discharged to the suppression pool.

4.2.5 Emergency Power

The ABWR has three emergency diesel generators (EDGs) to power the ECCS equipment in the event of a loss of normal power. Failure of one EDG will disable one of the LPFL pumps. RCIC is independent of the EDG and is available in the case of a station blackout. Failure of either of the other two EDGs will disable one HPCF pump and one LPFL pump. Figure 4-2 shows the breakdown of ECCS equipment by electrical division. The ECCS can also be manually powered by the combustion turbine generator (CTG). However, power supply from the CGT is not credited in the LOCA analysis.

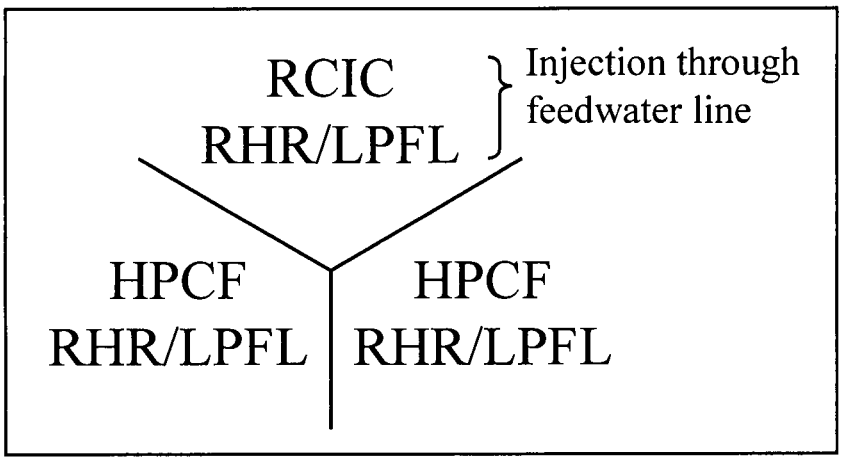

Figure 4-2 Schematic of ECCS Divisions

4.3 DESCRIPTION OF ABWR EVALUATION MODEL

4.3.1 GOBLIN Model

4.3.1.1 Nodalization

The typical ABWR GOBLIN nodalization for the Westinghouse ABWR Evaluation Model is shown in Figure 4-3. This nodalization scheme has been developed based on previous nodalization studies (References 3, 4, and 7). The major difference in the ABWR ECCS performance Evaluation Model is the increased number of nodes to model the active core. The benchmarking of the FRIGG loop experiments, as described in Section 5.3, showed improved results when [ ]^{a,c} were used to model the heated test section. GOBLIN nodalization of the ABWR may be changed, depending on the application of the model, to ensure that the appropriate thermal/hydraulic phenomena are captured in sufficient detail.

The steam dome is represented by a single control volume. During a LOCA transient with total loss of offsite power, the steam line is isolated rapidly by closure of the turbine stop valves (TSVs), fast closure of the turbine control valves (TCVs) or closure of the main steam isolation valves (MSIVs) and the steam dome is generally a stagnant vapor space.

The upper and lower downcomer regions are made up of nine sub-volumes. Feedwater as well as RCIC and LPCF injection are directed into the upper portion of the lower downcomer. Two-phase mixture level tracking is calculated throughout the entire downcomer. This means that the actual volume boundary nearest the mixture level is placed at the location of the mixture level. More detail about the level tracking feature is provided in Section 3.3.2 of Reference 2.

The lower plenum is divided into four control volumes. The lowermost sub-volume receives flow from the RIPs. This noding is similar in detail to the noding used in the BWR Evaluation Model.

The core is represented by five parallel channels, two channels representing the average core and its associated water-cross channel, two channels representing the hot assembly and its associated water-cross channel, and the fifth channel representing the core bypass region. The four channels representing average core and hot assembly channels, including their respective water cross, are comprised of [ ]^{a,c} each. The active region of the core and hot assembly are represented by [ ]^{a,c}. There are unheated sub-volumes at the top and bottom.

The core bypass and guide tube region are connected. These regions are partitioned into a total of seven control volumes, two of which represent the guide tubes. This noding is also similar to the noding detail used in the BWR Evaluation Model.

The upper plenum is divided into four sub-volumes. Three of the sub-volumes represent the region above the active core and one sub-volume represents the standpipes and steam separators. This is a region where the HPCF flow is injected. This noding is also similar in detail to the BWR Evaluation Model.

4.3.1.2 Hot Assembly Power

The ABWR design does not result in the hot assembly uncovering for any break in piping connected to the reactor pressure vessel (RPV), even when the limiting single active failure of ECCS equipment is assumed. As a result, the hot assembly power in the ABWR LOCA analysis may be established in a conservative manner [ ]^{a,c}. The process used is as follows:

The methodology assumes a symmetrical axial power shape (chopped cosine) with a 1.5 axial peaking factor. It is recognized that the axial power shape at the beginning of cycle is bottom peaked and that the peak power location generally moves upward during the cycle to become slightly top-peaked at the end of cycle. However, the axial shape used in the analysis is reasonably conservative and representative. The power at the hottest axial node is set to correspond to [ ]^{a,c}. The resulting initial assembly power is considerably higher than any that would occur during operation. This is confirmed for each reload.

The break spectrum analysis is performed using the predicted PCT in the GOBLIN hot assembly to identify the limiting break size/location case that will be subsequently evaluated in the CHACHA heatup calculation. The single failures of ECCS equipment have no impact on this analysis because the PCT occurs before any of the ECCS equipment has actuated. The break spectrum/single failure analysis results are also used to confirm that the performance of the ECCS equipment is sufficient to ensure that any uncovery is minimal and there is no appreciable cladding heat-up.

When the limiting break size/location has been determined, the boundary conditions from the hot assembly node applicable to the lattice being evaluated are applied to a CHACHA heatup calculation. The nodal power in the CHACHA heatup calculation is set so that [

]^{a,c}. The resulting conditions from the analysis are shown to be less than the 10 CFR 50.46 criteria, with regard to PCT and maximum local oxidation. [

]^{a,c}

4.3.2 CHACHA-3D Model

The CHACHA calculations performed in this report were for the SVEA-96 Optima2 fuel design. However, any fuel design approved by the NRC can be considered. The CHACHA-3D model is identical to the model described in Section 5.3 of Reference 7. Previous sensitivity studies described in Section 4.3.1 of Reference 3 and Section 6.3.1 of Reference 4 have shown little sensitivity to fuel rod noding. The standard fuel rod noding, which consists of seven radial nodes having equal volume to represent the fuel pellet and three nodes having equal radial increments to represent the cladding, is used. Similarly, the channel/water cross is represented by a single node with a constant thickness. Because previous studies have shown little sensitivity to channel thickness, the average thickness of the channel and water cross structures is used.

4.3.3 ABWR ECCS Performance Methodology

The reactor coolant pressure boundary contains numerous connecting pipes of varying lengths, diameters, and elevations. A postulated LOCA may be initiated by a break in connecting piping of a wide range of sizes and locations. A 10 CFR 50 Appendix K LOCA analysis requires that the worst possible single failure of the ECCS be assumed when demonstrating ECCS performance. A spectrum of pipe breaks sizes, locations, and single failures is necessary in the evaluation of an ECCS performance.

4.3.3.1 Break Spectrum

For typical LOCA Evaluation Models, the limiting break is the combination of break size, location, and single failure that yields the highest calculated PCT. However in the case of the ABWR, the PCT is not a sufficient measure of ECCS performance.

There is a short duration cladding temperature excursion in the first few seconds of a LOCA due to the rapid loss of core flow after the RIPs lose power. This temperature excursion occurs whether or not a LOCA has occurred and the magnitude of the PCT is independent of ECCS performance. Even though the return to nucleate boiling is prevented in the Evaluation Model, the cladding temperature reduces quickly as the reactor power reduces and the hot assembly remains cooled by a two-phase mixture throughout the rest of the ABWR LOCA transient.

The purpose of the ECCS in the ABWR design is to provide sufficient makeup to the core to prevent heat-up of the cladding subsequent to initial brief heat-up caused by boiling transition associated with the rapid decrease in core flow. Therefore, in the case of the ABWR, the relative performance of the ECCS is best determined by comparing the minimum system inventories for the various cases analyzed and showing that adequate core cooling is not interrupted at any core location. A demonstration of this analysis is presented in Section 4.4 and the case that resulted in the least inventory during the transient is described in Section 4.7.1.

4.3.3.2 Compliance with Acceptance Criteria

The Code of Federal Regulations, 10 Part 50.46 prescribes the following five acceptance criteria for an ECCS performance evaluation for light water nuclear power reactors:

1. Peak cladding temperature – The calculated maximum fuel element cladding temperature shall not exceed 2200°F.

2. Maximum cladding oxidation – The calculated total oxidation of the cladding shall nowhere exceed 0.17 times the total cladding thickness before oxidation.

3. Maximum hydrogen generation – The calculated total amount of hydrogen generated from the chemical reaction of the cladding with water or steam shall not exceed 0.01 times the hypothetical amount that would be generated if all the metal in the cladding cylinders surrounding the fuel, excluding the cladding surrounding the plenum volume, were to react.

4. Coolable geometry – Calculated changes in core geometry shall be such that the core remains amenable to cooling.

5. Long-term cooling – After any calculated successful initial operation of the ECCS, the calculated core temperature shall be maintained at an acceptably low value and decay heat shall be removed for the extended period of time required by the long-lived radioactivity remaining in the core.

As discussed in Section 4.3.3.1, the PCT that occurs during a LOCA for an ABWR is not associated with the performance of the ECCS because it occurs before the ECCS is actuated. However, there is a requirement to demonstrate that the 10 CFR 50.46 criteria are met for all postulated LOCAs. The following process is used to demonstrate that these criteria are met:

1. The GOBLIN system response analysis includes an analysis of the hot assembly that has been initialized at a conservative initial power per Section 4.3.1.2. The maximum cladding temperature and the node where it occurs are recorded for each of the break spectrum analyses and single failure studies.

2. The GOBLIN case resulting in the maximum peak cladding temperature is determined.

3. Boundary conditions from the limiting case (e.g., convective heat transfer coefficient, normalized power, rod plenum surface temperatures), which are appropriate for the lattice being evaluated,

are extracted from the GOBLIN system response analysis for the limiting break scenarios(s) as established by the maximum cladding temperature calculated by GOBLIN.

4. These boundary conditions are provided to the hot plane analysis using CHACHA and the nodal power is increased in the CHACHA analysis so that the hottest fuel rod in the lattice is at a linear heat generation rate corresponding to the TMOL.

5. The PCT, maximum oxidation and transient oxidation are recorded and used to demonstrate that the acceptance criteria are met.

The three remaining criteria, maximum hydrogen generation, coolable geometry and long term cooling, are clearly met by the ABWR. The short duration of the cladding heatup and the low maximum cladding temperature ensure that the transient cladding oxidation will be below the established acceptance criterion. For similar reasons, the fuel cladding will retain sufficient ductility to maintain the fuel structure intact and amenable to long-term cooling which is ensured by the long-term operation of the ECCS.

a,c

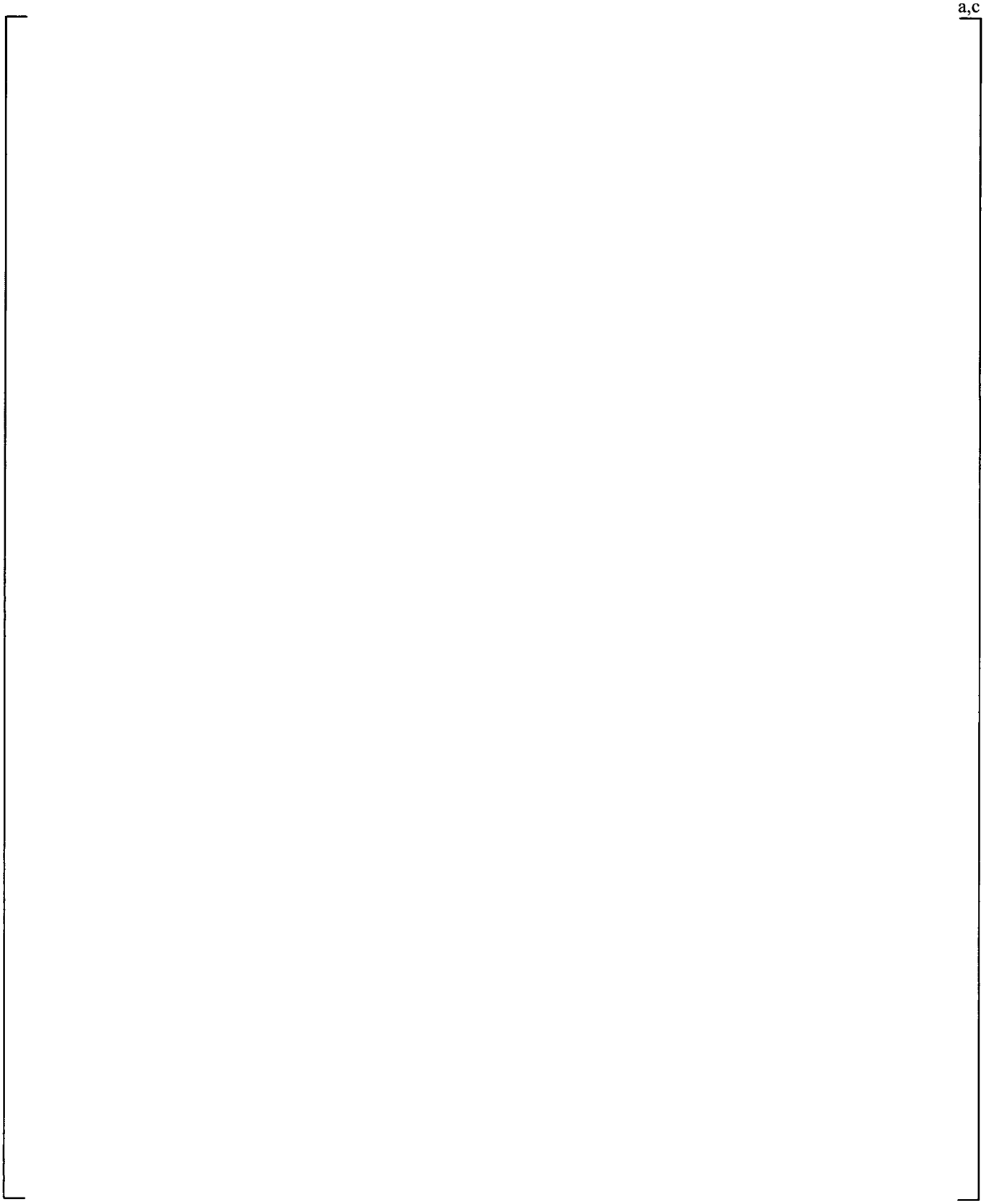

Figure 4-3 Typical GOBLIN Nodalization for ABWR

4.4 RESPONSE OF THE ABWR SYSTEMS TO A LOCA WITH LOSS OF OFFSITE POWER

In the ABWR there are one high pressure reactor core isolation (RCIC) system, two high pressure core flooder (HPCF) systems, three low pressure flooder (LPFL) systems available for any postulated pipe break, and the automatic depressurization system (ADS) available to mitigate a postulated LOCA. Given a break and the limiting single failure, there remains at least one high pressure and one low pressure injection system available to mitigate the event. Although loss of offsite power is assumed to occur at the start of the event, the analysis bounds the various time delays by assuming that the Emergency Diesel Generators (EDGs) start on the low water level ECCS initiation signal plus a fixed time delay. Because the EDGs start also on a high drywell pressure signal that occurs prior to the low water level signal in general, this assumption results in a conservative start time for ECC systems.

4.4.1 Reactor Scram

There are three automatic reactor scram signals that might occur following a LOCA with coincident loss of offsite power:

- Water level < LWL 3
- Drywell pressure > High drywell pressure signal
- MSIV stem position < 0.9 (steam line break)

With the exception of high drywell pressure, the other two reactor scram signals will be modeled.

4.4.2 Steam Line Isolation

The steam line will isolate following a LOCA. The two MSIVs on each steam line, which receive a close signal on LWL 1.5 or on high steam flow, are the safety grade system for isolating the steam lines. However, sensitivity studies, which are described in this report, show that an earlier and faster steam line isolation is conservative because it reduces the amount of voiding in the core as the pumps coast down due to its impact on system pressure. Therefore, it is assumed that the control grade fast closure of the turbine control valves (TCVs) isolates the steam lines on the generator trip signal coincident with the loss of offsite power.

4.4.3 Feedwater Isolation

The feedwater pumps lose motive power on the loss of offsite power. Although the feedwater pumps would coastdown due to inertia, the feedwater flow is assumed to ramp to zero flow in 1 second.

4.5 BREAKS INSIDE CONTAINMENT

Because the ABWR has no external recirculation lines, the largest line breaks are those postulated in a steam line, a feedwater line, or the RHR shutdown suction line. In comparison to external recirculation loop BWRs, the maximum ABWR line break size is only ~15% of the maximum double-ended recirculation line break. In addition, all of the large ABWR lines are located above the core. Breaks in smaller lines such as the RHR injection line, the HPCF injection line, and the bottom head drain line are also considered along with smaller breaks in the larger connecting lines. Table 4-1 lists the breaks considered inside the containment and the corresponding limiting single failure. Note that the limiting single failure is based on minimum inventory predicted during the event because failures in ECCS equipment do not impact the predicted PCT, which occurs before any ECCS equipment is activated. The limiting single failure is the one that provides the least makeup when considering the impact of the break location on the ECCS. The breaks listed in Table 4-1 are piping systems with RPV penetrations. There are other branch lines that connect to these lines, such as reactor water clean-up (RWCU), RCIC injection line, and the RCIC turbine steam supply line. Breaks in these lines are bounded by the break spectrum of lines that connect directly to the RPV.

A conservative assumption made in the ABWR LOCA analysis is that all offsite AC power is lost simultaneously with the initiation of the LOCA. In this case, four of the RIPs will automatically trip off. If reactor water level continues to drop and reaches LWL-2, the remaining six RIPs will be tripped, three immediately and the final three after a preset time delay. However, in the analysis, all of the RIPs are assumed to coast down rapidly as a result of the loss of power. The resulting rapid core flow coastdown produces a calculated departure from nucleate boiling in the hot assemblies within a fraction of a second after the accident. If offsite power were available, the RIPs would continue to run until a LWL-2 signal is generated and the pump coastdown would not begin until after the reactor scram.

Table 4-1 Line Breaks Inside Containment

Break Location	Available ECCS				Remarks
	RCIC	HPCF	LPFL	ADS	
HPCF Line Break	1	0	2	8	HPCF break + single failure of 1EDG
Main Steam Line Break	1 -	1 1	2 2	8 8	Single failure of 1 EDG RCIC side MSLB
Feedwater Line Break	- 1	1 1	2 1	8 8	RCIC side FWLB + single failure of 1 EDG LPFL side FWLB + single failure of 1 EDG
RHR Shutdown Suction Line Break	1	1	2	8	Single failure of 1 EDG
RHR Injection Line Break	1	1	1	8	LPFL break + single failure of 1 EDG
Drain Line Break	1	1	2	8	Single failure of 1 EDG

4.5.1 HPCF Line Break

There are two HPCF injection nozzles that attach to the RPV near the elevation of the shroud dome. Each nozzle is connected to one of the two HPCF loops. Each injection line is isolated from the RPV by

two valves, one a testable check valve and the other a normally closed motor operated valve (MOV), which opens on the HPCF actuation signal. Internal piping connects each nozzle to a sparger within the upper plenum of the reactor. Each sparger contains a number of nozzles that distribute the injected water above the core.

In the event of a break in the HPCF injection line between the check valve and the RPV, coolant from the RPV will discharge directly into the drywell. The flow of coolant exiting the RPV is limited by the combined flow area of the sparger nozzles. A break in the injection line will prevent any makeup from the water injected from the affected HPCF system. The limiting single active failure is the failure of the EDG that powers the unaffected HPCF loop. This results in the following available equipment:

1 RCIC + 2 LPFL + 8 ADS

Because the combined flow area of the sparger nozzles is small, the system pressure is maintained by the SRVs until actuation of ADS. The RCIC system receives an actuation signal when the measured water level decreases below LWL-2. The LPFL system and ADS delay timer receive an actuation signal when the measured water level decreases below LWL-1. Although the LPFL pumps will start, the LPFL injection valve will not open until the system pressure decreases below a permissive setpoint.

4.5.1.1 HPCF Line Break Results

Six cases were run with the power in the hot assembly set to simulate the hot rod at the TMOL. Table 4-2 summarizes the results of those cases. As shown, the variations in PCT are small when the steam line is isolated by TCV fast closure. The variations in minimum mass for a given break size were minimal. The minimum system mass increases with decreasing break size as expected.

Table 4-2 HPCF Line Break Results

Case	Core Flow	Break Location	Break Size	Steam Line Isolation	PCT (GOBLIN)	Minimum Mass
hpcf3	90%	HPCF Line	100%	TCV fast closure	708°C	133.3 E3 kg
hpcf4	111%	HPCF Line	100%	TCV fast closure	692°C	132.2 E3 kg
hpcf5	90%	HPCF Line	100%	Pressure regulator	661°C	133.7 E3 kg
hpcf7	90%	HPCF Line	75%	TCV fast closure	708°C	138.1 E3 kg
hpcf8	90%	HPCF Line	50%	TCV fast closure	708°C	143.6 E3 kg
hpcf9	90%	HPCF Line	25%	TCV fast closure	708°C	151.3 E3 kg

4.5.1.2 Sensitivity Studies

Core Flow Rate

Cases hpcf3 and hpcf4 show the effects of different initial core flow rates. The higher initial core flow rate will result in a higher initial mass in the core due to lower void content and additional margin to dryout.

Figure 4-4 compares the system pressure response and the maximum cladding temperature in the hottest GOBLIN node. As shown, the initial pressure responses are identical. However, ADS actuation occurs sooner for the base case, 90% core flow rate, because the water level decreases to the ADS actuation setpoint, LWL-1, sooner. The figure also shows that the PCT is slightly higher in the base case, which is a result of an earlier transition to dryout.

Figure 4-5 compares the system mass and ECCS flow rates. Although the initial mass is slightly higher in the high core flow case (hpcf4), there is a delay in the start of RCIC and LPFL injection which delays recovery. As a result, the minimum inventory is slightly less in the high core flow rate case.

Figure 4-6 compares the upper plenum average void and hot assembly exit quality. As shown, there is a period of time when the upper plenum does not contain any liquid (i.e., the void fraction becomes 1.0). This is because the break is located in the upper plenum and it eventually loses all liquid inventory. However, the figure also shows that the hot assembly exit quality indicates two-phase flow throughout the transient.

Steam Line Isolation

Cases hpcf3 and hpcf5 compare different ways of isolating the steam lines. The first, or base, case isolates the steam line by fast closure of the TCVs. The second case assumes that the pressure regulator controls the TCVs to maintain system pressure. As shown in Table 4-2, the PCT was lower in the second case. The minimum inventories were nearly identical.

As shown in Figure 4-7, the dome pressure responses are quite different. The base case maintains a higher pressure until ADS actuation. In this case, the initial system pressure is controlled by the opening and closing of the SRVs. The second case (hpcf5) shows the effect of the pressure regulator closing the TCVs, where system pressure is held approximately constant until the MSIV closure setpoint, LWL-1.5, is reached. After MSIV closure, the system pressure increases until ADS is actuated. The figure also shows that the base case has a higher PCT, which is due to reactivity feedback effect caused by the impact of the pressure response on the void distribution.

As shown in Figure 4-8, the initial break flow rate is higher when the steam line is isolated by the pressure regulator as in case hpcf5. This is because the combined break area (HPCF line and steam line) is larger as the steam is discharging through the TCVs for a longer time. The additional loss of inventory results in earlier ADS actuation, earlier actuation of the LPFL pumps, and earlier recovery. However, the minimum system masses are nearly identical.

Break Size

Cases hpcf3, hpcf7, hpcf8, and hpcf9 show the effects of different break sizes. As shown in Table 4-2, the PCTs are the same for all cases and the minimum inventory decreases as break size increases.

Figure 4-9 compares the dome pressure and PCT responses. As shown, the initial pressure responses are the same because the pressure is controlled by the opening and closing of the SRVs until ADS actuation. Because the loss of inventory occurs at a slower rate as the break size decreases, the water level reaches

the ADS actuation setpoint later as break size decreases. The figure also shows that the PCT, which occurs early due to the reduction in core flow, is independent of break size.

Figure 4-10 shows the effect of break size on system inventory and ECCS flow rate. As shown, the system mass decreases at a faster rate for the larger breaks, but recovery starts sooner due to earlier actuation of the LPFL pumps. As a result, the largest break has the smallest minimum inventory.

Figure 4-11 shows the upper plenum average void fraction and hot assembly exit quality for each of the break sizes. As shown, all cases have a period of time where the upper plenum void fraction becomes one. This is due to the break location being in the upper plenum. However, Figure 4-11 also shows that the hot assembly exit quality is substantially less than one, indicating that the hot assembly is cooled by a two-phase mixture throughout the transient.

Assembly Power

Although the hot assembly does not uncover during the event, assemblies with lower power do experience a short-term uncovery at the upper elevations for the HPCF injection line break. The difference in behavior between high and low power assemblies is due to the amount of steam generated in the two-phase region of the assembly. For high power assemblies, there is sufficient steam generation to swell the two-phase mixture to the top of the channel. However, for low power assemblies, the top of the two-phase mixture may not reach the exit of the channel. Sensitivity studies were performed where the power in the single channel was reduced. Figure 4-12 compares the cladding temperatures at the exit of the heated channel for several channel peaking factors. As shown, for peaking factors of 1.2 and lower, there is a temperature excursion after 280 seconds which recovers following LPFL injection.

Figure 4-13 compares the PCTs for several channel peaking factors. As shown, the highest power channel has the highest peak cladding temperature, occurring during the RIP coastdown phase of the event. Although the lower power bundles do not experience the early boiling transition during the RIP coastdown phase, there is a short duration heatup that occurs prior to LPFL injection when the system inventory is low. As shown, there is a channel peaking factor between 0.9 and 0.3 where this heatup will reach a maximum. However, the PCT during this heatup phase is of the same order as the initial cladding temperature.

The HPCF line break was the only break to exhibit this behavior because this is the only break located inside the core shroud region.

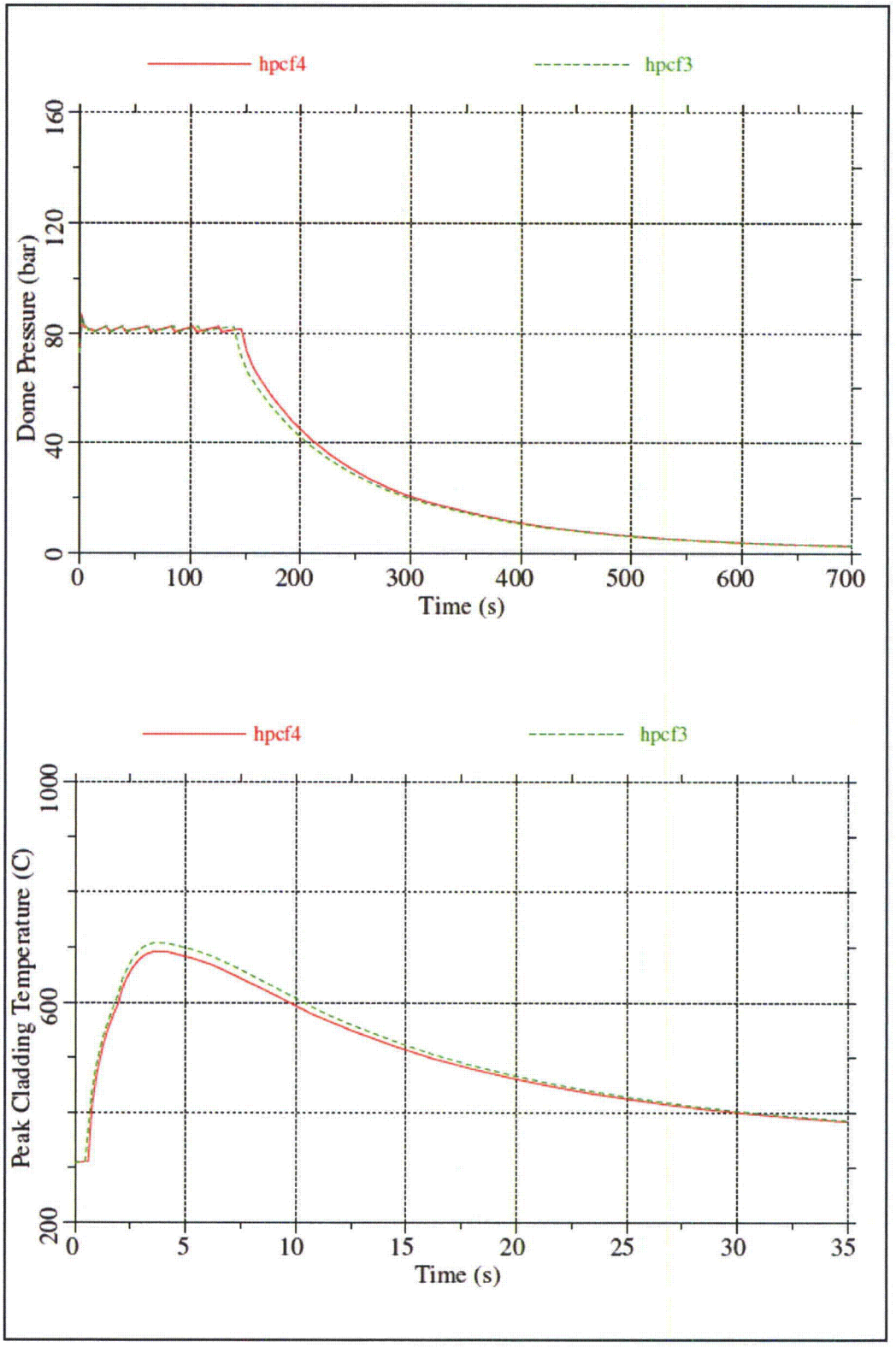

Figure 4-4 Core Flow Rate Sensitivity – Dome Pressure and GOBLIN PCT

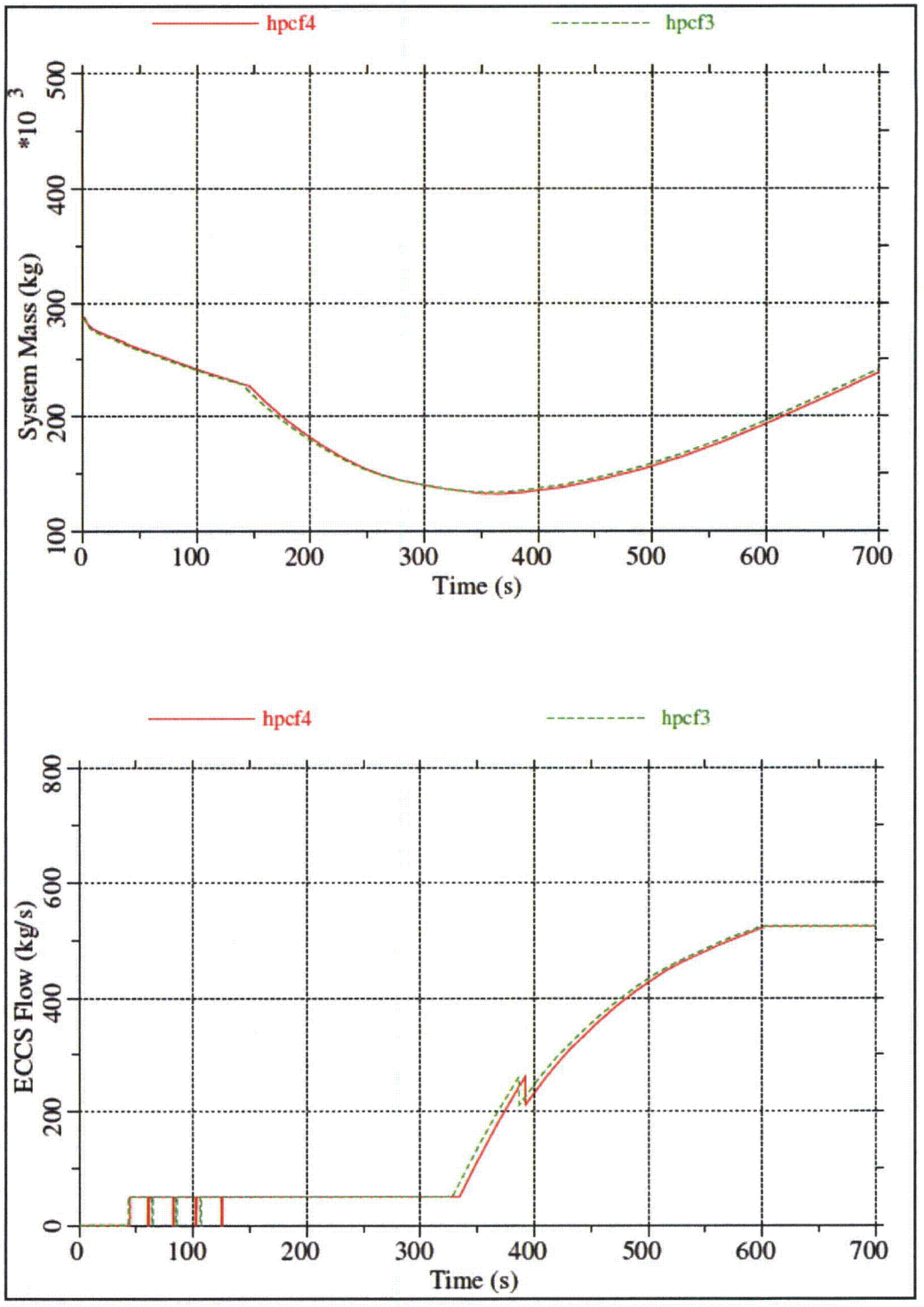

Figure 4-5 Core Flow Rate Sensitivity – System Mass and ECCS Flow Rate

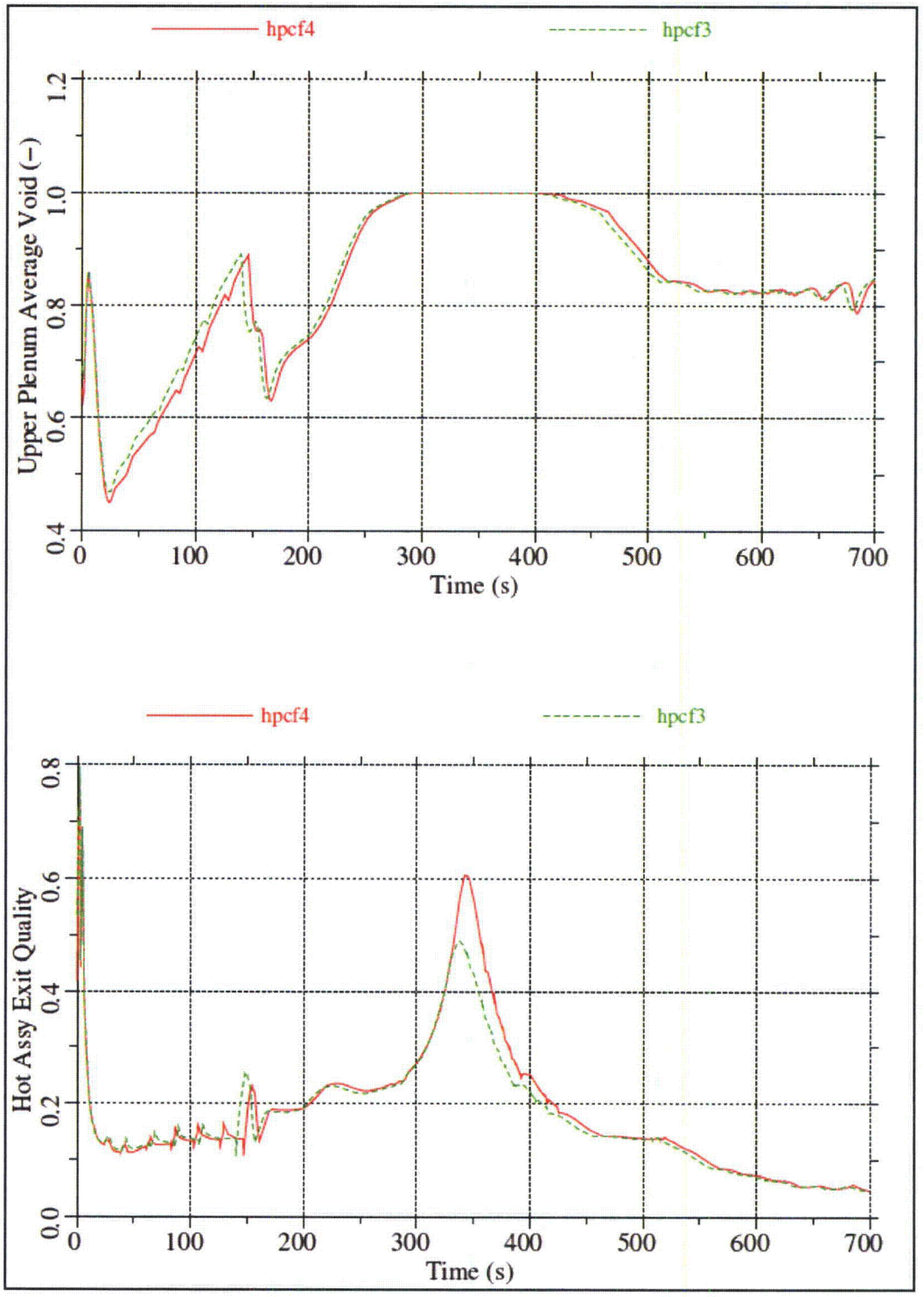

Figure 4-6 Core Flow Rate Sensitivity – Upper Plenum Void and Hot Assembly Exit Quality

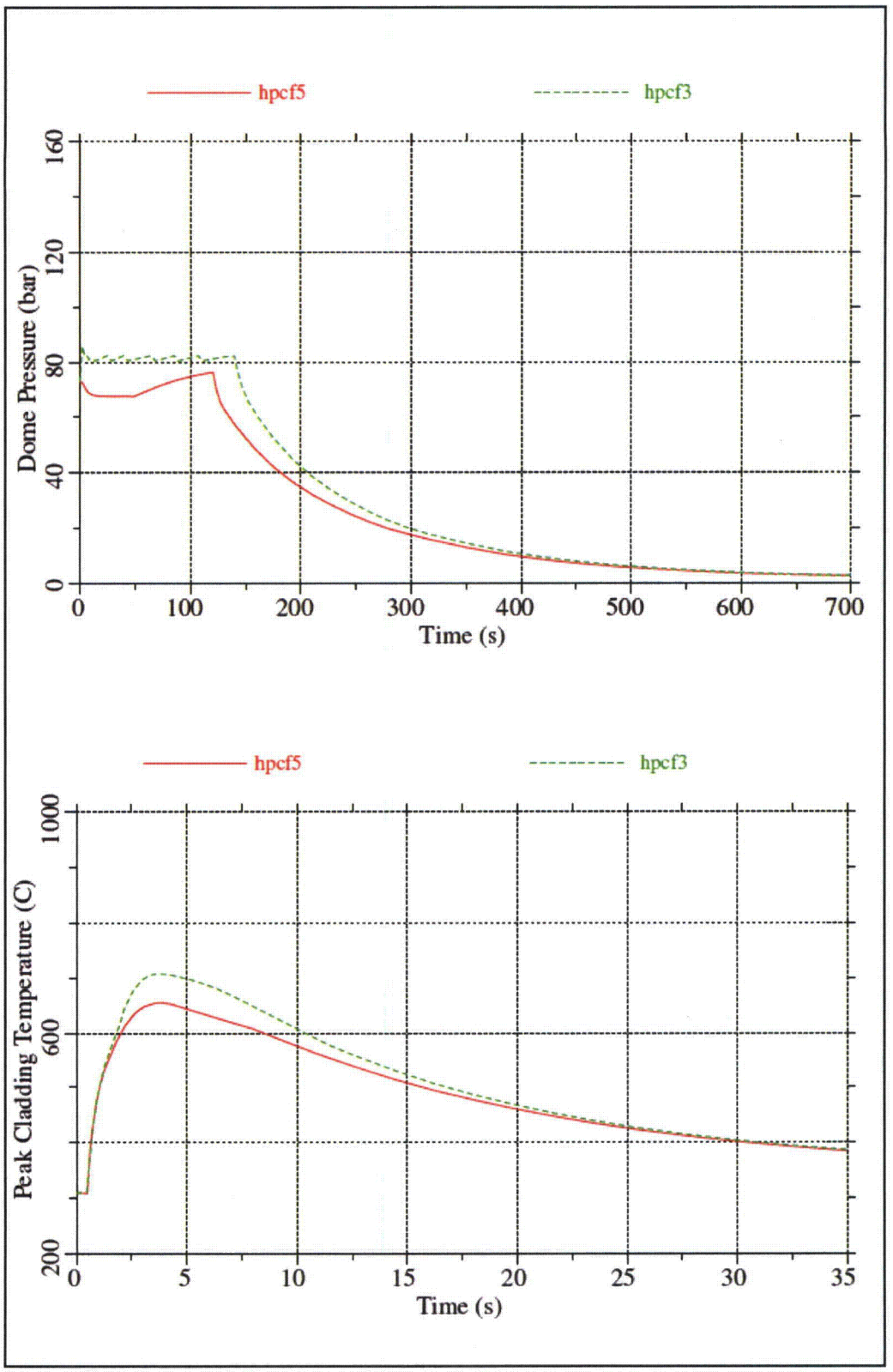

Figure 4-7 Steam Line Isolation Sensitivity –Dome Pressure and GOBLIN PCT

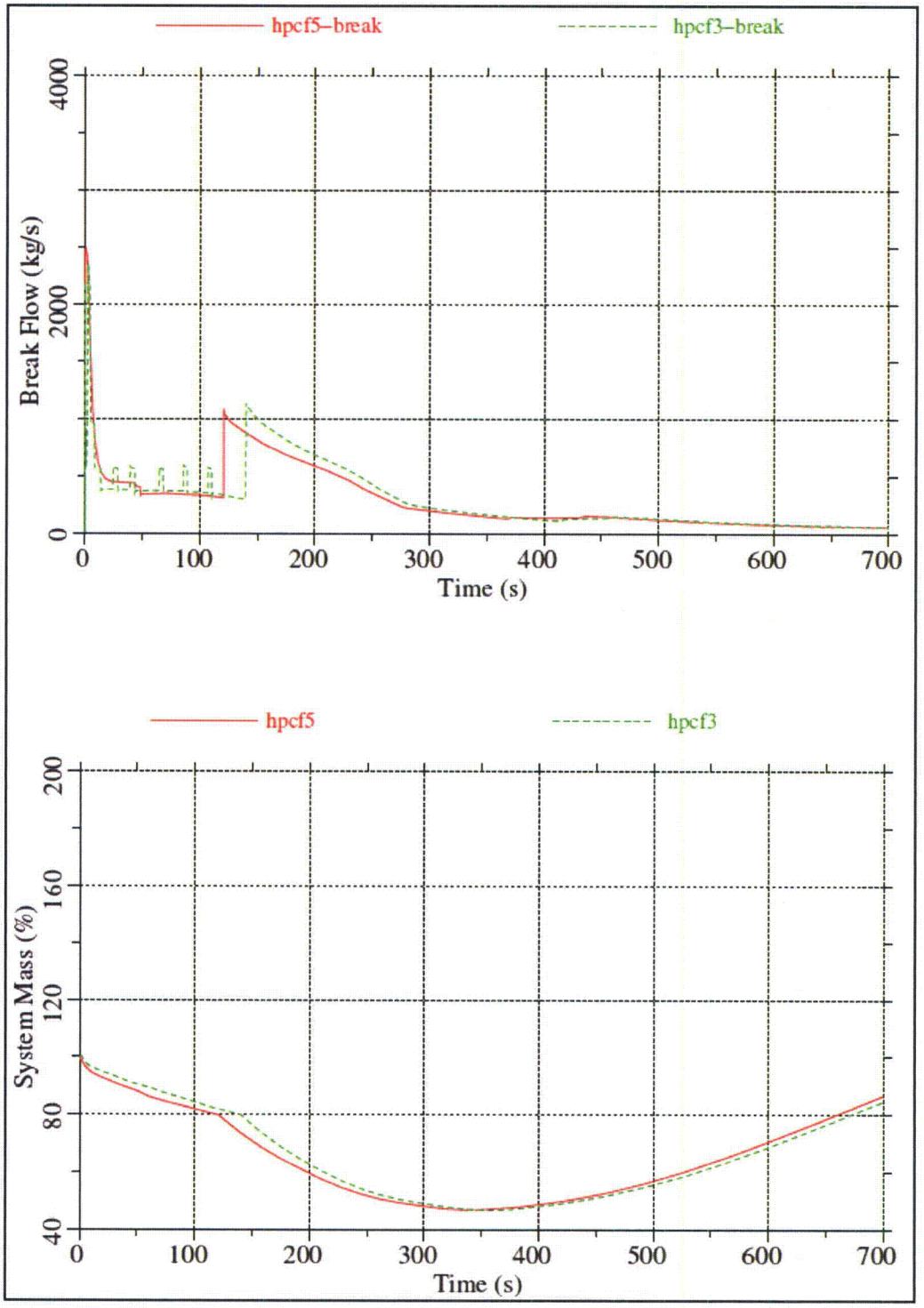

Figure 4-8 Steam Line Isolation Sensitivity – Break Flow Rate and System Mass

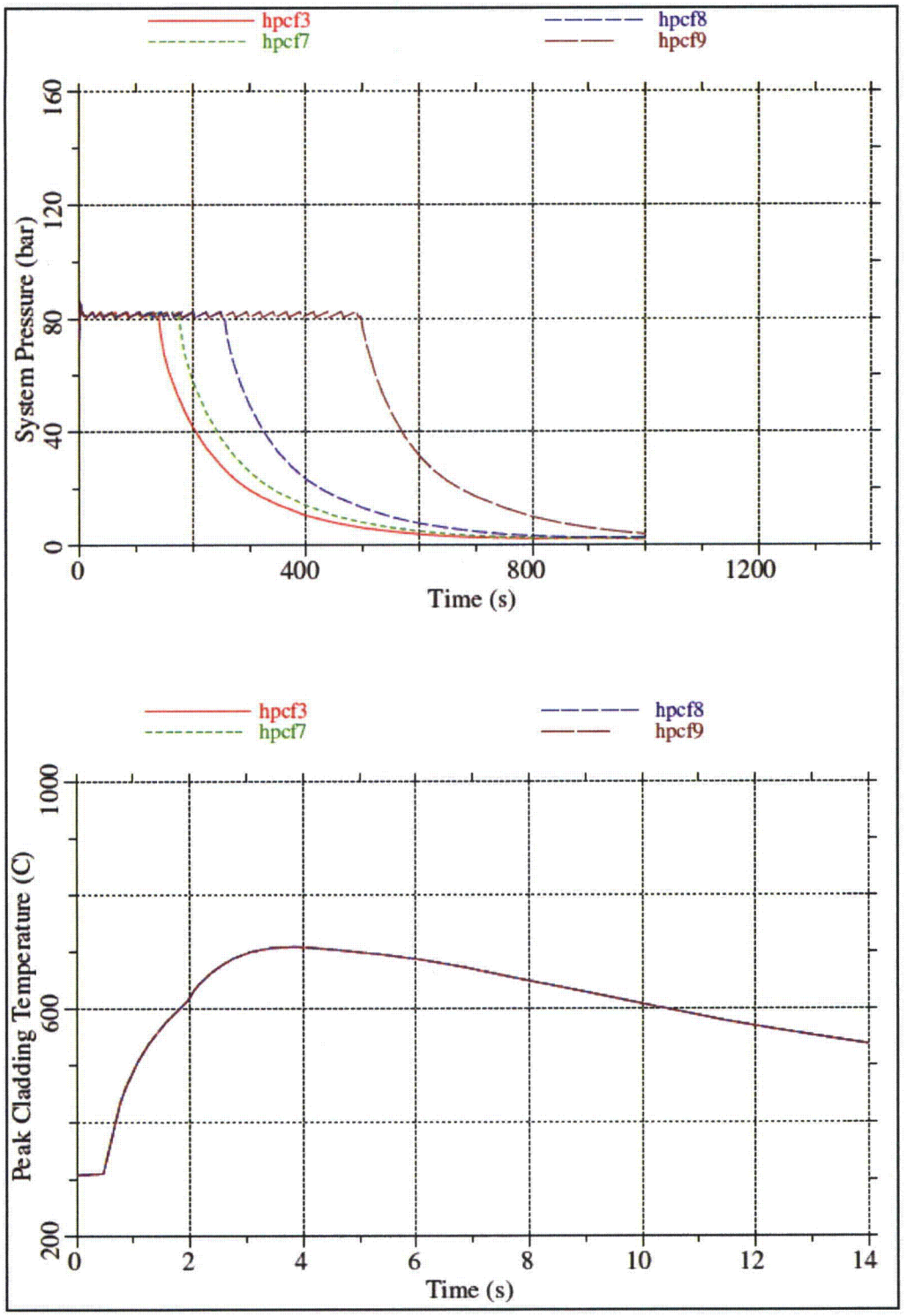

Figure 4-9 Break Size Sensitivity – Dome Pressure and PCT

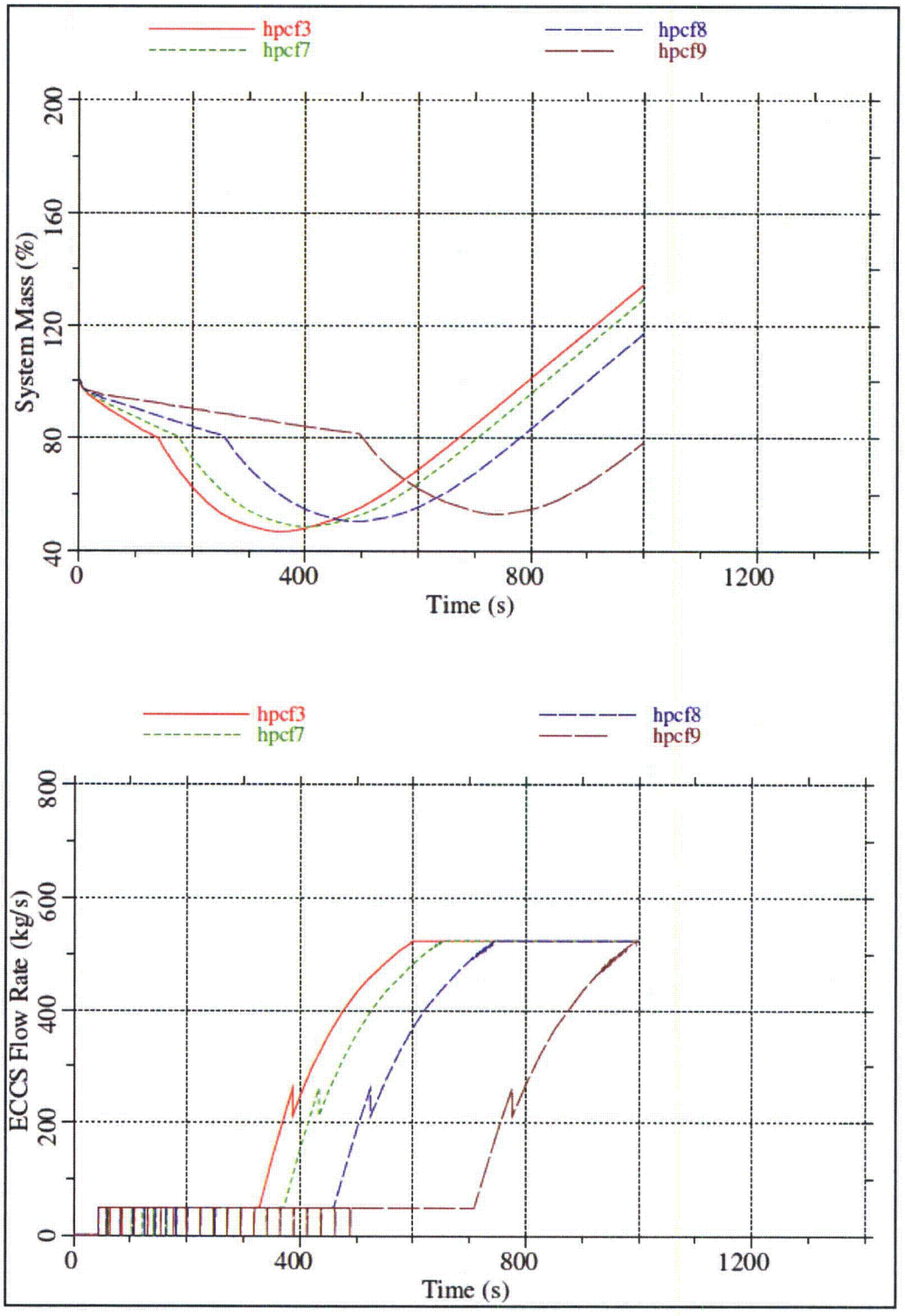

Figure 4-10 Break Size Sensitivity – System Mass and ECCS Flow Rate

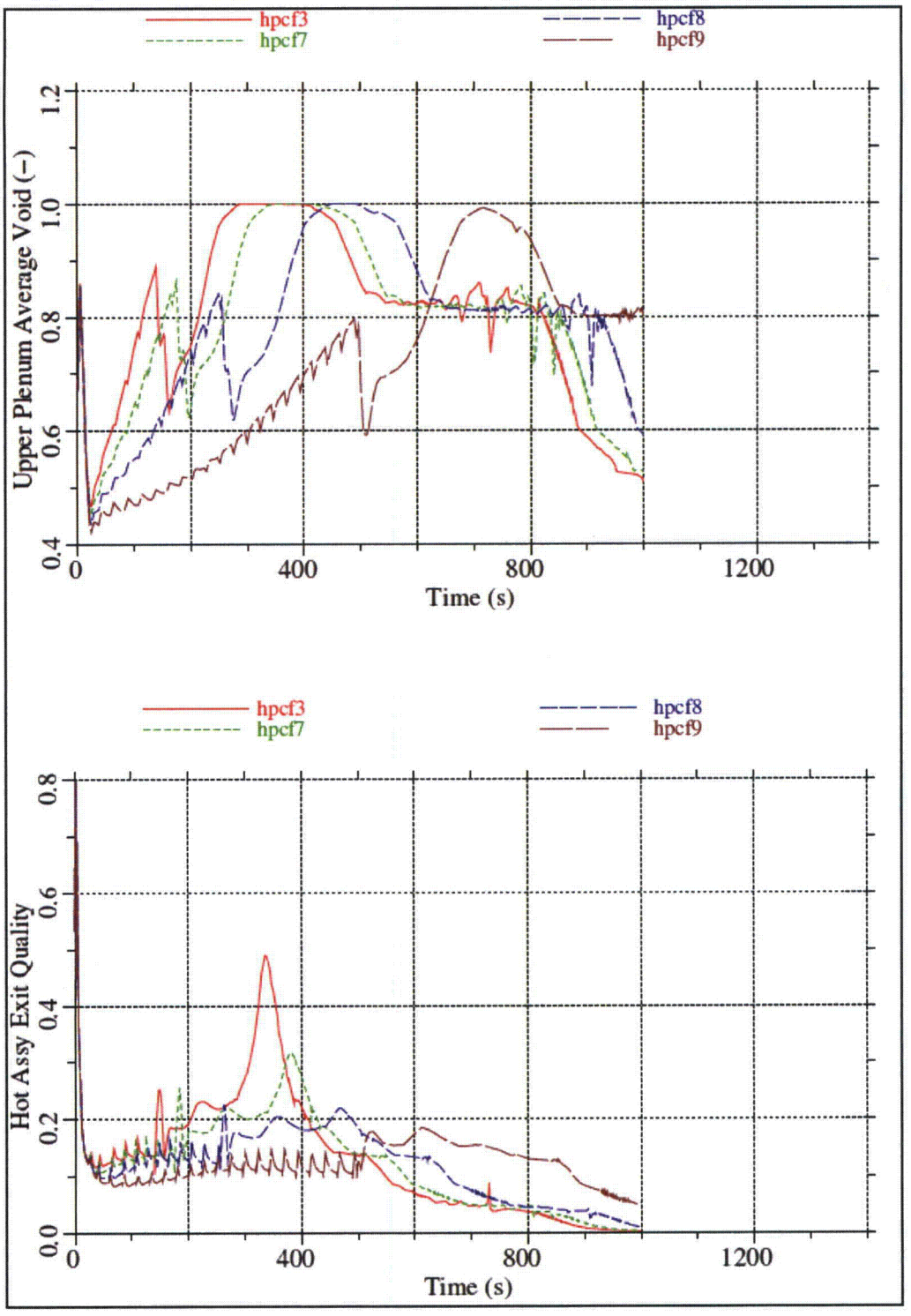

Figure 4-11 Break Size Sensitivity – Upper Plenum Void and Hot Assembly Exit Quality

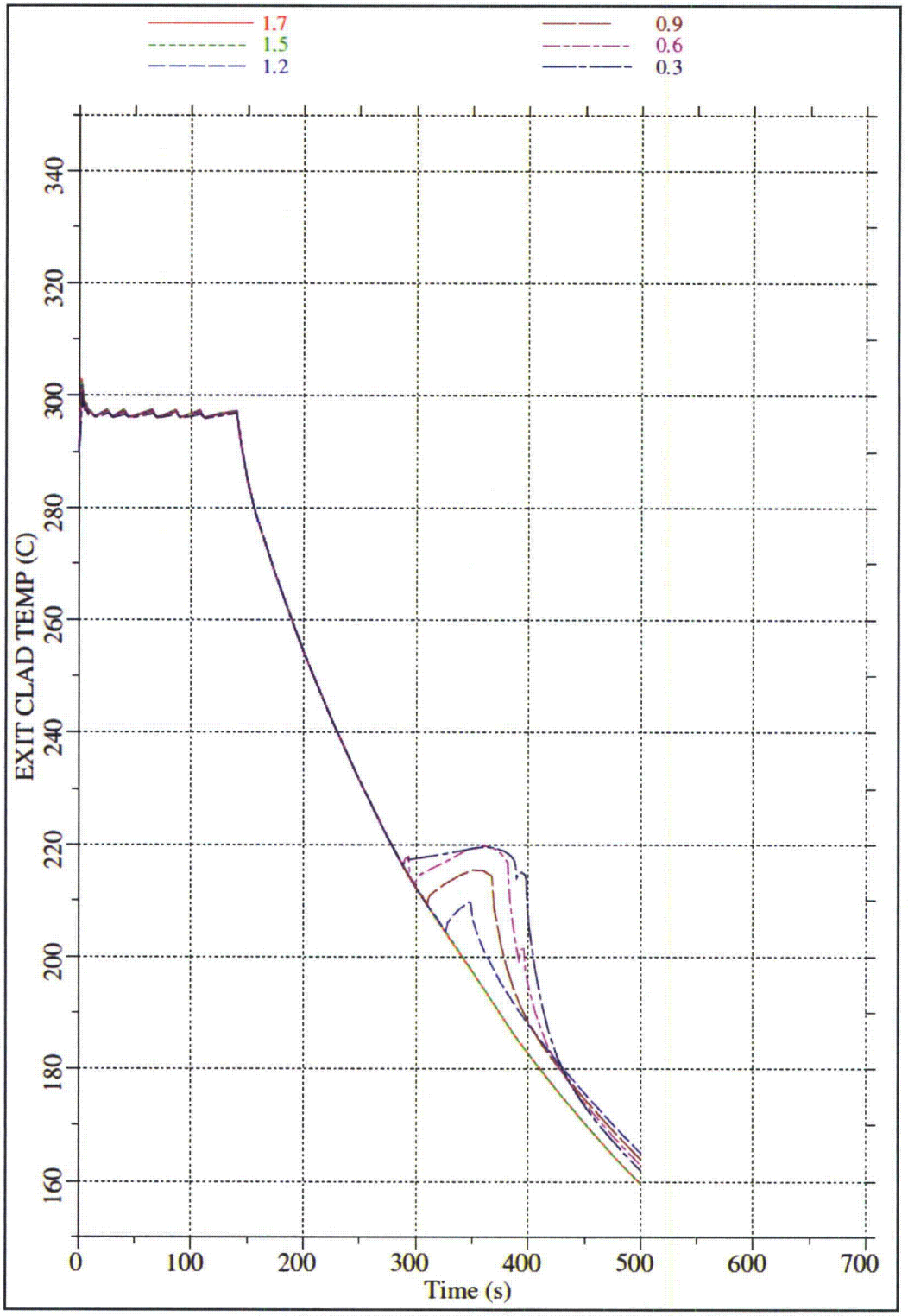

Figure 4-12 Assembly Power Sensitivity – Exit Cladding Temperature vs. Channel Peaking Factor

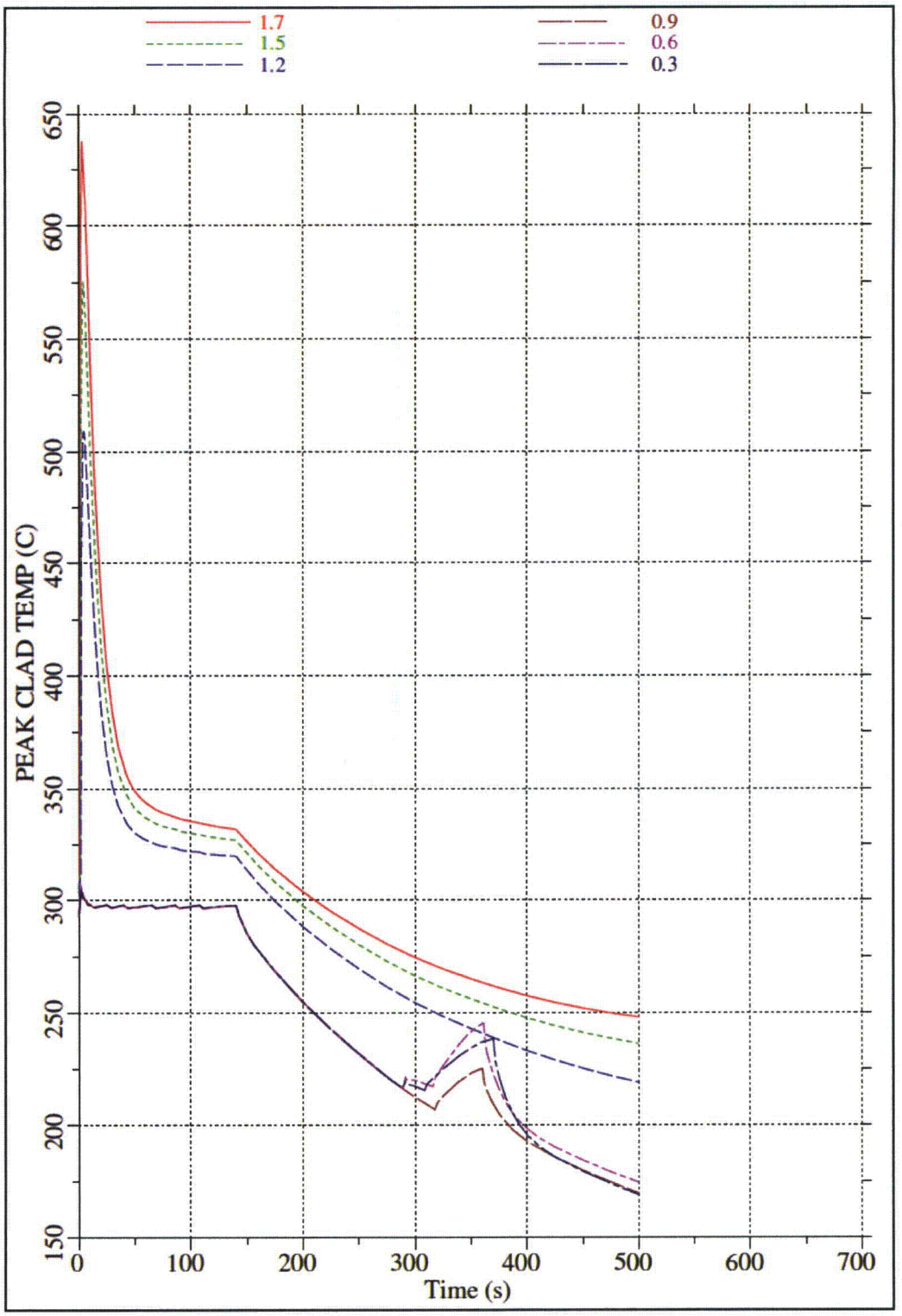

Figure 4-13 Assembly Power Sensitivity – GOBLIN PCT vs. Channel Peaking Factor

4.5.2 Main Steam Line Break (MSLB)

There are four main steam lines that attach to the reactor pressure vessel (RPV) at an elevation just above the bottom of the steam dryer. Each steam line nozzle has an integral flow restrictor, which limits the steam flow in the event of a steam line rupture. Each steam line can be isolated from the turbine by closure of the two MSIVs in each line. One MSIV is located inside the drywell; the other MSIV is located outside the drywell. In addition to the MSIVs, there are TCVs and TSVs between the steam header and the turbine. These valves can also isolate the steam lines from the turbine following a loss of electrical load. A main steam line break inside containment is a result of a break in one of the steam lines between the RPV and the first MSIV.

For a large steam line break coincident with loss of offsite power, the steam lines would be isolated from the turbine by fast-closure of the TCVs. Steam from the RPV would flow through the broken steam line directly to the break and from the intact steam lines through the steam header and back into the drywell via the broken steam line. The flow from the intact steam lines would continue until the MSIVs in the broken steam line close. As shown in Figure 4-14, once the MSIVs are closed, the break flow is only from the RPV through the broken line.

The MSIV closure is actuated by either the LWL-1.5 signal or the high steam flow signal. For large steam line breaks, the high steam flow signal would occur almost instantly. For small steam line breaks, the MSIVs would isolate on a LWL-1.5 signal.

The limiting single active failure that results in the least injection capability is the failure of the EDG that powers a HPCF pump and a LPFL pump with the steam line break located in the line that feeds the RCIC turbine. This results in the following available equipment:

1 HPCF + 2 LPFL + 8 ADS

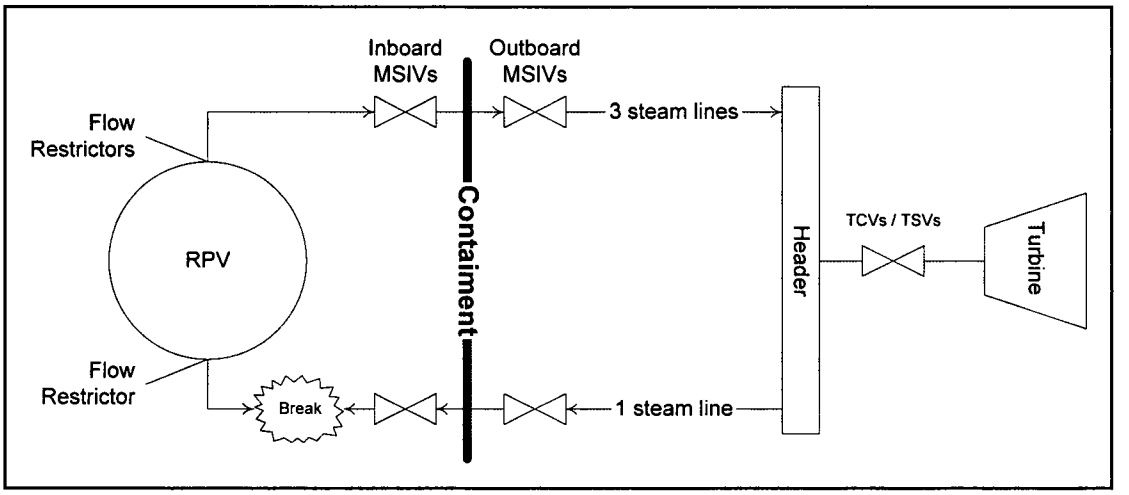

Figure 4-14 Schematic of Steam Line Break inside Containment

4.5.2.1 Main Steam Line Break Results

Four cases were run with the power in the hot assembly set to simulate a nodal power where the hot rod would be at the TMOL. As shown in Table 4-3, the variation in PCT and minimum mass were small.

Table 4-3 Steam Line Break Results

Case	Core Flow	Break Location	Break Size[1]	Steam Line Isolation	PCT (GOBLIN)	Minimum Mass
mslb6	90%	RCIC side	200%	TCV fast closure	657°C	164.1 E3 kg
mslb6a	111%	RCIC side	200%	TCV fast closure	648°C	162.6 E3 kg
mslb7	90%	RCIC side	150%	TCV fast closure	654°C	164.1 E3 kg
mslb8	90%	RCIC side	100%	TCV fast closure	656°C	164.1 E3 kg

Note:
1. Steam line breaks are simulated as double-ended breaks. However, MSIVs isolate steam line side of the break.

4.5.2.2 Sensitivity Studies

Core Flow Rate

Cases mslb6 and mslb6a compare the impact of initial core flow rate on steam line break results. As shown in Table 4-3, the case with the lowest initial core flow rate had the highest PCT.

Figure 4-15 compares the dome pressure and break flow rate responses for cases mslb6 and mslb6a. As shown, the first case depressurizes more rapidly in the first 20 seconds. This is a result of differing break flow during this period of time. In the base case the break flow quality is one until ~ 18 seconds. In the second, higher core flow, case the break flow quality transitions to a two-phase mixture at ~ 4 s. This causes the different depressurization rates mentioned above. As a result of the additional mass in the core, the break flow transitions from steam to a two-phase mixture sooner in the second case.

Figure 4-16 compares the system mass and ECCS flow rate for the two cases. As shown, the ECCS actuation for the second case, mslb6a, is slightly sooner. In this case, the higher break flow compensated for the higher initial system mass resulting in an earlier actuation of the ECCS pumps. However, the minimum inventories were nearly identical.

Figure 4-17 compares the GOBLIN PCTs. As shown, the base case had the highest PCT. The higher initial core flow rate in the second case provides additional margin to dryout. As a result, dryout occurs later in the second case and the PCT is lower.

Figure 4-18 compares the upper plenum average void fraction and hot assembly exit quality. As shown, a two phase mixture exists in the upper plenum and there is a two-phase mixture exiting the hot assembly throughout the transient.

Break Size

Cases mslb6, mslb7, and mslb8 simulate double-ended breaks of the steam line between the reactor pressure vessel and the first MSIV. The first case, mslb6, represents a full double-ended rupture of the steam line. However, the vessel side of the break is limited in flow area because of the integral flow restrictor, which has a flow area that is approximately 30% of the main steam line flow area. The second case represents a 75% steam line break. In this case, the vessel side of the break continues to be limited by the flow restrictor, but the turbine side of the break is reduced in flow area below that of the combined flow area of the three intact steam line flow restrictors. The third case represents a 50% steam line break. In this case, the vessel side of the break continues to be limited by the flow restrictor, but the steam line side of the break would be further reduced. In all cases, the MSIV closure signal was generated by the high steam flow signal due to the flow out of the break.

As shown in Figure 4-19, the break flow from the steam line side decreases with decreasing break size, but the effect is small due to closure of the MSIVs. As shown in Figure 4-20 and Figure 4-21, the effect of changing break size on system pressure, system mass, and PCT is also minimal.

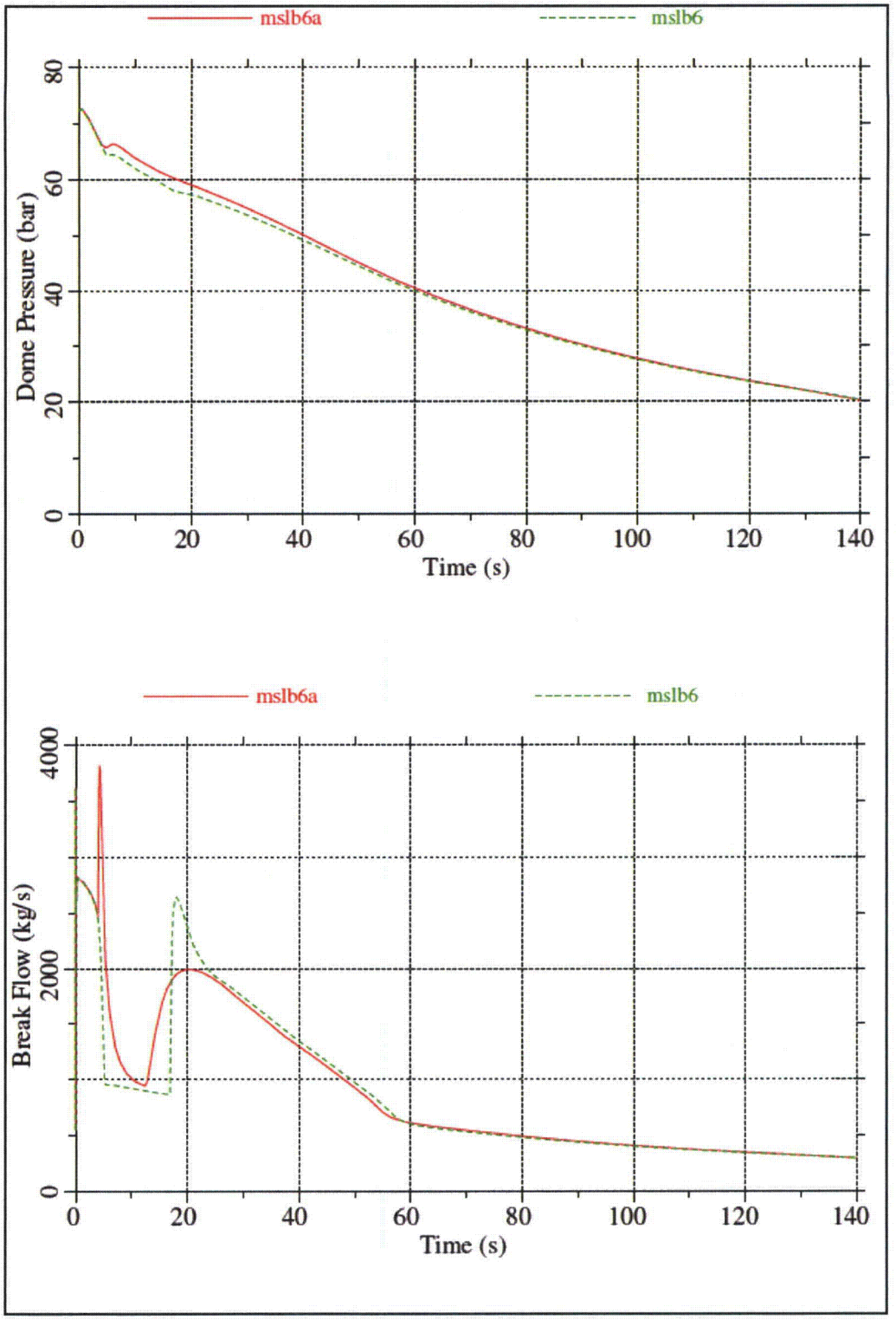

Figure 4-15 Core Flow Rate Sensitivity – Dome Pressure and Break Flow Rate

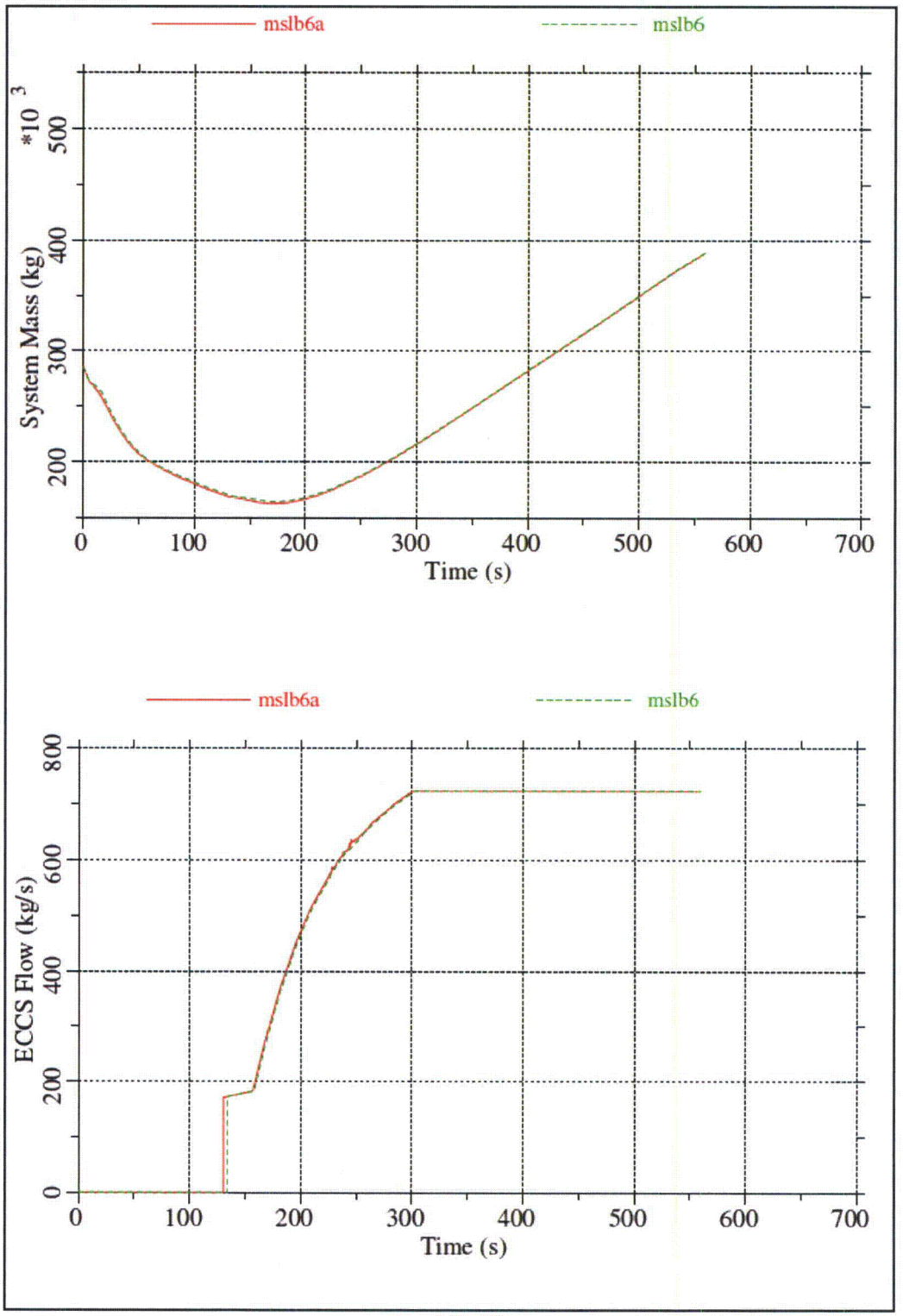

Figure 4-16 Core Flow Rate Sensitivity – System Mass and ECCS Flow Rate

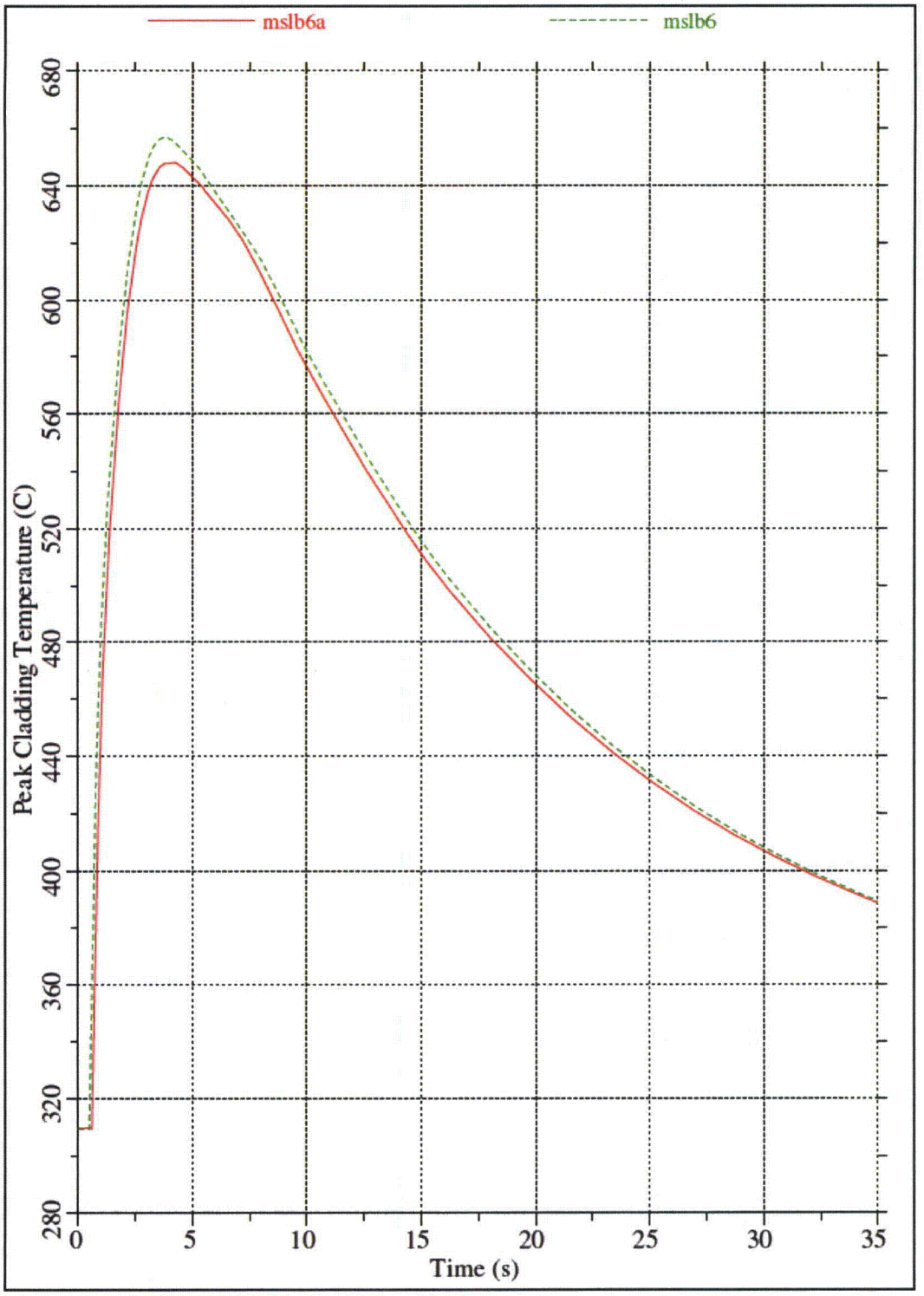

Figure 4-17 Core Flow Rate Sensitivity – GOBLIN PCTs

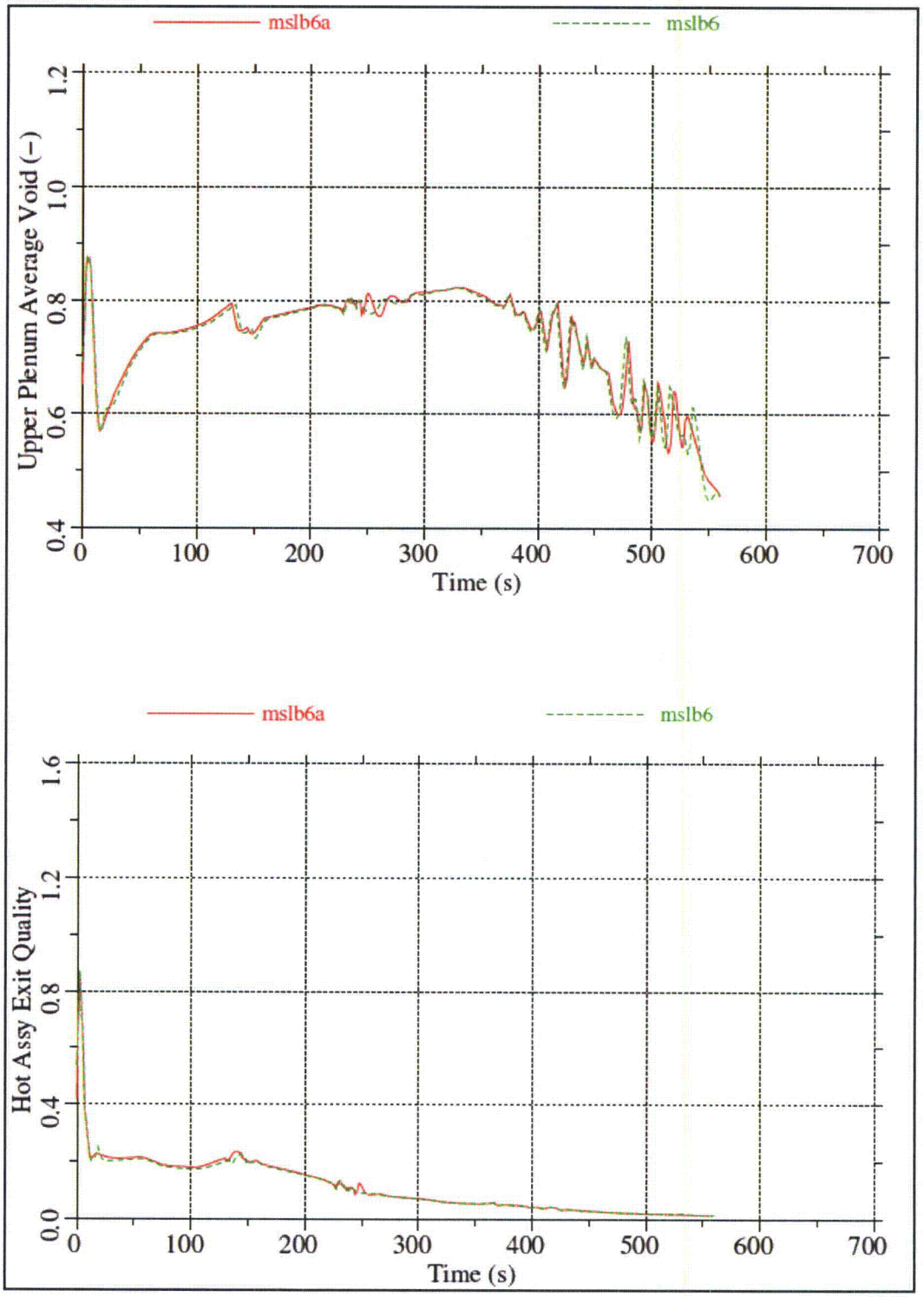

Figure 4-18 Core Flow Rate Sensitivity – Upper Plenum Void and Hot Assembly Exit Quality

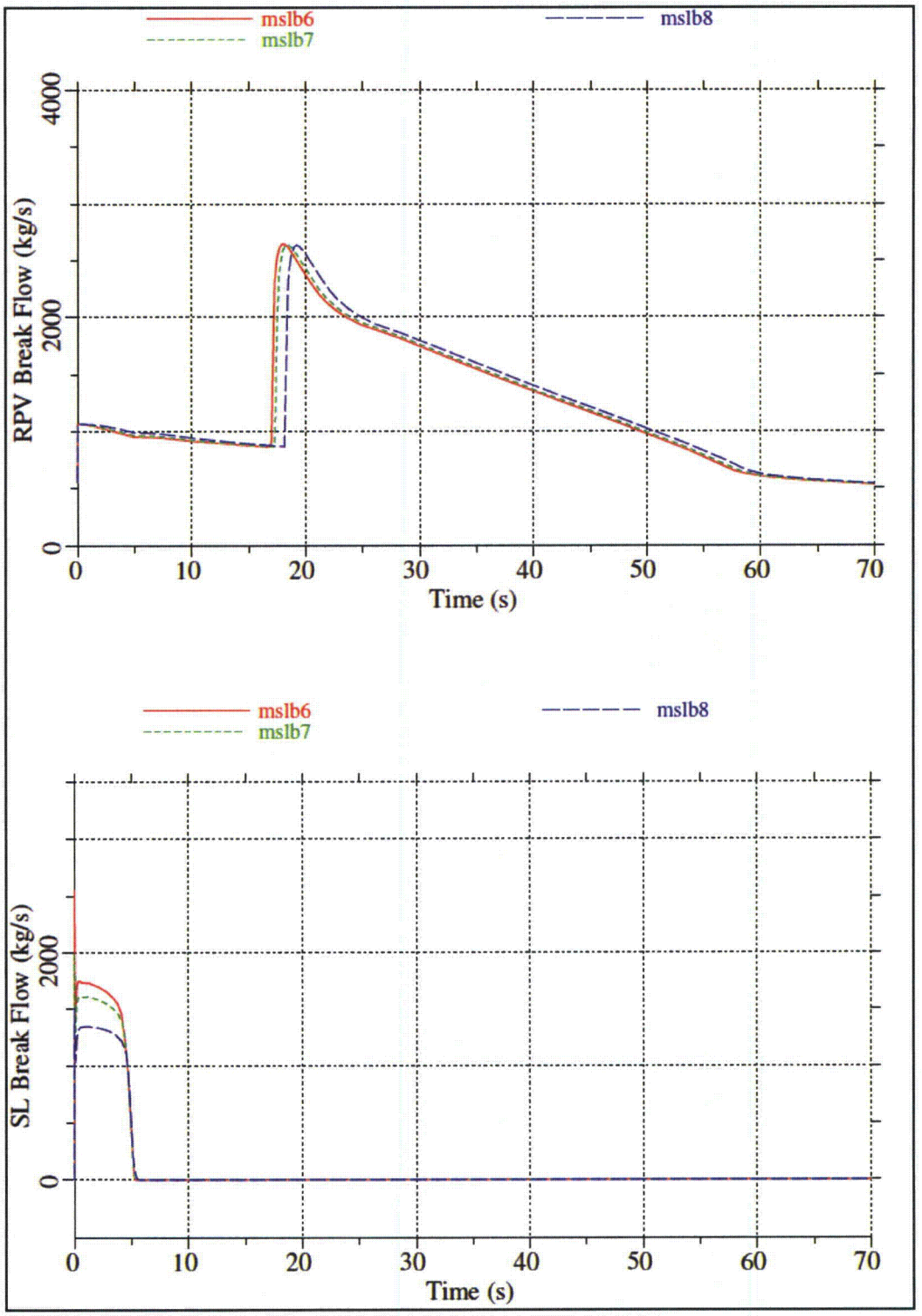

Figure 4-19 Break Size Sensitivity – Break Flow Rates

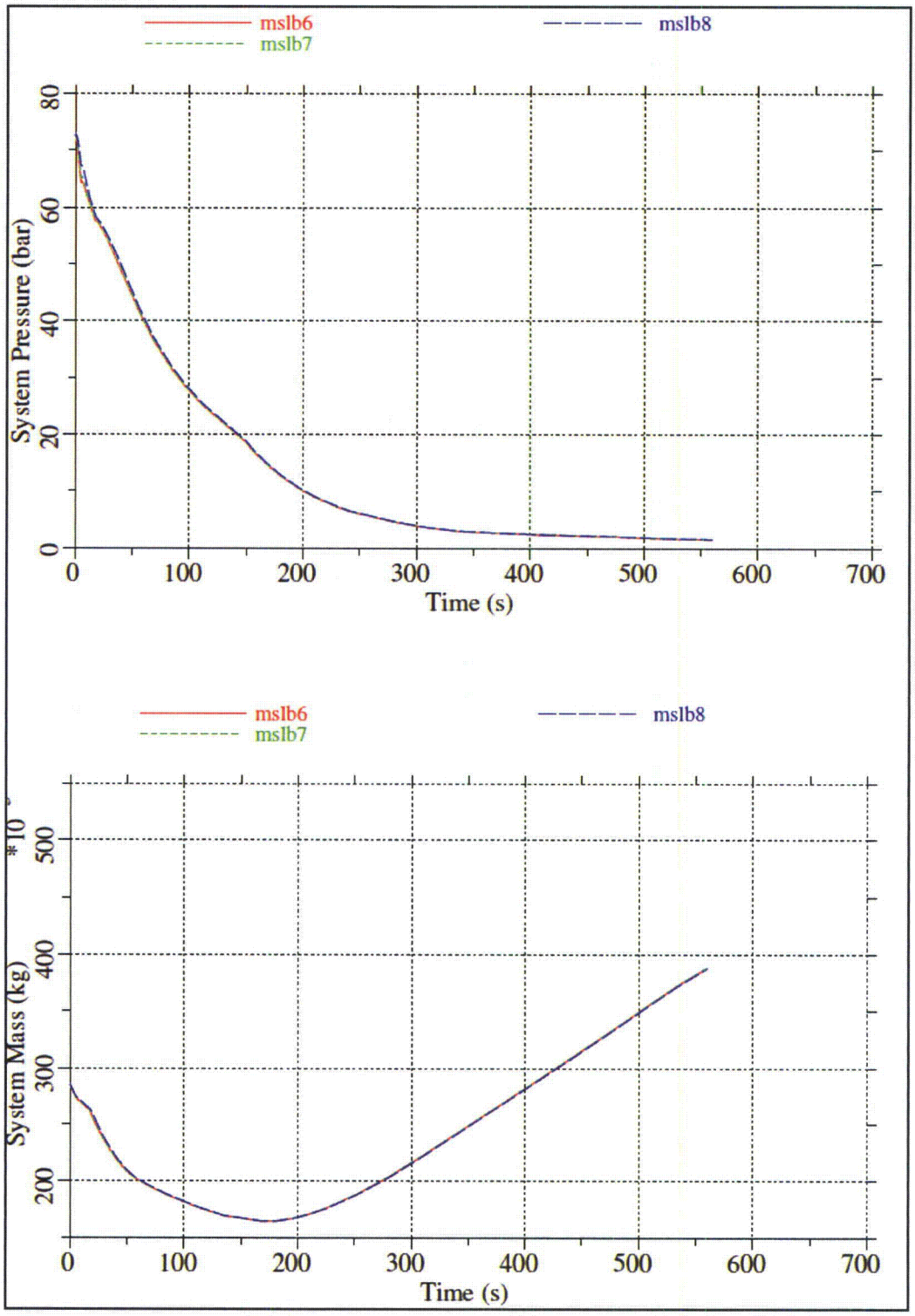

Figure 4-20 Break Size Sensitivity – Dome Pressure and System Mass

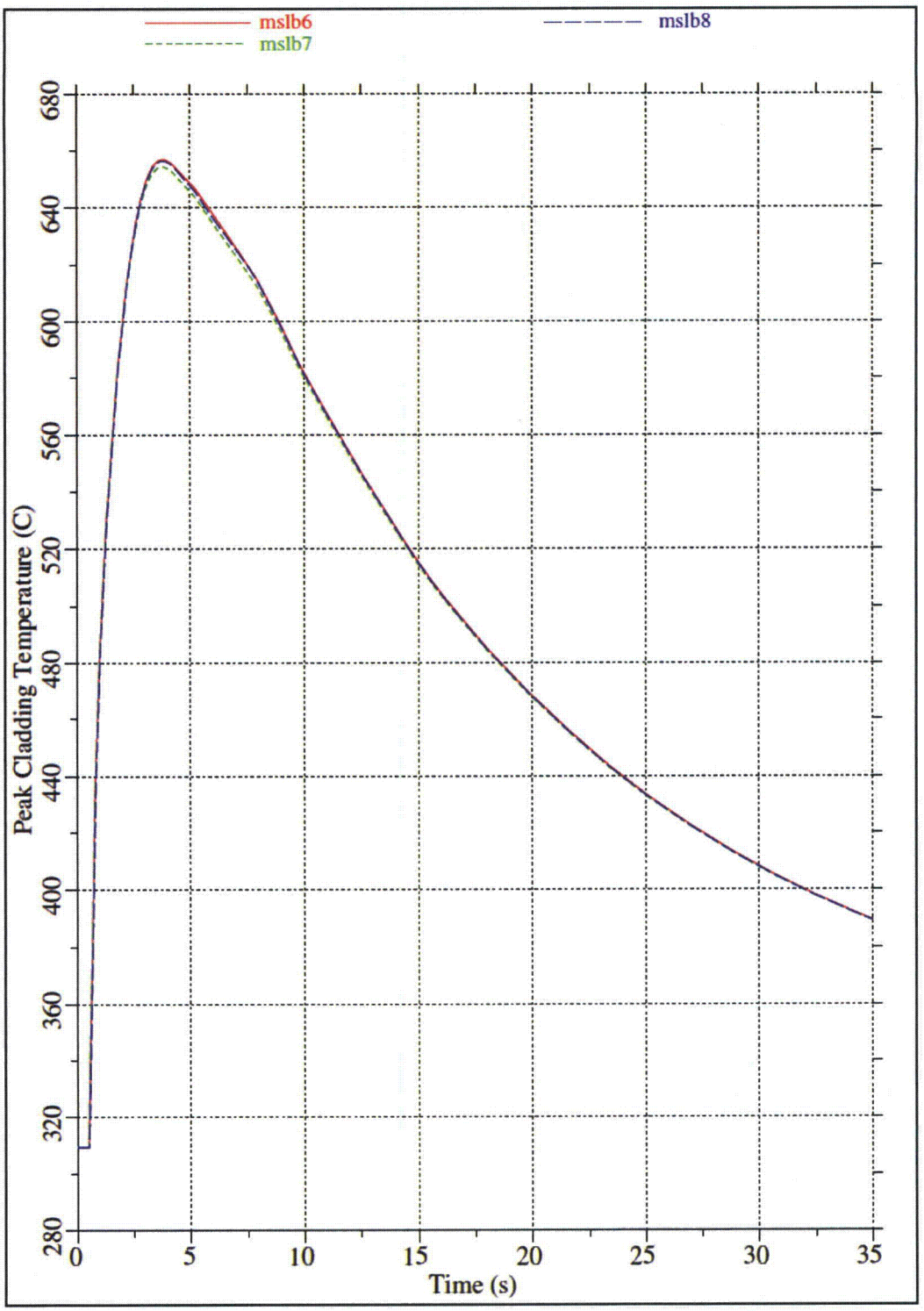

Figure 4-21 Break Size Sensitivity – GOBLIN PCTs

4.5.3 Feedwater Line Break (FWLB)

There are two feedwater lines that enter the drywell. Each feedwater line passes through two check valves, one inside the drywell and one outside the drywell. These two feedwater lines are connected to a common feedwater line outside the drywell. Inside the drywell each feedwater line branches into three lines that penetrate the RPV and connect to a sparger inside the downcomer annulus. The six feedwater spargers distribute feedwater in the annulus at an elevation corresponding to the top of the shroud dome. The three feedwater spargers associated with a single feedwater line penetrating the drywell have [ ]^{a,c} nozzles to distribute the feedwater in the annulus.

The feedwater line break inside the containment is postulated to occur between the RPV and the first check valve, as shown in Figure 4-22. For a complete rupture of the feedwater line inside the drywell, the flow would be restricted by the available flow area through the [ ]^{a,c} nozzles connected to the affected sparger. The check valves on the unaffected feedwater line prevent the loss of coolant through the other line.

Because one train of LPFL injects in one feedwater line and RCIC injects in the other feedwater line, the break will disable one of those systems. Failure of one of the EDGs powering a HPCF pump and a LPFL pump will result in the following equipment available:

RCIC side break: 1 HPCF + 2 LPFL + 8 ADS
LPFL side break: 1 RCIC + 1 HPCF + 1 LPFL + 8 ADS

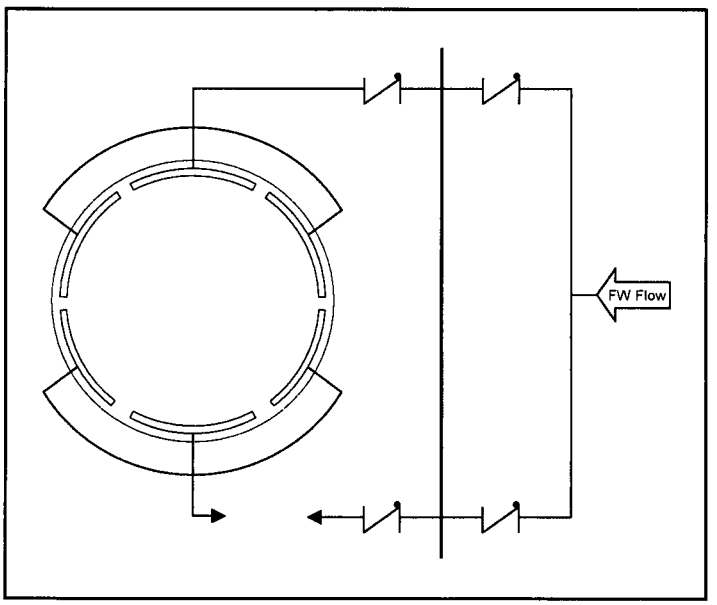

Figure 4-22 Schematic of Feedwater Line Break

4.5.3.1 Feedwater Line Break Results

Seven cases were run with the power in the hot assembly set to simulate a nodal power so that the hot rod would be at the TMOL. Table 4-4 summarizes the results of those cases. As shown, the variations in PCT are small when the steam line is isolated in the same way. Also, the variation in minimum system mass depends mainly on break size.

Table 4-4 Feedwater Line Break Results

Case	Core Flow	Break Location	Break Size	Steam Line Isolation	PCT (GOBLIN)	Minimum Mass
fwlb3	90%	RCIC side	100%	TCV fast closure	708°C	126.5 E3 kg
fwlb4	111%	RCIC side	100%	TCV fast closure	684°C	123.5 E3 kg
fwlb5	90%	RCIC side	100%	Pressure Regulator	661°C	126.0 E3 kg
fwlb6	90%	RHR side	100%	TCV fast closure	708°C	125.9 E3 kg
fwlb7	90%	RCIC side	75%	TCV fast closure	705°C	136.9 E3 kg
fwlb8	90%	RCIC side	50%	TCV fast closure	707°C	148.4 E3 kg
fwlb9	90%	RCIC side	25%	TCV fast closure	710°C	215.6 E3 kg

4.5.3.2 Sensitivity Studies

Core Flow Rate

Cases fwlb3 and fwlb4 compare the impact of core flow rate on the system and hot assembly responses. As shown in Table 4-4 and Figure 4-23, the GOBLIN PCT was lower for the high core flow rate case. Similar to cases described previously, this was caused by a delay in the time of boiling transition due to the higher core flow rate and increased margin to dryout. Table 4-4 also shows that the minimum system inventory was slightly lower in the case with the higher initial core flow rate.

As shown in Figure 4-24, the lower minimum system inventory was caused by a delay in HPCF injection due to the different level response resulting in later HPCF actuation.

Figure 4-25 shows that there is significant liquid in the upper plenum and that the core is cooled by a two-phase mixture throughout the transient in both cases.

Steam Line Isolation

Cases fwlb3 and fwlb5 compare the impact of steam line is isolation on the system and hot assembly responses. As shown in Figure 4-26, the dome pressure increases initially when the steam line is isolated by TCV fast closure. Node 17 exhibited the highest PCT in both cases and, as shown, case fwlb3 has a larger PCT than case fwlb5. The difference is due to the initial reactor power transient prior to reactor scram (i.e., the increasing pressure in case fwlb3 results in a slower increase in average void).

As shown in Figure 4-27, the initial break flow is higher when the pressure regulator is used to isolate the steam line. This is due to the additional inventory lost from the steam line until the break is finally isolated. As a result, the minimum inventory for case fwlb5 is slightly less than for case fwlb3.

Break Location

Comparing cases fwlb3 and fwlb6 shows the effect of break location. In the first case the break is located in the feedwater line where the RCIC injects. The limiting single failure of one EDG disables one HPCF pump and one LPFL pump. In the other case, the break is located in the feedwater line where one of the LPFL pumps injects. The limiting single failure of one EDG disables one HPCF and one LPFL pump. The available ECCS systems for these cases are as follows:

fwlb3 – 1 HPCF + 2 LPFL + 8 ADS
fwlb6 – 1 RCIC + 1 HPCF + 1 LPFL + 8 ADS

As shown in Table 4-4, there is no difference in the predicted PCT, because the time of PCT occurs well before ECCS injection. There is a small effect on minimum system inventory caused by the different ECCS pumps that are available. As shown in Figure 4-28, initially there is more injection in the second case, but the injection of 2 LPFL pumps in the first case results in a faster recovery and a slightly higher minimum inventory.

Break Size

Cases fwlb3, fwlb7, fwlb8, and fwlb9 show the sensitivity to break size for feedwater line breaks. As shown in Figure 4-29, the initial system pressure responses were nearly identical because they were affected primarily by the steam line isolation. However, the long term pressure responses were quite different due to the differing break sizes. As shown in Figure 4-30, the PCTs for all cases were nearly the same.

As shown in Figure 4-31, the largest break had the greatest loss of inventory before recovery. The figure also shows that the system did not lose enough inventory for the smallest break (fwlb9) to actuate ADS and one HPCF pump provided enough injection to recover the lost inventory.

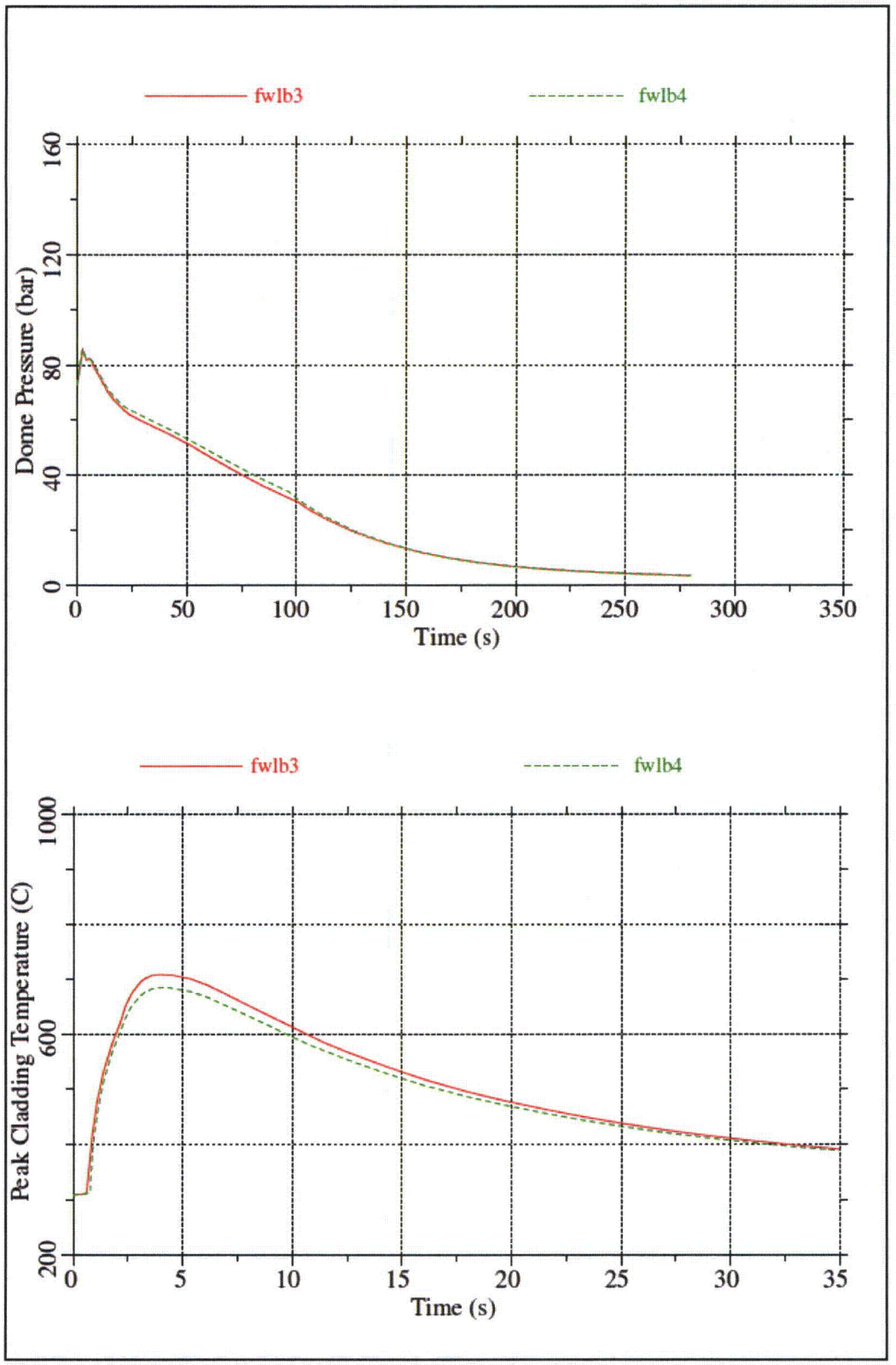

Figure 4-23 Core Flow Rate Sensitivity – Dome Pressure and GOBLIN PCTs

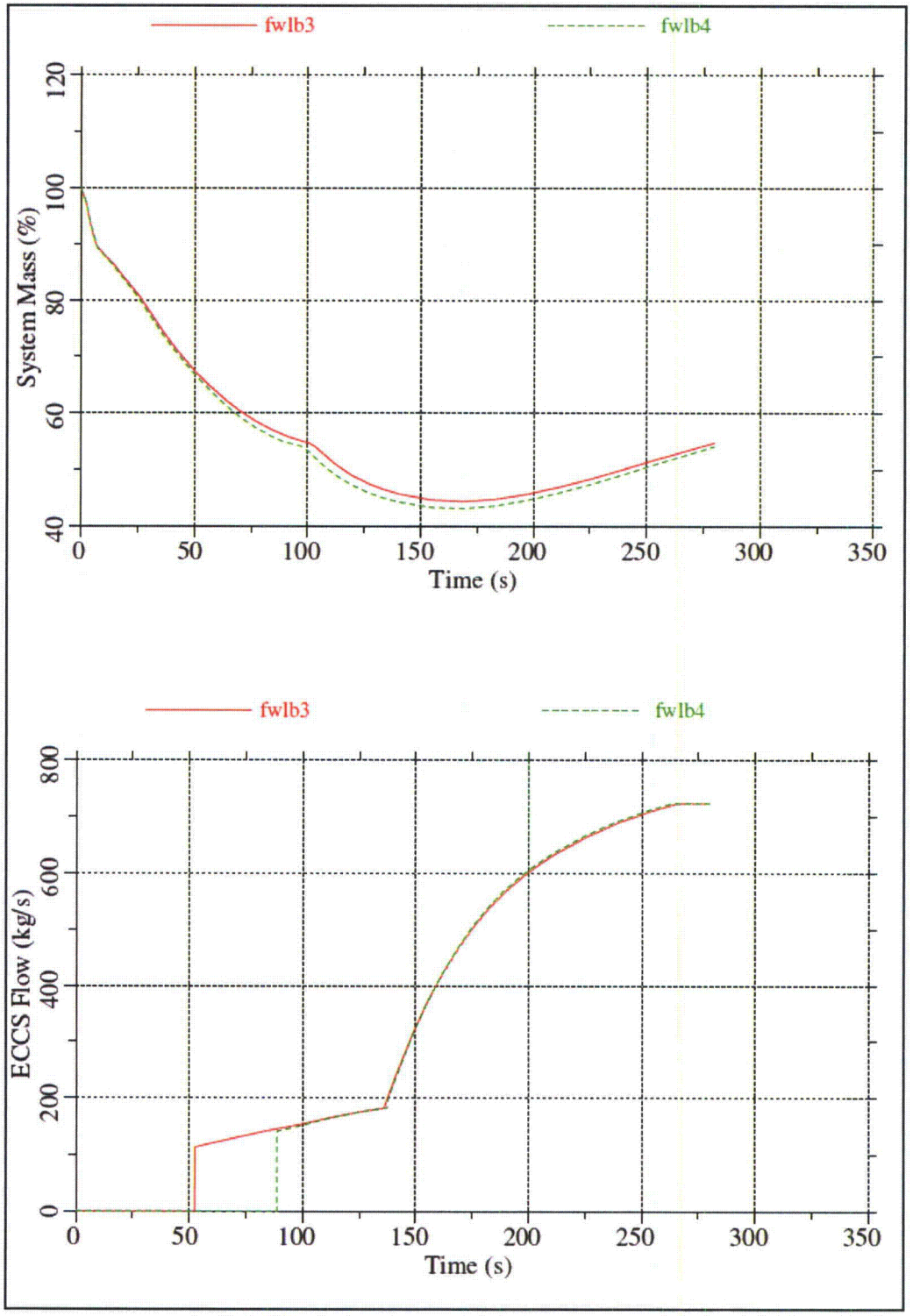

Figure 4-24 Core Flow Rate Sensitivity – System Mass and ECCS Flow Rates

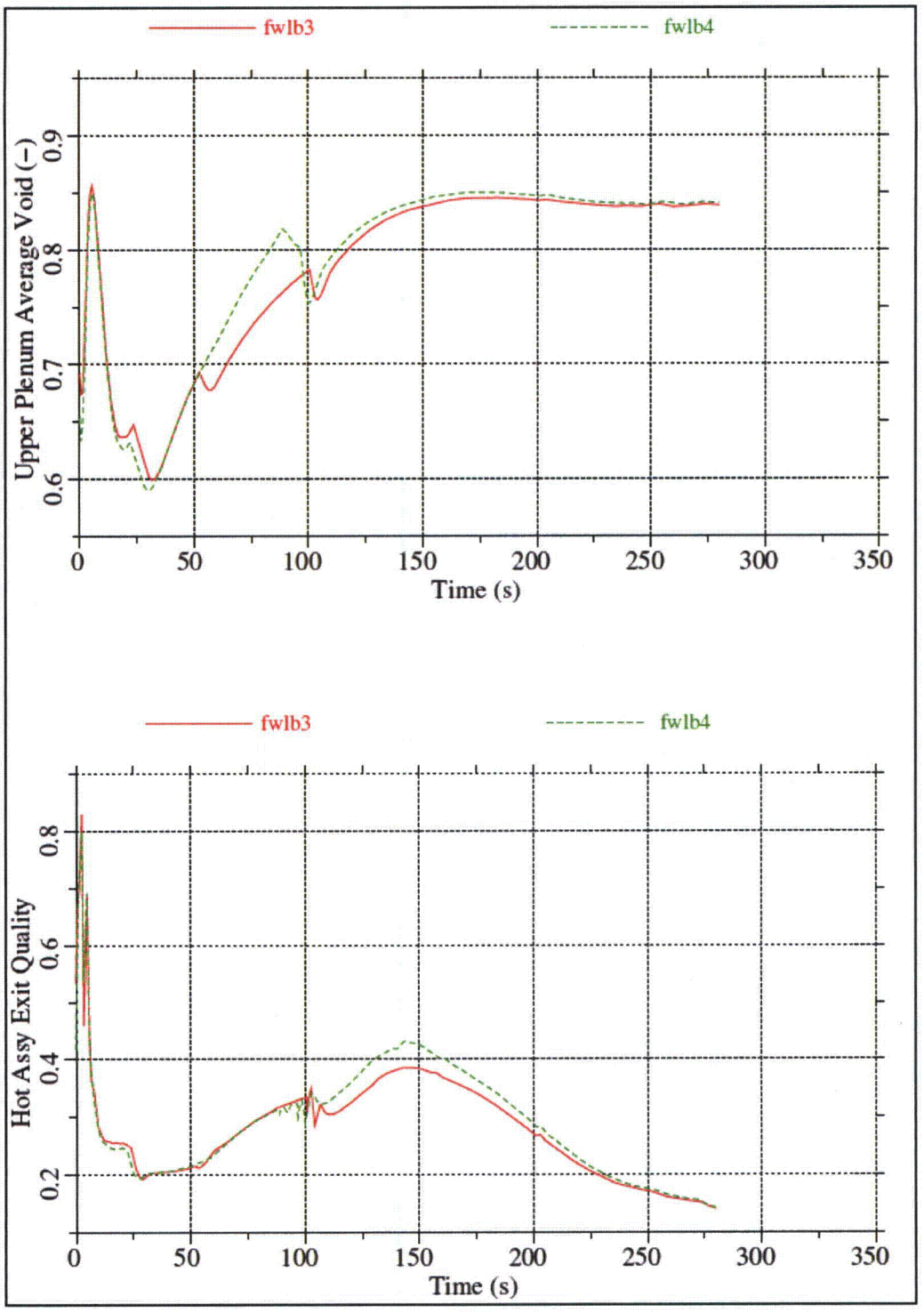

Figure 4-25 Core Flow Rate Sensitivity – Upper Plenum Void and Hot Assembly Exit Quality

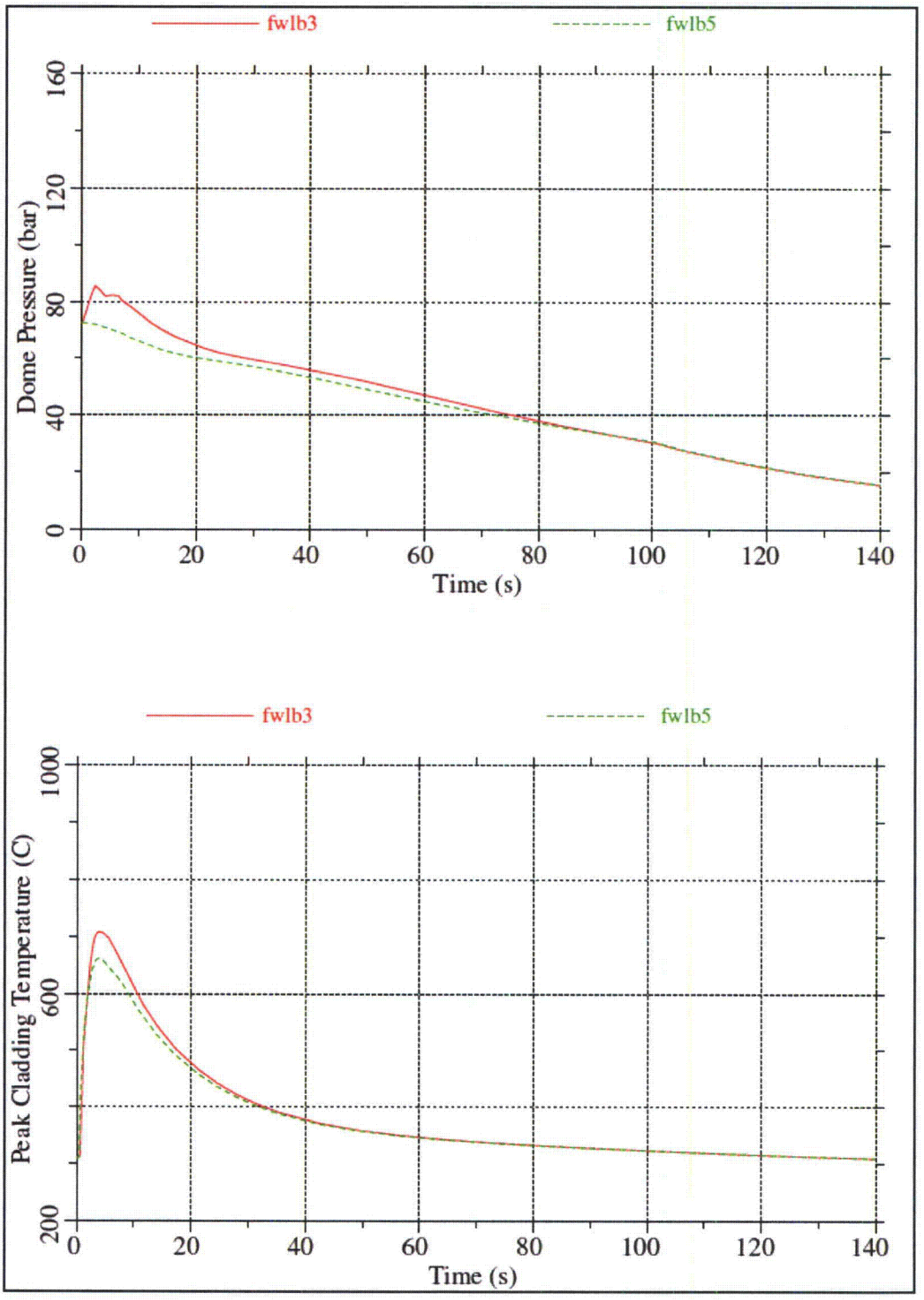

Figure 4-26 Steam Line Isolation Sensitivity – Dome Pressure and GOBLIN PCTs

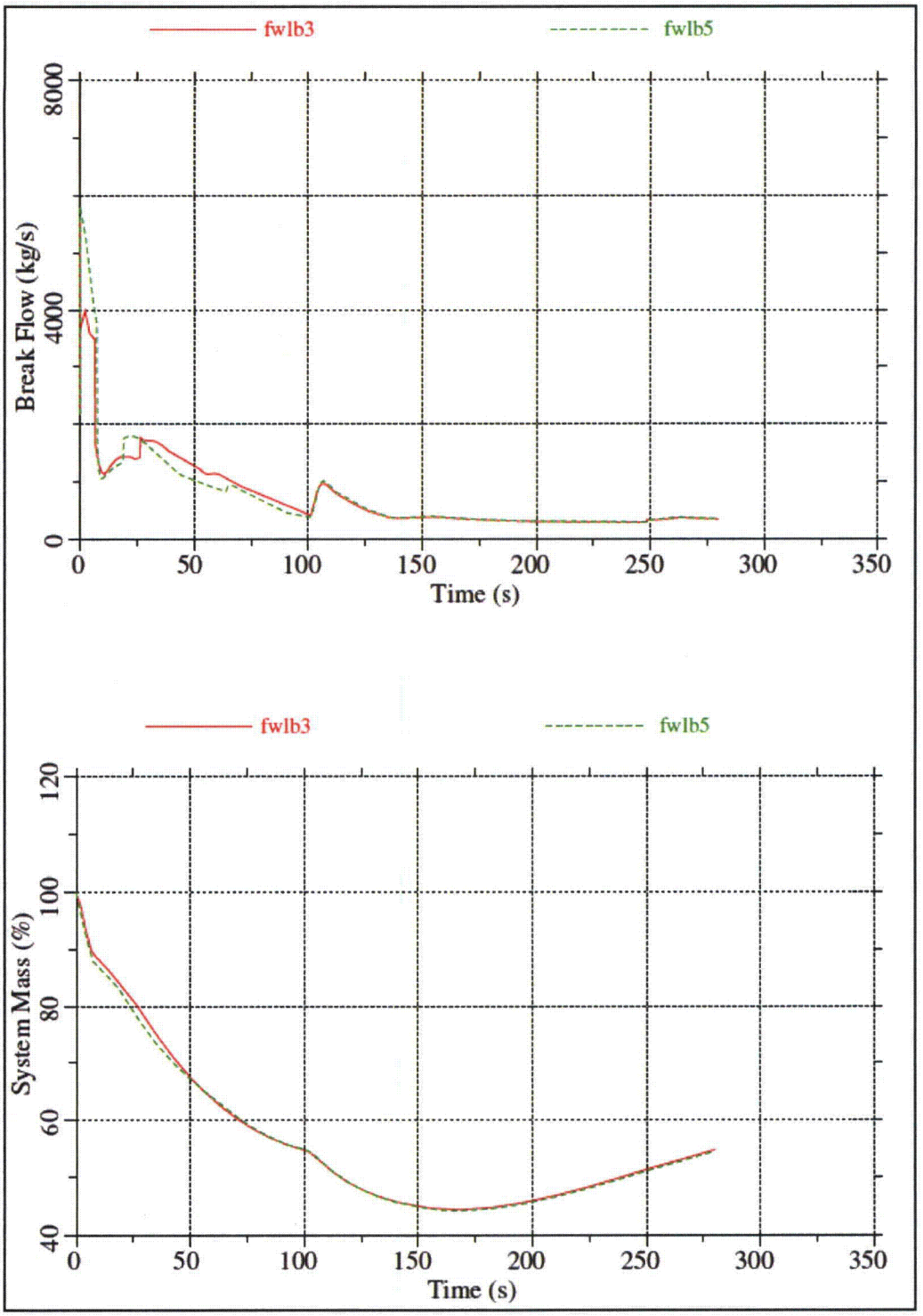

Figure 4-27 Steam Line Isolation Sensitivity – Break Flow Rate and System Mass

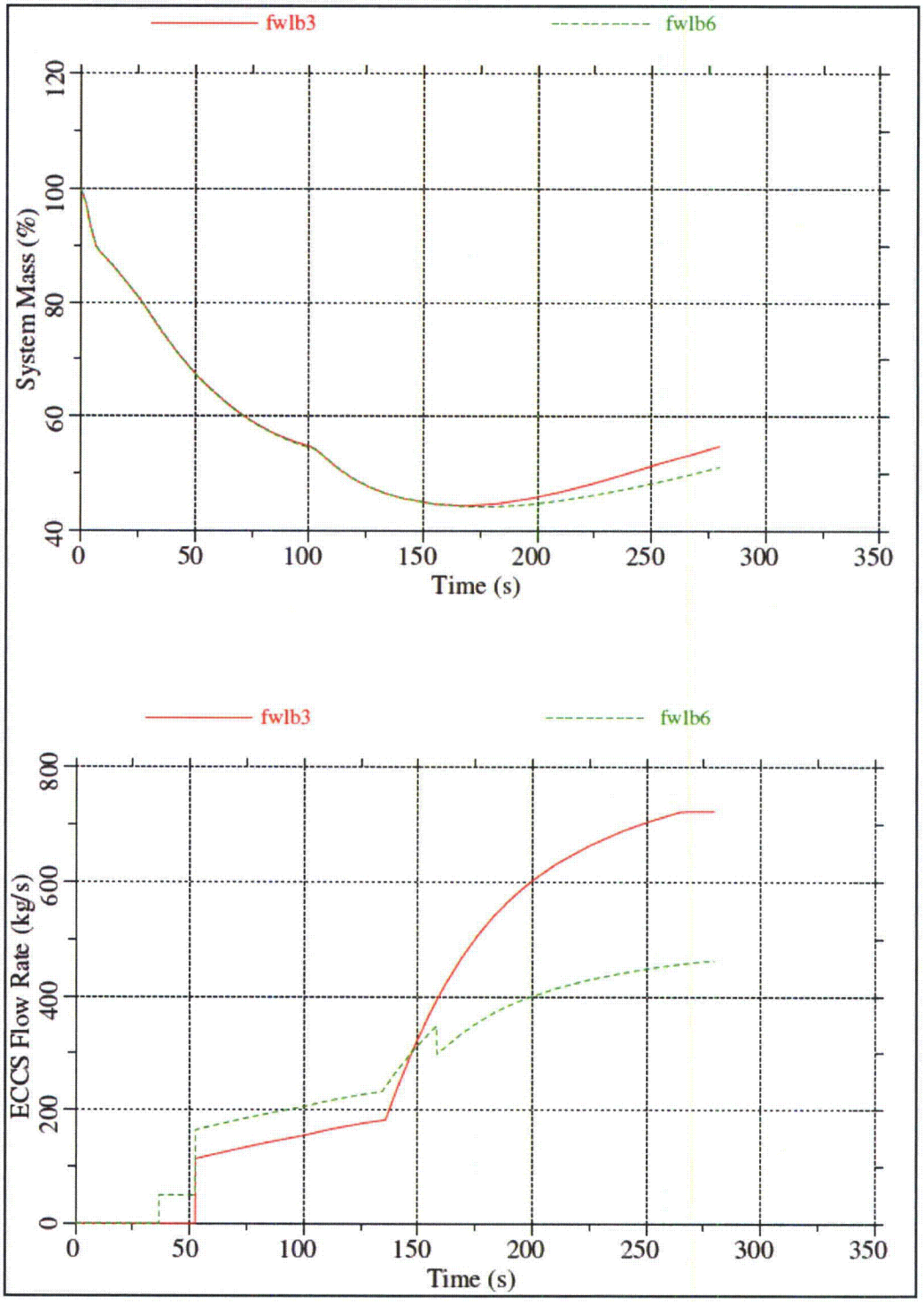

Figure 4-28 Break Location Sensitivity – System Mass and ECCS Flow Rates

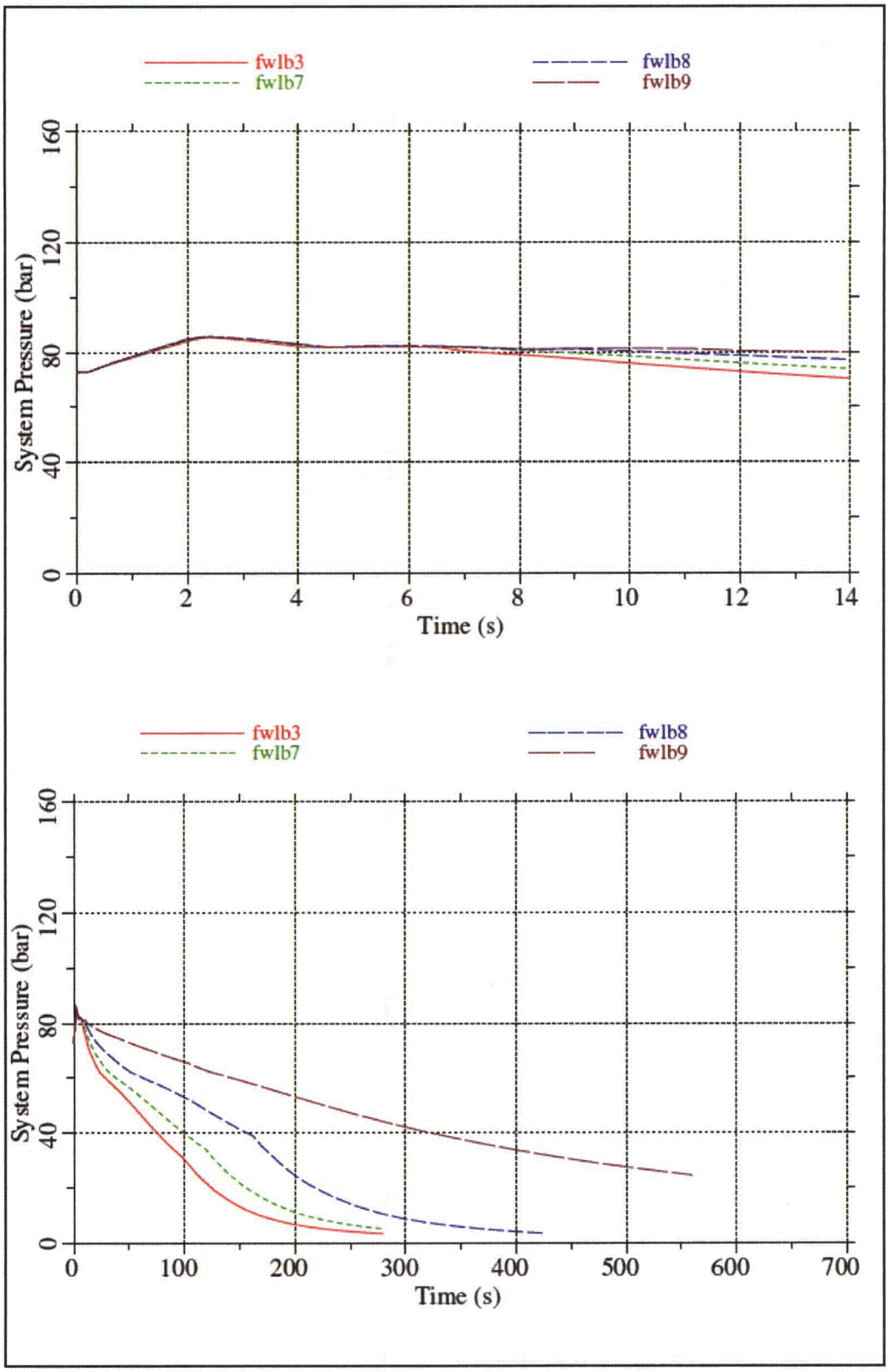

Figure 4-29 Break Size Sensitivity – Dome Pressure (Short-term and Long-term)

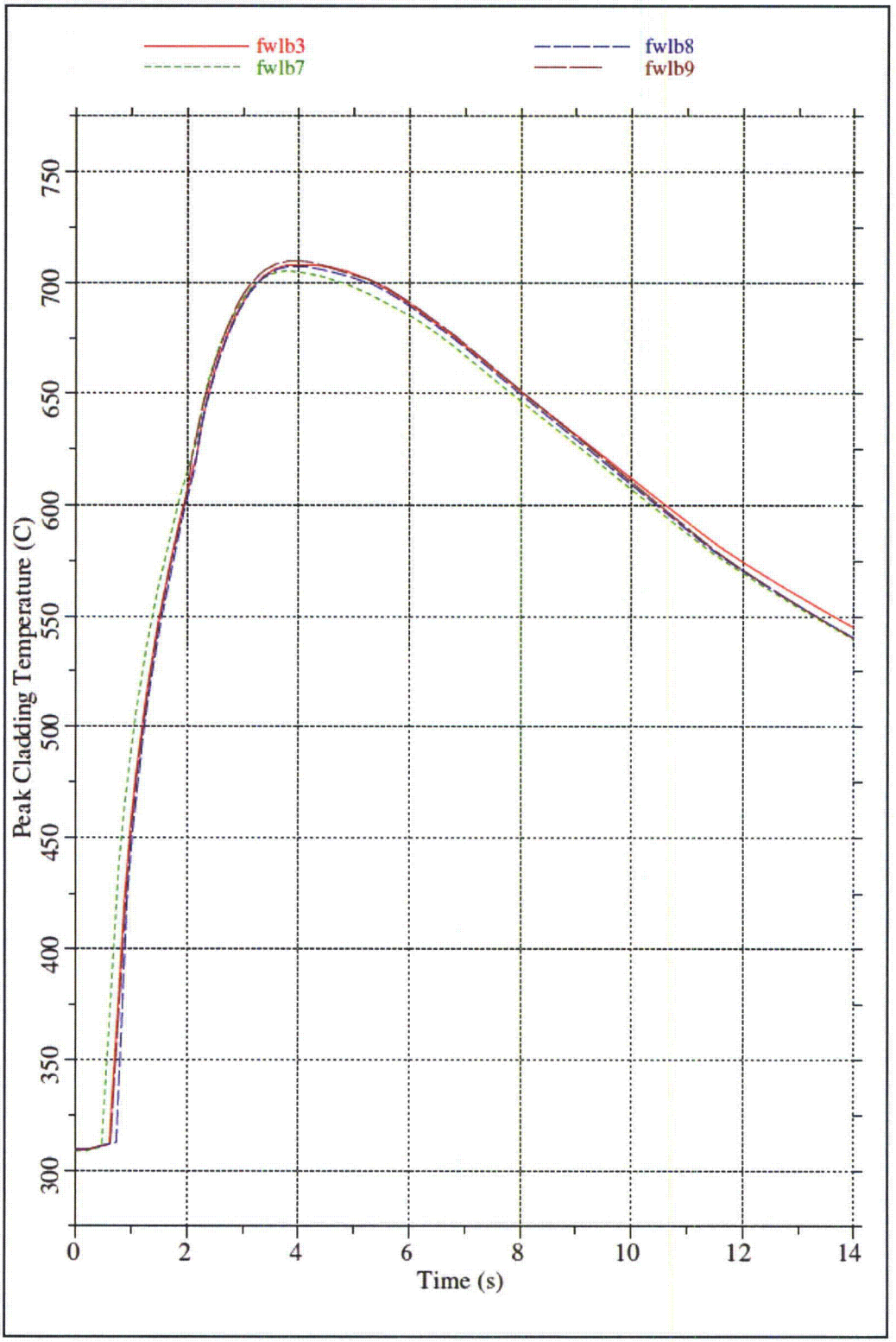

Figure 4-30 Break Size Sensitivity – GOBLIN PCTs

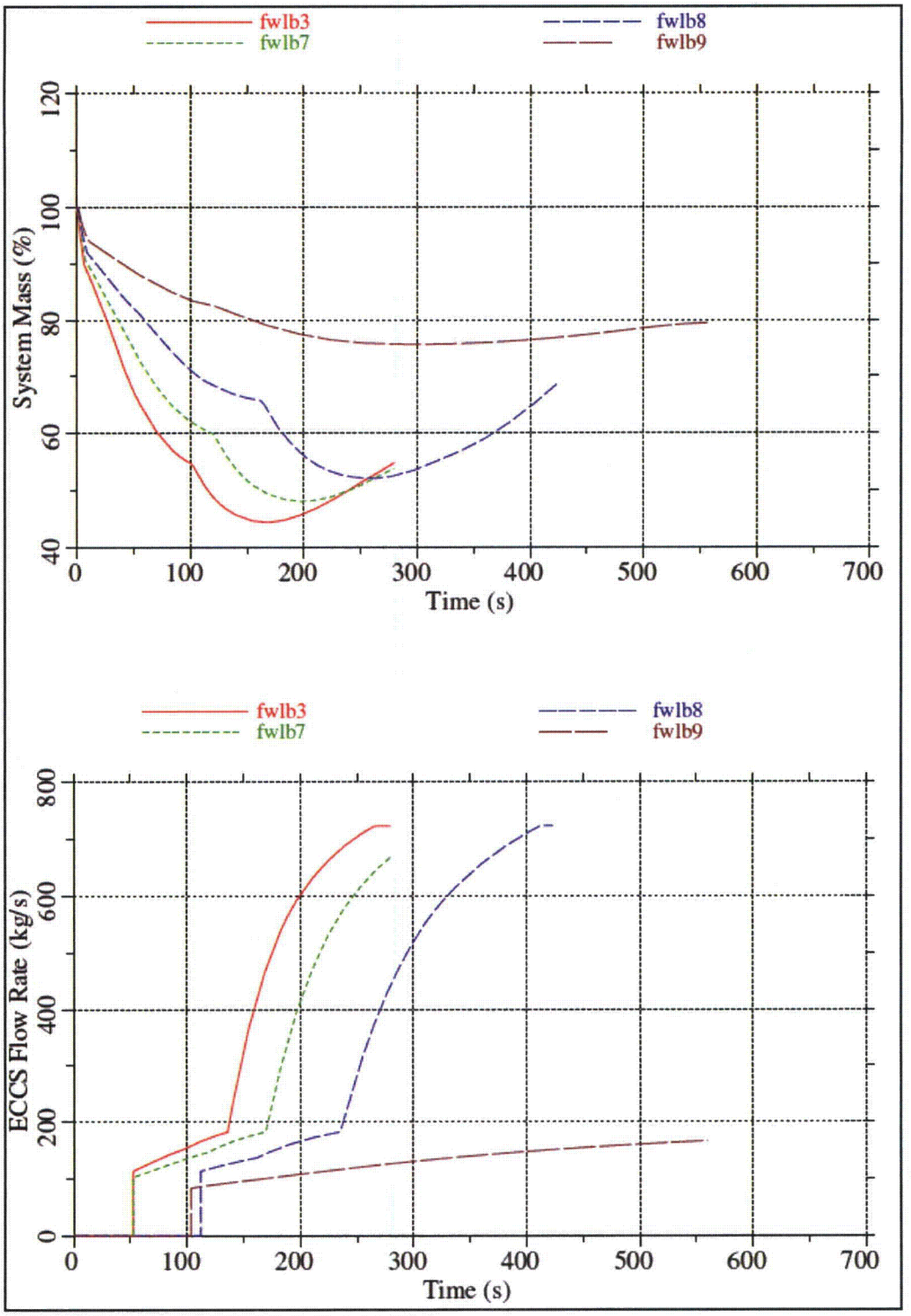

Figure 4-31 Break Size Sensitivity – System Mass and ECCS Flow Rates

4.5.4 RHR Suction Line Break

The RHR suction line nozzle is located between the elevation of the feedwater nozzle and the HPCF line nozzle. As shown in Figure 4-32, the RHR suction line also connects to the bottom head drain line. As a result, a break in the RHR suction line will result in a loss of coolant from the upper annulus and from the lower plenum of the RPV through the bottom drain line. Because of the piping configuration, the break flow from the upper annulus is limited by the flow area of the RHR suction nozzle, and the break flow from the lower head is limited by the flow area of the bottom drain nozzle. In this case the limiting single failure is that one of the EDGs that provides power to a HPCF pump does not start. This results in the following available ECCS equipment:

1 RCIC + 1 HPCF + 2 LPFL + 8 ADS

4.5.4.1 RHR Suction Line Break Results

Five cases were run with the power in the hot assembly set to simulate a nodal power so that the hot rod would be at the TMOL. Table 4-5 summarizes the results of those cases. As shown, the variation in PCT is small when the steam line is isolated in the same manner. The table also shows that the variation in minimum mass is primarily a function of break size.

Table 4-5 RHR Suction Line Break Results

Case	Core Flow	Break Location	Break Size	Steam Line Isolation	PCT (GOBLIN)	Minimum Mass
rhrlb3dlb	90%	RHR SL	100%	TCV fast closure	708°C	125.9 E3 kg
rhrlb4dlb	111%	RHR SL	100%	TCV fast closure	691°C	124.6 E3 kg
rhrlb5dlb	90%	RHR SL	100%	Pressure regulator	662°C	125.5E3 kg
rhrlb7dlb	90%	RHR SL	75%	TCV fast closure	709°C	135.7 E3 kg
rhrlb8dlb	90%	RHR SL	50%	TCV fast closure	710°C	147.6- E3 kg

a,c

Figure 4-32 Schematic of RHR Suction Line Break

4.5.4.2 Sensitivity Studies

Core Flow Rate

Cases rhrlb3dlb and rhrlb4dlb show the impact of initial core flow rate. As shown in Table 4-5, the minimum system masses are about the same, but the first case, rhrlb3dlb, had the highest PCT. Similar to previous sensitivity studies, the case with the higher initial core flow rate has more margin to dryout, and therefore goes through boiling transition later and have a lower peak cladding temperature. The cladding temperatures in the hot nodes are compared in Figure 4-33.

As shown in Table 4-5, the minimum inventories are nearly identical. Figure 4-34 shows that significant water is maintained in the upper plenum and that a two-phase mixture provides cooling in the hot assembly throughout the transient.

Cases rhrlb3dlb and rhrlb5dlb show the impact of steam line isolation on the LOCA transient. As shown in Table 4-5, the PCT is significantly reduced when the steam line is isolated more slowly by the pressure regulator. The minimum inventories for the two cases are nearly identical.

Figure 4-35 compares the short term dome pressure responses and the cladding temperatures of the hot nodes. As shown, fast closure of the TCVs causes the system pressure to increase initially whereas the case crediting the pressure regulator results in a slowly decreasing system pressure. Similar to previous sensitivity studies, the PCT responses are a result of different void reactivity feedback caused by the different system pressure responses.

Break Size

Cases rhrlb3dlb, rhrlb7dlb, and rhrlb8dlb show the impact of break size. These cases represent a 100%, 75%, and 50% break of the RHR suction line. The drain line break size is unchanged. As shown in Table 4-5 and Figure 4-36, the minimum inventory increases as the break size is decreased, while the PCT changes minimally.

4.5.5 RHR Injection Line Break

There are two RHR injection line nozzles located below the feedwater nozzles. The RHR injection lines are used by two of the three LPFL trains. The third LPFL train injects into one of the feedwater lines. Spargers located within the annulus connect to each of the RHR injection nozzles. The break flow associated with a break in one of the RHR injection lines is limited by the [ ]^{a,c} nozzles on each of the RHR injection spargers. A break in one of these lines would disable one of the LPFL divisions. The limiting single failure is to the EDG which powers the other division. The remaining ECCS equipment is:

1 RCIC + 1 HPCF + 1 LPFL + 8 ADS

4.5.5.1 RHR Injection Line Break Results

Two cases were run with the power in the hot assembly set to simulate a nodal power so that the hot rod would be at the TMOL. Table 4-6 summarizes the results of these cases. As shown, the variation in minimum inventory is small, and the sensitivity to initial core flow rate is similar to other cases in that the higher initial core flow rate provides additional margin to dryout and a slightly lower PCT.

Table 4-6 RHR Injection Line Break Results

Case	Core Flow	Break Location	Break Size	Steam Line Isolation	PCT (GOBLIN)	Minimum Mass
rhrilb3	90%	RHR IL	100%	TCV fast closure	707°C	215.0 E3 kg
rhrilb4	111%	RHR IL	100%	TCV fast closure	655°C	213.1 E3 kg

4.5.5.2 Sensitivity Studies

Core Flow Rate

Figure 4-37 compares the PCT transient predicted by GOBLIN for the hot assembly, which occurs in Node 18. As shown, the case with the lower initial core flow rate is more limiting as described above. Figure 4-38 compares the system pressures and masses. The small differences in the response are due to different actuation times for the HPCF pump. The water level recovers before actuation of the LPFL pump.

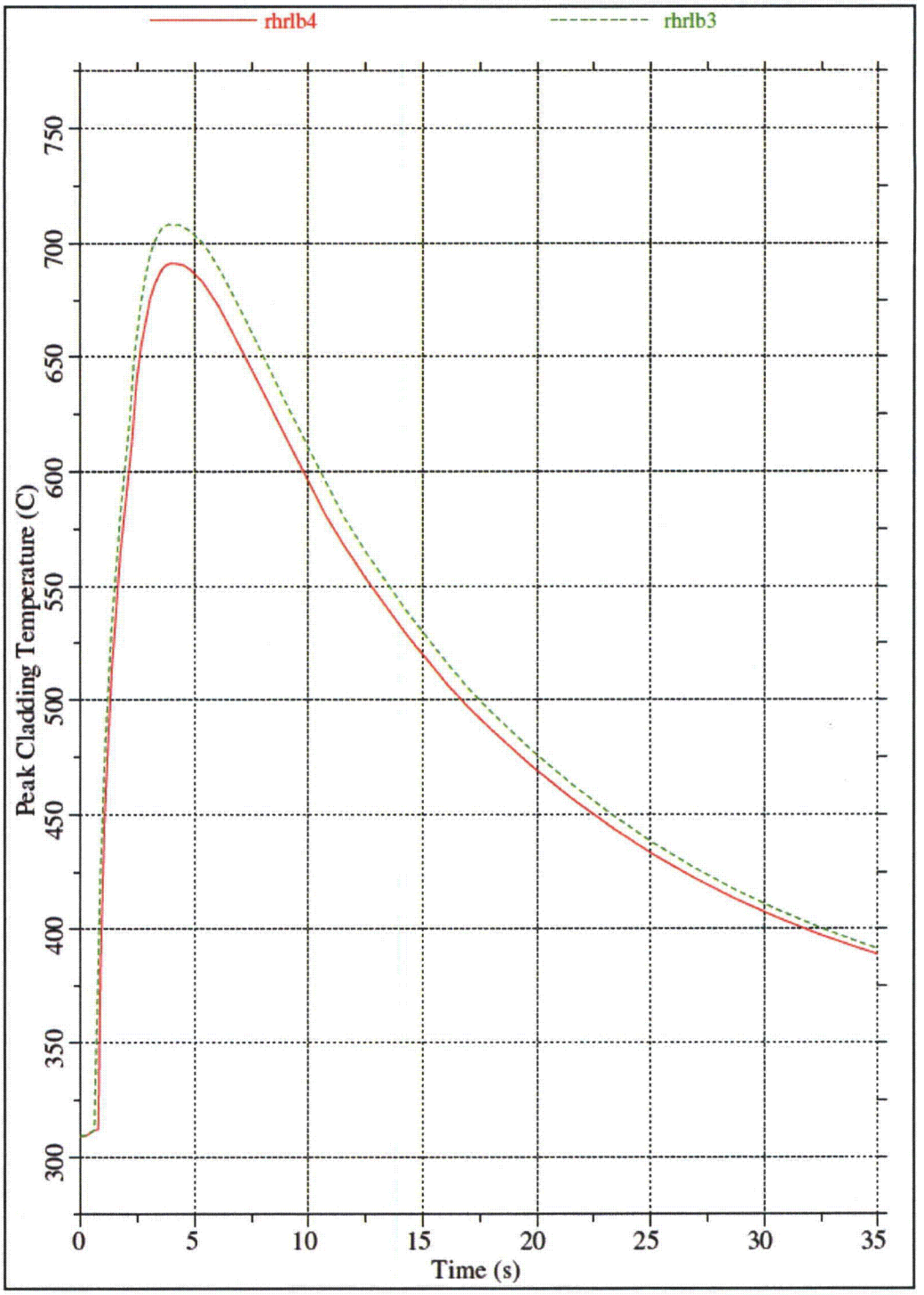

Figure 4-33 Core Flow Rate Sensitivity – GOBLIN PCTs

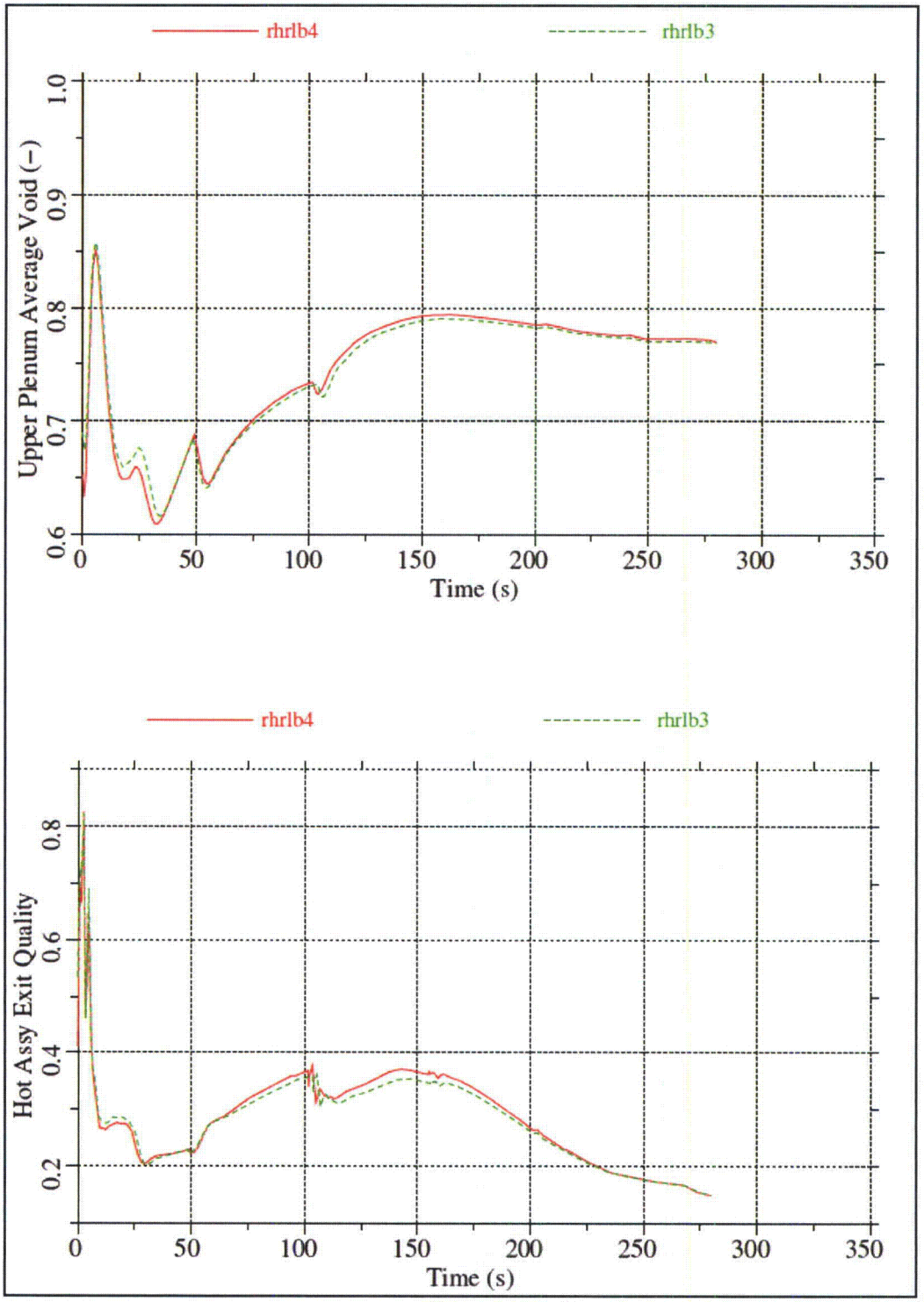

Figure 4-34 Core Flow Rate Sensitivity – Upper Plenum Void and Hot Assembly Exit Quality

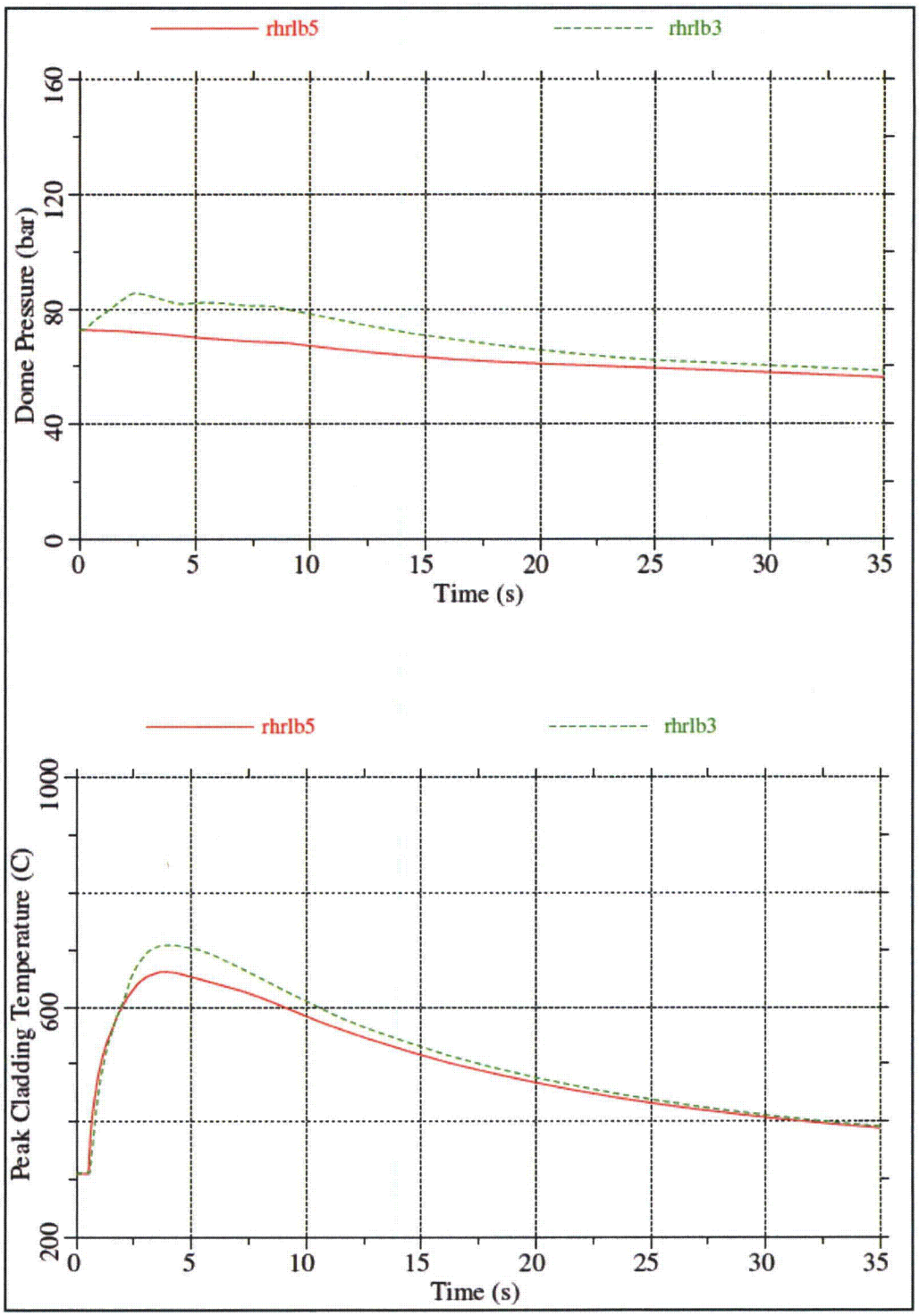

Figure 4-35 Steam Line Isolation Sensitivity – Dome Pressure and GOBLIN PCT

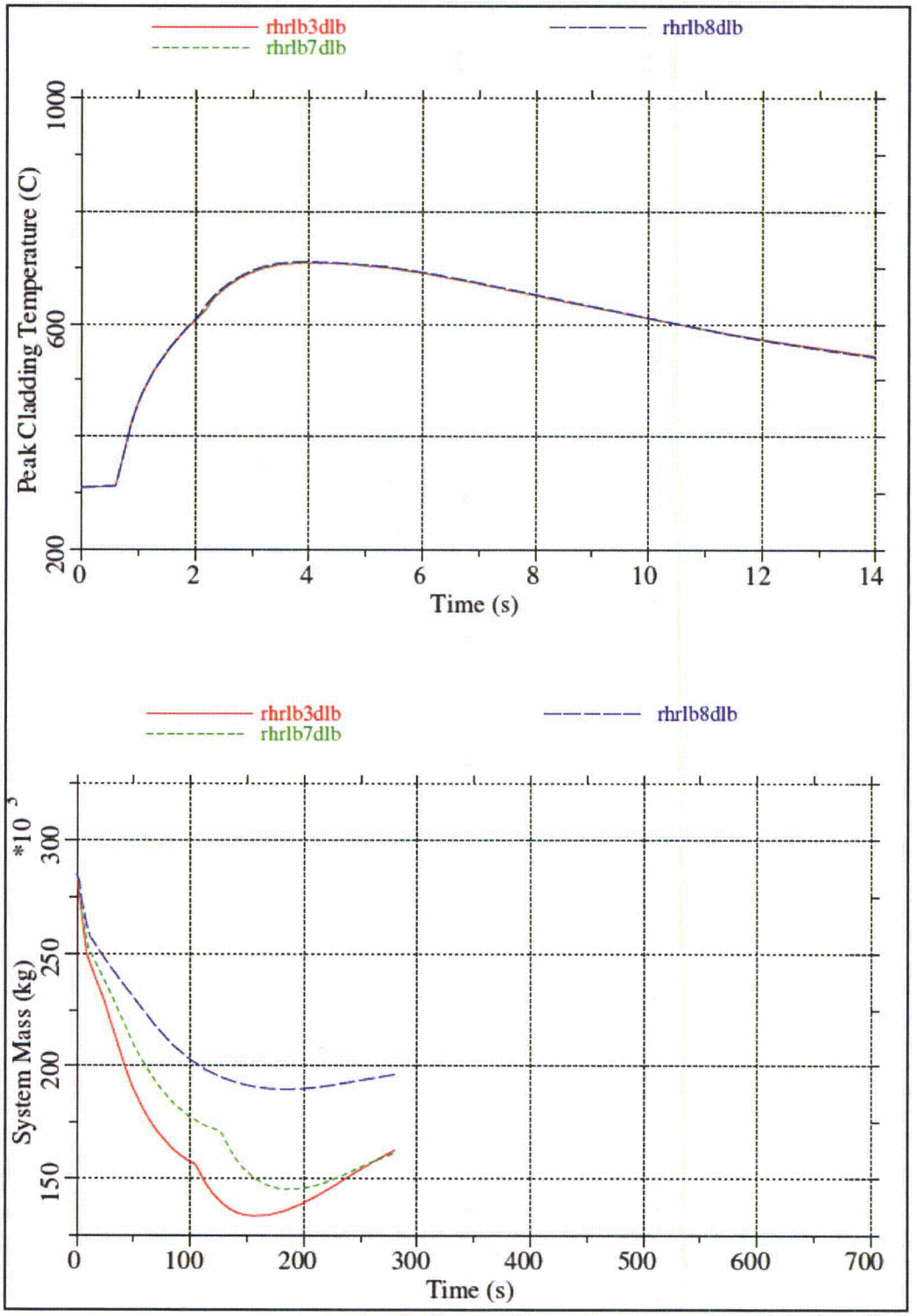

Figure 4-36 Break Size Sensitivity – GOBLIN PCT and System Mass

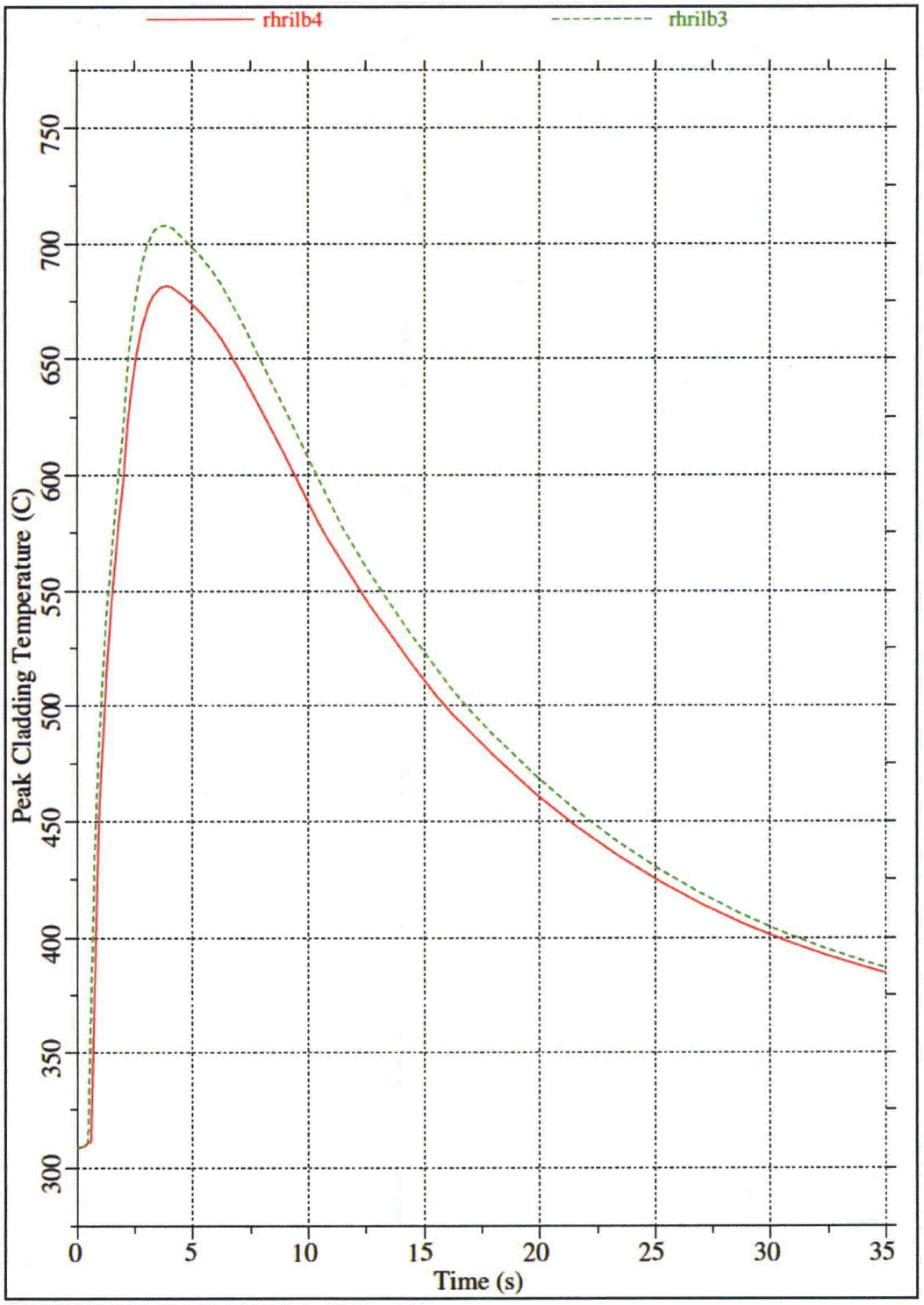

Figure 4-37 Core Flow Rate Sensitivity – GOBLIN PCT

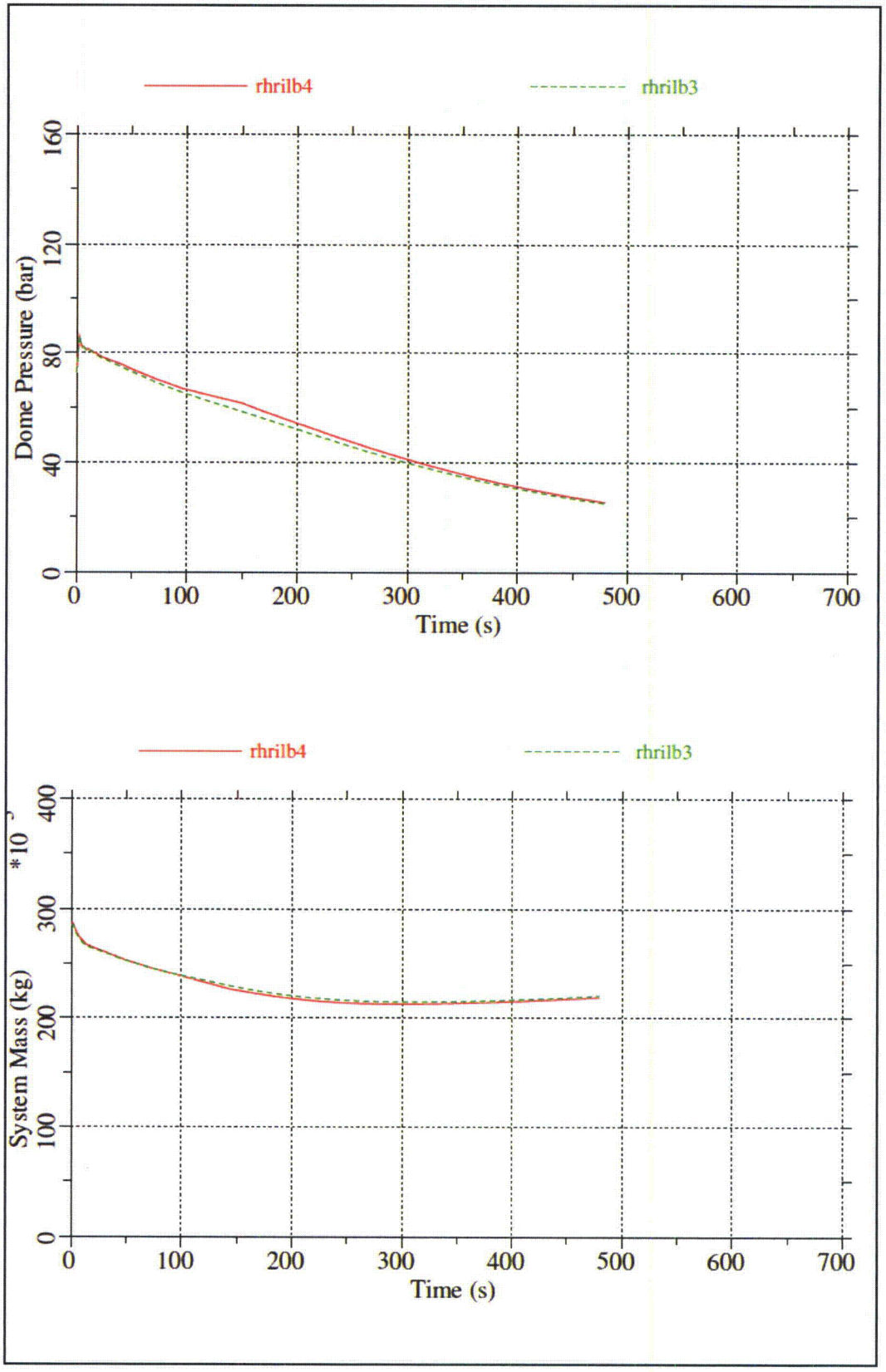

Figure 4-38 Core Flow Rate Sensitivity – Dome Pressure and System Mass

4.5.6 Drain Line Break

The drain line nozzle is connected to the bottom head. As shown in Figure 4-39, the drain line is also connected to the RHR suction line. Therefore, a break in the drain line will also result a loss of coolant from the upper annulus. In the case of a double-ended break in the drain line in the vicinity of the drain line nozzle, the break flow from the RHR suction line side of the break is limited by the smaller diameter of the piping near the bottom head drain. The limiting single failure is that one of the EDGs that provides power to a HPCF pump does not start. The remaining ECCS equipment is:

1 RCIC + 1 HPCF + 2 LPFL + 8 ADS

4.5.6.1 Drain Line Break Results

One case was run to simulate the drain line break. The results are summarized in Table 4-7. Comparing these results to those for the RHR suction line break, case rhrlb3dlb Table 4-5, shows that the PCTs predicted by GOBLIN are the same, but that the minimum inventory in this case is significantly greater as a result of the much smaller combined break flow area.

The drain line break is compared to the RHR suction line break in Figure 4-40 and Figure 4-41. As shown, the peak cladding temperature responses are nearly identical, but the drain line break loses significantly less inventory due to the smaller break size.

Table 4-7 Drain Line Break Results

Case	Core Flow	Break Location	Break Size	Steam Line Isolation	PCT (GOBLIN)	Minimum Mass
dlb	90%	Drain Line	100%	TCV fast closure	708°C	245.0 E3 kg

a,c

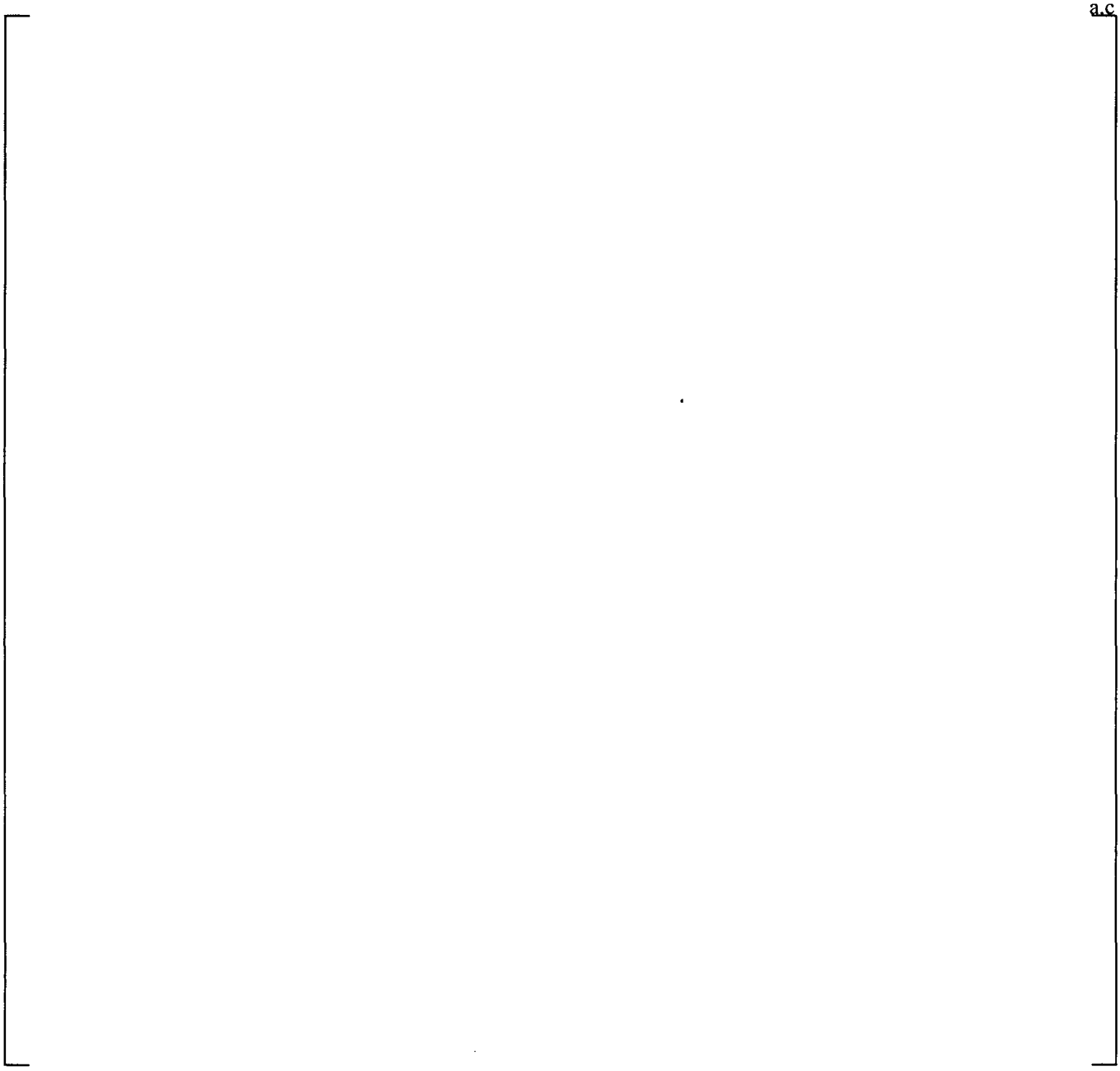

Figure 4-39 Schematic of Drain Line Break

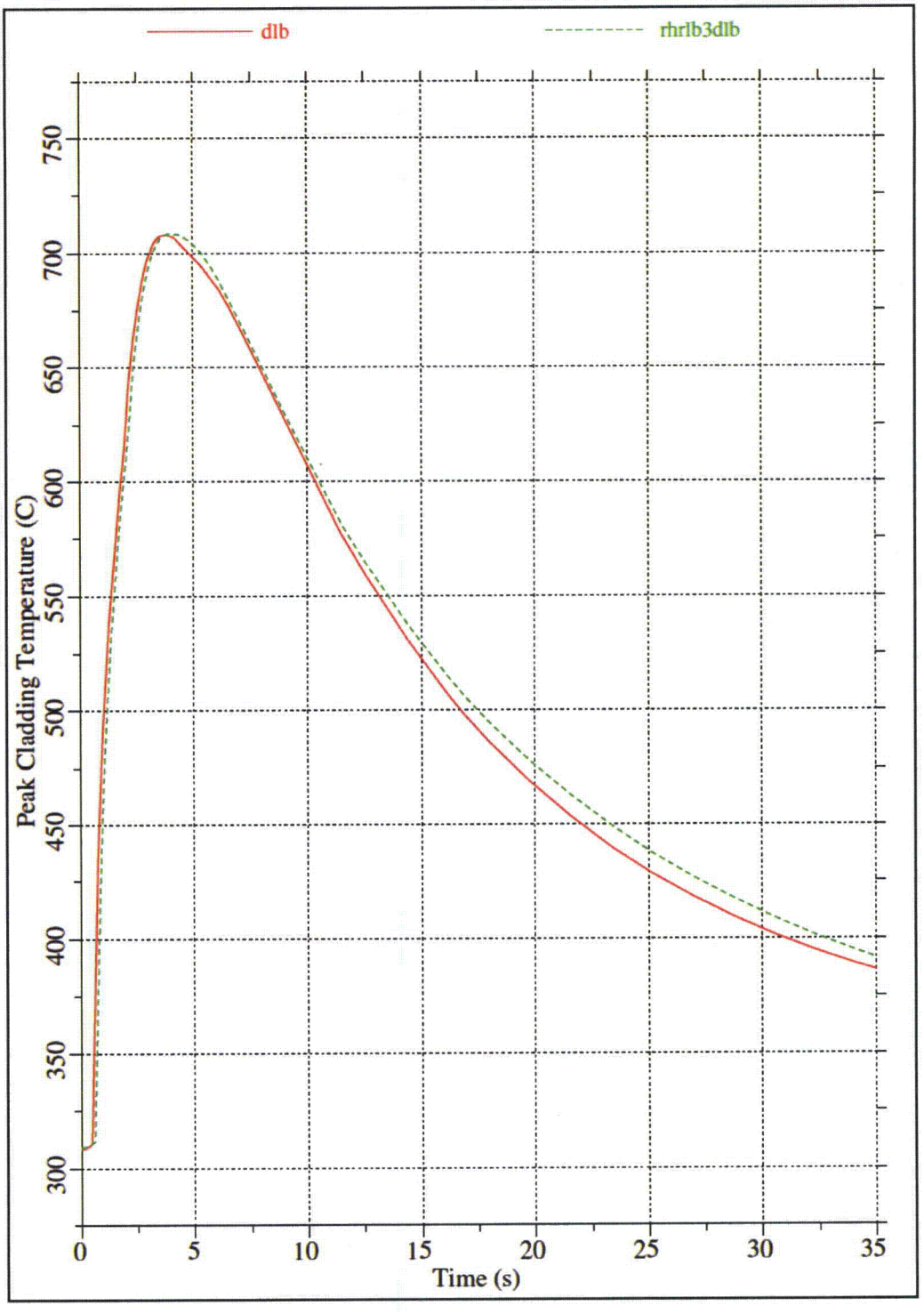

Figure 4-40 Comparison of DLB to RHRSLB – GOBLIN PCTs

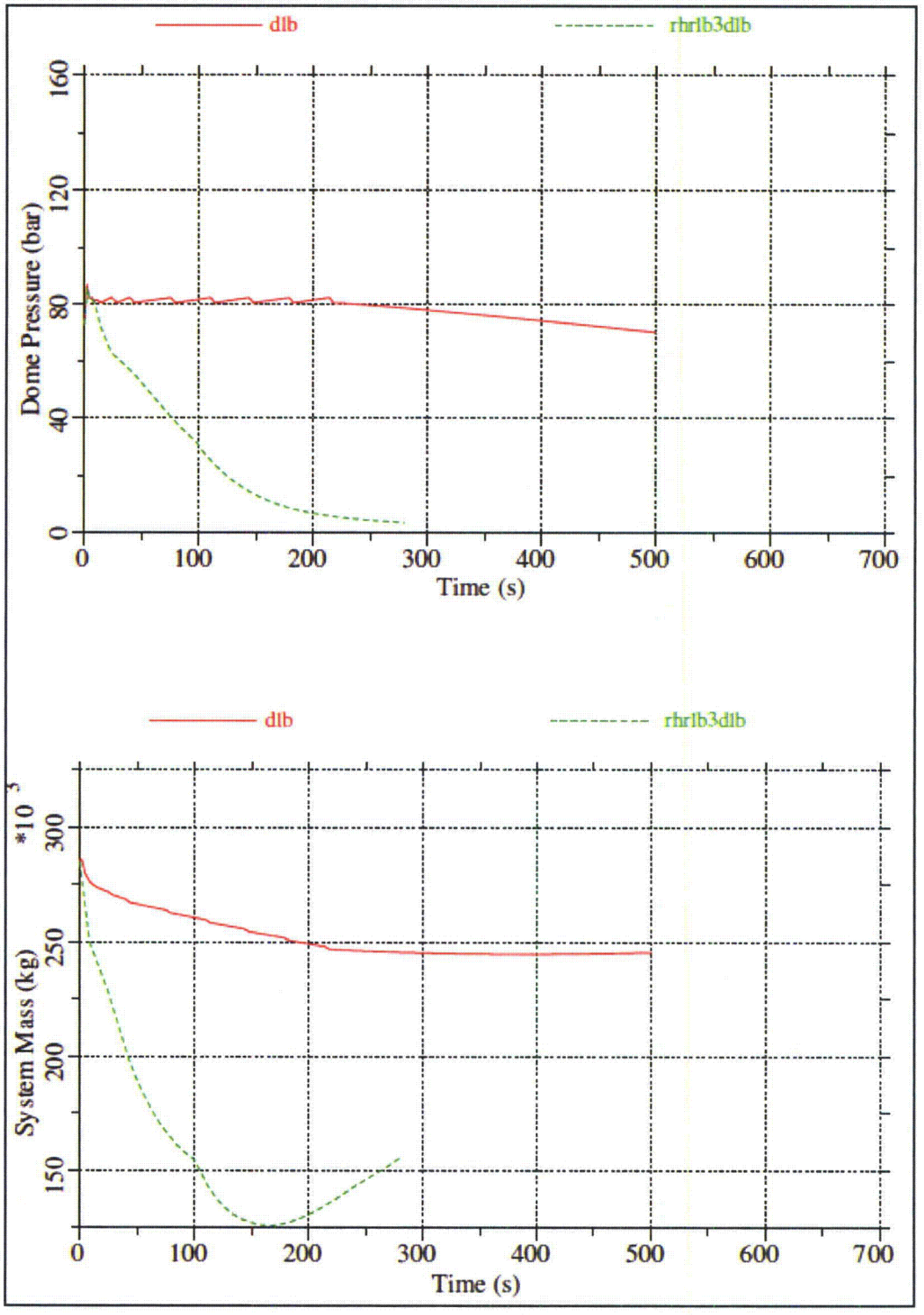

Figure 4-41 Comparison DLB to RHRSLB – Dome Pressure and System Mass

4.6 BREAKS OUTSIDE CONTAINMENT

Breaks outside of containment are characterized by isolation of the break by the MSIVs. Because the main steam line break outside the containment produces more vessel inventory loss before isolation than other breaks in this category, the results of this case are bounding for breaks in this group.

A postulated guillotine break of one of the four main steam lines outside the containment is shown schematically in Figure 4-42. A pipe rupture in this location results in mass loss from each end of the break until the MSIVs close. The MSIVs receive a close signal due to high steam flow rate through the integral flow restrictors or due to LWL 1.5. Closure of the MSIVs limits the amount of flow that will be discharged outside the containment. Once the MSIVs close, the RPV will pressurize until the SRVs open. The SRVs will control system pressure and discharge steam to the suppression pool. The RCIC system or one of the HPCF systems can provide adequate flow to the vessel to maintain core cooling.

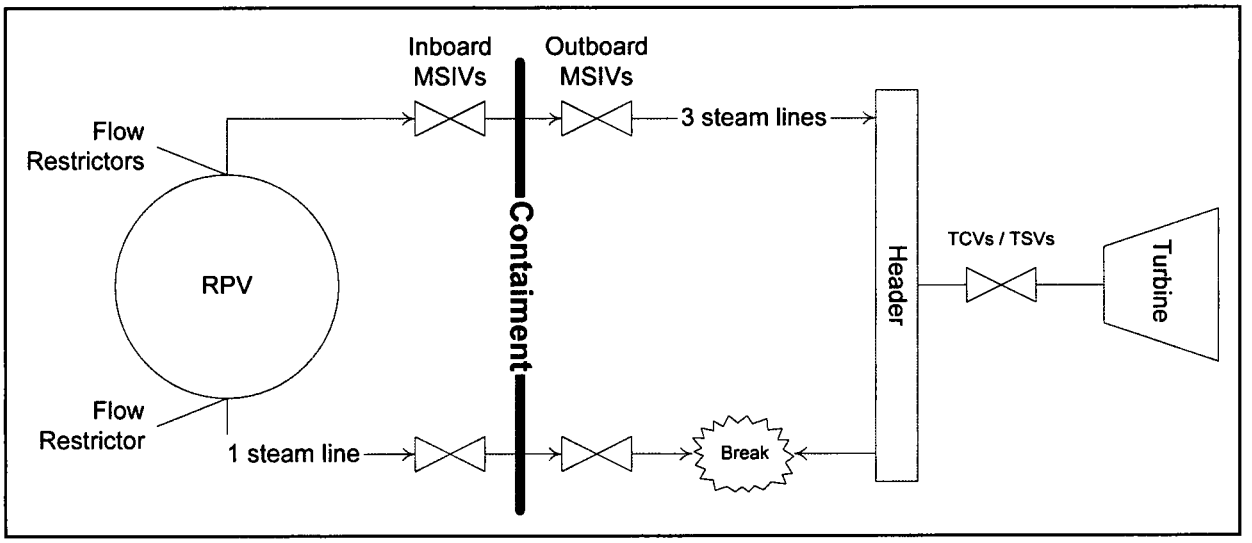

Figure 4-42 Schematic of Steam Line Break Outside Containment

4.6.1 Steam Line Break Outside Containment Results

The limiting single failure is that one of the EDGs that provides power to a HPCF pump does not start. This results in one RCIC pump, one HPCF pump, and two LPFL pumps available to mitigate the event. Although the RCIC turbine takes suction from one of the steam lines, closure of the MSIVs ensures that there is a long-term supply of steam for the RCIC turbine. However, a more limiting case is evaluated where the RCIC is assumed unavailable. In this case the assumed available equipment is:

1 HPCF + 2LPFL + 8 ADS

In this case, the LPFL systems would not actuate as the system inventory is stabilized before ADS actuation.

Table 4-8 summarizes the results for this case. As shown, the PCT and minimum system mass are not as limiting as other cases. Figure 4-43 shows that the PCT occurs early in the transient before ECCS

actuation. Figure 4-44 shows that the system pressure decreases at the beginning of the transient. However, the pressure increases after MSIV closure until actuation of the SRVs controls the pressure for the remainder of the event. Figure 4-44 also shows that the mass of the system decreases rapidly until MSIV closure, and that the system mass is maintained after HPCF injection.

Table 4-8 Main Steam Line Break Outside Containment Results

Case	Core Flow	Break Location	Break Size	Steam Line Isolation	PCT (GOBLIN)	Minimum Mass
mslboc6a	90%	SL outside containment	100%	MSIV closure	668°C	241.4 E3 kg

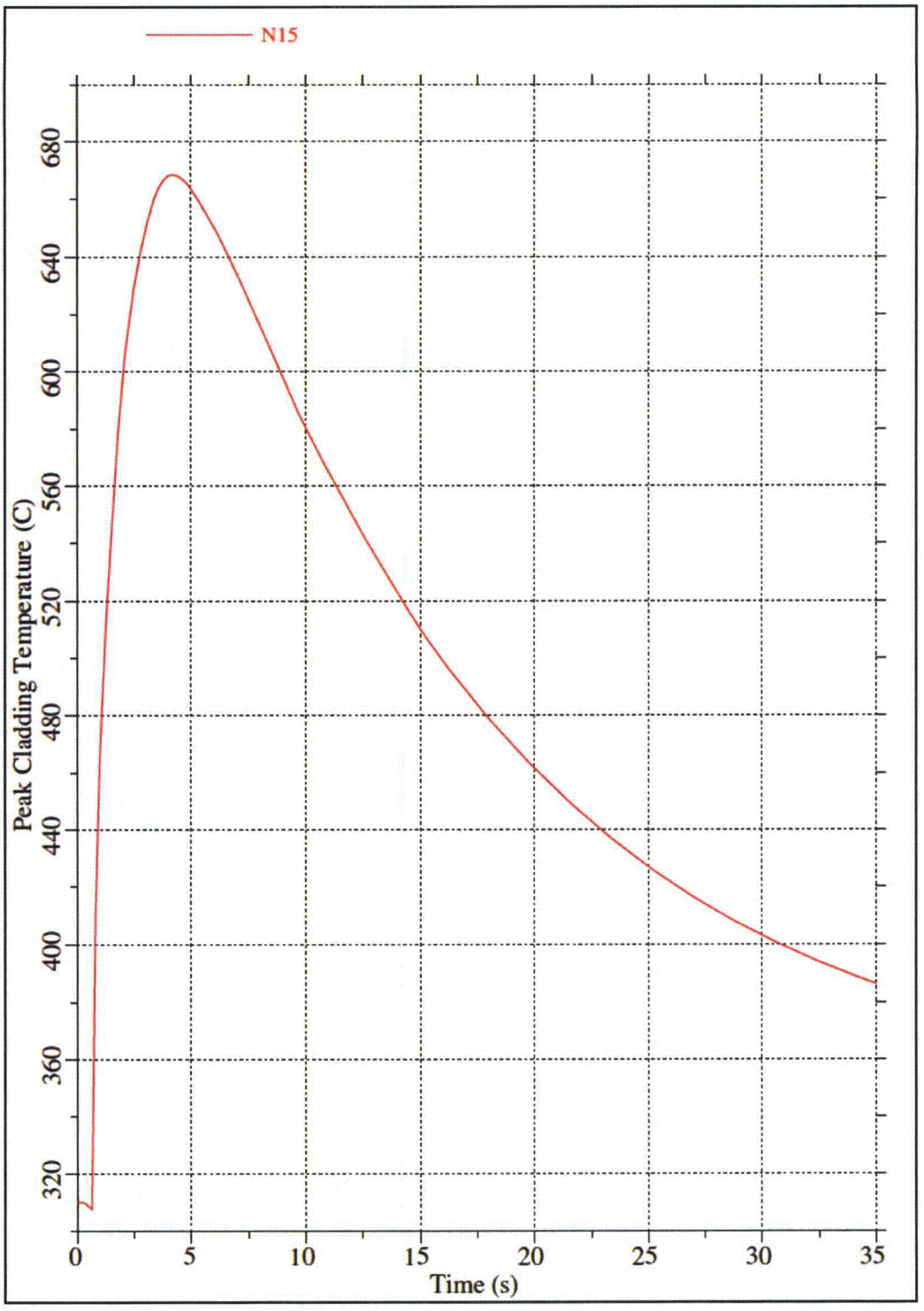

Figure 4-43 Steam Line Break Outside Containment – GOBLIN PCT

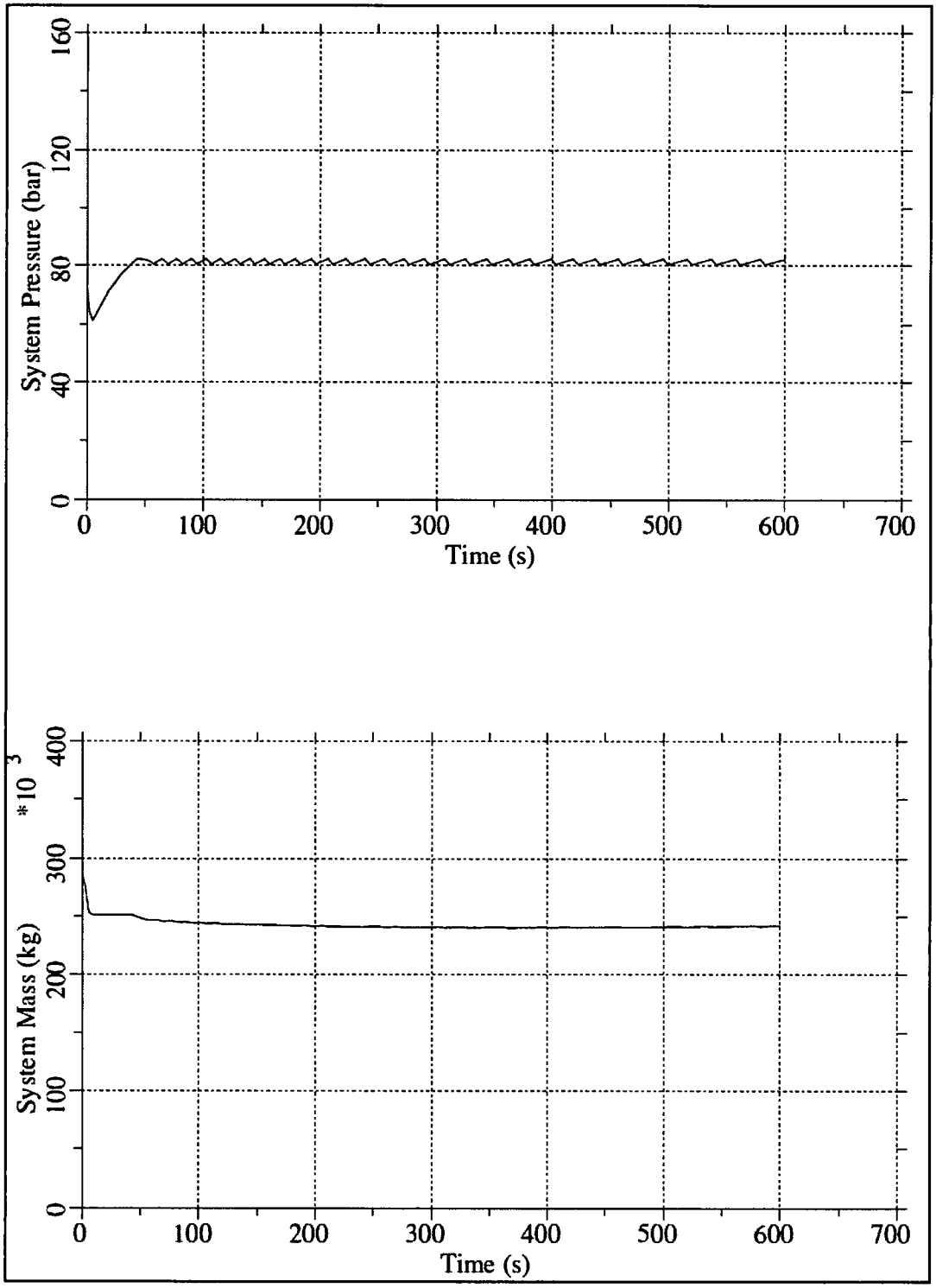

Figure 4-44 Steam Line Break Outside Containment – Dome Pressure and System Mass

4.7 SUMMARY OF LIMITING CASES

The resulting peak cladding temperature and minimum system inventory for each case is presented in Table 4-9. These results are shown as a function of break size in Figure 4-45 and Figure 4-46.[2]

As shown in Figure 4-44, the peak cladding temperature does not vary appreciably with break size. The variations in PCT are caused by different initial conditions such as high core flow rate vs. low core flow rate and the method assumed for isolating the steam line. As shown, the higher PCTs result from cases that are initiated from the lower core flow rate and cases where the steam line was isolated quickly (fast closure of the TCVs). Additionally, alternative axial power distributions were considered. The mid-peaked chopped cosine power distribution was confirmed as limiting, and applied to all cases summarized below.

As shown in Figure 4-46, the minimum inventory varies with break size. For a similar set of available ECCS equipment, minimum inventory decreased as break size increased.

Table 4-9 Summary of Break Spectrum Study Results

Case	Core Flow	Break Location	Break Size	Steam Line Isolation	PCT (GOBLIN)	Minimum Mass
hpcf3	90%	HPCF Line	100%	TCV fast closure	708°C	133.3 E3 kg
hpcf4	111%	HPCF Line	100%	TCV fast closure	692°C	132.2 E3 kg
hpcf5	90%	HPCF Line	100%	Pressure regulator	661°C	133.7 E3 kg
hpcf7	90%	HPCF Line	75%	TCV fast closure	708°C	138.1 E3 kg
hpcf8	90%	HPCF Line	50%	TCV fast closure	708°C	143.6 E3 kg
hpcf9	90%	HPCF Line	25%	TCV fast closure	708°C	151.3 E3 kg
mslb6	90%	SL – RCIC side	200%	TCV fast closure	657°C	164.1 E3 kg
mslb6a	111%	SL – RCIC side	200%	TCV fast closure	648°C	162.6 E3 kg
mslb7	90%	SL – RCIC side	150%	TCV fast closure	654°C	164.1 E3 kg
mslb8	90%	SL – RCIC side	100%	TCV fast closure	656°C	164.1 E3 kg
fwlb3	90%	FWL – RCIC side	100%	TCV fast closure	708°C	126.5 E3 kg
fwlb4	111%	FWL – RCIC side	100%	TCV fast closure	684°C	123.5 E3 kg
fwlb5	90%	FWL – RCIC side	100%	Pressure Regulator	661°C	126.0 E3 kg
fwlb6	90%	FWL – RCIC side	100%	TCV fast closure	708°C	125.9 E3 kg
fwlb7	90%	FWL – RCIC side	75%	TCV fast closure	705°C	136.9 E3 kg
fwlb8	90%	FWL – RCIC side	50%	TCV fast closure	707°C	148.4 E3 kg
fwlb9	90%	FWL – RCIC side	25%	TCV fast closure	710°C	215.6 E3 kg

2. The results of the steam line break outside containment are not shown in the figures because the break isolates rapidly, preventing a meaningful comparison.

Table 4-9 (cont.) Summary of Break Spectrum Study Results

Case	Core Flow	Break Location	Break Size	Steam Line Isolation	PCT (GOBLIN)	Minimum Mass
rhrlb3dlb	90%	RHR Suction Line	100%	TCV fast closure	708°C	125.9 E3 kg
rhrlb4dlb	111%	RHR Suction Line	100%	TCV fast closure	691°C	124.6 E3 kg
rhrlb5dlb	90%	RHR Suction Line	100%	Pressure regulator	662°C	125.5E3 kg
rhrlb7dlb	90%	RHR Suction Line	75%	TCV fast closure	709°C	135.7 E3 kg
rhrlb8dlb	90%	RHR Suction Line	50%	TCV fast closure	710°C	147.6 E3 kg
rhrilb3	90%	RHR Injection Line	100%	TCV fast closure	707°C	215.0 E3 kg
rhrilb4	111%	RHR Injection Line	100%	TCV fast closure	655°C	213.1 E3 kg
dlb	90%	Drain Line	100%	TCV fast closure	708°C	245.0 E3 kg
mslboc6a	90%	SL Outside Containment	200%	MSIV closure	668°C	241.4 E3 kg

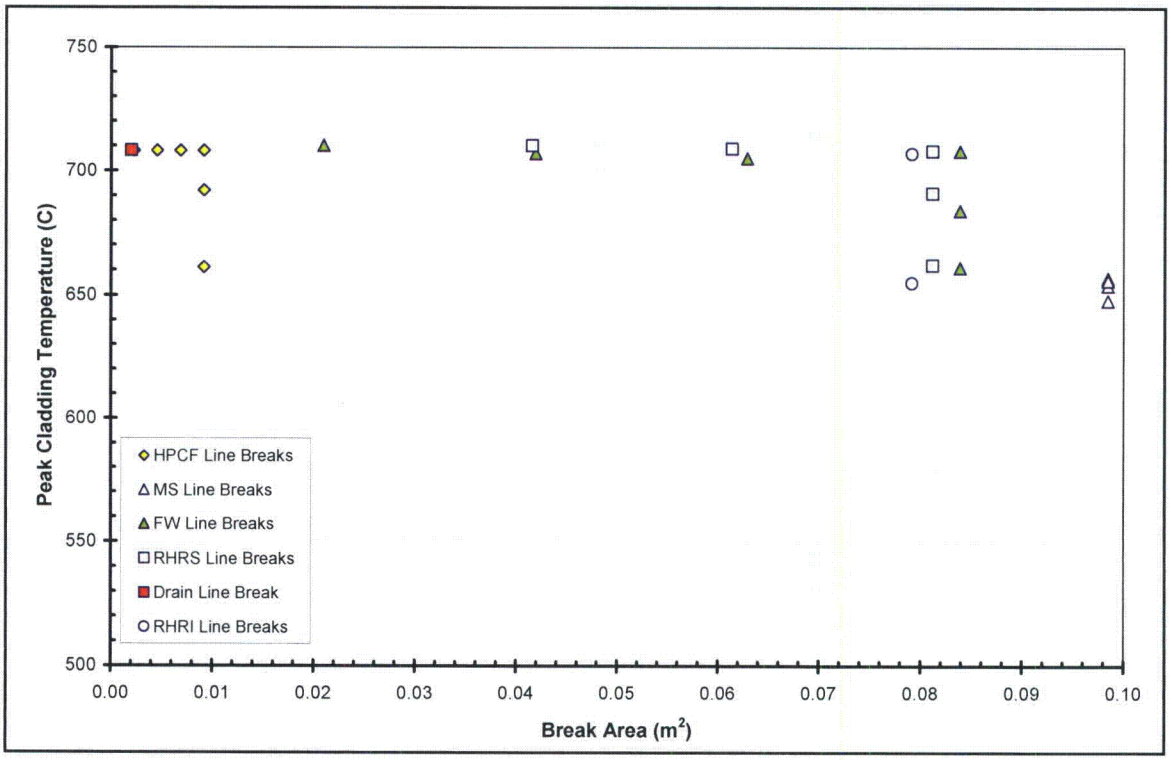

Figure 4-45 Summary of Peak Cladding Temperature Results vs. Break Size

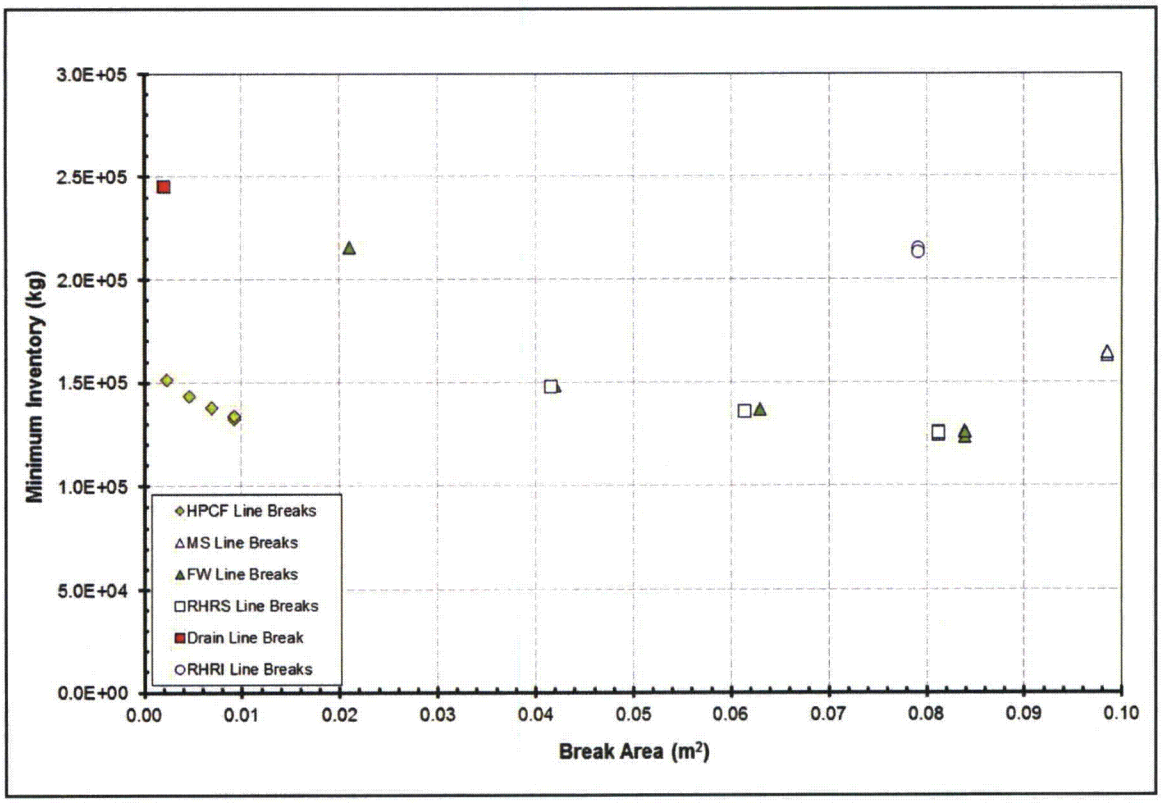

Figure 4-46 Summary of Minimum Inventory Results vs. Break Size

4.7.1 Case with Minimum Inventory

The case having the minimum system inventory was the case where the feedwater line break initiated with maximum core flow rate. Although the steam line break has a greater flow area than the feedwater line break, the feedwater line break has the smallest minimum inventory due to the lower quality fluid flowing out the break. In spite of having the least minimum inventory, the core remains cooled by a two-phase mixture throughout the transient.

4.7.2 Case with Maximum Peak Cladding Temperature

There is no clear case having the highest peak cladding temperature from the GOBLIN hot assembly analysis. As shown in Table 4-9, two cases have a PCT of 710°C as predicted by GOBLIN. The small feedwater line break initiated from 90% core flow rate, fwlb9, is selected for the heatup analysis using CHACHA.

Several exposure points are evaluated to show that the combination of nodal power and pin-to-pin peaking results in the hot rod being at the TMOL. The range of exposures encompasses beginning of life to [ ]^{a,c}.
It is typical of BWR/ABWR fuel to have the largest pin-to-pin peaking factors early in life. However, the high power rods burn down with exposure, causing the rod power distribution to become flatter at larger cycle exposures. [
]^{a,c} Figure 4-47 shows the results of a calculation for a typical lattice design over a range of

burnups [ ]^{a,c}. As shown, the PCT increases slightly with burnup. However, the PCT remains below the licensing limit for ECCS performance analysis.

Due to the relatively low PCT, the maximum local oxidation and core wide oxidation are below the licensing limits.

A similar evaluation is performed for each reload to confirm that the 10 CFR 50.46 criteria are met when the [ ]^{a,c} for the limiting LOCA event.

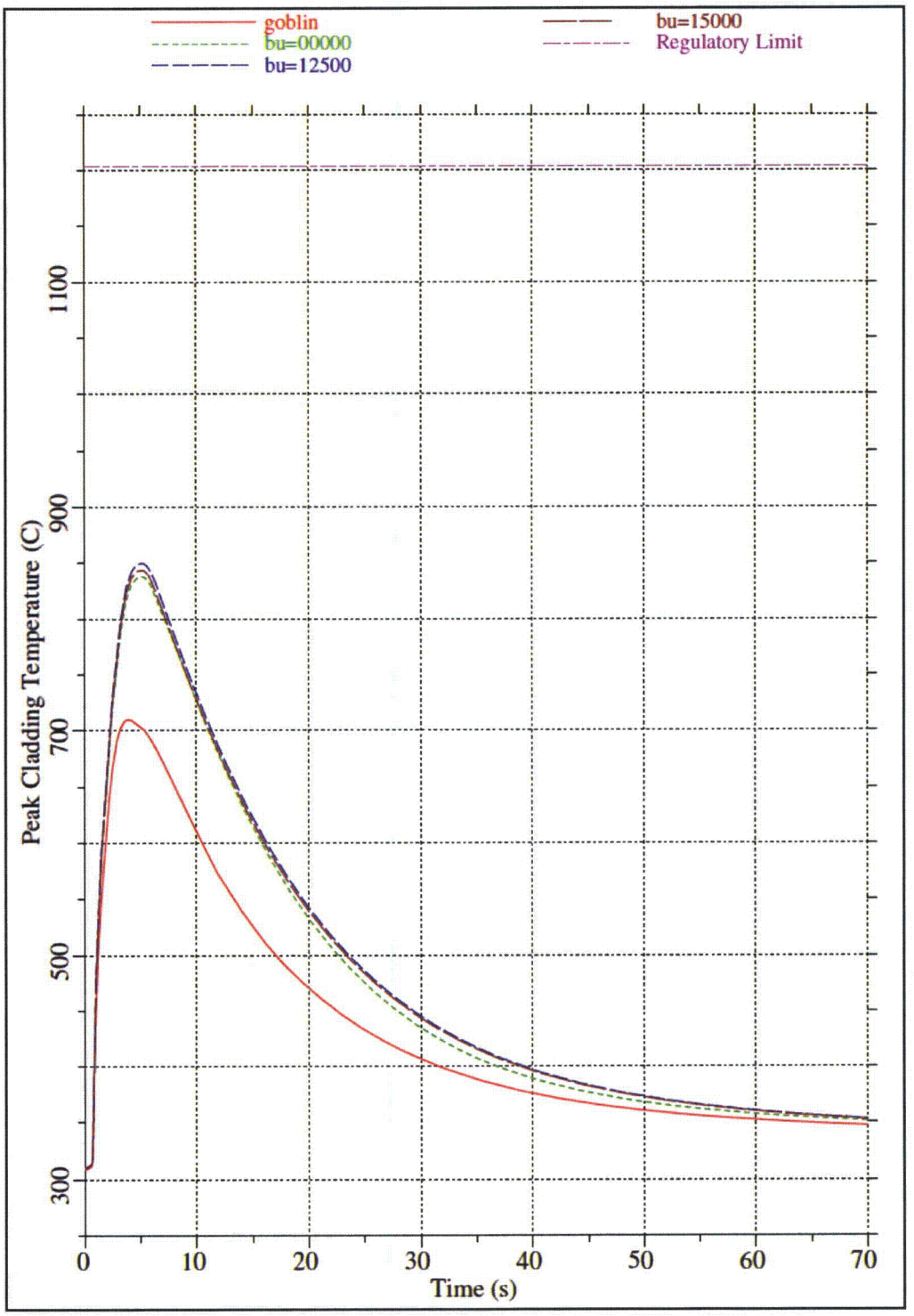

Figure 4-47 Peak Cladding Temperature For Limiting Case

5 QUALIFICATION OF ABWR EVALUATION MODEL

As described in Section 1, the main differences between a LOCA in a BWR and in an ABWR arise from the different elevations of piping connections to the RPV and the different inertias of the RIPs and external recirculation pumps. The lower inertia of the RIPs results in a faster coastdown of the pumps following a loss of power. The rapid coastdown causes an early boiling transition in the transient and a brief heat-up of the cladding. This occurs well before the ECCS actuates.

To ensure that the rapid coastdown of core flow and the effect of such a coastdown on boiling transition are accurately modeled in GOBLIN, the following two additional qualifications are performed:

- Predicted behavior of internal recirculation pumps are compared to the minimum design acceptance criterion for the ABWR RIPs and to Okiluoto 1 (OL1) plant startup test data.
- The results of GOBLIN simulations of the FRIGG loop are compared to FRIGG loop test data that simulated flow coastdown.

5.1 RECIRCULATION PUMP MODEL

The recirculation pump model is described in RPB 90-93-P-A (Reference 2). The behavior of the pumps is modeled by the conservation of angular momentum:

$$I\frac{d\varpi}{dt} = T$$

where:

ω = angular velocity
t = time
T = net torque
I = moment of inertia

The coolant conservation equations and the pump angular momentum equation are coupled in the GOBLIN code through the 4-quadrant pump homologous curves. The fluid conservation equations are solved simultaneously with the pump conservation of angular momentum equation using numerical integration techniques to obtain the transient pump coastdown. The pump angular momentum equation uses several inputs, including pump/motor assembly inertia, hydraulic torque and frictional torque.

The data that is usually provided for the pump includes the pump homologous curves for head and hydraulic torque and the following parameters:

ω_r = rated pump speed
W_r = rated pump flow
H_r = rated pump head
T_r = rated pump torque

ρ_r = rated density of pump fluid
η = pump efficiency (minimum)

The GOBLIN input data include the following parameters:

H_2 = frictional torque coefficient for high pump speed
H_3 = lower limit of angular velocity for high speed frictional torque
H_4 = constant frictional torque for when angular velocity < H3
H_6 = rated pump speed
H_9 = rated hydraulic torque

The rated hydraulic torque is calculated using the rated torque and the minimum efficiency as follows:

$$H_9 = \eta \times T_r$$

This results in a conservatively high frictional torque at rated conditions. The frictional torque relationship in GOBLIN is assumed to vary as the square of the pump speed. The coefficient in that expression is then determined as follows:

$$H_2 = \frac{-(T_r - H_9)}{\varpi_r^2}$$

The constant frictional torque at low speed (H_4) is not typically provided. However, other information is usually provided (e.g., pump coastdown time constant or pump coastdown data from a startup test), which allows the low speed frictional torque to be tuned so that the pump coastdown is simulated conservatively. The speed where these two curves cross (H_3) is then determined as follows:

$$H_3 = \sqrt{H_4 / H_2}$$

The frictional torque as a function of speed then becomes:

$$T_f(\omega) = H_2 \times \varpi \times |\varpi| \quad \text{if } |\varpi| > H_3$$

$$T_f(\omega) = H_4 \times \frac{\varpi}{|\varpi|} \quad \text{otherwise}$$

This approach is used for the initial approximation, and the results are compared to the specification for the minimum safety analysis limit for the pump coastdown time constant of [ ]^{a,c}. If the resulting coastdown time constant is greater than this value, the model is adjusted so that this specification is met. The calculated pump coastdown transient, which is shown in Figure 5-1, demonstrates that the time constant of [ ]^{a,c} is met [ ]^{a,c}. In this case the pump speed does not decrease to zero. This is a result of the core flow, which transitions from forced flow to natural circulation, driving the pump rotor.

a,c

Figure 5-1 Calculated ABWR Pump Trip Transient

5.2 INTERNAL PUMP COASTDOWN

5.2.1 Okiluoto 1 Pump Trip

The OL1 reactor is an internal recirculation pump reactor operated by Teollisuuden Voima Oy (TVO) on the west coast of Finland. The plant, which is an Asea-Atom design, contains 500 fuel assemblies and 6 internal recirculation pumps. GOBLIN was used to simulate a pump trip test that was performed during plant start-up. The simulation is described in Section 6.1.8 of Reference 2. Although the purpose of the simulation was to validate the point kinetics model in GOBLIN, it also showed that the calculated flow compares well with the measured flow, Figure 5-2.

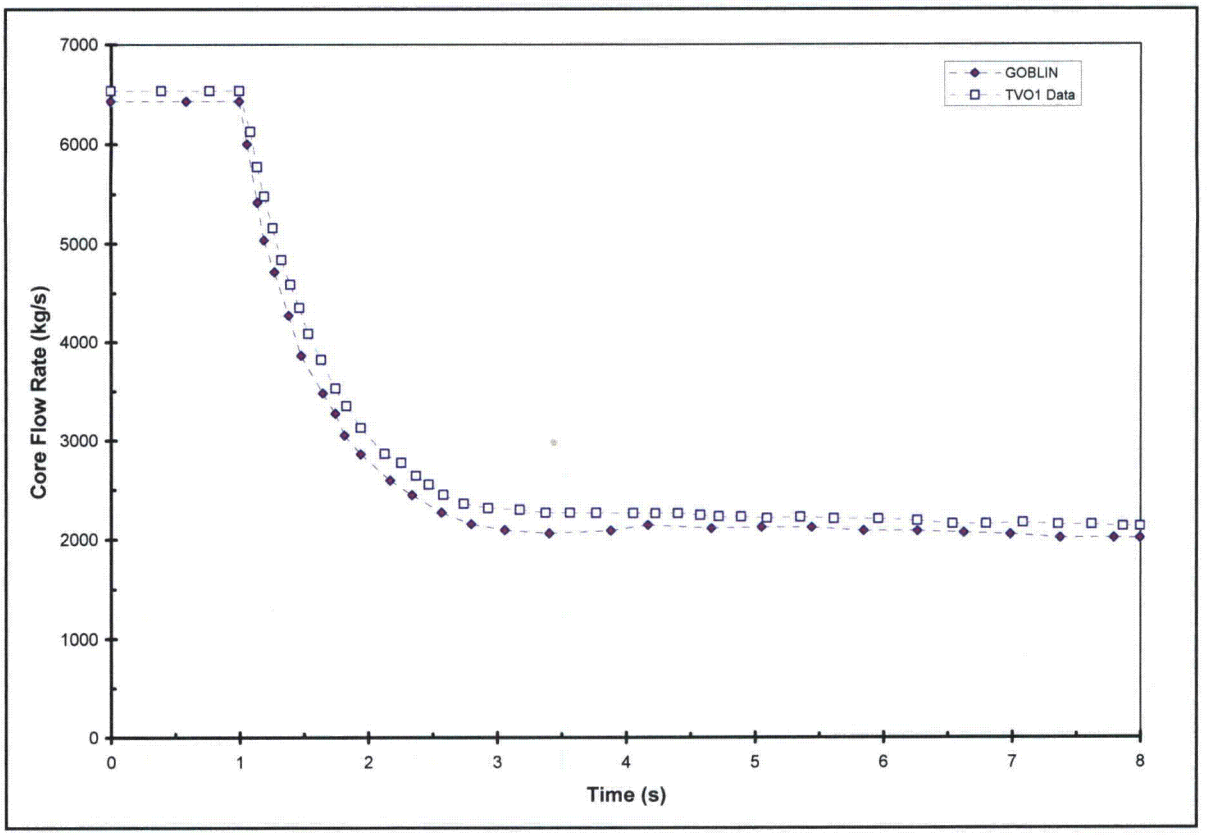

Figure 5-2 Comparison of Core Channel Inlet Flow Rate for OL1 Pump Trip Transient

5.3 PREDICTION OF BOILING TRANSITION

The ABWR LOCA event coincident with the loss of offsite power is characterized by a rapid coastdown of the RIPs. The rapid decrease in coolant flow through the core causes an abrupt change of the fuel rod heat transfer regime from nucleate boiling to film boiling. The typical ABWR LOCA is characterized by departure from nucleate boiling shortly after the onset of the LOCA event. Even though the core remains covered by a two-phase mixture throughout the LOCA event, the transition to film boiling results in a cladding temperature increase until the reactor trip reduces the heat generation. Because the peak cladding temperature occurs during this time, the predicted time of boiling transition is important.

As described in Section 4.1 of Reference 5, the onset of boiling transition in GOBLIN is calculated using a boiling length CPR correlation that was developed for the fuel being analyzed. For example, the D4.1.2 CPR correlation, which has been implemented in GOBLIN, is used for the SVEA-96 Optima2 fuel design. The CPR correlation was developed from steady-state test data collected from the FRIGG loop in the Westinghouse laboratories in Västerås, Sweden. Derivation of the correlation is described in detail in Section 5 of Reference 8.

5.3.1 FRIGG Loop Comparison

In addition to the steady-state tests, another set of FRIGG transient dryout experiments was performed by increasing the bundle power and/or reducing the bundle inlet flows. These tests are described in Section 7 of Reference 8. The transient results are used for the validation of D4.1.2's implementation in GOBLIN.

The test section consists of a pressure vessel, a Zircaloy flow channel, and a replica of a SVEA-96 Optima2 sub-bundle with 24 heater rods. Each heater rod contains a heater element, electrical insulation, and Inconel-600 cladding. The heater element is made from a Monel K-500 tube. The heater rod non-uniform axial power profiles were generated by laser cutting a spiral on the Monel tube with a variable pitch. Three of the rods in each sub-bundle are part-length rods (PLRs), two being two-thirds of the length of a full-length rod and are placed adjacent to the central channel of the water cross. The other is one-third of the length of a full-length rod and is placed in the outer corner of the sub-bundle. An orifice plate is installed at the inlet of the flow channel to provide an even distribution of flow into the channel. The loss coefficient of the orifice plate closely approximates that of the lower tie plate in standard SVEA-96 Optima2 fuel. The heater rods are constrained by eight Inconel spacers of the same type used in the standard SVEA-96 Optima2 sub-bundle as seen in Figure 5-3.

[

]^{a,c}

Eighty five of the 253 FRIGG transient tests were used to validate the GOBLIN dryout prediction capability. The test cases selected included all axial power shapes and power/flow transients that are relevant to ABWR LOCA analyses. The three axial power shapes included in the validation were a bottom-peaked shape with a 1.5 axial peak located at 22% core height; a chopped cosine shape with a 1.4 axial peak; and a top-peaked shape with a 1.5 axial peak located at 78% core height.

The power transients evaluated were typically ones where the power was rapidly increased above the initial power by 50% to 70%. Power was then held power constant for a short time and subsequently reduced to 30% of its initial value. The flow was held constant during these tests.

The flow transients typically ramped flow down from an initial value at a fixed rate until it decreased to 30% of its initial value. During the flow transients, the power was ramped down at a fixed rate over 4 seconds where it reached 30% of its initial value.

A comparison of the measured vs. predicted dryout times is shown in Figure 5-4. As shown, with the exception of a few power-transient tests, the predictions are more conservative than the measurements. All of the flow transient tests are predicted conservatively.

A typical ABWR LOCA transient is characterized by a rapid decrease in flow and a slow decrease in reactor power in the first 3 seconds of the event. Therefore, the slight non-conservatism shown in the power transient tests does not impact the overall conclusion that GOBLIN predicts boiling transition time conservatively.

a,c

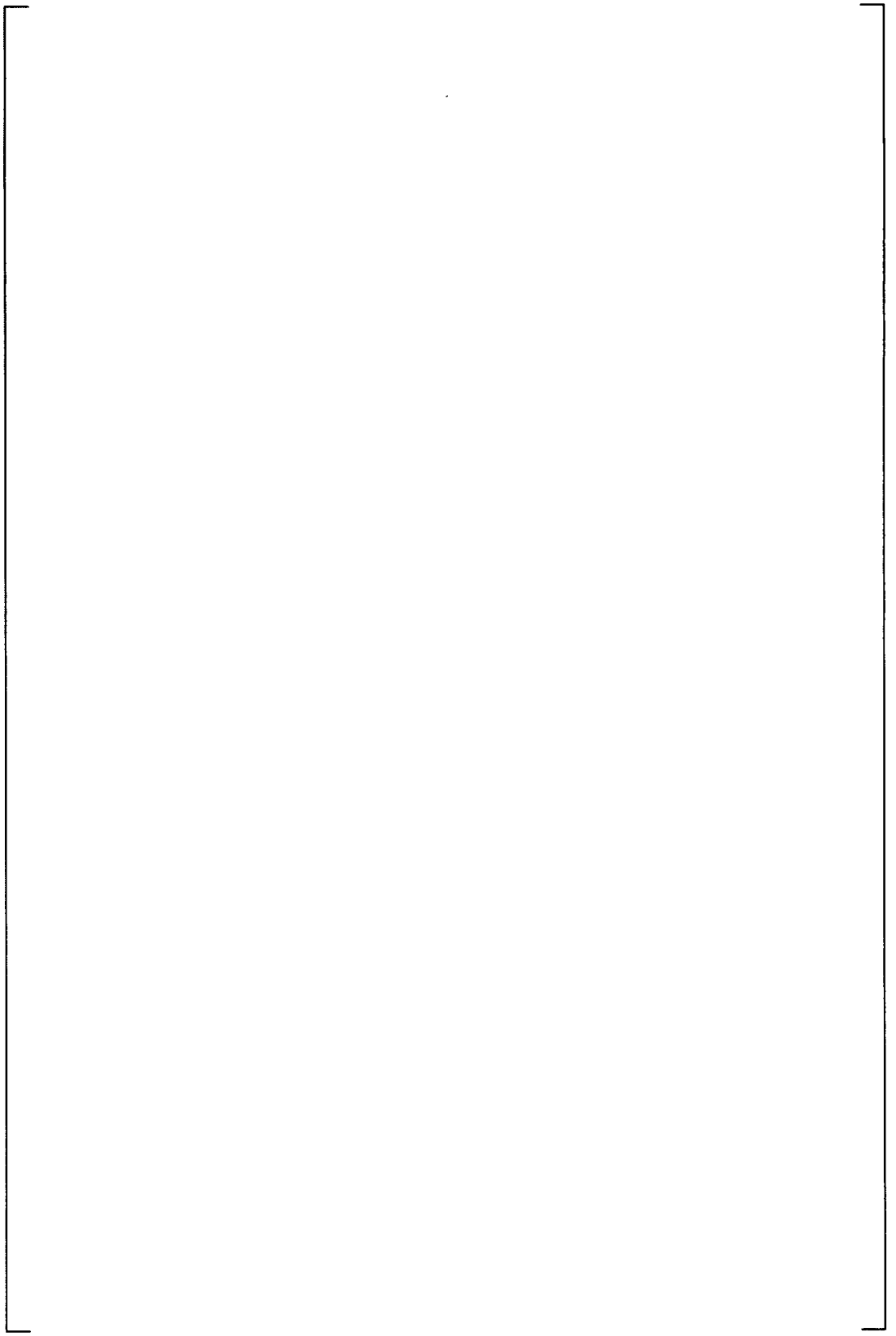

Figure 5-3 FRIGG Loop Test Section

a,c

Figure 5-4 Comparison of Measured and Predicted Dryout Times

6 COMPLIANCE WITH 10 CFR 50 APPENDIX K

This section describes the Westinghouse ABWR ECCS Evaluation Model compliance with the requirements of 10 CFR 50 Appendix K.

6.1 SOURCES OF HEAT DURING THE LOCA

Section I.A of Appendix K:

> *For the heat sources listed in paragraphs I.A.1 to 4 of this appendix it must be assumed that the reactor has been operating continuously at a power level at least 1.02 times the licensed power level (to allow for instrumentation error), with the maximum peaking factor allowed by the technical specifications. An assumed power level lower than the level specified in this paragraph (but not less than the licensed power level) may be used provided the proposed alternative value has been demonstrated to account for uncertainties due to power level instrumentation error. A range of power distribution shapes and peaking factors representing power distributions that may occur over the core lifetime must be studied. The selected combination of power distribution shape and peaking factor should be the one that results in the most severe calculated consequences for the spectrum of postulated breaks and single failures that are analyzed.*

Evaluation Model Compliance with Section I.A:

> Westinghouse may account for power level instrumentation uncertainties less than 2 percent, but no less than the power level uncertainty that has been demonstrated.

6.1.1 Initial Stored Energy in the Fuel

Section I.A.1 of Appendix K:

> *The steady-state temperature distribution and stored energy in the fuel before the hypothetical accident shall be calculated for the burn-up that yields the highest calculated cladding temperature (or, optionally, the highest calculated stored energy.) To accomplish this, the thermal conductivity of the UO2 shall be evaluated as a function of burn-up and temperature, taking into consideration differences in initial density, and the thermal conductance of the gap between the UO2 and the cladding shall be evaluated as a function of the burn-up, taking into consideration fuel densification and expansion, the composition and pressure of the gases within the fuel rod, the initial cold gap dimension with its tolerances, and cladding creep.*

Evaluation Model compliance with Section I.A.1:

> The [
>
>]^{a,c}

[

]^{a,c}

6.1.2 Fission Heat

Section I.A.2 of Appendix K:

> *Fission heat shall be calculated using reactivity and reactor kinetics. Shutdown reactivities resulting from temperatures and voids shall be given their minimum plausible values, including allowance for uncertainties, for the range of power distribution shapes and peaking factors indicated to be studied above. Rod trip and insertion may be assumed if they are calculated to occur.*

Evaluation Model compliance with Section I.A.2:

> Fission heat is calculated by a point kinetics model as described in Section 3.7 of Reference 3. The model includes feedback effects from voiding, Doppler broadening, moderator temperature, and control rod worth. The point kinetics parameters are generated from the nuclear design code PHOENIX for a range of power distributions, peaking factors, and void fractions throughout the fuel life. Conservative values for these parameters, i.e., those which yield the highest fission heat generation, are used in the GOBLIN model. Specifically:
>
> - The delayed neutron fraction (β) will be given its highest calculated value, typically corresponding to the beginning-of-life conditions.
> - The void and Doppler reactivity coefficients will be given their highest calculated value (lowest absolute value).
> - The reactivity worth of the control rods will be given a conservative (low) value.
>
> This methodology and sensitivity studies demonstrating the conservatism of the fission heat generation are provided in Reference 4.

6.1.3 Decay of Actinides

Section I.A.3 of Appendix K:

> *The heat from the radioactive decay of actinides, including neptunium and plutonium generated during operation, as well as isotopes of uranium, shall be calculated in accordance with fuel cycle calculations and known radioactive properties. The actinide decay heat chosen shall be that appropriate for the time in the fuel cycle that yields the highest calculated fuel temperature during the LOCA.*

Evaluation Model compliance with Section I.A.3:

The actinide decay energy release contribution is determined by calculating the equilibrium concentrations of the isotopes U^{239} and Np^{239}, and then using the energy per disintegration and half-life for these isotopes to evaluate the time dependence of the energy release after shutdown. The elements U^{239} and Np^{239} are the only significant activation products that contribute to the decay energy release in the time range of interest for LOCAs. The energy release from the activation products of U^{235} namely U^{236} and U^{237} are insignificant, approximately a factor of 20-30 less, when compared to the energy release of U^{239} and Np^{239} for this range.

The actinide decay power is determined from the decay rate equations described in the American Nuclear Society Standard 5.1 (Reference 9) and is modeled in GOBLIN as the decay power groups 12, 13, and 14 (see Section 3.7.1 of Reference 2).

The U^{239} production per fission, $Cr\sigma_{25}/\sigma f_{25}$, is chosen to yield the highest actinide decay power throughout the fuel life, typically end of life.

6.1.4 Fission Product Decay

Section I.A.4 of Appendix K:

The heat generation rates from radioactive decay of fission products shall be assumed to be equal to 1.2 times the values for infinite operating time in the ANS Standard (Proposed American Nuclear Society Standards--"Decay Energy Release Rates Following Shutdown of Uranium-Fueled Thermal Reactors." Approved by Subcommittee ANS-5, ANS Standards Committee, October 1971). This standard has been approved for incorporation by Reference by the Director of the Federal Register. A copy of the standard is available for inspection at the NRC Library, 11545 Rockville Pike, Rockville, Maryland 20852-2738. The fraction of the locally generated gamma energy that is deposited in the fuel (including the cladding) may be different from 1.0; the value used shall be justified by a suitable calculation.

Evaluation Model compliance with Section I.A.4:

Decay of U^{235} fission products is computed by a relationship in the form of the summation of eleven decay equations. The fission product decay model is described in Section 3.7.1 of Reference 2. Comparison with the tabulated 1971 ANS proposed standard (Reference 9) is shown in Table 3-3 of Reference 2. The agreement is excellent. The local decay heat power calculated by this model is multiplied by 1.2 in accordance with the requirement in paragraph I.A.4. The fraction of gamma energy deposited in the fuel along with gamma and neutron deposition in the coolant may be specified as a function of time through the transient. The actual deposition fractions are described and justified in Reference 3.

6.1.5 Metal-Water Reaction Rate

Section I.A.5 of Appendix K:

> *The rate of energy release, hydrogen generation, and cladding oxidation from the metal/water reaction shall be calculated using the Baker-Just equation (Baker, L., Just, L.C., "Studies of Metal Water Reactions at High Temperatures, III. Experimental and Theoretical Studies of the Zirconium-Water Reaction," ANL-6548, page 7, May 1962). This publication has been approved for incorporation by reference by the Director of the Federal Register. A copy of the publication is available for inspection at the NRC Library, 11545 Rockville Pike, Two White Flint North, Rockville, Maryland 20852-2738. The reaction shall be assumed not to be steam limited. For rods whose cladding is calculated to rupture during the LOCA, the inside of the cladding shall be assumed to react after the rupture. The calculation of the reaction rate on the inside of the cladding shall also follow the Baker-Just equation, starting at the time when the cladding is calculated to rupture, and extending around the cladding inner circumference and axially no less that 1.5 inches each way from the location of the rupture, with the reaction assumed not to be steam limited.*

Evaluation Model compliance with Section I.A.5:

> The heat generation due to local metal-water reaction is considered in the cladding temperature calculation as described in Section 3.7.2 of Reference 2 for GOBLIN and Section 4.4 of Reference 2 for CHACHA. In these models, the reaction between Zircaloy cladding and steam is assumed to follow the parabolic rate law of Baker and Just.

6.1.6 Reactor Internals Heat Transfer

Section I.A.6 of Appendix K:

> *Heat transfer from piping, vessel walls, and non-fuel internal hardware shall be taken into account.*

Evaluation Model compliance with Section I.A.6:

> Heat transfer from piping, vessel walls, and non-fuel internal hardware is accounted for according to the method described in Sections 3.5 and 3.6 of Reference 2.

6.2 SWELLING AND RUPTURE OF THE CLADDING AND FUEL ROD THERMAL PARAMETERS

Section I.B of Appendix K:

> *Each Evaluation Model shall include a provision for predicting cladding swelling and rupture from consideration of the axial temperature distribution of the cladding and from the difference in pressure between the inside and outside of the cladding, both as functions of time. To be acceptable the swelling and rupture calculations shall be based on applicable data in such a way*

that the degree of swelling and incidence of rupture are not underestimated. The degree of swelling and rupture shall be taken into account in calculations of gap conductance, cladding oxidation and embrittlement, and hydrogen generation.

The calculations of fuel and cladding temperatures as a function of time shall use values for gap conductance and other thermal parameters as functions of temperature and other applicable time-dependent variables. The gap conductance shall be varied in accordance with changes in gap dimensions and any other applicable variables.

Evaluation Model compliance with Section I.B:

Section 6.2 of Reference 5 describes the comparison of mechanistic swelling and rupture model to the applicable set of data. Section 4.1 of Reference 6 describes the revision to the Westinghouse BWR LOCA Evaluation Model, which considers burst to occur when [

]^{a,c}

Therefore, neither the incidence of rupture nor the degree of swelling is underestimated.

6.3 BLOWDOWN PHENOMENA

6.3.1 Break Characteristics and Flow

6.3.1.1 Break Spectrum

Section I.C.1.a of Appendix K:

In analyses of hypothetical loss-of-coolant accidents, a spectrum of possible pipe breaks shall be considered. This spectrum shall include instantaneous double-ended breaks ranging in cross-sectional area up to and including that of the largest pipe in the primary coolant system. The analysis shall also include the effects of longitudinal splits in the largest pipes, with the split area equal to the cross-sectional area of the pipe.

Evaluation Model compliance with Section I.C.1.a:

The LOCA sensitivity study topical report (Reference 3) reports the results of a break spectrum analysis including the double-ended guillotine break of the largest pipe in a typical BWR design. A break spectrum analysis is used to justify the selection of the worst case in a plant-specific BWR LOCA analysis.

A similar study for the ABWR design is described in Sections 4.5 and 4.6 of this report. This study includes a series of double-ended guillotine and longitudinal split breaks of the largest pipe connected to the reactor pressure vessel, as well as breaks in other piping connected to the reactor pressure vessel. The break spectrum analysis is used to identify the limiting cases for a plant-specific ABWR LOCA analysis.

6.3.1.2 Discharge Model

Section I.C.1.b of Appendix K:

> *For all times after the discharging fluid has been calculated to be two-phase in composition, the discharge rate shall be calculated by use of the Moody model (F.J. Moody, "Maximum Flow Rate of a Single Component, Two-Phase Mixture," Journal of Heat Transfer, Trans American Society of Mechanical Engineers, 87, No. 1, February, 1965). This publication has been approved for incorporation by reference by the Director of the Federal Register. A copy of this publication is available for inspection at the NRC Library, 11545 Rockville Pike, Rockville, Maryland 20852-2738. The calculation shall be conducted with at least three values of a discharge coefficient applied to the postulated break area, these values spanning the range from 0.6 to 1.0. If the results indicate that the maximum clad temperature for the hypothetical accident is to be found at an even lower value of the discharge coefficient, the range of discharge coefficients shall be extended until the maximum clad temperatures calculated by this variation has been achieved.*

Evaluation Model compliance with Section I.C.1.b:

> The Moody model is used to calculate the two-phase discharge rate. The application and integration of the Moody model into the complete break flow model for all regimes is described in Section 3.3.6 of Reference 2.

6.3.1.3 End of Blowdown

Section I.C.1.c of Appendix K:

> *(Applies Only to Pressurized Water Reactors.) For postulated cold leg breaks, all emergency cooling water injected into the inlet lines or the reactor vessel during the bypass period shall in the calculations be subtracted from the reactor vessel calculated inventory. This may be executed in the calculation during the bypass period, or as an alternative the amount of emergency core cooling water calculated to be injected during the bypass period may be subtracted later in the calculation from the water remaining in the inlet lines, downcomer, and reactor vessel lower plenum after the bypass period. This bypassing shall end in the calculation at a time designated as the "end of bypass," after which the expulsion or entrainment mechanisms responsible for the bypassing are calculated not to be effective. The end-of-bypass definition used in the calculation shall be justified by a suitable combination of analysis and experimental data. Acceptable methods for defining "end of bypass" include, but are not limited to, the following:*
> *(1) Prediction of the blowdown calculation of downward flow in the downcomer for the remainder of the blowdown period; (2) Prediction of a threshold for droplet entrainment in the upward velocity, using local fluid conditions and a conservative critical Weber number.*

Evaluation Model Compliance with Section I.C.1.c:

> This requirement applies only to pressurized water reactors.

6.3.1.4 Noding Near the Break and the ECCS Injection Points

Section I.C.1.d of Appendix K:

> *The noding in the vicinity of and including the broken or split sections of pipe and the points of ECCS injection shall be chosen to permit a reliable analysis of the thermodynamic history in these regions during blowdown.*

Evaluation Model compliance with Section I.C.1.d:

> Reference 3 shows the LOCA peak clad temperature sensitivity to noding near the break for a BWR. These results demonstrate that the break noding used in the evaluation model is sufficient to adequately represent the hydraulic behavior and reactor vessel geometry in the vicinity of the break.
>
> Noding near the break in the ABWR LOCA analysis is similar to that used in the BWR LOCA analysis. Since the PCT for an ABWR occurs as a result of the rapid coastdown of the reactor internal pumps, the resulting PCT is less sensitive to break modeling than for a BWR.

6.3.2 Frictional Pressure Drops

Section I.C.2 of Appendix K:

> *The frictional losses in pipes and other components including the reactor core shall be calculated using models that include realistic variation of friction factor with Reynolds number, and realistic two-phase friction multipliers that have been adequately verified by comparison with experimental data, or models that prove at least equally conservative with respect to maximum clad temperature calculated during the hypothetical accident. The modified Baroczy correlation (Baroczy, C. J., "A Systematic Correlation for Two-Phase Pressure Drop," Chem. Enging. Prog. Symp. Series, No. 64, Vol. 62, 1965) or a combination of the Thom correlation (Thom, J.R.S., "Prediction of Pressure Drop During Forced Circulation Boiling of Water," Int. J. of Heat & Mass Transfer, 7, 709-724, 1964) for pressures equal to or greater than 250 psia and the Martinelli-Nelson correlation (Martinelli, R. C. Nelson, D.B., "Prediction of Pressure Drop During Forced Circulation Boiling of Water," Transactions of ASME, 695-702, 1948) for pressures lower than 250 psia is acceptable as a basis for calculating realistic two-phase friction multipliers.*

Evaluation Model compliance with Section I.C.2:

> The frictional losses are calculated using models that include a realistic variation of the friction factor with Reynolds number and realistic two-phase friction multipliers that are based on acceptable open literature correlations and test data as described in Section 3.3.3 of Reference 2.

6.3.3 Momentum Equation

Section I.C.3 of Appendix K:

> *The following effects shall be taken into account in the conservation of momentum equation: (1) temporal change of momentum, (2) momentum convection, (3) area change momentum flux, (4) momentum change due to compressibility, (5) pressure loss resulting from wall friction, (6) pressure loss resulting from area change, and (7) gravitational acceleration. Any omission of one or more of these terms under stated circumstances shall be justified by comparative analyses or by experimental data.*

Evaluation Model compliance with Section I.C.3:

> The momentum equation used in GOBLIN includes all of the required effects as described in Section 3.1.3 of Reference 2 and Section 4.2 of Reference 5.

6.3.4 Critical Heat Flux

Section I.C.4 of Appendix K:

a. *Correlations developed from appropriate steady-state and transient-state experimental data are acceptable for use in predicting the critical heat flux during LOCA transients. The computer programs in which these correlations are used shall contain suitable checks to assure that the physical parameters are within the range of parameters specified for use of the correlations by their respective authors.*

b. *Steady-state CHF correlations acceptable for use in LOCA transients include, but are not limited to, the following:*

   (1) *W 3. L. S. Tong, "Prediction of Departure from Nucleate Boiling for an Axially Non-uniform Heat Flux Distribution," Journal of Nuclear Energy, Vol. 21, 241-248, 1967.*

   (2) *B&W-2. J. S. Gellerstedt, R. A. Lee, W. J. Oberjohn, R. H. Wilson, L. J. Stanek, "Correlation of Critical Heat Flux in a Bundle Cooled by Pressurized Water," Two-Phase Flow and Heat Transfer in Rod Bundles, ASME, New York, 1969.*

   (3) *Hench-Levy. J. M. Healzer, J. E. Hench, E. Janssen, S. Levy, "Design Basis for Critical Heat Flux Condition in Boiling Water Reactors," APED-5186, GE Company Private report, July 1966.*

   (4) *Macbeth. R. V. Macbeth, "An Appraisal of Forced Convection Burnout Data," Proceedings of the Institute of Mechanical Engineers, 1965-1966.*

(5) *Barnett. P. G. Barnett, "A Correlation of Burnout Data for Uniformly Heated Annuli and Its Uses for Predicting Burnout in Uniformly Heated Rod Bundles," AEEW-R-463, 1966.*

(6) *Hughes. E. D. Hughes, "A Correlation of Rod Bundle Critical Heat Flux for Water in the Pressure Range 150 to 725 psia," IN-1412, Idaho Nuclear Corporation, July 1970.*

c. *Correlations of appropriate transient CHF data may be accepted for use in LOCA transient analyses if comparisons between the data and the correlations are provided to demonstrate that the correlations predict values of CHF which allow for uncertainty in the experimental data throughout the range of parameters for which the correlations are to be used. Where appropriate, the comparisons shall use statistical uncertainty analysis of the data to demonstrate the conservatism of the transient correlation.*

d. *Transient CHF correlations acceptable for use in LOCA transients include, but are not limited to, the following:*

(1) *GE transient CHF. B. C. Slifer, J. E. Hench, "Loss-of-Coolant Accident and Emergency Core Cooling Models for General Electric Boiling Water Reactors," NEDO-10329, General Electric Company, Equation C-32, April 1971.*

e. *After CHF is first predicted at an axial fuel rod location during blowdown, the calculation shall not use nucleate boiling heat transfer correlations at that location subsequently during the blowdown even if the calculated local fluid and surface conditions would apparently justify the reestablishment of nucleate boiling. Heat transfer assumptions characteristic of return to nucleate boiling (rewetting) shall be permitted when justified by the calculated local fluid and surface conditions during the reflood portion of a LOCA.*

Evaluation Model compliance with Section I.C.4:

The critical heat flux in the system and hot assembly analyses is determined using an NRC-approved CPR correlation that is applicable to the fuel design.

6.3.5 Post-CHF Heat Transfer Correlations

Section I.C.5 of Appendix K:

a. *Correlations of heat transfer from the fuel cladding to the surrounding fluid in the post-CHF regimes of transition and film boiling shall be compared to applicable steady-state and transient-state data using statistical correlation and uncertainty analyses. Such comparison shall demonstrate that the correlations predict values of heat transfer co-efficient equal to or less than the mean value of the applicable experimental heat transfer data throughout the range of parameters for which the correlations are to be used. The comparisons shall quantify the relation of the correlations to the statistical uncertainty of the applicable data.*

b. *The Groeneveld flow film boiling correlation (equation 5.7 of D.C. Groeneveld, "An Investigation of Heat Transfer in the Liquid Deficient Regime," AECL-3281, revised December 1969) and the Westinghouse correlation of steady-state transition boiling ("Proprietary Redirect/Rebuttal Testimony of Westinghouse Electric Corporation," USNRC Docket RM-50-1, page 25-1, October 26, 1972) are acceptable for use in the post-CHF boiling regimes. In addition, the transition boiling correlation of McDonough, Milich, and King (J.B. McDonough, W. Milich, E.C. King, "An Experimental Study of Partial Film Boiling Region with Water at Elevated Pressures in a Round Vertical Tube," Chemical Engineering Progress Symposium Series, Vol. 57, No. 32, pages 197-208, (1961) is suitable for use between nucleate and film boiling. Use of all these correlations is restricted as follows:*

   (1) *The Groeneveld correlation shall not be used in the region near its low-pressure singularity,*

   (2) *The first term (nucleate) of the Westinghouse correlation and the entire McDonough, Milich, and King correlation shall not be used during the blowdown after the temperature difference between the clad and the saturated fluid first exceeds 300°F,*

   (3) *Transition boiling heat transfer shall not be reapplied for the remainder of the LOCA blowdown, even if the clad superheat returns below 300°F, except for the reflood portion of the LOCA when justified by the calculated local fluid and surface conditions.*

c. *Evaluation Models approved after October 17, 1988, which make use of the Dougall-Rohsenow flow film boiling correlation (R.S. Dougall and W.M. Rohsenow, "Film Boiling on the Inside of Vertical Tubes with Upward Flow of Fluid at Low Qualities," MIT Report Number 9079 26, Cambridge, Massachusetts, September 1963) may not use this correlation under conditions where nonconservative predictions of heat transfer result. Evaluation Models that make use of the Dougall-Rohsenow correlation and were approved prior to October 17, 1988, continue to be acceptable until a change is made to, or an error is corrected in, the Evaluation Model that results in a significant reduction in the overall conservatism in the Evaluation Model. At that time continued use of the Dougall-Rohsenow correlation under conditions where nonconservative predictions of heat transfer result will no longer be acceptable. For this purpose, a significant reduction in the overall conservatism in the Evaluation Model would be a reduction in the calculated peak fuel cladding temperature of at least 50°F from that which would have been calculated on October 17, 1988, due either to individual changes or error corrections or the net effect of an accumulation of changes or error corrections.*

Evaluation Model compliance with Section I.C.5:

The heat transfer correlations and regimes modeled in GOBLIN are described in Section 3.5 of Reference 2. The post-CHF convective heat transfer coefficient is calculated using the Groeneveld 5.7 correlation, the NRC-approved Westinghouse upper-head injection correlation, the modified Bromley correlation, and single-phase steam correlations. The Groeneveld

correlation is used for flow film boiling in the higher pressure range. For lower pressures, where the Groeneveld correlation has a singularity, a transition is made to the Westinghouse UHI correlation. This NRC-approved correlation is more conservative than the Dougall-Rohsenow correlation, which is non-conservative when compared to some heat transfer data.

The lower limit to the heat transfer coefficient is calculated using the modified Bromley correlation, which is based on zero flow. The modified Bromley correlation has been demonstrated to be a conservative lower limit when compared to a wide range of tests. A more detailed discussion of the applicability of this correlation is given Section 6.1.7 of Reference 2.

Once dryout is calculated to occur, the heat transfer mode is forced to remain in the post-dryout regime, even if rewet and transition boiling are calculated to occur.

6.3.6 Pump Modeling

Section I.C.6 of Appendix K:

The characteristics of rotating primary system pumps (axial flow, turbine, or centrifugal) shall be derived from a dynamic model that includes momentum transfer between the fluid and the rotating member, with variable pump speed as a function of time. The pump model resistance used for analysis should be justified. The pump model for the two-phase region shall be verified by applicable two-phase pump performance data. For BWR's after saturation is calculated at the pump suction, the pump head may be assumed to vary linearly with quality, going to zero for one percent quality at the pump suction, so long as the analysis shows that core flow stops before the quality at pump suction reaches one percent.

Evaluation Model compliance with Section I.C.6:

The recirculation pump model is described in Section 3.4.1 of Reference 2 and Section 3.4.1 of this report. An angular momentum balance is solved for the pump, including all contributing torques. Single-phase and degraded two-phase pump performance are modeled through user-specified performance curves.

6.3.7 Core Flow Distribution During Blowdown

Applies only to pressurized water reactors.

6.4 POST-BLOWDOWN PHENOMENA; HEAT REMOVAL BY THE ECCS

6.4.1 Single Failure Criterion

Section I.D.1 of Appendix K:

> *An analysis of possible failure modes of ECCS equipment and of their effects on ECCS performance must be made. In carrying out the accident evaluation the combination of ECCS subsystems assumed to be operative shall be those available after the most damaging single failure of ECCS equipment has taken place.*

Evaluation Model compliance with Section I.D.1:

> The evaluation of the LOCA is performed assuming the single active component failure that results in the most severe consequences. The combinations of ECC subsystems assumed to be operating are those remaining after the component failure has occurred.
>
> In an ABWR, no single active failure of ECCS equipment results in an extended uncovery of the core. The limiting single failure is determined as the one that results in the least transient system inventory.

6.4.2 Containment Pressure

Section I.D.2 of Appendix K:

> *The containment pressure used for evaluating cooling effectiveness during reflood and spray cooling shall not exceed a pressure calculated conservatively for this purpose. The calculation shall include the effects of operation of all installed pressure-reducing systems and processes.*

Evaluation Model compliance with Section I.D.2:

> The ABWR Evaluation Model will assume atmospheric pressure in the containment analysis throughout the LOCA transient.

6.4.3 Calculation of Reflood Rate

Applies only to Pressurized Water Reactors.

6.4.4 Steam Interaction with Emergency Core Cooling Water

Applies only to Pressurized Water Reactors.

6.4.5 Refill and Reflood Heat Transfer

Applies only to Pressurized Water Reactors.

6.4.6 Convective Heat Transfer Coefficients for Boiling Water Reactor Fuel Rods Under Spray Cooling

Section I.D.6 of Appendix K:

Following the blowdown period, convective heat transfer shall be calculated using coefficients based on appropriate experimental data. For reactors with jet pumps and having fuel rods in a 7 x 7 fuel assembly array, the following convective coefficients are acceptable:

- *During the period following lower plenum flashing but prior to the core spray reaching rated flow, a convective heat transfer coefficient of zero shall be applied to all fuel rods.*
- *During the period after core spray reaches rated flow but prior to reflooding, convective heat transfer coefficients of 3.0, 3.5, 1.5, and 1.5 Btu-hr^{-1}-ft^{-2}°F-1 shall be applied to the fuel rods in the outer corners, outer row, next to outer row, and to those remaining in the interior, respectively, of the assembly.*
- *After the two-phase reflooding fluid reaches the level under consideration, a convective heat transfer coefficient of 25 Btu-hr-1^{-ft}-2°F^{-1} shall be applied to all fuel rods.*

Evaluation Model compliance with Section I.D.6:

This requirement applies to BWRs with jet pumps. The ABWR has internal recirculation pumps with the feedwater nozzles representing the lowest of the large piping systems connected to the reactor pressure vessel. As a result, the ABWR LOCA transient does not experience the same phenomena as a BWR in that the ABWR core does not experience extended uncovery during the event, even for the most limiting break location and single failure. The PCT is predicted to occur early in the transient when the reactor internal pumps coastdown due to their loss of motive power. The two-phase convective heat transfer coefficients predicted by GOBLIN will be used in the rod heatup calculation.

6.4.7 The Boiling Water Reactor Channel Box Under Spray Cooling

Section I.D.7 of Appendix K:

Following the blowdown period, heat transfer from, and wetting of, the channel box shall be based on appropriate experimental data. For reactors with jet pumps and fuel rods in a 7 x 7 fuel assembly array, the following heat transfer coefficients and wetting time correlation are acceptable.

- *During the period after lower plenum flashing, but prior to core spray reaching rated flow, a convective coefficient of zero shall be applied to the fuel assembly channel box.*
- *During the period after core spray reaches rated flow, but prior to wetting of the channel, a convective heat transfer coefficient of 5 Btu-hr-1-ft-2-°F-1 shall be applied to both sides of the channel box.*

- *Wetting of the channel box shall be assumed to occur 60 seconds after the time determined using the correlation based on the Yamanouchi analysis ("Loss-of-Coolant Accident and Emergency Core Cooling Models for General Electric Boiling Water Reactors," General Electric Company Report NEDO-10329, April 1971). This report was approved for incorporation by reference by the Director of the Federal Register. A copy of the report is available for inspection at the NRC Library, 11545 Rockville Pike, Rockville, Maryland 20852-2738.*

Evaluation Model compliance with Section I.D.7:

This requirement applies to BWRs with jet pumps. The ABWR has internal recirculation pumps with the feedwater nozzles representing the lowest of the large piping systems connected to the reactor pressure vessel. As a result, the ABWR LOCA transient does not experience the same phenomena as a BWR in that the extended uncovery of the core is not predicted during the transient and the channel box remains wet throughout the transient.

7 REFERENCES

1. RPB 90-93-P-A, "Boiling Water Reactor Emergency Core Cooling System Evaluation Model: Code Description and Qualification," October 1991.

2. CENPD-300-P-A, "Reference Safety Report for Boiling Water Reactor Reload Fuel," July 1996.

3. RPB 90-94-P-A, "Boiling Water Reactor Emergency Core Cooling System Evaluation Model: Code Sensitivity," October 1991.

4. CENPD-283-P-A, "Boiling Water Reactor Emergency Core Cooling System Evaluation Model: Code Sensitivity for SVEA-96 Fuel," July 1996.

5. CENPD-293-P-A, "BWR ECCS Evaluation Model: Supplement 1 to Code Description and Qualification," July 1996.

6. WCAP-15682-P-A, "Westinghouse BWR ECCS Evaluation Model: Supplement 2 to Code Description, Qualification and Application," April 2003.

7. WCAP-16078-P-A, "Westinghouse BWR ECCS Evaluation Model: Supplement 3 to Code Description, Qualification and Application to SVEA-96 Optima2 Fuel," November 2004.

8. WCAP-16081-P-A, "10x10 SVEA Fuel Critical Power Experiments and CPR Correlation: SVEA-96 Optima2," March 2005.

9. ANS-5.1 1973 Decay Energy Release Rates Following Shutdown of Uranium-Fueled Thermal Reactors, Draft ANS-5.1 / N18.6, October 1973.

10. Code of Federal Regulations, 10 Part 50, Office of the Federal Register, National Archives and Records Administration, 1986.

APPENDIX A
ROADMAP TO THE METHODOLOGY CHANGES

A.1 INTRODUCTION

The original BWR LOCA Evaluation Model, USA1, which was approved by the NRC in 1989, is described in RPB 90-93-P-A (Reference A-1) and RPB 90-94-P-A (Reference A-2). This methodology was revised in 1996 with the USA2 Evaluation Model, described in CENPD-283-P-A (Reference A-3) and CENPD-293-P-A (Reference A-4); in 2003 with the USA4 Evaluation Model described in WCAP-15682-P-A (Reference A-5); and in 2004 with USA5 Evaluation Model described in WCAP-16078-P-A (Reference A-6). The USA6 Evaluation Model is described in WCAP-16865-P (Reference A-7), which was withdrawn in February 2009. WCAP-16865-P has been revised and will be resubmitted for review and approval in late 2009. All of the documents mentioned above apply only to BWRs.

The Evaluation Model described in this report, USA7, pertains to ABWR applications. Because of the unique features of the ABWR, approval of the USA6 Evaluation Model is not required for ABWR applications.

A.2 MAJOR ASPECTS OF THE EVALUATION MODEL

A.2.1 Momentum Equation

As described in Reference A-4, Section 4.2:

> The spatial acceleration term in the momentum equation has been modified to account more accurately for uneven velocities of water and steam. This change has insignificant effects on typical LOCA transients and has been introduced to improve the consistency of the fluid flow model as shown in Section 7.4 of Reference A-4. The new formulation was assessed and qualified by repeating pertinent cases in the GOBLIN qualification.

Per the NRC SER of Reference A-4:

> The Technical Evaluation attached to the SER acknowledged the change to the momentum equation and cited a study showing that the GOBLIN code with the new formulation resulted in an early prediction of dryout time and in a slightly higher temperature than in old analysis. No limitations or conditions were placed upon the use of this modification.

A.2.2 Countercurrent Flow Limitation (CCFL) Model

As described in Reference A-3, Section 7.1:

> The BWR LOCA Evaluation Model has a comprehensive CCFL model for determining the rate of liquid drainage into the SVEA-96 fuel assembly. The correlation is documented in Reference A-1, Section 3.3. The CCFL correlation was originally developed for 8 x 8 fuel

assemblies. Since its original development, the correlation has been generalized and validated for many geometries. Further, the correlation, with its general geometric dependence, has been confirmed valid for QUAD+ fuel through comparisons with experimental data (see response to Question 8 in Reference A-1). The SVEA-96 geometry is basically the same as the SVEA-64 and QUAD+ geometry. Differences in area of the flow restrictions are accounted for in the CCFL correlation. In the LOCA Evaluation Model, the CCFL correlation with the appropriate geometric parameters for SVEA-96 fuel will be used.

Per the NRC SER of Reference A-3:

> The coefficients in the CCFL correlation that were shown to be insensitive for the SVEA-96 fuel should not be extended to other fuels without being validated by experimental data.
>
> In addition, Westinghouse was required to demonstrate the acceptability the CCFL coefficient in any instance when the calculated PCT is greater than 2100°F. In this case, the CCFL correlation shall include a conservative bias that bounds the scatter in the database. The bias introduced to the base CCFL correlation will be such that conservative bounding predictions are obtained from the database of all fuel assembly components that were used to derive the basic CCFL correlation.

As described in Reference A-6, Section 5.4.2:

> The change to the CCFL model removes the restriction placed on the USA2 Evaluation Model. This change was made to the CCFL correlation to apply a conservative bias such that it bounds all scatter in the correlation database.
>
> The present CCFL correlation replaces the wetted perimeter term in one of the correlation coefficients with one composed of an effective diameter relation that is a function of the local cross-sectional flow area. The more restrictive effective diameter relation better represents the observed data and eliminates the restriction placed on earlier versions of the Evaluation Model.
>
> To qualify the applicability of the modified CCFL model to SVEA-96 Optima2 fuel, Westinghouse performed a sensitivity study demonstrating the effect of the new fuel design and the modified CCFL correlation on the overall LOCA response.

Per the NRC SER of Reference A-6:

> The staff concurred that the change to the CCFL acts in the same manner as the imposed restriction required by the SER of Reference A-3 and found that the CCFL model with appropriate geometric parameters is acceptable for applications involving SVEA-96, SVEA-96+, and SVEA-96 Optima2 fuel designs.

A.2.3 Two-Phase Level Tracking

The GOBLIN code has the capability to specify a series of control volumes in which a two-phase level is to be calculated and tracked with time. The level tracking model replaces a fixed control volume boundary with a moving boundary located at the two-phase level. The model can be used when it is important to know the location of the two-phase mixture level.

As described in Reference A-3, Section 6.1.2:

> As a result of a sensitivity study on the use of level tracking in the upper plenum, it was determined that it is conservative to deactivate the level tracking option, and that the additional accuracy of tracking the upper plenum level is not warranted.

Per the NRC SER of Reference A-3:

> The TER attached to the SER acknowledged the level tracking sensitivity study. The SER made no limitations or conditions regarding the use of level tracking in the upper plenum.

As described in Reference A-6, Section 5.1.1:

> The level tracking model calculates the motion of the control volume interface such that it moves with the two-phase mixture level. The intent of the level tracking model is to capture the transient interaction of the mixture level with flow paths or with ECCS injection when it is impractical to do so by additional noding detail. Sensitivity studies were presented on the level tracking feature in Section 4.1.3 of RPB 90-94-P-A (Reference A-2) and Section 6.1.2 of CENPD-283-P-A (Reference A-3). The focus of these sensitivity studies was the use of level tracking in the upper plenum. Section 6.1.2 of CENPD-283-P-A (Reference A-3) provided the basis for not using the level tracking feature in the upper plenum.
>
> The focus of the sensitivity study presented in this section is on the use of level tracking in the lower plenum. Cases were run with the level tracking feature activated and deactivated in the lower plenum. The results were virtually identical. Because level tracking in the lower plenum does not affect the timing of these key events, the heat transfer coefficients that are used to determine the cladding temperature response of the hot plane will be identical. As a result, the cladding temperature response will also be identical. This sensitivity shows that the use of the level tracking feature in the lower plenum is not warranted. Therefore, standard practice will be to not use level tracking in the lower plenum of the USA5 Evaluation Model unless warranted by the specific application.
>
> However, level tracking remains an option to capture important thermal-hydraulic phenomena when it is not practical to do so with fixed control volumes. Level tracking continues to be used in the reactor vessel annulus to ensure that conditions upstream of the break are determined correctly.

Per the NRC SER of Reference A-6:

> The SER indicated that the use of the optional level tracking model in the lower plenum of the GOBLIN vessel model is acceptable.

A.2.4 Convective Spray Heat Transfer Coefficients

As described in Reference A-3, Section 4.3:

> Convective spray heat transfer coefficients as specified in 10 CFR 50 Appendix K are applicable for 7 x 7 fuel designs. Convective heat transfer coefficients have been derived for open lattice 8 x 8, SVEA-64/QUAD+ fuel from the coefficients prescribed in 10 CFR 50 Appendix K. These coefficients also were confirmed by experimental tests for 8 x 8 and SVEA-64/QUAD+. An extension of this application provides spray heat transfer coefficients for SVEA-96 fuel.
>
> The approved values of convective heat transfer coefficients per Reference A-3 are presented in Table A-2.

Per the NRC SER of Reference A-3:

> The SER concurred with the procedure to show conservatism in the method used to determine the spray cooling heat transfer coefficients. However, since the procedure was not supported by experimental data, it should not be extended to other fuels without experimental verification.

As described in Reference A-6, Section 6.1.1:

> The convective spray heat transfer coefficients described in Section 7.2 of CENPD-283-P-A (Reference A-3) are applied without modification to analyses determining the hot plane heatup response for a reactor containing SVEA-96 Optima2 fuel. The spray cooling heat transfer coefficients are given in Table A-3.

Per the NRC SER of Reference A-6:

> Because of the similarity of the lattice layout to the SVEA-96/96+ fuel design, the staff found applying SVEA-64 spray coefficients to the Optima2 fuel to be conservative and acceptable.

A.2.5 Critical Power Ratio (CPR) Correlation

As described in Reference A-3, Section 4.2:

> The SVEA-96 CPR correlation was developed through a full-scale thermal-hydraulic verification program in the ABB Atom FRIGG loop. The resultant correlation is documented in Reference A-7, which has been approved by the U.S. NRC. This correlation, denoted by XL-S96, is implemented into the GOBLIN/DRAGON code. The implementation is analogous to the previous approved QUAD+ CPR correlation application.

Per the NRC SER of Reference A-3:

> The SER (Reference A-8) on UR-89-210-P-A (Reference A-7) approved the use of the XL-S96 CPR correlation with the BISON computer code. However, Reference A-8 requires that when this correlation is implemented in other computer codes, the vendor must submit documentation of adequate implementation to the NRC. The SER also requires that the correlation be used to evaluate the SVEA-96 fuel assemblies for the revised range of applicability.
>
> The adequacy of implementation of the XL-S96 CPR correlation into the GOBLIN series will be reviewed with CENPD-293-P (Reference A-4), because this version of GOBLIN/DRAGON/ CHACHA-3C was viewed to be an intermediary state.

As described in Reference A-4, Section 4.1:

> A CPR correlation using the critical quality-boiling length formulation has been introduced in the thermal-hydraulic code system GOBLIN/DRAGON.
>
> The GEXL correlation, also described in Reference A-7, is chosen as the basis for all critical quality-boiling length type CPR correlations. The implementation of this base correlation is described in Section 4.1.2 of Reference A-4. As a sample case of the critical quality-boiling length CPR correlation, the implementation of the XL-S96 correlation is described in Section 4.1.3 of Reference A-4, and verification of proper implementation of the correlation is given in Section 7.1 of Reference A-4.

Per the NRC SER of Reference A-4:

> The SER placed a condition on the use of the XL-S96 CPR correlation requiring that it be subject to the SER conditions in UR 89-210-P-A (Reference A-7) and Reference A-8.

As described in Reference A-6, Section 5.4.1:

> CPR correlations are part of the heat transfer model in GOBLIN and DRAGON. The CPR correlation is used to determine the initial power of the hot assembly. The CPR correlation may also determine when boiling transition occurs during the LOCA transient if the fluid conditions are within the range of applicability of the correlation. The Westinghouse USA5 BWR ECCS Evaluation Model will use the SVEA-96 Optima2 CPR correlation that is approved by the NRC for applications involving the SVEA-96 Optima2 fuel design.
>
> An NRC-approved CPR correlation that is applicable to the fuel-design being analyzed is used in the ECCS Evaluation Model RPB 90-93-P-A (Reference A-1). At the time this topical report was written, the CPR correlation for SVEA-96 Optima2 had not been approved by the NRC. Qualification of the SVEA-96 Optima2 CPR correlation was subsequently provided. The CPR correlation was installed in the GOBLIN code in accordance with the process described in Section 3.3.2.2 of Reference A-6 and has been used for licensing. The NRC will be informed of the resulting change to the GOBLIN code via the 10 CFR 50.46 reporting process.

Per the NRC SER of Reference A-6:

> The SER indicated that the SVEA-96 Optima2 CPR correlation was being reviewed by the staff. After it is approved, Westinghouse may implement it into the USA5 EM model and report to the NRC through the 10 CFR 50.46 annual report process.
>
> A new fuel design normally requires a specific CPR correlation approved by the NRC. The implementation of a new CPR correlation into GOBLIN has become a routine code update process, which includes the source code development, new CPR correlation validation, and non-Westinghouse fuel justifications. Westinghouse requested that this process be evaluated through the 10 CFR 50.46 annual report process. Therefore, the staff does not necessarily review the details of the implementation process. The staff has previously reviewed the proposed process from Reference 10 and determined that the requested process is acceptable as long as the new CPR correlation has been approved by the NRC and the change to the LOCA method is reported to the NRC through the 10 CFR 50.46 reporting process.
>
> For version USA5, the currently approved CPR correlations (i.e., XL-S96, ABBD1.0, ABBD2.0) can still be used within the approved ranges of applicability. However, the new CPR correlation for SVEA-96 Optima2 fuel has not yet been approved by the NRC. Therefore, the current version of the SVEA-96 Optima2 fuel CPR correlation in USA5 cannot be used until it has received the approval of the staff.
>
> On December 9, 2004, the NRC staff issued its safety evaluation (SE) approving Topical Report WCAP-16081-P-A, "10x10 SVEA Fuel Critical Power Experiments and CPR Correlation: SVEA-96 Optima2." As provided in the FSER for NRC license amendments issued on April 4, 2006 for the transition of the Quad Cities and Dresden units to Westinghouse Fuel, the NRC staff verified that all the conditions and limitations of the NRC-approved BWR LOCA methods were satisfied for this application.

A.2.6 Fuel Rod Conduction Model

As described in Reference A-4, Section 5.1:

> The fuel rod conduction model described in Section 4.1 of Reference A-1 is unchanged. An optional feature is added to explicitly model the heat resistance due to crud on the cladding surface. The effective outside surface heat transfer coefficient is a function of the previous coefficient, the depth of the crud layer, and the thermal conductivity of the crud layer.
>
> The depth of the crud layer is calculated using an NRC-approved fuel rod performance code and the thermal conductivity of crud used is consistent with the fuel performance code properties. For example, applications in the foreseen future shall use a crud depth from the STAV6.2 code and a crud thermal conductivity of 0.5 (W/m/°K), which is also consistent with STAV6.2.

Per the NRC SER of Reference A-4:

> The Technical Evaluation attached to the SER acknowledged the addition of the crud resistance model. The SER placed no limitations or conditions on its use.

As described in Reference A-6, Section 5.5.2.3:

> A model has been introduced in the STAV7.2 code to describe the burnup-induced degradation of the fuel pellet conductivity. This model has replaced the STAV6.2 fuel pellet conductivity model in CHACHA-3D.

Per the NRC SER of Reference A-6:

> The SER acknowledged the addition of the revised fuel pellet conductivity model but placed a condition upon its use until the NRC approval of the STAV7.2 code was complete. Westinghouse provided a letter to the NRC (Reference A-9), as required by the condition, after NRC approval of the STAV7.2 code was complete. The letter indicated that the applicable STAV7.2 models have been implemented in CHACHA-3D.

A.2.7 Heat Generation Model

As described in Reference A-4, Section 5.2:

> The heat generation model, as described in Section 4.3 of Reference A-4, is unchanged except for the radial power distribution within the fuel pellet, and will be supplied from the appropriate NRC-approved fuel performance code. For example, results from the STAV6.2 code will be used as input to CHACHA-3. In addition, options are available in CHACHA-3 to assume a uniform radial power distribution, or a Bessel function based radial power distribution.

Per the NRC SER of Reference A-4:

> The Technical Evaluation attached to the SER acknowledged the use of the uniform radial power distribution model and the Bessel function model in CHACHA. No conditions or limitations were placed upon their use in the SER.

As described in Reference A-6, Section 5.5.2.3:

> The burnup-dependent TUBRNP model in STAV7.2 has been implemented in CHACHA-3D and will be used in the USA5 Evaluation Model. This model takes into account power generation by plutonium isotopes, resulting in a more precise radial power distribution in the pellet rim region.

Per the NRC SER of Reference A-6:

> The SER acknowledged the change to the pellet heat generation model, but placed a condition upon its use until NRC approval of the STAV7.2 code was complete. Westinghouse provided a letter to the NRC (Reference A-9), as required by the condition, after NRC approval of the STAV7.2 code was complete. The letter indicated that the applicable STAV7.2 models have been implemented in CHACHA-3D.

A.2.8 Metal-Water Reaction

As described in Reference A-4, Section 5.3:

> The metal-water reaction model remains unchanged from that described in Section 4.4 of Reference A-1. The initial oxide depth on the cladding outer surface is calculated using an NRC-approved fuel performance code. For example, the STAV6.2 code (Reference A-10) will replace the PAD fuel rod performance code, identified in Reference A-2.

Per the NRC SER of Reference A-4:

> The NRC SER indicated that acceptance of this change should be determined in the review of CENPD-285-P (Reference A-10). The NRC SER of Reference A-10 placed no restrictions on the use of the initial oxide depth except for limiting the rod average burnup range of STAV6.2 to 50 GWd/MTU.

As described in Reference A-6, Section 5.5.2.3:

> The initial oxide depth of the cladding outer surface is determined by the STAV7.2 fuel performance code.

Per the NRC SER of Reference A-6:

> The SER acknowledged the change from STAV6.2 to STAV7.2, but placed a condition on the use of this feature in that it could not be used until the staff's review of STAV7.2 (Reference A-11) was complete. The SER of Reference A-11 did not place any condition on the use of STAV7.2 except for limiting the rod average burnup range of STAV7.2 to 62 GWd/MTU. Westinghouse provided a letter to the NRC (Reference A-9), as required by the condition, after NRC approval of the STAV7.2 code was complete.

A.2.9 Thermal Radiation Model

As described in Reference A-4, Section 5.4:

> The basic model of thermal radiation, as described in Section 4.5 and 4.5.1 of Reference A-1, remains unchanged.
>
> The gray body factors used in the radiation model are still calculated with the BILBO code as described in Section 4.5.2 of Reference A-1. However, the gray body factors are now calculated throughout the transient. To facilitate this, the BILBO code has been incorporated into CHACHA-3. The change was done to make the radiation model consistent with the new rod deformation model (described in Section 5.6 of Reference A-4), which calculates individual time-dependent dimensions for each fuel rod. The gray body factors are first calculated by BILBO at the beginning of the CHACHA-3 calculation using the initial geometry. They are updated transiently when a significant change in geometry or emissivity has occurred.

Per the NRC SER of Reference A-4:

> The SER acknowledged the change to the CHACHA code and placed no limitations or conditions on the use of the change.

A.2.10 Gas Plenum Temperature and Pressure Model

As described in Reference A-6, Section 5.5.1:

> The detailed fuel heatup computer code (CHACHA-3D) has been revised to provide a new plenum type that permits a conservative prediction of the plenum temperature of the PLRs. For this plenum type, the gas temperature in the rod plenum is determined conservatively by equating it to the maximum of the plenum cladding outer surface temperature, which is calculated in the hot channel analysis, and the gas temperature determined using the conventional plenum model.

Per the NRC SER of Reference A-6:

> The SER acknowledged the new PLR plenum model and found it acceptable. No limitations or conditions were placed on its use.

A.2.11 Pellet-Cladding Gap Heat Transfer Model

As described in Reference A-4, Section 5.5:

> Due to the replacement of the PAD code with the STAV6.2 code, the pellet-cladding gap heat transfer model in the original CHACHA code was replaced with that from the STAV6.2 code with one modification. The contact conductance term is neglected in the CHACHA model to ensure conservatism when the clad and fuel are computed to be in contact.

Per the NRC SER of Reference A-4:

> Because the model was identical to that in STAV6.2, a detailed review of this model was not performed because it was to be done as part of the review of CENPD-285-P (Reference A-10). The SER for CENPD-285-P-A did not place any restriction on the use of the STAV6.2 gap heat transfer model except for the limitation to a rod average burnup of 50 GWd/MTU.

As described in Reference A-12, Appendix A:

> The input to CHACHA from STAV6.2 consists of all the data describing the fuel conditions at the initiation of the LOCA. The fuel rod heatup calculations used to derive the inputs to the CHACHA gap heat transfer model make use of bounding input for model parameters, fuel geometry, and power history. A conservative representation of a reference core limiting power history was used.

Per the NRC SER for Reference A-12:

> The SER adopted the TER evaluation, which acknowledged the conservative approach and concluded that the use of the STAV6.2 initialization for LOCA was acceptable. No limitations or conditions were placed on the use of STAV6.2 to provide initial conditions for CHACHA using the approach described.

As described in Reference A-6, Section 5.5.2.3:

> No changes were made to the CHACHA gap heat transfer model as a result of the change to the STAV7.2 fuel performance except that initial conditions for the model would be taken from the STAV7.2 calculations.

Per the NRC SER for Reference A-6:

> The SER acknowledged that CHACHA would receive inputs from the STAV7.2 code to initialize the gap heat transfer model, but placed a condition on approval of this change pending completion of the NRC review of the STAV7.2 code. Westinghouse provided a letter to the NRC (Reference A-9), as required by the condition, after NRC approval of the STAV7.2 code was complete.

As described in Reference A-13, Section 4.4.4:

> The fuel rod heatup calculations used to derive the inputs to the CHACHA gap heat transfer model are based on bounding segmented power histories and conservative fuel parameters.

Per the NRC SER for Reference A-13:

> The SER acknowledged the use of the segmented power history approach to bound all operation defined by the thermal mechanical operating limit (TMOL) and concluded that the LOCA initialization methods were acceptable. No limitations or conditions were placed upon the use of this methodology other than to limit its application to a peak rod average burnup of 62 GWd/MTU.

A.2.12 Cladding Strain and Rupture Model

As described in Reference A-4, Section 5.6:

> The mechanistic models described in Section 5.6 replaced the empirical correlations presented in Section 4.9 of Reference A-1. The mechanical models for the fuel rod cladding are used to determine the geometry of the fuel rods (outside diameter of the rods, size of the gap between the UO2 pellet and the cladding, and cladding thickness).
>
> The mechanistic model for cladding burst, which gives a burst stress as a function of material properties and temperature, accounts for the influence of surface oxide and oxygen that has diffused into the Zircaloy. The burst stress is compared to the true, actual stress to detect

a rupture. The true, actual stress is calculated as a function of the pressures inside and outside the rod and the strained dimensions of the rod.

Per the NRC SER of Reference A-4:

The SER acknowledged the revision to the cladding strain and rupture model but placed a condition on its use that requires a bias of -0.5 MPa to be placed on the burst stress.

As described in Reference A-5, Section 4.1:

In addition to the cladding burst criterion described in Section 5.6 of Reference A-4, a second criterion was added to require cladding burst upon rod-to-rod contact.

Thus, the criteria for determining fuel rod rupture became that cladding rupture occurs when either the cladding contacts a neighboring rod or the burst stress criterion is exceeded – whichever comes first. The MAPLHGR is limited to a value that ensures the 10 CFR 50.46 acceptance criteria are met.

Per the NRC SER of Reference A-5:

The NRC acknowledged the change and concluded that the change complies with 10 CFR Part 50, Appendix K, in that the swelling and rupture calculations are based on applicable data in such a way that the degree of swelling and incidence of rupture are not underestimated. No limitations or conditions were placed on the application of this change.

A.2.13 Fuel Bundle Material Properties

As described in Reference A-4, Appendix A:

The fuel properties in CHACHA were changed to be consistent with fuel performance models derived from the STAV6.2 fuel performance code of Reference A-10. This includes density, thermal conductivity, and specific heat for uranium oxide (with and without Gd2O3), Zircaloy-2 and Zircaloy-4, and zirconium oxide.

Per the NRC SER of Reference A-4:

The SER placed a condition on the revisions to CHACHA that were based on STAV6.2 to be subject to the review findings of Reference A-10. The only condition resulting from this review was that applications must be to peak rod average burnups less than or equal to 50 GWd/MTU.

As described in Reference A-6, Section 5.5.2:

A model to account for the burnup-induced degradation of fuel pellet conductivity was introduced in CHACHA. This model was consistent with the STAV7.2 fuel performance code.

Per the NRC SER of Reference A-6:

> The SER placed a condition on the revisions to CHACHA that were based on STAV7.2 to be subject to the review findings of STAV7.2, which were ongoing at the time. Westinghouse provided a letter to the NRC (Reference A-9), as required by the condition, after NRC approval of the STAV7.2 code was complete. No limitations were placed on the model other than to limit applications to peak rod average burnups less than or equal to 62 GWd/MTU.

A.3 APPLICATION OF THE EVALUATION MODEL TO A NEW FUEL DESIGN

The U.S. version of the Westinghouse BWR ECCS Evaluation Model has been qualified and approved for application to several fuel designs. The specific designs are QUAD+, SVEA-96, SVEA-96+, and SVEA-96 Optima2. The same methodology has been applied in Europe to additional fuel designs (e.g., open lattice 8 x 8, SVEA-64, SVEA-100, and SVEA-96 Optima).

The qualification process described for various fuel designs, which is discussed in Reference A-14, is shown in Figure A-1 and summarized below.

A.3.1 Methodology

If all the qualification criteria are met, the ECCS Evaluation Model is acceptable for application to the specific fuel mechanical design. If any step described below does not fulfill the qualification criteria, then the LOCA ECCS Evaluation Model may not be applied for the new fuel mechanical design prior to specific NRC review and approval.

- Nodalization – Fuel design-specific models are developed for the GOBLIN, DRAGON, and CHACHA-3D codes that capture fuel design geometrical characteristics that are important to the key phenomena of a LOCA event.

- CPR Correlation – The CPR correlation used is NRC-approved and has been shown to conservatively predict early boiling transition in a LOCA event for the specific fuel design.

- CCFL Correlation – The CCFL model used is demonstrated as conservative relative to applicable experimental data for the specific mechanical fuel design.

- Spray Cooling Convective – The spray cooling heat transfer coefficients used are demonstrated as conservative relative to applicable experimental data for the specific mechanical fuel design.

- Transition Cores – A full core configuration of the specific fuel design is used in LOCA ECCS performance evaluation applications. Acceptability for transition cores is confirmed by comparing the following reactor system responses for analyses performed assuming a full core of the applicable co-resident fuel designs:

  - time of reactor trip
  - time of boiling transition at the midplane of the hot assembly
  - time of end of lower plenum flashing

- times of ECCS actuation
- time of reflood of the midplane of the hot assembly

The following sections provide discussion of each item above in the methodology statement.

A.3.2 Nodalization

The GOBLIN average reactor core and hot channel nodalization are selected to represent the fuel design features important to ECCS performance analysis. These features include the fuel rod dimensions, fuel assembly active cross-sectional flow areas, locations and characteristics of inter- and intra-assembly flow paths, grid spacers, and tie plates. Axial node size in the GOBLIN models is selected to ensure there is sufficient detail to characterize thermal-hydraulic conditions along the channel and at the hot plane. When it is impractical to reduce axial node size sufficiently to capture important mixture level dynamics, GOBLIN's two-phase level tracking feature may be used to determine the position of the mixture level more precisely.

The CHACHA-3D geometric model is selected to represent fuel design-specific rod or rod lattice configuration, channel configuration, fuel pellet, cladding and gap dimensions, and fuel rod plenum dimensions.

A.3.3 CPR Correlation

The CPR correlation is used to (1) determine the initial power of the hot assembly that will have it operating at bounding operating conditions, and (2) determine the time of boiling transition during the blowdown phase of the LOCA. GOBLIN has several CPR correlations available to the user. The CPR correlation applicable to the fuel design being evaluated or demonstrated to be conservative relative to a NRC-approved correlation for that fuel design is selected by the analyst to ensure that the hot assembly power and the time of dryout are predicted conservatively. To ensure that the critical power is calculated conservatively, a modified pool boiling correlation is also used to determine the critical power. The code then determines the critical power by selecting the smaller of the two calculated values. The following NRC-approved CPR correlations are currently available to the user:

CPR Correlation	Application
XL-S96	SVEA-96
ABBD1.0	SVEA-96
ABBD2.0	SVEA-96+
D4.1.2	SVEA-96 Optima 2

CPR correlations are applicable to specific fuel designs or a group of fuel designs. The SER for RPB 90-93-P-A (Reference A-1) requires that an appropriate NRC-approved CPR correlation be used when GOBLIN is used in a licensing analysis. The NRC-approved correlation may be one that has been developed specifically for the fuel design or one shown to be conservative relative to an NRC-approved correlation for that fuel design. Changes to GOBLIN are necessary when a new CPR correlation is implemented. The process described below is used by Westinghouse to install and test NRC-approved

CPR correlations. Changes to GOBLIN following this process do not require specific NRC review and approval. Such changes will be communicated to the NRC via the 10 CFR 50.46 annual reporting process.

The process used to install and qualify a CPR correlation in GOBLIN is as follows:

1. Develop coding to represent the new correlation. The coding includes checks on correlation parameters to ensure that inputs to the correlation are within valid ranges of those parameters. If a parameter is outside its range of validity, the [
]^{a,c}

2. Validation of the implemented CPR correlation is performed by:

   a. Transient code simulation of transient experimental data, or

   b. Transient code to transient code comparisons where the reference transient code implementation of the CPR correlation has been qualified against transient experimental data.

3. Ensure NRC approval of CPR correlation for the fuel design prior to its use in licensing applications.

4. Inform the NRC of the change to GOBLIN via the 10 CFR 50.46 annual reporting process.

If a LOCA analysis of non-Westinghouse fuel is required, Westinghouse may not have direct access to the accepted correlation for the resident fuel. In this case, sufficient information is obtained from the utility company to either:

1. Allow renormalization of an NRC-approved Westinghouse CPR correlation for Westinghouse fuel to describe the CPR performance of the fuel, or

2. Show that the NRC-approved Westinghouse CPR correlation for Westinghouse fuel is conservative.

CPR correlations are valid within specified ranges of parameters (e.g., system pressure, core mass flux, inlet subcooling). When a CPR correlation is implemented in GOBLIN, it is only applied when conditions in the core are within its range of applicability. If any parameter is outside its valid range, a pool boiling CHF correlation is used. Because the system pressure and core flow decrease rapidly following a large-break LOCA, the prediction of boiling transition is often the result of exceeding the [ ]^{a,c}. Experience has shown that the fuel-specific CPR correlation selected [

]^{a,c}

[

]^{a,c}

The process for developing the renormalized CPR correlation is described in Section 5.3.2.5 of Reference A-14. Implementation of the renormalized CPR correlation in GOBLIN follows the process outlined above.

A.3.4 CCFL Model

The CCFL model has been approved for a variety of fuel designs. In accordance with CENPD 283-P-A (Reference A-3), this correlation will not be extended to fuel designs outside the range of approved applicability without being supported by experimental data. NRC review and approval of the new CCFL model is required prior to its use in licensing applications.

The change to the CCFL model in GOBLIN that is described in Section 5.4.2 of Reference A-6 removes a restriction placed on the USA2 Evaluation Model.[2]

A.3.5 Spray Cooling Convective Heat Transfer

A methodology to extrapolate spray cooling heat transfer coefficients for application to a variety of fuel designs has been approved. In accordance with CENPD-283-P-A (Reference A-3), this methodology will not be extended to fuel designs outside the range of applicability without being supported by experimental data. If the spray cooling heat transfer coefficients cannot be demonstrated as applicable, spray cooling heat transfer coefficients must be determined either from a detailed analysis that has been validated by experimental data or taken directly from applicable data. NRC review and approval of the new spray cooling heat transfer coefficients are required prior to their use in licensing applications.

A.3.6 Transition Cores

The BWR fuel channel and fuel mechanical designs are established to ensure hydraulic compatibility with co-resident fuel. This means that the system response to a LOCA event for one core of mixed fuel designs will be similar hydraulically to that of a full core of a single fuel design. This observation has been demonstrated for several fuel designs in References A-2 and A-3. It became a requirement to specifically analyze a transition core during the first reload analysis following the NRC acceptance of WCAP-16078-P-A (Reference A-6). If it is confirmed that a full core of Westinghouse fuel is bounding, then the Evaluation Model can be performed using the full-core Westinghouse fuel approach. Otherwise, the mixed-core model must be used. The Westinghouse Evaluation Model may not be used to calculate the MAPLHGR limits for non-Westinghouse fuel for a mixed-core analysis. If the transition core analysis indicates that the system performance of the mixed core is more limiting than the full-core analysis of the legacy fuel, Westinghouse must request the utility to contact the legacy fuel vendor for an evaluation of the impact of the mixed core on the MAPLHGR limits for their fuel.

2. In responding to a request for additional information relative to the NRC review of CENPD-283-P-A (Reference A-3), Westinghouse committed to applying a conservative bias to the CCFL correlation to bound all the scatter in the correlation database for LOCA applications in which the calculated peak cladding temperature exceeded 2100°F.

Tables for Appendix A

Table A-1 Roadmap to Evaluation Model Changes

Evaluation Model Element	Reference No.					Road Map Section
	A-1	A-4	A-3	A-5	A-6	
Thermal-Hydraulic Model – GOBLIN						
Mass Conservation Equations	3.1.1					
Energy Conservation Equations	3.1.2					
Momentum Conservation Equations	3.1.3	4.2				A.2
Fluid Properties	3.2.1					
Equation of State	3.2.2					
Two-Phase Energy Flow Model	3.3.1		7.1		5.4.2	A.2.2
Two-Phase Level Tracking	3.3.2		6.1.2		5.1.1	A.2.3
Frictional Pressure Drop Correlations	3.3.3					
Form Pressure Drop Correlations	3.3.4					
Injection Flow – Fluid Interaction	3.3.5					
Critical Flow Model	3.3.6					
Recirculation Pump Model	3.4.1					
Jet Pump Model	3.4.2					
Separator and Dryer Model	3.4.3					
Feedwater and Steam line Systems	3.4.4					
Reactor Measurement and Protection Systems	3.4.5					
Heat Transfer Regimes	3.5.1					
Convective Heat Transfer Coefficients	3.5.2		4.3		6.1	A.2.4
Critical Power Ratio Correlation	3.5.3	4.1	4.2		5.4.1	A.2.5
Transition Boiling	3.5.4					
Radiation Heat Transfer	3.5.5					
Fuel Rod Conduction Model	3.6.1					
Plate Conduction Model	3.6.2					
Material Properties	3.6.3					
Point Kinetics Model	3.7.1					
Metal-Water Reaction Model	3.7.2					
Point Kinetics Solution	3.8.1					

Table A-1 (cont.) Roadmap to Evaluation Model Changes

Evaluation Model Element	Reference No.					Road Map Section
	A-1	A-4	A-3	A-5	A-6	
Hydraulic Model Solution	3.8.2					
Heat Conduction and Transfer Solution	3.8.3					
Nodalization	3.9					
Rod Heatup Model – CHACHA						
Fuel Rod Conduction Model	4.1	5.1			5.5.2	A.2.6
Channel Temperature Model	4.2					
Heat Generation Model	4.3	5.2			5.5.2	A.2.7
Metal-Water Reaction Model	4.4	5.3			5.5.2	A.2.8
Thermal Radiation Model	4.5	5.4				A.2.9
Gas Plenum Temperature and Pressure Model	4.6				5.5.1	A.2.10
Channel Rewet Model	4.7					
Pellet-Cladding Gap Heat Transfer Model	4.8	5.5.1			5.5.2.3	A.2.11
Cladding Strain and Rupture Model	4.9	5.6		4.1		A.2.12
Fuel Bundle Material Properties	App. 4.A	App. A			5.5.2	A.2.13

Table A-2 Extrapolated Spray Cooling Heat Transfer Coefficients per Reference A-3

Geometry	Extrapolated from Appendix K Values (W/m^2-K)			
	Corner Rods	Side Rods	Inner Rods	Channel
Appendix K 7 x 7, 8 x 8, Isotropic Radiation	17.0	19.9	8.5	28.4
Appendix K 8 x 8, Anisotropic Radiation	16.8	19.4	11.9	28.4
SVEA-64, Anisotropic Radiation	15.0	17.3	10.6	25.3
SVEA-96, Anisotropic Radiation	15.0	17.3	10.6	25.3

Table A-3 Extrapolated Spray Cooling Heat Transfer Coefficients per Reference A-6

	Extrapolated from Appendix K Values (W/m^2-K)			
	Corner Rods	Side Rods	Inner Rods	Channel
SVEA-96, Anisotropic Radiation	15.0	17.3	10.6	25.3
SVEA-96 Optima2	15.0	17.3	10.6	25.3

Figures for Appendix A

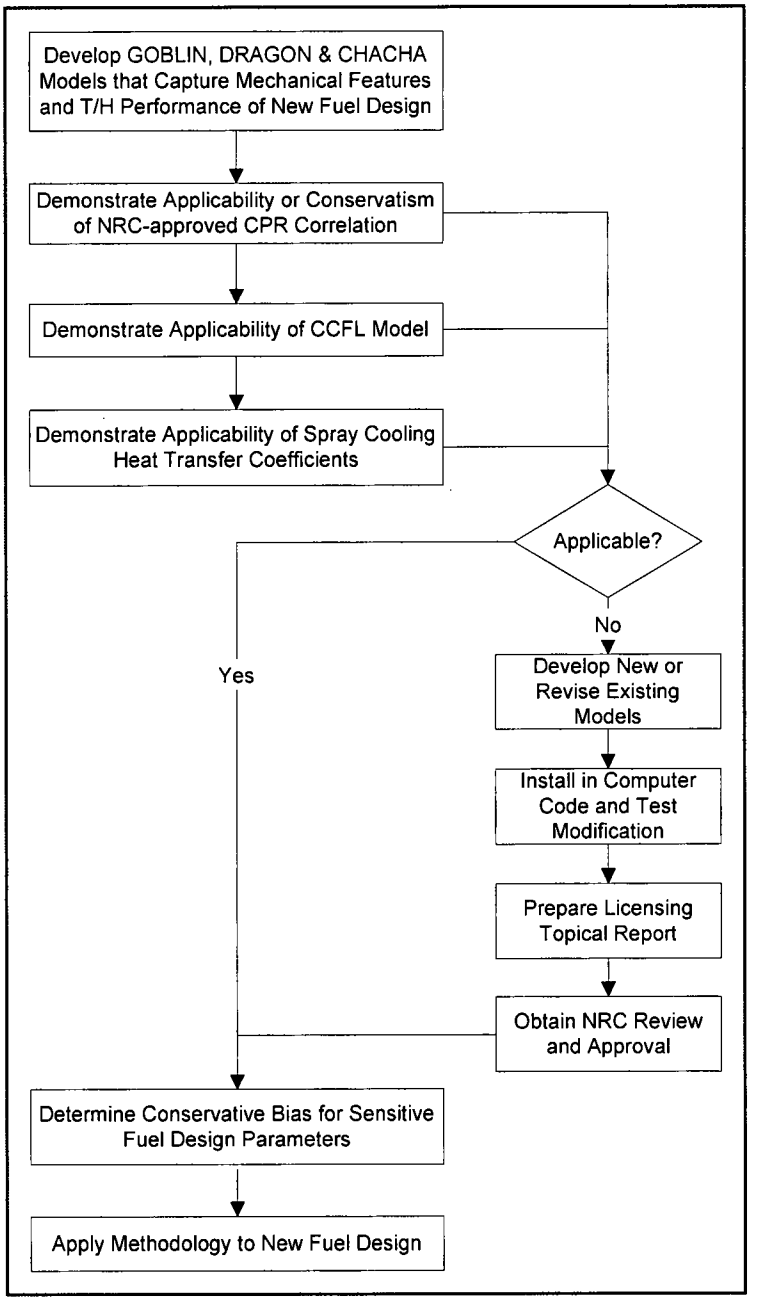

Figure A-1 Process for Applying Evaluation Model to New Fuel Mechanical Design

References for Appendix A

A-1 "Boiling Water Reactor Emergency Core Cooling System Evaluation Model: Code Description and Qualification," Westinghouse Report RPB 90-93-P-A (Proprietary), RPB 90-91-NP-A (Non-Proprietary), October 1991.

A-2 "Boiling Water Reactor Emergency Core Cooling System Evaluation Model: Code Sensitivity," Westinghouse Report RPB 90-94-P-A (Proprietary), RPB 90-92-NP-A (Non-Proprietary), October 1991.

A-3 "Boiling Water Reactor Emergency Core Cooling System Evaluation Model: Code Sensitivity for SVEA-96 Fuel," Westinghouse Report CENPD-283-P-A (Proprietary), CENPD-283-NP-A (Non-Proprietary), July 1996.

A-4 "BWR ECCS Evaluation Model: Supplement 1 to Code Description and Qualification," Westinghouse Report CENPD-293-P-A (Proprietary), CENPD-293-NP-A (Non-Proprietary), July 1996.

A-5 "Westinghouse BWR ECCS Evaluation Model: Supplement 2 to Code Description, Qualification and Application," Westinghouse Report WCAP-15682-P-A (Proprietary), WCAP-15682-NP-A (Non-Proprietary), April 2003.

A-6 "Westinghouse BWR ECCS Evaluation Model: Supplement 3 to Code Description, Qualification and Application to SVEA-96 Optima2 Fuel," Westinghouse Report WCAP-16078-P-A (Proprietary), WCAP-16078-NP-A (Non-Proprietary), November 2004.

A-7 "SVEA-96 Critical Power Experiments on a Full Scale 24-rod Sub-bundle," ABB Atom Report UR 89-210-P-A, October 1993.

A-8 Letter from A.C. Thadani (NRC) to W. R. Russell (ABB Atom), "Waiver of CRGR Review of the Safety Evaluation of ABB Supplemental Information Regarding UR 89-210 Safety Evaluation Report," July 12, 1993.

A-9 Letter from B. F. Maurer (Westinghouse) to F. M. Akstulewicz (NRC), "Westinghouse response to Condition 1 in the FINAL SAFETY EVALUATION FOR TOPICAL REPORT WCAP-16078-P, "Westinghouse BWR ECCS Evaluation Model: Supplement 3 to Code Description, Qualification and Application to SVEA-96 Optima2 Fuel" (TAC NO. MB8908), October 21, 2004," LTR-NRC-06-1, January 4, 2006.

A-10 "Fuel Rod Design Methods for Boiling Water Reactors," Westinghouse Report CENPD-285-P-A (Proprietary), CENPD-285-NP-A (Non-Proprietary), July 1996.

A-11 "Fuel Rod Design Methods for Boiling Water Reactors – Supplement 1," Westinghouse Report WCAP-15836-P-A (Proprietary), WCAP-15836-NP-A (Non-Proprietary), April 2006.

A-12 "Fuel Rod Design Methodology for Boiling Water Reactors," Westinghouse Report CENPD-287-P-A, July 1996.

A-13 "Fuel Assembly Mechanical Design Methodology for Boiling Water Reactors Supplement 1 to CENP-287," Westinghouse Report WCAP-15942-P-A (Proprietary), WCAP-15942-NP-A (Non-Proprietary), March 2006.

A-14 "Reference Safety Report for Boiling Water Reactor Reload Fuel," CENPD-300-P-A (Proprietary), CENPD-300-NP-A (Non-Proprietary), July 1996.

APPENDIX B
ABWR LOCA ANALYSIS MODEL INPUT PARAMETERS

Table B-1 of this appendix provides key input parameters that were used in the analyses described herein. Note that some of input parameters were revised after the analyses were completed. Although the changes were small, they and any other plant specific changes will be incorporated into the final analyses prior to the first plant application of the methodology.

Table B-1 ABWR LOCA Analysis Model Input Parameters

Parameter	Toshiba/W Values	
Volumes (see Figure B-1)	a,c	
WV-A	[ ]	m^3
WV-B	[ ]	m^3
WV-C	[ ]	m^3
WV-D	[ ]	m^3
WV-E	[ ]	m^3
WV-F	[ ]	m^3
WV-G (Control Rods Fully Inserted)	[ ]	m^3
WV-H	[ ]	m^3
WV-J	[ ]	m^3
WV-K	[ ]	m^3
WV-N1	[ ]	m^3
WV-N2	[ ]	m^3
WV-L	[ ]	m^3
WV-M	[ ]	m^3
WV-P	[ ]	m^3
WV-Q	[ ]	m^3
WV-R1	[ ]	m^3
WV-R2	[ ]	m^3
WV-R3	[ ]	m^3
WV-R4	[ ]	m^3
WV-R5	[ ]	m^3
WV-S1	[ ]	m^3
WV-S2	[ ]	m^3
WV-S3	[ ]	m^3
WV-S4	[ ]	m^3
WV-S5	[ ]	m^3
WV-T1	[ ]	m^3
WV-T2	[ ]	m^3
WV-T3	[ ]	m^3

Table B-1 ABWR LOCA Analysis Model Input Parameters (cont.)

Parameter		Toshiba/W Values	
VSL1-A (Main Steam Line A from RPV to first MSIV)		a,c	m^3
VSL1-B			m^3
VSL1-C			m^3
VSL1-D			m^3
Elevations (from vessel zero)		a,c	
Z1	Internal pump discharge port upper end height		m
Z2	Bottom of active fuel		m
Z3	Top of active fuel		m
Z4	Upper plenum upper end (inside)		m
Z5	Feedwater sparger discharge port height		m
Z6	Normal water level		m
Z7	Steam separator upper end		m
Z8	Shroud support leg lower end height		m
Z9	Control rod guide tube lower end		m
Z10	Control rod guide tube upper end		m
Z11	Core support plate height		m
Z12	Fuel channel upper end height		m
Z13	Steam dryer skirt lower end height		m
Z14	Steam dryer lower end height		m
Z15	Steam dryer upper end height		m
Z16	Pressure vessel upper end height		m
Z17	Water level reference point height		m
Z18	HPCF sparger height		m
Z19	LPFL sparger height		m
Z20	Main steam line inlet height		m
Z21	Internal pump inlet height		m
Z22	Internal pump discharge port lower end height		m
Z23-1	Water level indictor nozzle (wide range)[1]		m
Z23-2	Water level indicator nozzle (narrow range)		m
Zcs	Top of core support mounting flange height		m
Zf	Elevation of vessel flange parting line		m
Zbc	Elevation of intersection of vessel bottom curvature		m
Zut	Elevation of upper tap for water level measurement		m

[1] The ABWR level measurement instruments are compensated for changes in reactor pressure. The analyses described in Section 4 assume uncompensated level instrumentation.

Table B-1 (cont.) ABWR LOCA Analysis Model Input Parameters

Parameter		Toshiba/W Values	
Dimensions of Core Structures			
Reactor Pressure Vessel		a,c	
Di	Pressure vessel shell inner diameter		m
Rhu	Top head radius		m
Rhb	Bottom head radius		m
TV1	Upper head wall thickness		m
TV2	Flange thickness		m
TV3	Vessel wall thickness		m
TV4	Bottom wall thickness		m
TV5	Bottom head thickness		m
TL1	Vessel wall liner thickness		m
TL2	Bottom wall liner thickness		m
Hfh	Flange head height		m
Control Rod Drive (CRD) Guide Tube and Control Rod (CR) Housing (see Figure B-2)		a,c	
Dgt	CRD guide tube outer diameter		m
Tgt	CRD guide tube thickness		m
Ngt	Number of CRD		–
Doit	Outer diameter of index tube		m
Docrd	Outer diameter of CR housing		m
Dicrd	Inner diameter of CR housing		m
In-core Monitor Guide Tubes (see Figure B-2)			
Dm	Outer diameter of in-core monitor guide tubes		m
Tm	Wall thickness of in-core monitor guide tubes		m
Nm	Number of in-core monitors		–
Core Support Plate (see Figure B-2)			
Dcs	Diameter of core support plate		m
Tcs	Wall thickness of core support plate		m
Lbt	Total length of beams		m
Dcs	Hole diameter		m
Hcs	Support ring height		m
Shroud (see Figure B-3)			
Dup	Inner diameter of shroud at upper plenum part		m
Do	Inner diameter of shroud at core part		m
Dip	Inner diameter of shroud at lower plenum part		m
Tsh	Wall thickness of core shroud part		m
Rsh	Shroud head curvature		m

Table B-1 (cont.) ABWR LOCA Analysis Model Input Parameters

Parameter		Toshiba/W Values	
Lsh1	Height of shroud	[a,c]	m
Lsh2	Height of shroud head		m
Lcy	Elevation of shroud support cylinder		m
Tfl	Width of shroud head flange		m
Tsl	Thickness of shroud support leg		m
Tsc	Thickness of shroud support cylinder		m
Separators (see Figure B-4)		[a,c]	
Lsp	Length of standpipe		m
Asp	Flow area of standpipe		m
Dsp	Inner diameter of standpipe		m
Tsp	Wall thickness of standpipe		m
Dsp1~3	Outer diameter of surface of separators		m
Tsp1~3	Wall thickness of separators		m
Lsp1	Length of separator skirts (1st)		m
D1~3	Outer diameter of inner wall surface of separators		m
T1~3	Wall thickness of inner wall surface of separators		m
L1	Length of inner wall surface of separators (1st)		m
Lsp2	Length of separator skirts (2nd)		m
L2	Length of inner wall surface of separators (2nd)		m
Lsp3	Length of separator skirts (3rd)		m
L3	Length of inner wall surface of separators (3rd)		m
Zsp1	Height at top of standpipe (from vessel zero)		m
Nsp	Number of separators		–
	Carry under		–
	Carry over		–
Steam Dryer		[a,c]	
Asd	Total heating surface area		m^2
Nsd	Number of packages		–
Tsd	Plate thickness		m
Wdr	Width of dryer unit		m
Tdr1	End thickness of dryer unit		m
Tdr2	Another end thickness of dryer unit		m
Ndr	Number of dryer plate units		–
Dd	Dryer skirt mean diameter		m
Tds	Dryer skirt thickness		m
Dsr	Dryer support ring outer diameter		m
Hsr	Dryer support ring height		m

Table B-1 (cont.) ABWR LOCA Analysis Model Input Parameters			
Parameter		**Toshiba/W Values**	
Sparger Rings		a,c	
Dmfw	Mean diameter of feedwater sparger ring	[ ]	m
Dfw	Outer diameter of feedwater sparger ring tubes	[ ]	m
Tfw	Wall thickness of feedwater sparger ring tubes	[ ]	m
Afw	Cross section of feedwater sparger ring outlet nozzle	[ ]	m^2
Dmhp	Mean diameter of HPCF sparger ring	[ ]	m
Dhp	Outer diameter of HPCR sparger ring tubes	[ ]	m
Thp	Wall thickness of HPCF sparger ring tubes	[ ]	m
Ahp	Cross section of HPCF sparger ring outlet nozzle	[ ]	m^2
Dmlp	Mean diameter of LPFL sparger ring	[ ]	m
Dlp	Outer diameter of LPFL sparger ring tubes	[ ]	m
Tlp	Wall thickness of LPFL sparger ring tubes	[ ]	m
Alp	Cross section of LPFL sparger ring outlet nozzle	[ ]	m^2
Main Steam (MS) Line			
D1~4	Inner diameter of MS line (from RPV to first MSIV)	[ ]a,c	m
Reactor Internal Pump (RIP)		a,c	
Ddf	Diameter of RIP discharge	[ ]	m
Ldf	Length of RIP discharge	[ ]	m
Ath	Flow area of RIP	[ ]	m^2
Did	Inner diameter of RIP diffuser ring	[ ]	m
Ts	Thickness of shroud support leg (internal support thickness)	[ ]	m
Nrp	Number of RIP	[ ]	–
Assumed pump trip time		[ ]	s
Rated pump speed		[ ]	rpm
Rated pump flow rate (per pump)		[ ]	m^3/h
Rated pump head		[ ]	m
Rated pump torque (includes hydraulic and frictional torque)		[ ]	Nm
Pump moment of inertia		[ ]	kg/m^3
Rated density of pump fluid		[ ]	kg/m^3
Pump efficiency (minimum value)		[ ]	%
Minimum inertia time constant (speed dropping to 50%)		[ ]	s
Maximum inertia time constant (speed dropping to 50%)		[ ]	s
Top Guide		a,c	
Ttg	Thickness of top guide	[ ]	m
Wth	Weight of top guide	[ ]	kg

Table B-1 (cont.) ABWR LOCA Analysis Model Input Parameters

Parameter	Toshiba/W Values	
Material	a,c	
Reactor pressure vessel		
RIP diffuser ring		
Internal support		
Shroud support		
Other internals		
Initial Conditions	a,c	
Core Thermal Power (102% of rated thermal power)		MWt
Core Inlet Flow Rate (90% rated)		kg/s
Core Inlet Flow Rate (111% rated)		kg/s
Steam Flow Rate		kg/s
Feedwater Flow Rate		kg/s
Feedwater Enthalpy		kJ/kg
Core Inlet Enthalpy (90% core flow)		kJ/kg
Core Inlet Enthalpy (111% core flow)		kJ/kg
Dome Pressure		MPa
Water Level (slightly above scram water level)		m
Break Areas	a,c	
HPCI Injection Line (area of 18 sparger nozzles)		cm^2
Main Steam Line (corresponds area of one flow limiter)		cm^2
Feedwater Line (area of 54 sparger nozzles)		cm^2
RHR Shutdown Cooling Suction Line		cm^2
RHR Injection Line		cm^2
Bottom Drain Line		cm^2
ECCS Performance		
High Pressure Core Flooder (HPCF)		
ΔP a,c	Flow a,c	
MPa (dif)	m^3/h	
MPa (dif)	m^3/h	
MPa (dif)	m^3/h	
MPa (dif)	m^3/h	
Time delay from actuation signal (includes all delays)	[ ]a,c	s
Actuation signals	a,c	
High drywell pressure, OR		MPa
Low water level (LWL-1.5)		m
Number of pumps		–

Table B-1 (cont.) ABWR LOCA Analysis Model Input Parameters

Parameter	Toshiba/W Values	
Reactor Core Isolation Cooling (RCIC)		
ΔP	Flow	
[ ]a,c MPa (dif)	[ ]a,c m^3/h	
MPa (dif)	m^3/h	
MPa (dif)	m^3/h	
MPa (dif)	m^3/h	
Time delay from actuation signal (includes all delays)	[ ]a,c	s
Actuation signals	[ ]a,c	
High drywell pressure, OR		MPa
Low water level (LWL-2)		m
Number of pumps		–
Low Pressure Flooder (LPFL)		
ΔP [ ]a,c	Flow [ ]a,c	
MPa (dif)	m^3/h	
MPa (dif)	m^3/h	
MPa (dif)	m^3/h	
Time delay from low pressure permissive (includes all delays)	[ ]a,c	s
Pressure permissive for LPFL injection valve		MPa
Actuation signals	[ ]a,c	
High drywell pressure, OR		MPa
Low water level (LWL-1)		m
Number of pumps		–
Automatic Depressurization System (ADS)	[ ]a,c	
Number of valves		–
Capacity per valve		kg/s
Pressure at rated capacity		MPa
Time delay from actuation signal		s
Actuation signals	[ ]a,c	
High drywell pressure, AND		MPa
Low water level (LWL-1), AND		m
Indication that at least 1 LPFL or 1 HPCF pump is operating		

Table B-1 (cont.) ABWR LOCA Analysis Model Input Parameters

Parameter						Toshiba/W Values	
ECCS water temperature						[ ]^{a,c}	°C
Safety Relief Valve (safety function)							
Setpoints for spring action							
	Open$_{a,c}$		Close$_{a,c}$		Number$_{a,c}$	Capacity$_{a,c}$	*
1st	[ ]	MPa (gage)	[ ]	MPa (gage)	[ ]	[ ]	kg/s
2nd	[ ]	MPa (gage)	[ ]	MPa (gage)	[ ]	[ ]	kg/s
3rd	[ ]	MPa (gage)	[ ]	MPa (gage)	[ ]	[ ]	kg/s
4th	[ ]	MPa (gage)	[ ]	MPa (gage)	[ ]	[ ]	kg/s
5th	[ ]	MPa (gage)	[ ]	MPa (gage)	[ ]	[ ]	kg/s
* capacity is per valve							
Opening/closing time						[ ]^{a,c}	s
Reactor Scram						a,c	
Low water level (LWL-3)						[ ]	m
MSIV position						[ ]	% open
Time delay from actuation signal (low water level)						[ ]	s
Time delay from actuation signal (MSIV position)						[ ]	s
Scram insert time						[ ]	s
Feedwater Flow Isolation							
Time feedwater flow rate decreases to zero (from time of event)						[ ]^{a,c}	s
Steam Line Isolation							
Turbine control valve fast closure							
[ ]^{a,c}							
A_{ti} is the steam line flow area upstream of the turbine, t is time from the loss of normal power							
Main Steam Isolation Valves (MSIVs)							
[ ]^{a,c}							
A is the MSIV flow area, A_{ms} is the flow area of the main steam line, t is time from actuation signal							
Main Steam Flow Control (pressure regulator)							
[ ]^{a,c}							
A_{ti} is the steam line flow area upstream of the turbine, P_d is the dome pressure in MPa.							
Actuation signals							
TCV fast closure							
Loss of normal power							
MSIV						a,c	
Low water level (LWL-1.5)						[ ]	m
High steam flow						[ ]	% rated

Table B-1 (cont.) ABWR LOCA Analysis Model Input Parameters

Parameter	Toshiba/W Values	
Reactivity Inputs		
Moderator density reactivity coefficients*	[ ]a,c	
Linear coefficient (C_1)		m^3/kg
Quadratic coefficient (C_2)		m^6/kg^2
Cubic coefficient (C_3)		m^9/kg^3
[ ]a,c		
Fuel temperature reactivity coefficients		
Square root coefficient (B_3)	[ ]a,c	$1/°C^{1/2}$
[ ]a,c	[ ]a,c	
Scram rod worth		

% Inserted	Scram reactivity
[ ]a,c	[ ]a,c

Fraction delayed neutrons in group i	[ ]a,c	
Group 1		--
Group 2		--
Group 3		--
Group 4		--
Group 5		--
Group 6		--
Total delayed neutron fraction		--
Decay constant for delayed neutron group i	[ ]a,c	
Group 1		1/s
Group 2		1/s

Table B-1 (cont.) ABWR LOCA Analysis Model Input Parameters

Parameter					Toshiba/W Values	
Group 3					[ ]a,c	1/s
Group 4						1/s
Group 5						1/s
Group 6						1/s
Fuel rod gap heat transfer coefficient						
Average core						
	Avg. fuel temperature		HGAP			
	[ ]a,c	°C	[ ]a,c	W/m^2-°C		
		°C		W/m^2-°C		
		°C		W/m^2-°C		
		°C		W/m^2-°C		
		°C		W/m^2-°C		
		°C		W/m^2-°C		
		°C		W/m^2-°C		
		°C		W/m^2-°C		
		°C		W/m^2-°C		
		°C		W/m^2-°C		
		°C		W/m^2-°C		
		°C		W/m^2-°C		
		°C		W/m^2-°C		
Hot Assembly						
	Avg. fuel temperature		HGAP			
	[ ]a,c	°C	[ ]a,c	W/m^2-°C		
		°C		W/m^2-°C		
		°C		W/m^2-°C		
		°C		W/m^2-°C		
		°C		W/m^2-°C		
		°C		W/m^2-°C		
		°C		W/m^2-°C		
		°C		W/m^2-°C		
		°C		W/m^2-°C		
		°C		W/m^2-°C		
		°C		W/m^2-°C		
		°C		W/m^2-°C		
		°C		W/m^2-°C		

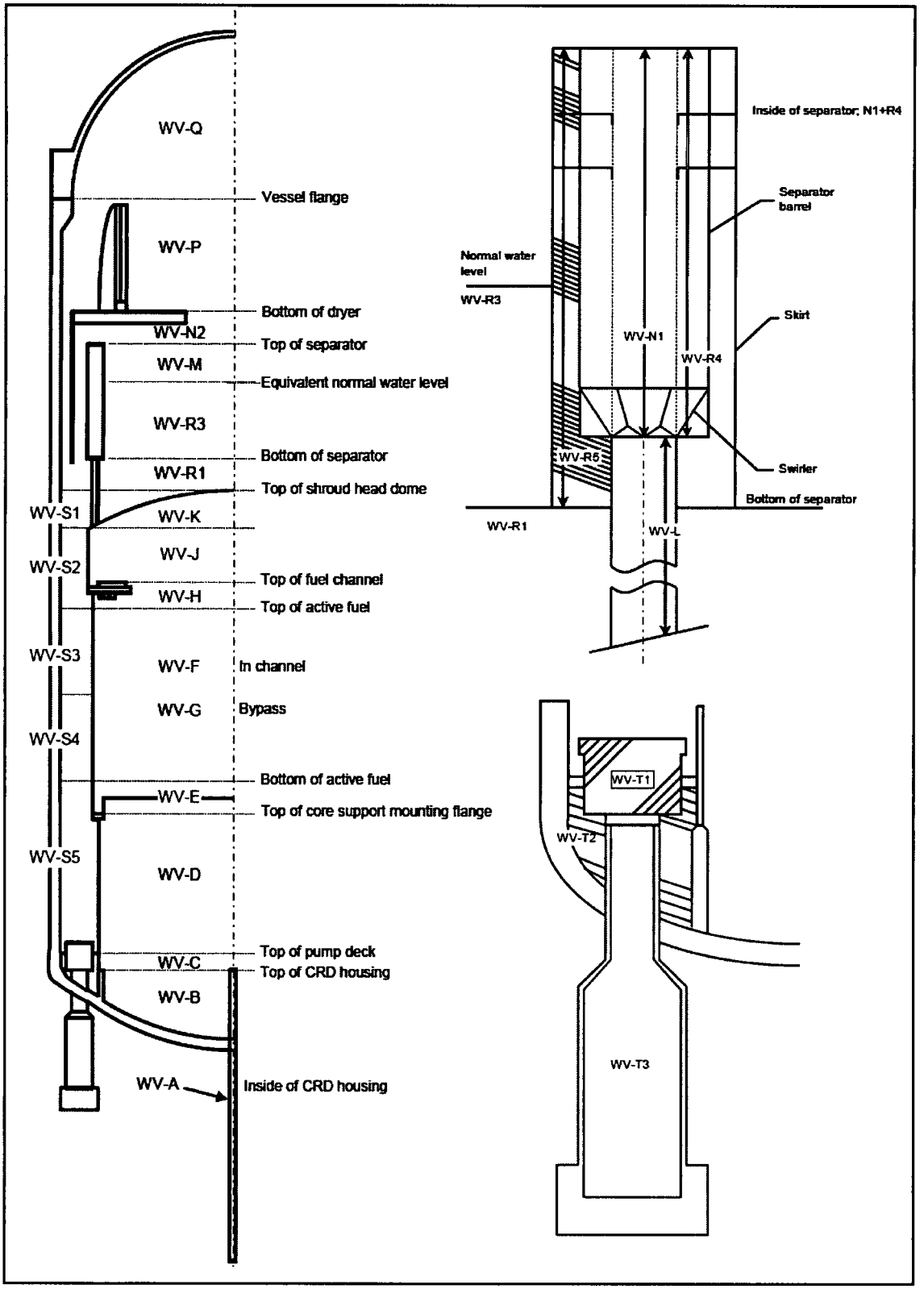

Figure B-1 Schematic of Reactor Pressure Vessel Internals

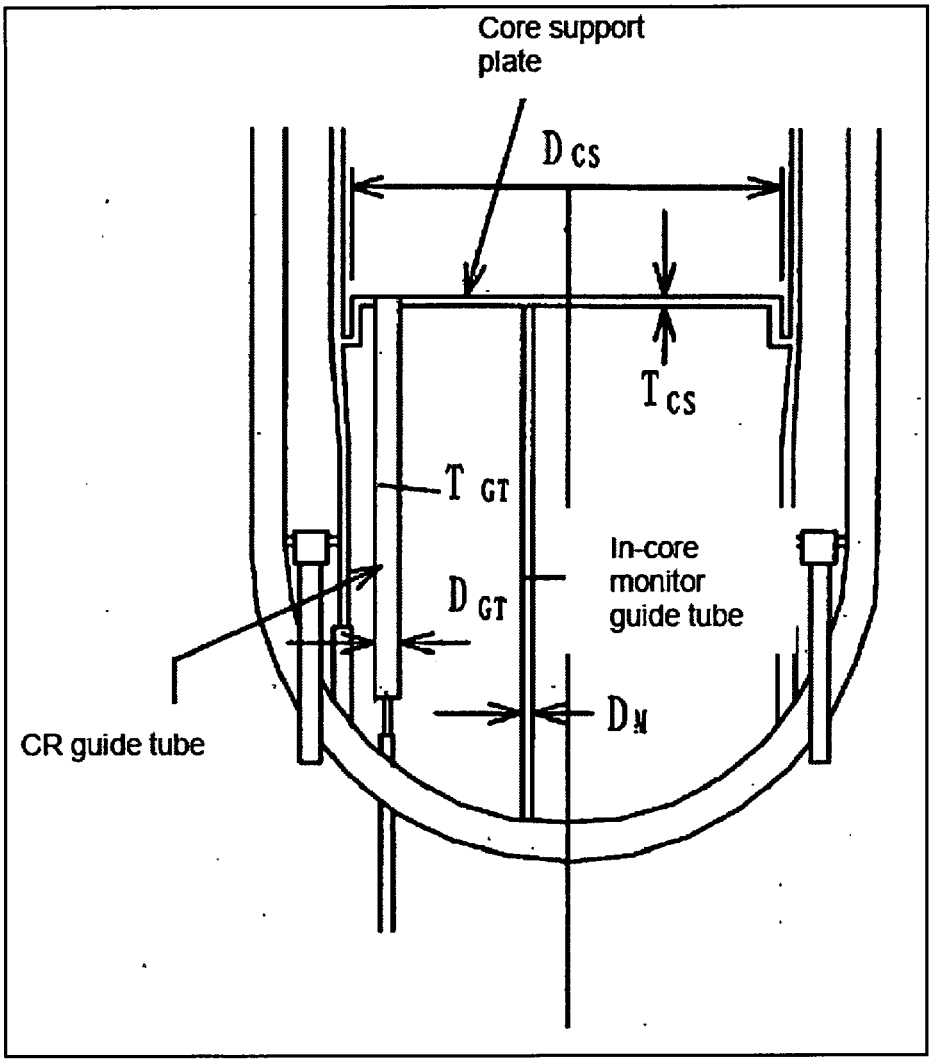
Core support plate
D CS
T CS
T GT
D GT
In-core monitor guide tube
D M
CR guide tube

Figure B-2

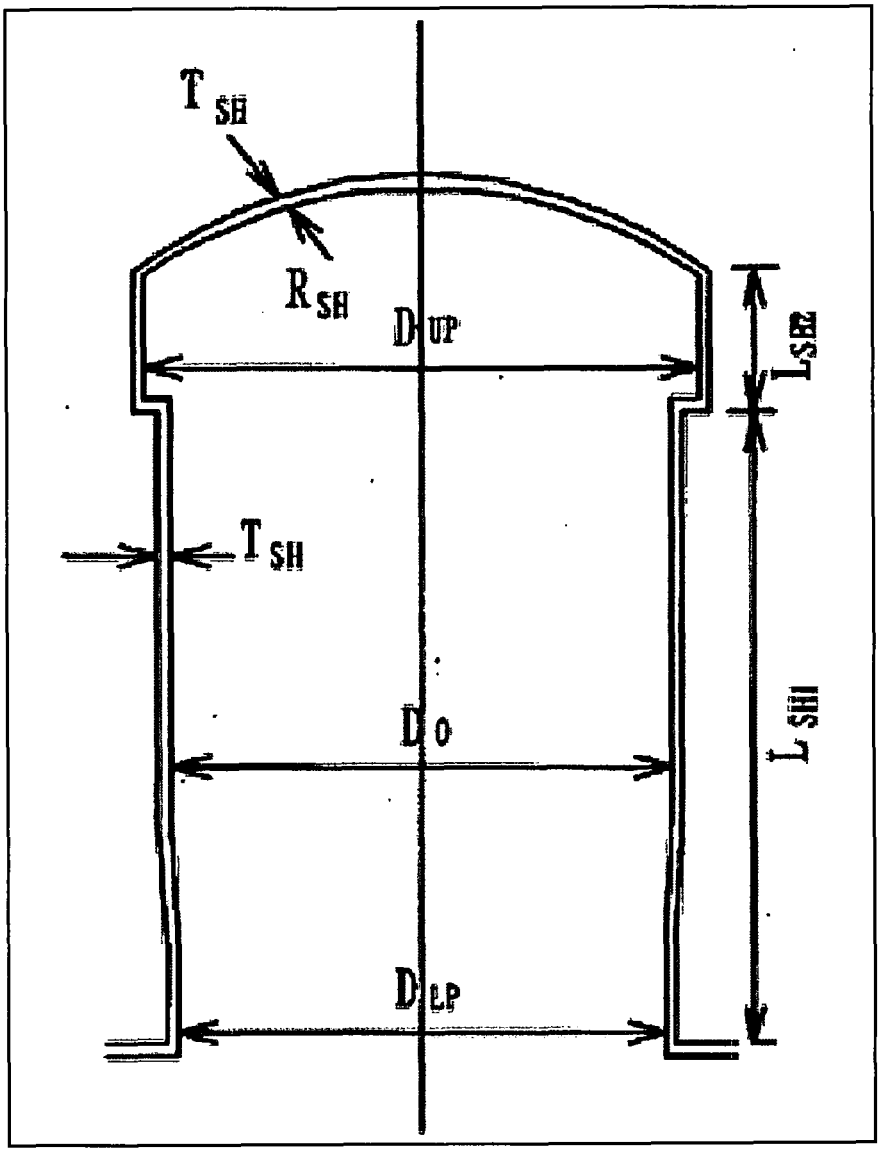

Figure B-3

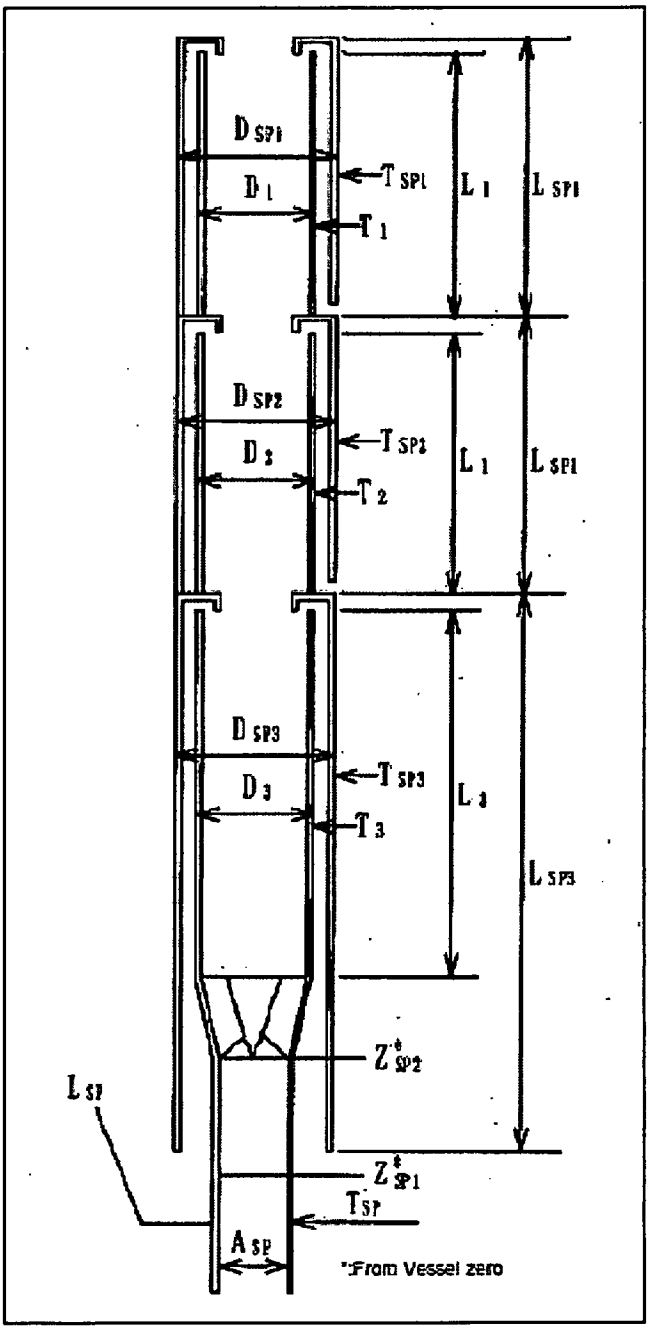
D SP1
T SP1
L 1
L SP1
D 1
T 1
D SP2
T SP2
L 1
L SP1
D 2
T 2
D SP3
T SP3
L 3
L SP3
D 3
T 3
Z* SP2
L S1
Z* SP1
T SP
A SP
*:From Vessel zero

Figure B-4

APPENDIX C
CHANGES INCORPORATED IN THE APPROVED VERSION RESULTING FROM VARIOUS RAI RESPONSES

The following changes have been made to the approved version of this report as a result of NRC review and subsequent RAI responses:

- The analyses supporting Section 4.5.4.1 "RHR Suction Line Break Results" were revised to correct the number of credited HPCF pumps. Table 4-5 of this report has been corrected, as well as Summary Table 4-9 and Summary Figure 4-46. See the response to RAI 32 Supplement 2, for further discussion.

- The analyses supporting Section 4.5.6.1 "Drain Line Break Results" were revised to correct the number of credited HPCF pumps. Table 4-7 and Figure 4-41 of this report have been corrected, as well as Summary Table 4-9 and Summary Figure 4-46. See the response to RAI 32 Supplement 2, for further discussion.

- Section 4.7 of this report has been revised to indicate the mid-peaked chopped cosine power distribution was confirmed as limiting. See the responses to RAI 19 Supplement 1 and RAI 32 Supplement 2 for further discussion.

- Changes have been made to Table B-1 regarding reactivity inputs. The units of the moderator density reactivity coefficients were corrected. Also, the equations for the moderator density reactivity and fuel temperature reactivity were missing from the review version of the report and have been added. See the response to RAI 13 Supplement 1 for further discussion.

- Footnote 1, referenced from parameter Z23-1, has been added to Table B-1 to indicate that the ABWR water level instruments are compensated for variations in reactor pressure. See the response to RAI 32 Supplement 2 for further discussion.

APPENDIX D
NRC RAIS AND RESPONSES

RAI-1

QUESTION

Section 11.3 of Appendix K to 1 OCFR50 requires that "appropriate sensitivity studies shall be performed for each evaluation model, to evaluate the effect on the calculated results of variations in noding, phenomena assumed in the calculation to predominate, including pump operation or locking, and values of parameters over their applicable ranges. For items to which results are shown to be sensitive, the choices made shall be justified."

a) Section 4.3.1.1 of WCAP-17116-P mentions that the GOBLIN active core was increased to 25 axial nodes based on results of benchmarking calculations against the FRIGG test data. As required by Section 11.3 of Appendix K, please elaborate if any nodalization studies were performed using the ABWR GOBLIN model to confirm that the selected noding scheme can be considered as appropriate and that there is no strong sensitivity of the calculated results to the selected node size.

b) Section A.3.2 of WCAP-17116-P notes that the two-phase level tracking feature can be introduced when it is impractical to reduce the node size below a certain limit. What is the significance of the two-phase level tracking feature when it is not convenient to add nodes? Does this imply a variable clad temperature within a node?

RESPONSE

a) Data collected from the FRIGG critical power test facility was used to validate the GOBLIN early dryout prediction capability during a postulated ABWR LOCA event. To determine the optimal GOBLIN node size that is required to conservatively predict the early boiling transition, a sensitivity study was performed by varying the number of axial nodes in the GOBLIN channel component that simulates the heated segment of the FRIGG test section. In the sensitivity study performed, data collected from the cosine axial power shape series presented in the LTR is used, and 15, 25, and 50 axial nodes are used to represent the heat region.

Figure 1-1 shows the comparisons of GOBLIN predicted dryout times for the three nodalization schemes with the test results. It shows that, for 25 nodes as compared to 15 nodes, a much higher percentage of the data points exhibit GOBLIN-calculated dryout times that are more conservative (that is, shorter) than the measured values. This is illustrated by the higher percentage of 25 node data points as compared to 15 node data points that fall below the ideal line, which represents the GOBLIN calculated dryout times being equal to the measured values. The figure further shows that there is no significant change to the dryout time by increasing the number of nodes from 25 to 50. Based on the result of this sensitivity study, 25 axial nodes are used in the ABWR GOBLIN core heated region.

Note that for the utilized 25-node scheme, [ ]^{a,c} analyzed fall into the non-conservative region. For further discussion on predicted dryout and CPR conservatism, see RAI-21.

a,

[

]

Figure 1-1 - Comparison of Measured vs. Predicted Dryout Times
for Different Nodalization Schemes

b) When the level tracking model is activated, the mixture level replaces the fixed control volume boundary that contains the mixture level with a moving boundary. The flow rate through the boundary is determined by maintaining continuity of phasic flow rates through the two-phase level for a given level velocity. The phasic flow rates are calculated for the volume above and below the mixture level by the drift flux correlation.

One impact of using the two-phase level tracking in the break region is a better resolution of the break flow calculation as the two-phase level moves across the break elevation. This is demonstrated by repeating the feedwater line break case (fwlb3) and turning the level tracking off in the downcomer region where the break is located. The fwlb3 case is chosen because it is similar to both fwlb4, the minimum inventory case (100% break size) and fwlb9, the maximum PCT case (low flow condition), and can give insight into the impact on inventory as well as PCT.

Figure 1-2 shows the dome pressure comparison between the cases, and it shows no significant change in the pressure response when the level tracking is turned off. Figure 1-2 also compares the downcomer two-phase level for the base case and the break flows. It shows that the break flow changes are more responsive when the two-phase level elevation drops below the elevation of the break location.

The clad temperatures of the upper most heated node are compared in Figure 1-3. It confirms that the use of level tracking has no discernable effect on clad temperature, and that the core does not heat up during the transient, with and without the level tracking. The second plot in Figure 1-3 compares the total system masses. It shows that the time dependent system mass remains the same, with and without level tracking. The minimum system inventory decreases from 126.5E3 kg to 126.2E3 kg when the level tracking is off.

The conclusion from the sensitivity study is that, with level tracking in the downcomer region, there is no major impact on the predicted system response for the feedwater line break. With the two-phase level tracking model activated, the break flow is more responsive as the two-phase level drops below the elevation of the break location, and the minimum total system inventory is slightly decreased.

The two-phase level tracking model is only used in the upper and lower annular downcomer regions in the GOBLIN ABWR model, and does not affect the calculation of the clad temperatures.

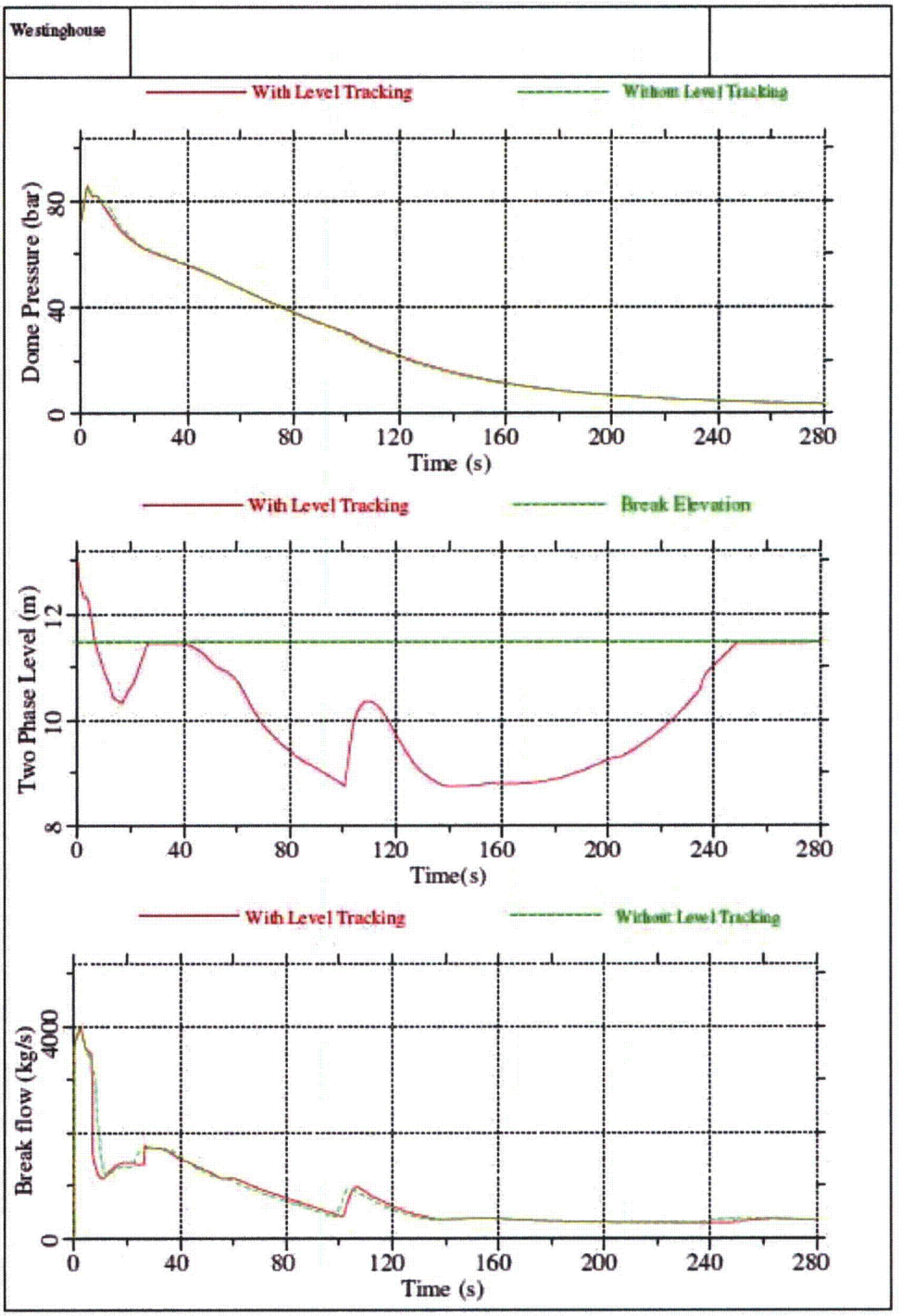

Figure 1-2 - Effect of Downcomer Level Tracking on Dome Pressure and Break Flow (Feedwater Line Break)

** For the first and third plots, the two curves lie on top of each other.

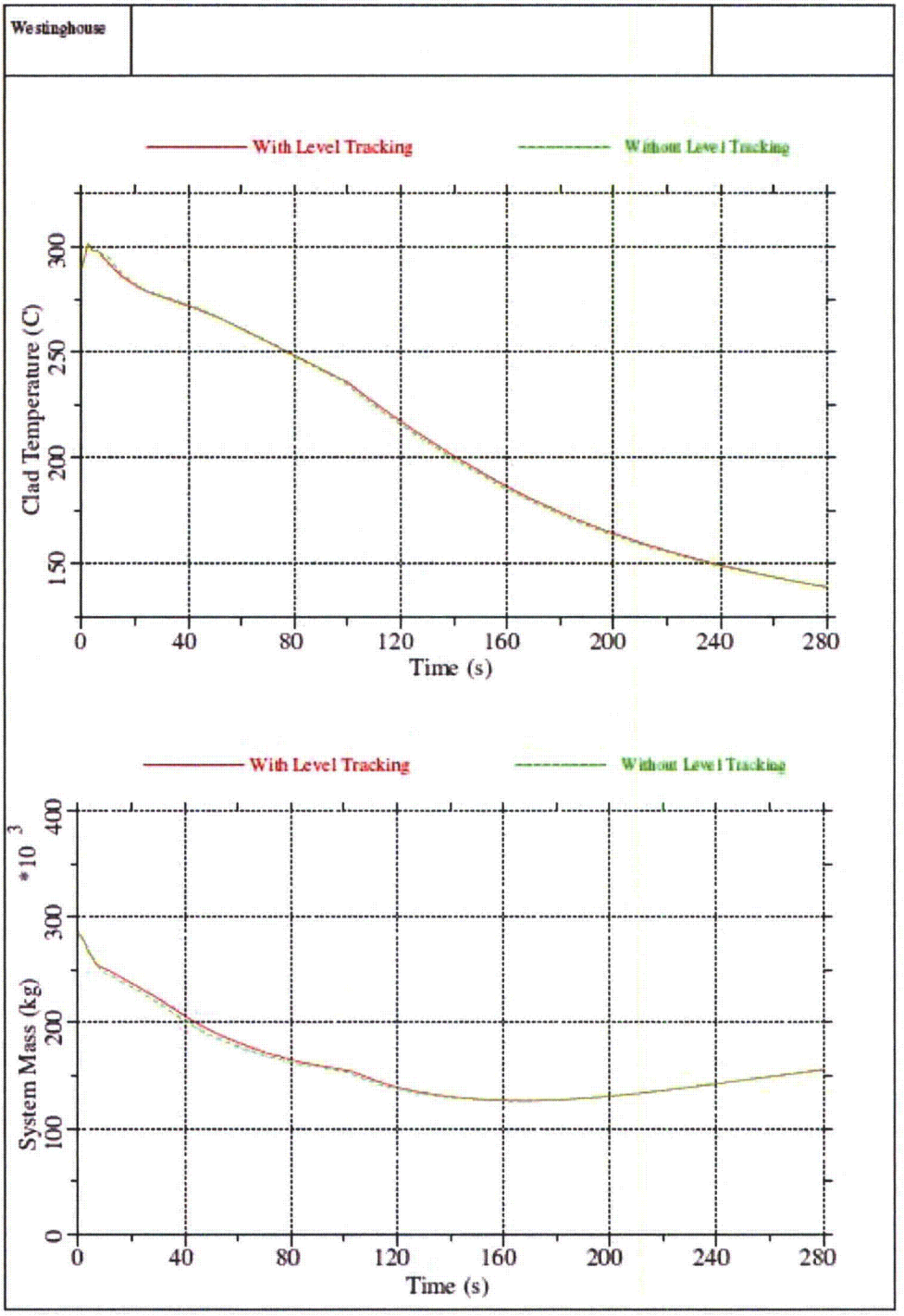

Figure 1-3 - Effect of Downcomer Level Tracking on Clad Temperatures and System Inventory (Feedwater Line Break)

*** For both plots in this figure, the curves lie on top of each other.

RAI-2

QUESTION:

In Section 4.4.2 of WCAP-17116, fast steam line isolation is stated to be a conservative assumption because it reduces voiding in the core at the start of accident. Would this apply to feedwater as well, noting that figures-of-merit such as PCT in ABWR appear to be a function of very early formation and collapse of voids in the reactor coolant rather than long-term coolant inventory makeup? Demonstrate that the assumption of fast (1 s) feedwater coast down is conservative from the standpoint of PCT.

RESPONSE:

To investigate the effect of feedwater coastdown time on the calculated Peak Clad Temperature (PCT), additional GOBLIN runs were performed with feedwater coastdown times of 0.01, 10 and 20 seconds. These calculations showed no difference in the calculated PCT for hot or average channels when varying the assumed feedwater coastdown time. Because the PCT occurs so early in the accident sequence, continued flow from feedwater pumps is unlikely to have a significant effect on the PCT. Figure 2-1, below, shows clad temperature for the limiting elevation of the hot channel as a function of feedwater coastdown time. Note that the curves for the four coastdown times are superimposed on top of each other.

These calculations conclude that feedwater coastdown times that are longer than the fast (1s) coast down time do not have an effect on the PCT.

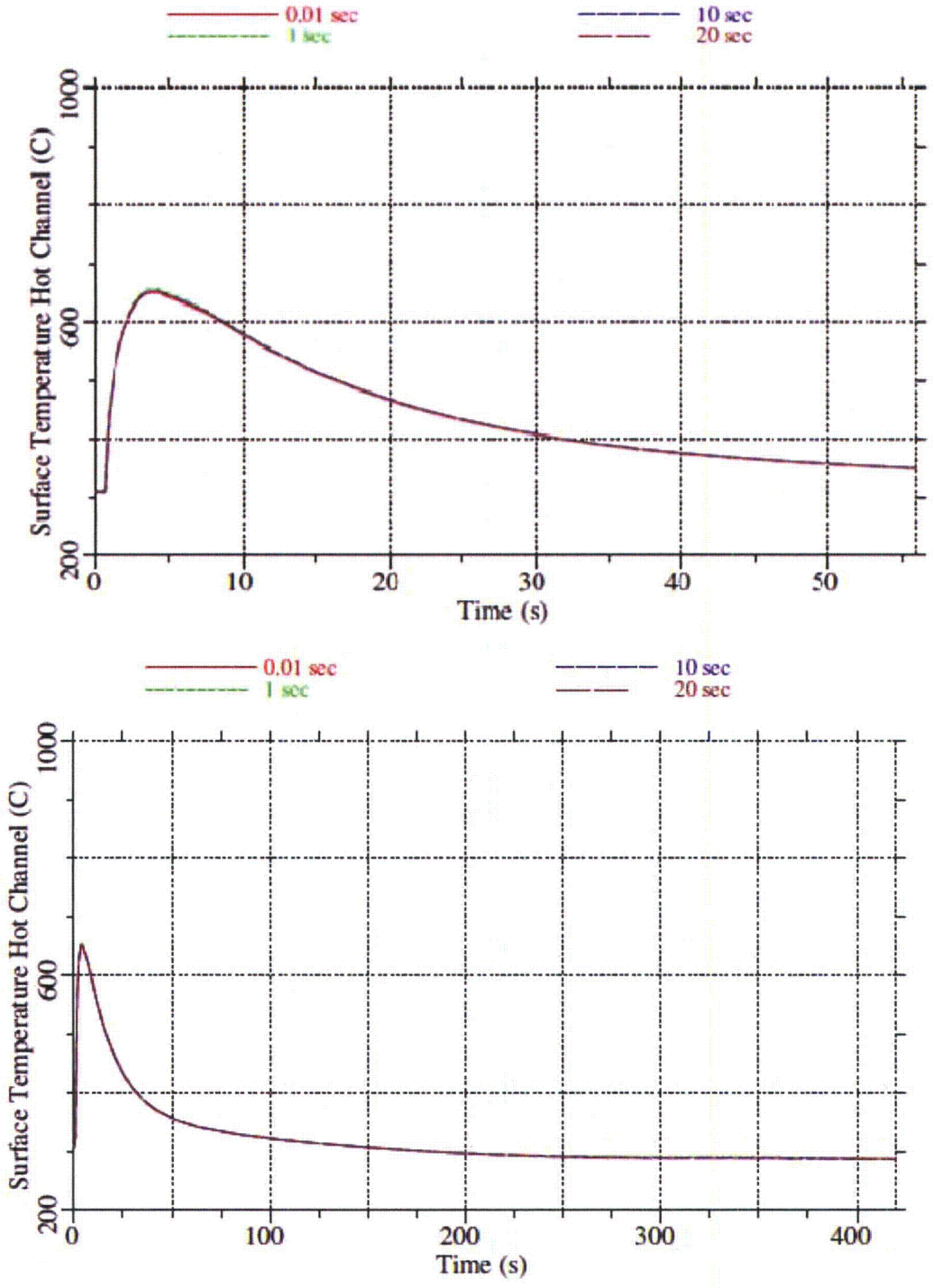

Figure 2-1 – PCT for Different Feedwater Coast Down Times

RAI-3

QUESTION:

Section 4.5.1.2 of WCAP-17116 (HPCF break spectrum sensitivity cases) describes how prediction of core uncovery is more likely in low-power assemblies than in high-power ones due to swelling of the two-phase mixture. In view of this, it is not intuitively obvious a priori which channel would be the most conservative one to consider (highest-power, lowest-power, or somewhere in between).

a) Can you demonstrate that no assembly would experience PCT significantly higher than the ones documented in the sensitivity analysis (i.e., would explicit modeling of an intermediate lower-power assembly yield more conservative results)?

b) What is the procedure for the identification of hottest channel?

RESPONSE:

a) The bundle power peaking factor values for the High Pressure Core Flooder (HPCF) break bundle power sensitivity study of 0.3, 0.6, 0.9, 1.2, 1.5 and 1.7 are expanded to cover peaking factors ranging from 0.1 to 1.7, and a peaking factor resolution of 0.1 is used.

   For each power level, the GOBLIN maximum cladding temperature during the core partial uncovery period after the automatic depressurization system (ADS) is actuated, is shown in Figure 3-1. The GOBLIN peak cladding temperature (PCT) due to the initial dryout is also included for comparison purposes.

   The results of the expanded study, as shown in Figure 3-1, show that the maximum cladding temperature during the partial uncovery is well below the PCT during the initial early dryout time, and the maximum cladding temperature is also a well behaved function of bundle power. Figure 3-1 also shows that the maximum cladding temperatures for these additional assumed bundle peaking factors are not significantly higher than the ones documented in the sensitivity analysis in WCAP-17116-P. Therefore, explicit modeling of lower power assemblies is not warranted.

b) Because the maximum cladding temperature during the partial core uncovery is well below the PCT that occurs during the initial dryout due to the pump coastdown, the hottest channel is the one with the channel power described in Section 4.3.1.2 of WCAP-17116-P.

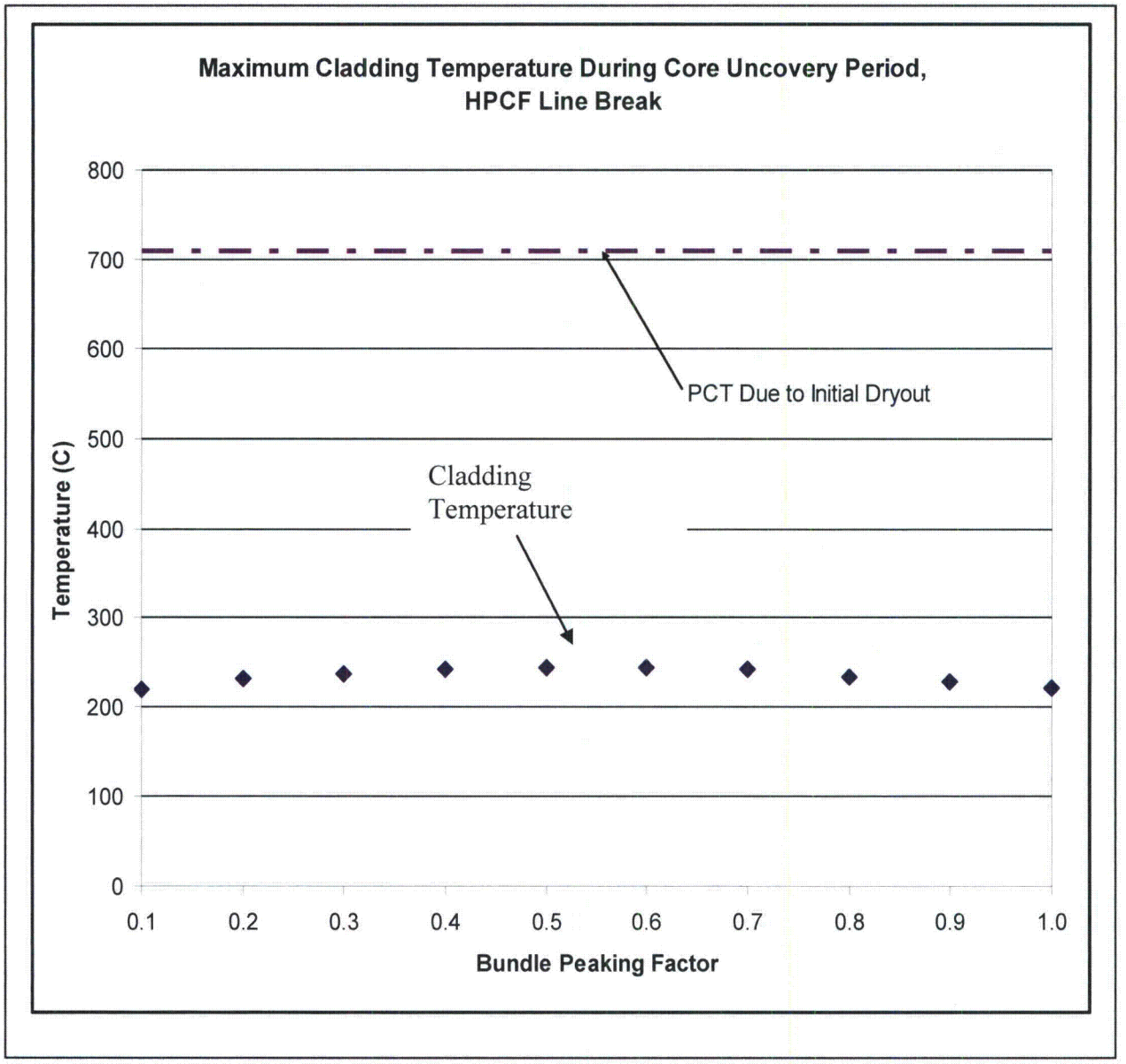

Figure 3-1 Variation of Maximum Cladding Temperature During Partial Core Uncovery with Respect to Bundle Peaking Factor

RAI-4

QUESTION:

Section I. D.1 of Appendix K to 10CFR50 requires that the most damaging single failure of ECCS be considered. In Section 6.4.1 of WCAP-17116-P, it is stated that the single failure for each location of break was chosen on the basis of which one results in the least transient system inventory. Results of the break spectrum analyses for ABWR as documented in WCAP-17116-P show that there is not necessarily any particular correlation between PCT and minimum system inventory (i.e., some cases with the highest PCT also have higher minimum inventory than other cases). Confirm that the single failures that were chosen for analysis do result in the highest PCT.

RESPONSE:

As stated in Section 2 of the LTR, the highest Peak Clad Temperature (PCT) occurs during the initial coast down of the Reactor Internal Pumps (RIPs) before actuation of the Emergency Core Cooling System (ECCS). Any cladding temperature excursion occurring after actuation of the ECCS did not result in a higher cladding temperature. This was true for all single failures evaluated. Therefore, there is no correlation between the single failure chosen and the resulting PCT.

RAI-5

QUESTION

The RIPs can regulate the reactor power output over an approximate range from 70% to 100% by regulating the flow rate without moving control rods. Sensitivity studies for initial core flow rates of 90% and 111% are presented in WCAP-17116-P describing the break spectrum analyses. For most of the break spectrum sensitivities documented in Section 4 of WCAP17116-P, initial core flow rate showed the greatest impact on PCT of any varied parameter (due to the effect on early boiling transition), with low (90%) core flow rate usually yielding highest PCT. In view of the apparent importance of this parameter:

a) As required by Section 11.3 of Appendix K, provide justification for core flow rates (90% and 111%) selected for the sensitivity study. Describe the potential effect of control rod position and power distributions on the core flow rate.

b) How many RIPs are assumed to be in operation for the 90% core flow case?

c) The ABWR DCD provides a power to flow map showing the percentage of core flow to the operating power. Provide the appropriate power to flow map for 9 of 10 and 10 of 10 internal pumps operating and indicate the operating conditions for which the LOCA analysis pump, power and core flow.

d) Was a calculation performed to obtain the steady state conditions for the reactor coolant system prior to the simulation of LOCA scenarios? If steady-state calculations were not performed prior to the simulation of various LOCA scenarios, provide justification that the LOCA results as presented are not affected by a lack of initially steady and stable conditions .

RESPONSE

a) Figure 5-1 below shows the power to flow points analyzed which were chosen to bound the allowable operating regions. Analysis is performed at the low flow and high flow points along the 102% power line. Lower permissible core flows, such as 70% core flow, would be accompanied by a lower operating power that results in less limiting LOCA results.

As discussed in ABWR DCD Subsection 4.4.3.3.5, control rod withdrawal and insertion result in power / flow changes along the constant pump speed lines. In order to achieve limiting LOCA results, the control rods are assumed to be positioned to achieve 102% of rated power.

The extent to which power distribution effects on core flow are relevant to LOCA results are based on the displayed effect of core flow on the transition time from nucleate boiling to film boiling. As discussed in Section 4.3.1.2 of WCAP-17116-P, the hot assembly power

distribution is established in a conservative manner, which bounds any effects it may have on core flow rate or timing of the transition from nucleate to film boiling. Figure 5-4 of WCAP-17116-P confirms that GOBLIN predicts boiling transition time in a conservative manner.

b) For the 90% core flow case, 10 RIPs are assumed operating and 90% flow is achieved by tuning the pump speed. 10 RIPs are assumed operating for all cases.

c) Figure 5-1 below shows the power to flow map for 10 of 10 RIPs operating. Figure 5-2 below shows power to flow map for fewer than 10 of 10 RIPs operating.

[a,c

]

Figure 5-1 – Power Flow Operating Map (10 RIPs)

As stated in Item (b) of this response, 10 RIPs are assumed for all cases analyzed in WCAP-17116-P. The 102/111 and 102/90 power to flow points are denoted in Figure 5-1 as points A and B, respectively.

[a,c

] a,c

Figure 5-2 – Power Flow Operating Map (less than 10 RIPs)

d) A steady state calculation was performed for each case utilizing GOBLIN in order to obtain the steady state conditions prior to event occurrence.

RAI-6

QUESTION

In Section 5 of WCAP-17116-P, qualification was provided for the GOBLIN model of internal recirculation pump coast down against Okiluoto 1 pump trip data. NUREG-0800 Section 15.0.2 Subsection 11.4 states that "calculations of actual plant transients or accidents can be considered, but only as confirmatory supporting assessments for the evaluation model. This is because the data available from plant instrumentation is usually not detailed enough to support code assessment of specific models. Plant data can be used for code assessment if it can be demonstrated that the available instrumentation provides measurements of adequate resolution to assess the code."

a) Provide validation of the GOBLIN internal recirculation pump model against separate effects single- and two-phase pump performance data.

Furthermore, Section I.C.6 of Appendix K to 10 CFR 50 requires that "[t]he pump model resistance used for analysis should be justified. The pump model for the two-phase region shall be verified by applicable *two-phase pump performance data.* For BWRs after saturation is calculated at the pump suction, the pump head may be assumed to vary linearly with quality, going to zero for one percent quality at the pump suction, so long as the analysis shows that core flow stops before the quality at pump suction reaches one percent."

b) Explain the following for the GOBLIN internal recirculation pump model:

i. The use of a constant frictional torque for low speed in contrast to a quadratic or cubic expression.

ii. The method for `tuning' the low speed frictional torque and "adjusting the model" to obtain the correct frictional torque as a function of speed.

iii. How is the conservatism of the model determined if the model is adjusted to meet the coast down conditions?

c) If pump head is assumed to vary linearly with suction quality in the GOBLIN internal recirculation pump model, in the manner described in 10 CFR 50 Appendix K, then confirm that the model meets the above stated requirement that core flow stops before the quality at pump suction reaches one percent.

d) Discuss the pump model behavior for reverse flow conditions and provide the frictional loss coefficient for reverse flow through locked rotor.

RESPONSE

Except for the pump-specific inputs, the pump model used for the ABWR evaluation model is the same model that has been used for the BWRs. The model is documented in Section 3.4.1 of Reference 6-1.

a) The ABWR pump model in GOBLIN makes use of the ABWR single phase homologous curves and the two-phase head degradation model described in Reference 6-2. The two-phase head degradation model is based on the Semiscale two-phase pump data. The model makes use of normalized head difference curves that provide the difference between the single-phase pump performance and the pump performance at a reference void fraction. A two-phase head multiplier is used to extrapolate this result to other void fractions. Although the specific speed of the ABWR internal pump is approximately double that of the Semiscale pump there is no significant correlation between pump head degeneration and the specific speed of the pumps at normal condition.

   In the ABWR LOCA transient, the peak cladding temperature (PCT) occurs very early in the transient when the internal pumps are coasting down and the conditions are single-phase. Therefore, the importance of two-phase pump modeling is low. The reduction of core flow due to pump coastdown is of primary importance, and the ABWR pump model is biased in a way to ensure a conservative coastdown by using a lower bound pump inertia.

b) See following responses:

   i. The GOBLIN pump model is described in Section 3.4.1 of Reference 6-1 and in Section 5.1 of WCAP-17116-P. It consists of solving the conservation of angular momentum for the pump at every time step simultaneously with the basic thermal-hydraulic conservation equations. The torque represents the net torque on the pump impeller. This torque consists of three components: a) hydraulic torque due to the interaction between the fluid and the pump impeller, b) the frictional torque due to frictional losses in the bearings and rotating machinery, and c) the pump motor torque. In GOBLIN, the frictional torque is modeled
   [

.]^{a,c}

Table 6-1 Pump Torque Data

a,c

Figure 6-1 Frictional Torque (N-m) as a Function of Pump Speed (rad/s)

ii. As described in Section 5.1 of WCAP-17116-P, the ABWR pump model is adjusted so that the pump coastdown meets the specified minimum coastdown time constant, which is defined as the time required for the pump speed to reduce to 50% of its initial value. In this case, the frictional hydraulic torques at zero speed and low speed were not provided for the ABWR RIP. Typical inputs for these two parameters were used for an internal pump of a similar design. The only adjustment necessary to meet the coastdown time constant was to reduce the pump inertia from a specified minimum value of [.]^{a,c}

iii. The conservatism in the model can be determined by comparing a case that results in the nominal coastdown time to the case presented in WCAP-17116-P using the minimum coastdown time.

A sensitivity study was performed in response to this RAI to quantify the third conservatism. The pump inertia was specified as having a range between [ ]^{a,c} for safety analysis purposes. The upper end of the inertia range was used in the sensitivity study. The input to the HPCF line break case hpcf3 was modified to increase the pump inertia. The modified case was called hpcf3a. The PCT predicted by GOBLIN was reduced 4° C [708°C to 704°C]. As shown in Figure 6-2 below, the PCT occurs before the pump speed reduces below 13 rad/s where the frictional hydraulic torque model switches to the low speed frictional torque model. Therefore, modifications to other parts of the pump model will not impact the predicted PCT.

c. Pump head is not assumed to vary linearly with quality. As described in item (a) of this RAI, the pump head during two-phase conditions is determined by the two-phase pump performance curves and a void fraction dependent multiplier from Reference 6-2.

d. The RIPs have an anti-rotation device that prevents reverse rotation of the impeller. Similarly, the evaluation model does not allow reverse rotation. The pump head data for the ABWR RIPs include pump head with reverse flow through the pump with a locked impeller. These data were used to generate the single-phase homologous head curves for the GOBLIN model. The pressure increase across the pump for reverse flow through the locked impeller is determined through the use of the homologous curves.

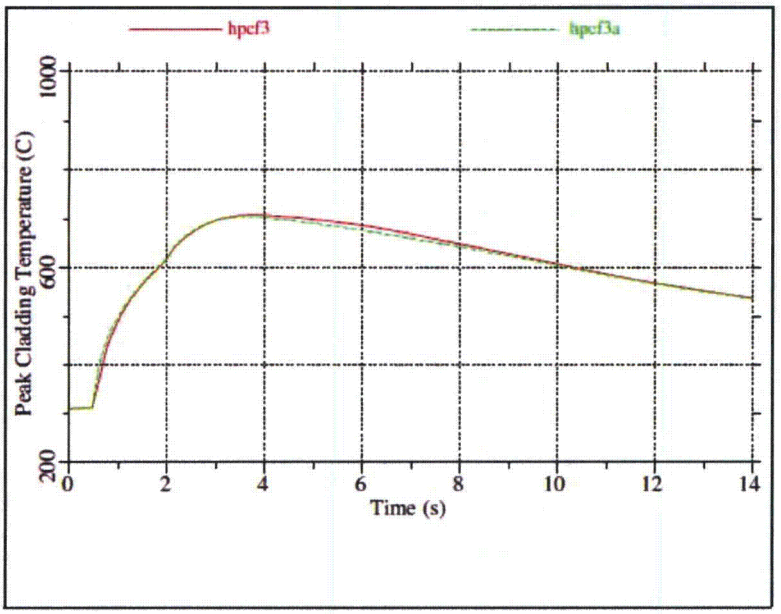

a,c

Figure 6-2 Sensitivity of PCT to RIP Inertia (HPCF Line Break)*

* For the first plot, the two curves lie on top of each other.

References

6-1 RPB 90-93-P-A, "Boiling Water Reactor Emergency Core Cooling System Evaluation Model: Code Description and Qualification," October 1989.

6-2 NUREG-75/056, "WREM: Water Reactor Evaluation Model," May 1975.

RAI-6 Supplement 1:

QUESTION:

In Section 5 of WCAP-17116-P, qualification was provided for the GOBLIN model of internal recirculation pump coast down against Okiluoto 1 pump trip data. NUREG-0800 Section 15.0.2 Subsection 11.4 states that "calculations of actual plant transients or accidents can be considered, but only as confirmatory supporting assessments for the evaluation model. This is because the data available from plant instrumentation is usually not detailed enough to support code assessment of specific models. Plant data can be used for code assessment if it can be demonstrated that the available instrumentation provides measurements of adequate resolution to assess the code."

a) Provide validation of the GOBLIN internal recirculation pump model against separate effects single- and two-phase pump performance data.

Furthermore, Section I.C.6 of Appendix K to 10 CFR 50 requires that "[t]he pump model resistance used for analysis should be justified. The pump model for the two-phase region shall be verified by applicable *two-phase pump performance data.* For BWRs after saturation is calculated at the pump suction, the pump head may be assumed to vary linearly with quality, going to zero for one percent quality at the pump suction, so long as the analysis shows that core flow stops before the quality at pump suction reaches one percent."

b) Explain the following for the GOBLIN internal recirculation pump model:

i. The use of a constant frictional torque for low speed in contrast to a quadratic or cubic expression.

ii. The method for `tuning' the low speed frictional torque and "adjusting the model" to obtain the correct frictional torque as a function of speed.

iii. How is the conservatism of the model determined if the model is adjusted to meet the coast down conditions?

c) If pump head is assumed to vary linearly with suction quality in the GOBLIN internal recirculation pump model, in the manner described in 10 CFR 50 Appendix K, then confirm that the model meets the above stated requirement that core flow stops before the quality at pump suction reaches one percent.

d) Discuss the pump model behavior for reverse flow conditions and provide the frictional loss coefficient for reverse flow through locked rotor.

SUPPLEMENT 1 RESPONSE:

The original response to RAI 6 was provided to the NRC in STPNOC Letter No. U7-C-STP-NRC-100227 dated October 14, 2010. At the NRC audit of WCAP-17116-P held in Windsor, CT the week of February 14, 2011, the NRC requested additional information concerning this response, which is identified in the Audit Plan. The specific request, which relates to Item (d) of this RAI, is to discuss the treatment of the RIP locked rotor flow resistance or, at a minimum, provide access to additional flow information for the transient cases provided in WCAP-17116-P. The purpose of this supplemental response is to provide this additional information.

As stated in the original response, the RIPs have an anti-rotation device that prevents reverse rotation. The pump homologous curves were developed based on pump data that includes forward and reverse flow through a fixed rotor. The pump head data for this condition is shown in Figure 6-1. These data are part of the data set used to develop the homologous curves. Although reverse flow through the pumps is not typical, if reverse flow through a locked rotor were predicted, the head loss would be determined by the homologous pump curves. A separate frictional loss coefficient is not used.

As stated in the original response, the flow through the pump is typically in the positive direction, because the flow through the pump, when the pump is not powered, is driven by natural circulation. As the flow rate through the pump decreases due to decreased driving head, the frictional torque will cause the rotor to stop while the flow rate remains positive as shown in Figure 6-2. When the rotors have 'locked', the flow rate through the pump is ~ 3% of rated flow as shown in Figure 6-3, and the resulting head loss is very small.

a,c

a,c

Figure 6-1 Pump Head vs. Pump Flow for Locked Rotor

[

]

Figure 6-2 Pump Speed vs. Time (hpcf3)

[

]a,c

Figure 6-3 Pump Flow vs. Time (hpcf3)

RAI-7

QUESTION:

In Section 6.3.1.1 of WCAP-17116-P, it is stated that the break spectrum analysis for ABWR includes a series of double-ended guillotine and longitudinal split breaks, in compliance with I.C.1.a of Appendix K. In the text of Sections 4.5 and 4.6 of WCAP-17116-P, some of the break spectrum scenarios were double-ended guillotine breaks and the rest were not identified clearly in this respect. Specify to which class of break each of the break spectrum scenarios in Sections 4.5 and 4.6 belongs.

RESPONSE:

Table 7-1 describes the breaks considered in Section 4.5 and 4.6. The break type is specified as SEG or DEG. A single-ended guillotine (SEG) is intended to represent the situation in which the connecting pipe is completely severed, but only one end of the pipe is left connected to the reactor vessel (e.g., a break in the High Pressure Core Flooder (HPCF) injection line). Any spillage from the other end of the severed line does not impact the loss of inventory from the reactor vessel. A double-ended guillotine (DEG) is used to represent the complete severance of a pipe connected to the reactor vessel in which both ends of the pipe are connected to the reactor vessel (e.g., a break in the steam line after it isolates from the turbine).

The results of longitudinal split breaks were not reported in the LTR. However, a sensitivity study (case mslb6b) was performed for a steam line break wherein a split break was assumed to occur having the same combined break area as the comparable double-ended guillotine break (case mslb6), which is described in Section 4.5.2.1. Figure 7-1 compares the total system mass and the peak cladding temperature predicted by GOBLIN for the hot assembly. As shown, the system responses were essentially identical. This result is expected because the break flow from the reactor vessel is limited by the integral flow restrictors in the steam line nozzles and the flow returning from the intact steam lines is quickly isolated by the Main Steam Isolation Valves (MSIVs).

Table 7-1 Breaks Types Considered

Case	Break Location	Break Type	Comment
hpcf3	HPCF Line	SEG	Break location disable 1 HPCF pump
hpcf4	HPCF Line	SEG	Break location disable 1 HPCF pump
hpcf5	HPCF Line	SEG	Break location disable 1 HPCF pump
hpcf7	HPCF Line	SEG	Break location disable 1 HPCF pump
hpcf8	HPCF Line	SEG	Break location disable 1 HPCF pump
hpcf9	HPCF Line	SEG	Break location disable 1 HPCF pump
mslb6	main steam line	DEG	Break location disables RCIC turbine
mslb6a	main steam line	DEG	Break location disables RCIC turbine
mslb7	main steam line	DEG	Break location disables RCIC turbine
mslb8	main steam line	DEG	Break location disables RCIC turbine
fwlb3	feedwater line	SEG	Break location disables 1 RCIC pump
fwlb4	feedwater line	SEG	Break location disables 1 RCIC pump
fwlb5	feedwater line	SEG	Break location disables 1 RCIC pump
fwlb6	feedwater line	SEG	Break location disables 1 LPFL pump
fwlb7	feedwater line	SEG	Break location disables 1 RCIC pump
fwlb8	feedwater line	SEG	Break location disables 1 RCIC pump
fwlb9	feedwater line	SEG	Break location disables 1 RCIC pump
rhrlb3dlb	RHR suction line	DEG	Connected to bottom drain
rhrlb4dlb	RHR suction line	DEG	Connected to bottom drain
rhrlb5dlb	RHR suction line	DEG	Connected to bottom drain
rhrlb7dlb	RHR suction line	DEG	Connected to bottom drain
rhrlb8dlb	RHR suction line	DEG	Connected to bottom drain
rhrilb3	RHR injection line	SEG	Break location disables 1 LPFL
rhrilb4	RHR injection line	SEG	Break location disables 1 LPFL
dlb	drain line break	DEG	Connected to RHR suction line

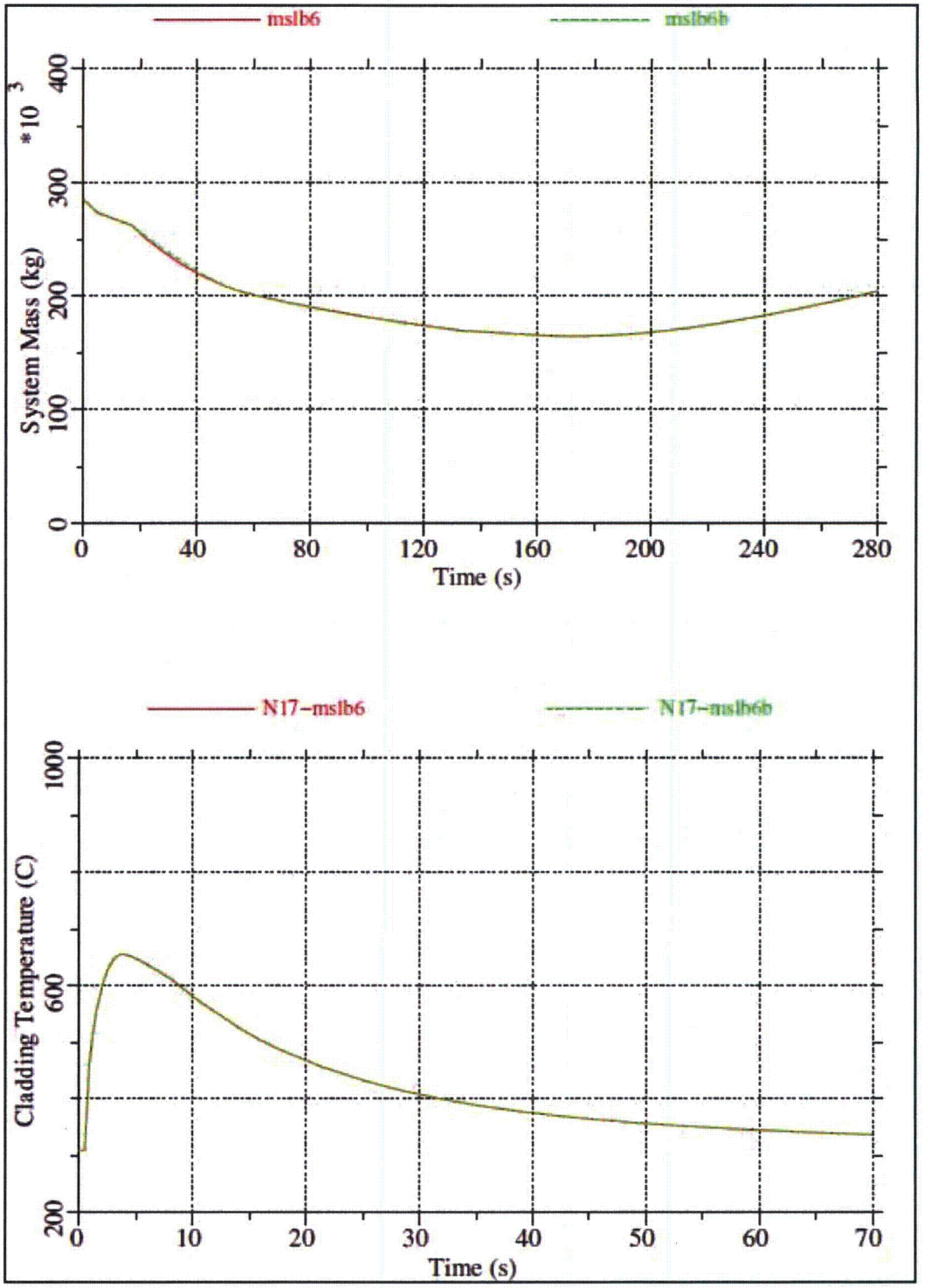

Figure 7-1 Comparison of Responses for DEG and Split of the Same Area (Steam Line Break)

RAI-7S01

QUESTION

RAI-7 had requested clarification on whether adequate consideration had been given to a variety of double-ended guillotine and longitudinal split break configurations, as required by Appendix K Section I.C.1.a. In their response as part of U7-C-STP-NRC-100155 STP replied that additional undocumented sensitivity studies of longitudinal split breaks in the main steam line have shown that the predicted behavior is very similar to that of an otherwise equivalent guillotine break. However, one might expect longitudinal split and double-ended guillotine breaks to behave similarly in cases of single-phase steam flow (as assumed by the STP undocumented sensitivity case). If the break location were to contain liquid and gas phases in close proximity, then entrainment of one phase into the other could result in significantly different break flow characteristics (also dependent upon whether the break is in the top, bottom, or side of the pipe). Demonstrate the adequacy of ECCS performance for ABWR in the presence of longitudinal splits in the feedwater line.

SUPPLEMENT RESPONSE

The GOBLIN code is based on a drift flux model and does not explicitly model entrainment. The current model for the feedwater (FW) line break, for example, considers the elevation of the two-phase mixture in the downcomer relative to the FW sparger nozzle elevation. When the mixture level drops below the nozzles, the break flow through the nozzles would transition to steam.

The FW line break analysis does not explicitly model the FW system. Rather, the analysis conservatively examines the reactor pressure vessel (RPV) side of the break, because this side of the break results in a loss of inventory. The break flow from the RPV is limited by the nozzles on the FW sparger until the break size is comparable to the total nozzle flow area. The diameter of each nozzle is approximately 1.75 inches and there are 54 nozzles per sparger, resulting in a total nozzle flow area of 0.9 ft^2 for the 100% break size. With regard to inventory loss from the RPV, the worst case 200% longitudinal split in the FW line would have the same inventory loss as a 100% double-ended guillotine (DEG) break in the FW line. For smaller longitudinal splits in the FW line, the flows from each side of the split would be competing for the flow area of the split. This would result in a reduced flow contribution from the RPV side of the split. Therefore, the longitudinal split is bounded by the DEG break with regard to minimum RPV inventory.

RAI-7 Supplement 2:

QUESTION:

RAI-7 had requested clarification on whether adequate consideration had been given to a variety of double-ended guillotine and longitudinal split break configurations, as required by Appendix K Section I.C.1.a. In their response as part of U7-C-STP-NRC-100155. STP replied that additional undocumented sensitivity studies of longitudinal split breaks in the main steam line have shown that the predicted behavior is very similar to that of an otherwise equivalent guillotine break. However, one might expect longitudinal split and double-ended guillotine breaks to behave similarly in cases of single-phase steam flow (as assumed by the STP undocumented sensitivity case). If the break location were to contain liquid and gas phases in close proximity, then entrainment of one phase into the other could result in significantly different break flow characteristics (also dependent upon whether the break is in the top, bottom, or side of the pipe). Demonstrate the adequacy of ECCS performance for ABWR in the presence of longitudinal splits in the feedwater line.

SUPPLEMENT 2 RESPONSE:

The original response to RAI 7 was provided to the NRC in STPNOC Letter No. U7-C-STP-NRC-100155 dated July 7, 2010. A supplemental response was provided in STPNOC Letter No. U7-C-STP-NRC-100242 dated October 25, 2010. At the NRC audit of WCAP-17116-P held in Windsor, CT the week of February 14, 2011, the NRC accepted the supplemental response that had been submitted on this RAI, as noted in the Audit Plan. However, the NRC also stated that the SER for WCAP-17116-P will highlight a limitation of the GOBLIN code for evaluation of longitudinal split breaks under conditions when choke flow does not exist. The purpose of this second supplemental response is to satisfy a commitment made at the audit to provide additional details on the feedwater line break flow modeling. This includes a comparison of the results for a number of break sizes assuming additional noding for the feedwater lines.

Although the feedwater line break is assumed to occur in one of the feedwater lines, the break flow is limited at the nozzles on the feedwater sparger (total area = 0.9 ft^2). Therefore, a simplification was made in WCAP-17116-P to simulate the break as a single-ended guillotine break discharging from the downcomer at the elevation of the feedwater line.

As shown in Figure 7-1, there are two 24-inch feedwater lines feeding each feedwater sparger. The flow area of the feedwater line is approximately 2.5 ft^2. The break flow from the reactor vessel due to a double-ended guillotine break of the feedwater line would be limited by the feedwater sparger nozzles. Such a limitation would not affect the discharge from the feedwater side of the break.

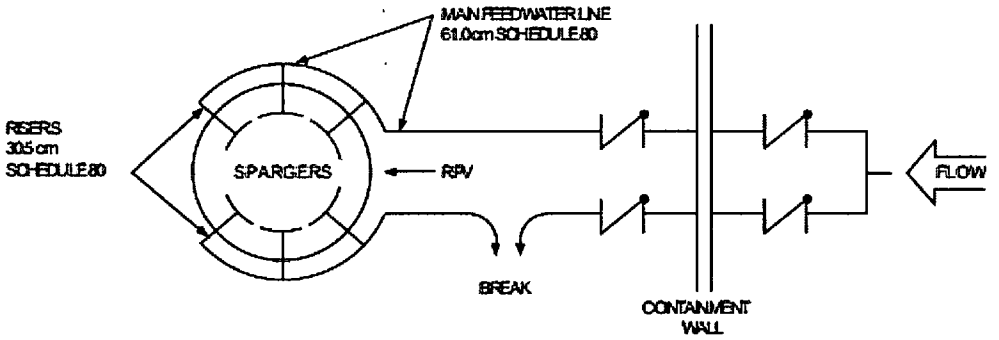

Figure 7-1 Schematic of Feedwater Lines

In the event of a large longitudinal split break (e.g., 200% split with area ~ 5 ft^2) in the feedwater piping, the stagnation pressure at the break is expected to decrease very rapidly such that the flow from the reactor vessel would be limited by choked flow through the feedwater nozzles. For smaller split breaks, there would be a break size where the flow through the feedwater nozzles would not be choked and the break flow would be influenced by the fluid discharging from the feedwater system. However, the break flow from the reactor vessel would be reduced relative to the way the break flow was determined in WCAP-17116-P.

To demonstrate this effect, several cases were run wherein the feedwater line was simulated by [ ]^{a,c} additional nodes as shown in Figure 7-2. As shown, a split break was simulated in node [ ]^{a,c} in which the feedwater pipe was assumed to have an internal diameter of 21.562 inches (0.548 m). A double-ended split break area becomes 0.4712 m^2. The flow path area [ ]^{a,c} simulated the connection of the feedwater line to the feedwater sparger with a flow area of the feedwater nozzles (0.08389 m^2). The size of the split break was varied from 200% to 25%. Note that the 25% break has an area of 0.0589 m^2, which is smaller than the combined area of the feedwater nozzles (0.08389 m^2).

Figure 7-3 compares the steam dome pressures. As shown, the original case (fwlb3) agrees closest with the largest break (200%). As expected, the smaller breaks indicate a slower depressurization.

Figure 7-4 compares the pressures downstream of the feedwater nozzles (node [ ]^{a,c} in this study). In the base case (fwlb3), the break was attached directly to the containment. As shown, the downstream pressure increases with decreasing break size as expected.

Figure 7-5 compares the mass flow rates leaving the reactor vessel. As shown, the flow rate for the 200% case is similar to the fwlb3 cases, although it is seen that even this break unchokes due to the influence of the discharge from the feedwater system.

Figure 7-6 compares the peak cladding temperature in the hot assembly as predicted by GOBLIN. This occurs in Node [ ]^{a,c}, which is [ ]^{a,c} nodes above the midplane, for all cases. As shown, the peak cladding temperatures occur at nearly the same time very early in the transient and are nearly identical.

Figure 7-7 compares the total reactor vessel inventories. As shown, the largest break (200%) has the lowest minimum inventory and is bounded by the base case (fwlb3). As the break area is

reduced, the flow from the reactor vessel through the feedwater nozzles is no longer choked and the resulting inventory loss is reduced.

In conclusion, the treatment of the feedwater line break in WCAP-17116-P is conservative in that the minimum reactor vessel inventory is predicted.

[a,c

]

Figure 7-2 Noding Added to Simulate Feedwater Piping

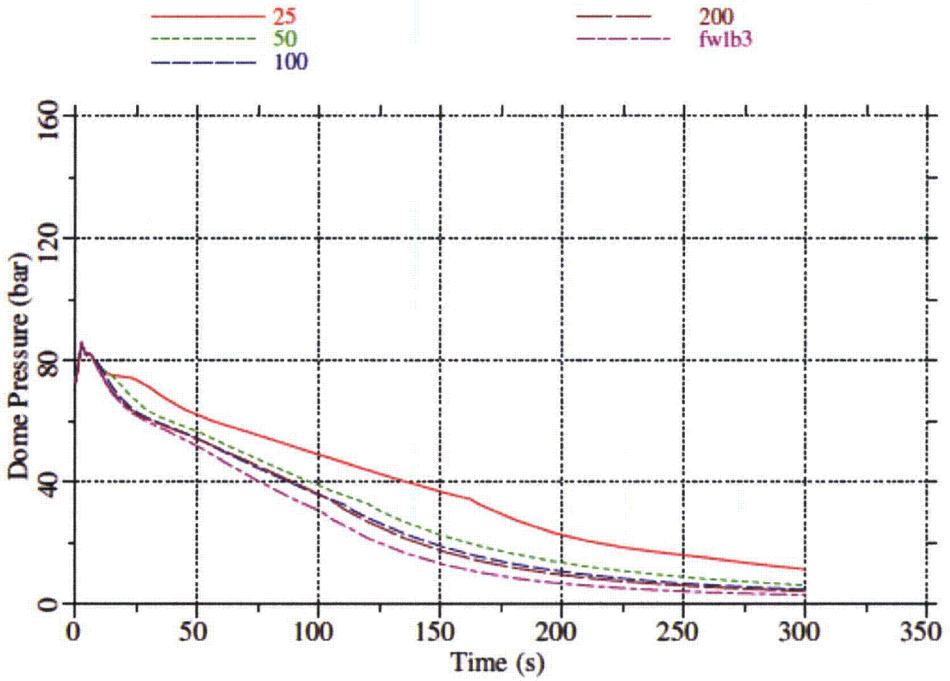

Figure 7-3 Comparison of Steam Dome Pressures

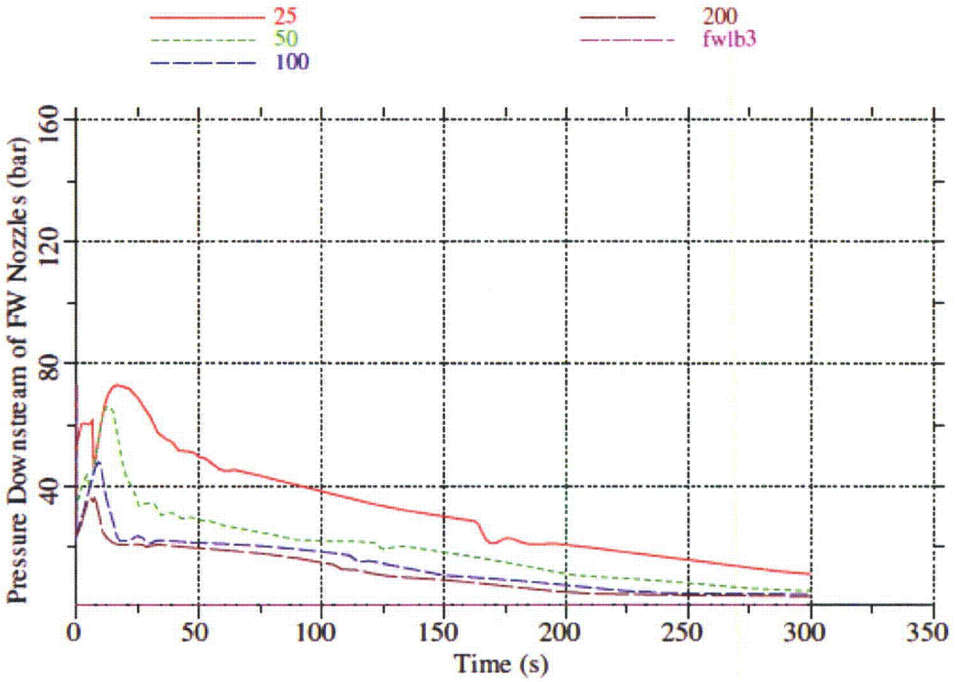

Figure 7-4 Comparison of Pressures Downstream of the FW Nozzles

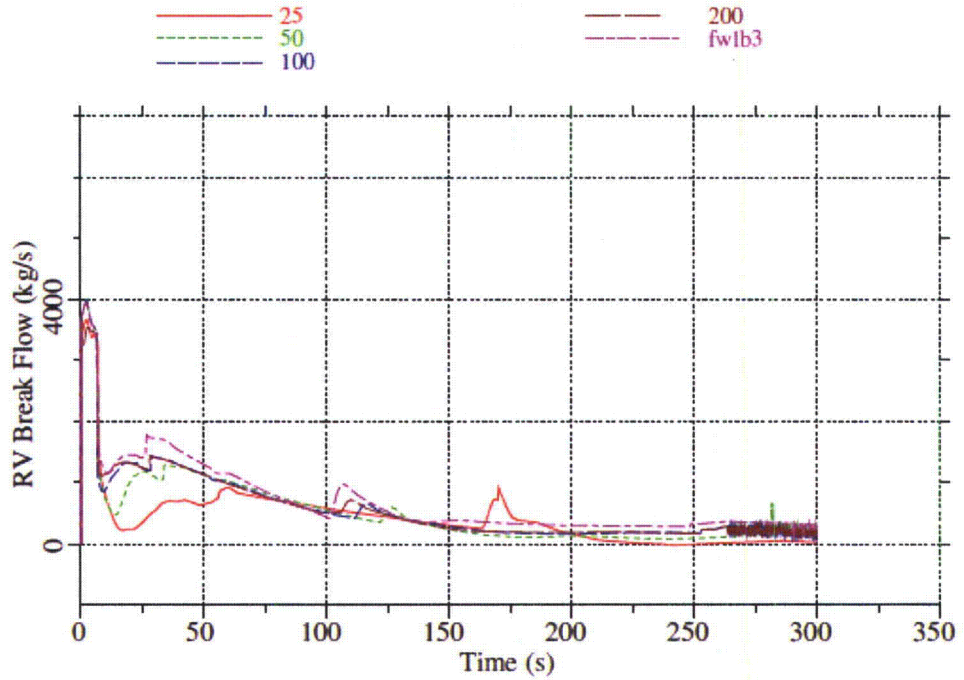

Figure 7-5 Comparison of Break Flows From the Reactor Vessel

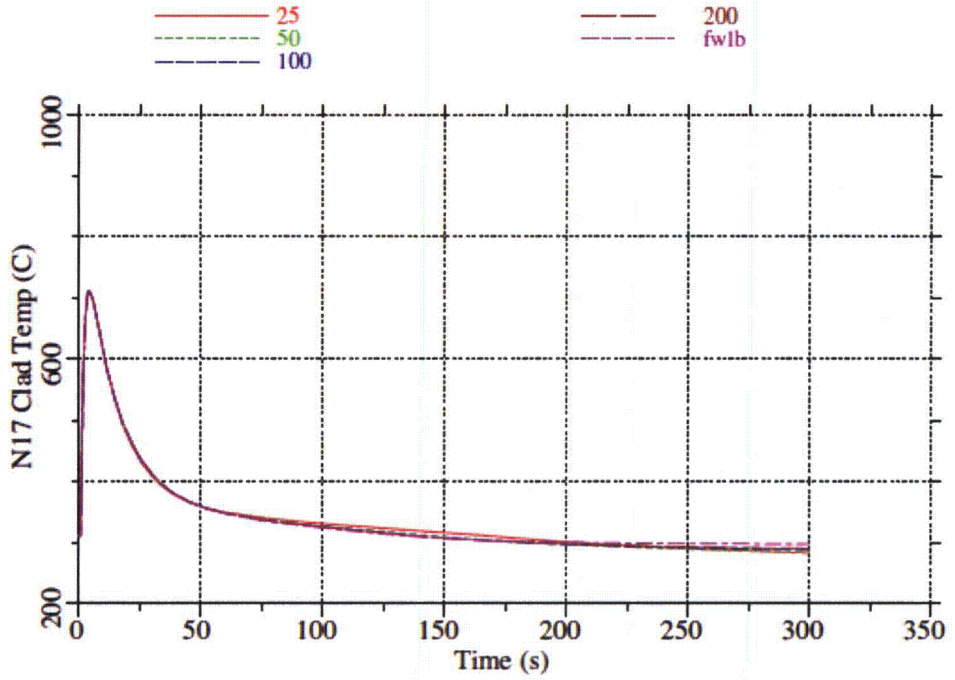

Figure 7-6 Comparison of GOBLIN Peak Cladding Temperatures

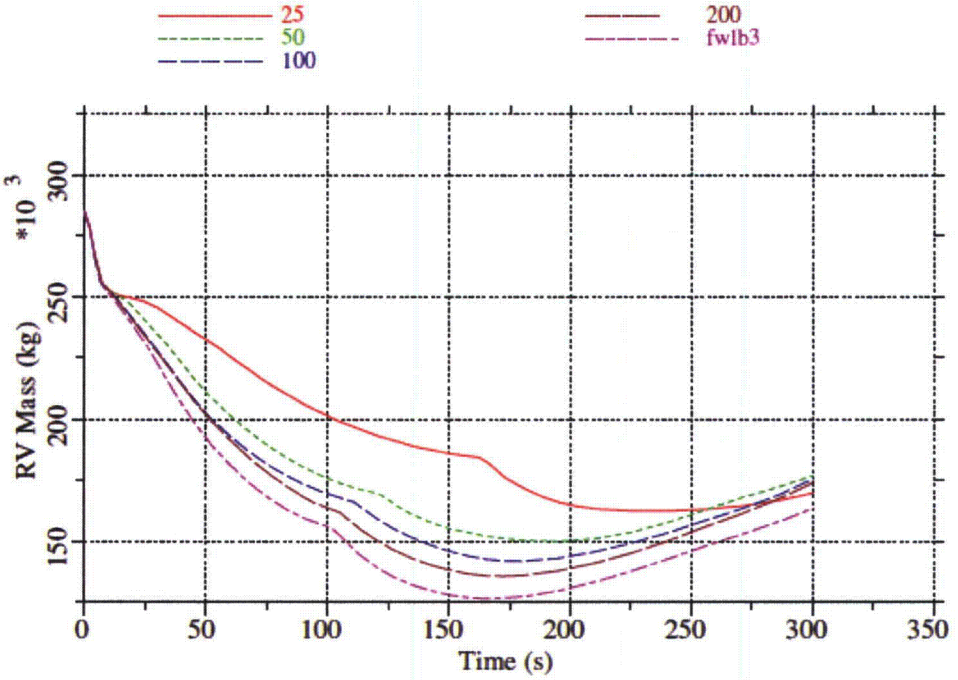

Figure 7-7 Comparison of Reactor Vessel Total Mass

RAI-8

QUESTION:

I.C.1.b of Appendix K requires that the licensee perform calculations with a range of break discharge coefficients ranging from 0.6 to 1.0. Clarify the evaluation model's compliance with this requirement, given that no values of break discharge coefficient are mentioned for the analyses presented in WCAP-17116-P.

RESPONSE:

The evaluation model, which is the basis for WCAP-17116-P, meets the above Appendix K, I.C.1.b requirement. The discharge coefficient is identified in WCAP-17116-P as "break size." A break size of 100% represents a fully open pipe break (discharge coefficient of 1.0). A break size of 50% would represent a break size of half the pipe cross-sectional area (discharge coefficient of 0.5), etc. Below is a summary of places in WCAP-17116-P that supply this information. In all cases, the range of discharge coefficients of 0.6 to 1.0, as noted in the RAI, is covered in the analyses.

- Table 4-2 in Section 4.5.1.1 shows the range of break sizes that were examined for a HPCF line break. Section 4.5.1.2 has a discussion of the effects of different break sizes.

- Table 4-3 in Section 4.5.2.1 shows the range of break sizes that were examined for a main steam line break. Section 4.5.2.2 has a discussion of the effects of different break sizes. Note that Table 4-3 shows break sizes of 200%, 150% and 100%. Because GOBLIN models the loss of reactor coolant from both sides of this break, a complete pipe break would result in a 200% break size case. As a result, a 200% main steam line break is analogous to a 100% single-sided break, a 150% break is analogous to a 75% single-sided break, and a break of 100% would be analogous to a 50% single-sided break. Therefore, the Appendix K range of 0.6 to 1.0 is covered in this case.

- Table 4-4 in Section 4.5.3.1 shows the range of break sizes that were examined for a feedwater line break. Section 4.5.3.2 has a discussion of the effects of different break sizes.

- Table 4-5 in Section 4.5.4.1 shows the range of break sizes that were examined for a Residual Heat Removal (RHR) suction line break. Section 4.5.4.2 has a discussion of the effects of different break sizes.

- Section 4.7, the summary of limiting cases, includes plots of minimum inventory and Peak Clad Temperature (PCT) as a function of break size.

RAI-9

QUESTION

WCAP-17116-P indicates that the objective of the ECCS analysis for the ABWR is to "simply show that either the core does not uncover or it uncovers minimally so that there is no appreciable cladding heat-up after the initial boiling transition to demonstrate the adequate performance of the ECCS equipment."

The ECCS design objective noted above, however, leaves open a number of questions regarding the definition of the terms for successful completion of the design objectives. *Minimal Core Uncovery* could translate into a two-phase mixture level 6-inches below the top of active fuel, one foot below the top of active fuel, or up to three feet below the top of active fuel. In each of these instances, cladding heat-up may not result if there is sufficient steam cooling and entrained liquid impingent upon spacer grids which would provide rewet cooling. Similarly, No *appreciable cladding heat-up* after the initial boiling transition can have a number of interpretations. It could mean that any secondary cladding heat-up is lower than the initial boiling transitions heat-up. This would still be well below the regulatory limit, but could translate into a two-phase mixture level up to 4 feet below the top of active fuel under steam cooling conditions. It could mean that the cladding temperature only exceeds the normal operating temperature by 50°F. In fact, the two-phase mixture level could be below the top of the core during the transient with the cladding temperature being below the normal operating temperature.

a) Provide quantitative explanations of the design objectives:

Minimal core uncovery, and

ii. No appreciable cladding heat-up after initial boiling transition

RESPONSE

Only one ABWR LOCA scenario shows complete depletion of upper plenum inventory and partial uncovery of fuel assemblies which is the High Pressure Core Flooder (HPCF) line break with failure of the emergency diesel generator (EDG) that powers the unaffected HPCF loop. The equipment available for this case is 1 RCIC + 2 LPFL + 8 Automatic Depressurization System (ADS).

In this case, the break is located in the upper plenum region, and, with both Reactor Core Isolation Cooling (RCIC) and Low Pressure Flooder (LPFL) delivering water to the Reactor Pressure Vessel (RPV) annular downcomer region, core inventory is replenished solely by reflooding from the bottom. Due to the small break size and the break elevation, core inventory is maintained until ADS is actuated. After the ADS is actuated, the loss of system inventory accelerates, and the core region becomes partially uncovered until LPFL refills the core from the bottom. During this period of partial core uncovery, the average core is filled with a two-phase

mixture and the severity of individual fuel channel uncovery depends on the local bundle power level. For the very low-power fuel channels, the lower rate of steam generation due to the removal of decay heat may not sustain a two- phase mixture level to the top of the fuel channel. For example, the top 20% of a low power channel would be cooled by steam generated in the lower 80% of the channel.

As documented in WCAP-17116-P, sensitivity studies of the impact of fuel bundle power on the severity of fuel channel uncovery and subsequent fuel rod heat up were performed by varying the single GOBLIN channel power peaking factor from 0.3 to 1.7. The results show that, while the two-phase mixture level decreases below the top of the low power fuel assemblies, the fuel rod temperature increase in those assemblies remains well below the peak clad temperature (PCT) that occurs during the initial dryout, which is well below the 10CFR50.46 acceptance criterion.

There are no design criteria for minimal core uncovery, since the real design criteria remain the acceptance criteria of 10CFR50.46.

RAI-10

QUESTION

The ABWR LOCA analysis presented in WCAP-17116-P assumes a loss of off-site power in combination with failure of one emergency diesel generator power as the limiting condition since it results in the lowest amount of ECCS flow for the breaks under consideration. Furthermore, all RIPs are assumed to coast down rapidly as a result of the loss of power. The rapid decrease in core flow leads to the boiling transition and excursion of cladding temperature.

Westinghouse has stated in WCAP-17116-P that the assumptions of loss of off-site power and trip of RIPs coincident with the LOCA are conservative. However, sensitivity analysis or justification supporting the above assumptions is not provided in WCAP-17116-P. With the offsite power available following a LOCA, the RIPs would continue to circulate flow until some pump trip criteria is reached. With the pumps powered; even though the core would remain cooled, the quality of fluid at the break location may be significantly lower resulting in substantially higher mass inventory loss. This is not a concern provided offsite power is maintained. If, however, it is lost during the transient and there is a subsequent failure of an emergency diesel generator to start, the same limiting flow conditions could result. In this case, the lower inventory conditions could result in an uncovering of the core and cladding heat-up that is more limiting than the initial cladding heat-up that results from the loss of flow transient in conjunction with the LOCA.

Section 11.3 of Appendix K to 10 CFR 50 requires that "appropriate sensitivity studies shall be performed for each evaluation model, to evaluate the effect on the calculated results of variations in noding, phenomena assumed in the calculation to predominate, including pump operation or locking, and values of parameters over their applicable ranges. For items to which results are shown to be sensitive, the choices made shall be justified."

a) Justify that the trip of RIPs coincident with the LOCA is the worst time for the RIPs to trip during the LOCA.

b) If the worst time for the RIPs to trip is not the time of initiation of LOCA:

i. Determine the worst time for the failure of RIPs.

ii. What is the minimum system inventory for LOCAs of various sizes if the RIPs continue to operate and offsite power is lost at the worst time?

iii. How is core cooling affected if offsite power is lost at the worst time for the RIPs to trip and the failure of an emergency diesel generator to start?

Furthermore, as discussed in Section 4.1 of WCAP-17116-P, the realistic response to the loss of off-site power would result in the operation of some RIPs for a longer period of time. In light

of the fact that RIP operation can affect the quality of flow at the break location, it is important to understand how the LOCA would respond to a more realistic response of the RIPs even if the initial temperature excursion is mitigated to some degree.

c) Describe the criteria for tripping the RIPs during LOCA conditions. Provide a discussion of the progression of events under LOCA accident conditions considering the realistic operation of the RIPs.

d) Does the mitigation of the temperature excursion, exceed the potential cladding heat-up that may result from a lower system mass inventory resulting from continued operation of some of the RIPs during the coast down of the M/G set?

e) As discussed earlier, the realistic response to the loss of off-site power would result in the operation of some RIPs for a longer period of time causing asymmetric distribution of flow in lower plenum and core. Under these circumstances, the hot assembly inlet flow rate, depending on location in the core, would be either lower or higher compared to the average core average flow rate. What are the effect of this type of flow asymmetry on the hot channel analysis and the results of LOCA analysis? If perfect mixing in the lower plenum cannot be justified, should the lower plenum be divided into additional nodes, with a set of lower plenum nodes feeding the average core and a set of nodes feeding the hot assembly? Please elaborate.

RESPONSE

a) For the LOCA analyses evaluated in WCAP-17116-P, the worst-case time for tripping of the RIP's, which results in the highest calculated peak clad temperature (PCT), is at the time of the LOCA. The discussion which follows provides a detailed justification.

The three LOCA scenarios considered in the WCAP-17116-P are the main steam line break (MSLB), the feedwater line break (FWLB), and the high pressure core flooder (HPCF) break. Each of these break scenarios are evaluated below.

In order to simulate the scenario described in this RAI, offsite power is assumed to be available until some time following the LOCA. To evaluate the effect of the RIPs continuing to run following the LOCA, the RIPs are assumed to trip at 5 seconds and 20 seconds post-LOCA. These times are considered sufficient to illustrate the trend resulting from increasing the RIP trip time.

The reactor is assumed to scram at time = 0 as in WCAP-17116-P.

Because continued offsite power is stipulated, for the MSLB and HPCF break scenarios, the feedwater pumps are assumed to continue functioning after the LOCA. To maintain conservatism, it is assumed that the feedwater is stopped at the time of RIP trip. For the FWLB case, feedwater flow is terminated at the time of the break because of the break location. In cases considered in WCAP-17116-P, fast closure of the the turbine closure valve

(TCV) was assumed due to loss of offsite power. Since offsite power is stipulated here, normal operation of TCVs is assumed until the time of RIP trip.

MSLB Scenario

For the MSLB, the feedwater pumps are assumed to continue to operate after the LOCA, because the break location does not prohibit it. With the reactor trip coincident with the LOCA and all of the pumps continuing normal operation until some later time, there is cooling flow for the duration of the heatup time. As shown in Figure 10-1, in all cases analyzed in which the RIPs are allowed to run post-LOCA, there is no heatup observed. Because the feedwater pumps supply more coolant than is being lost through the break, the total system inventory increases (see Figure 10-2) during that portion of the scenario when feedwater is available. In this event, regardless of the time of RIP trip, the PCT is reduced relative to pump trip at the time of LOCA, and total system inventory increases with longer RIP trip time. Consequently, the 5 second and 20 second cases are sufficient to demonstrate that the highest peak clad temperature occurs when the RIPs are assumed to trip at the time of the LOCA.

Figures 10-3 and 10-4 show the break flow quality and the break flow rate for different assumed RIP trip times. With delayed RIP trip, there is an increase in the amount of break flow caused by lower break quality, but because of the added feedwater flow, the total system mass increases. The analysis is shown until break quality returns to 1, and break flows are equal. From this point forward, the scenarios should produce the same results.

In summary, for the MSLB, assuming RIP trips after the LOCA results in higher coolant inventory and lower PCT compared with RIP trip coincident with the LOCA. Consequently, the worst time for the RIPs to trip is coincident with the LOCA.

FWLB Scenario

For the FWLB case considered in WCAP-17116-P, the water level crosses LWL-2 before 7 seconds. The last RIPs trip 6 seconds later (Reference 10-1), meaning that all RIP flow stops by 13 seconds after the LOCA (RIP trip criteria are discussed in detail in part c) of this response). The assumed upper value of 20 seconds for tripping all RIPs bounds that value with margin. Feedwater injection is assumed to stop at the start of the LOCA because of the break location. This means that any additional RIP action only shortens the time required to reach LWL-2, further justifying the conservatism of the assumed 20-second RIP trip time.

Figures 10-5, 10-6, 10-7, and 10-8 show the time-dependent clad surface temperature, total system mass, break flow quality, and break flow rate for this scenario. As shown in Figure 10-5, the PCT for cases with assumed RIP trip time after the onset of LOCA is less than for the case of RIP trip coincident with the LOCA. Subsequent break flow does not experience a consistent decrease in quality or increase in flow. There is no further heat up caused by RIP action.

There is a slight decrease in total system inventory, but by 220 seconds, the break flow for all cases converges. Despite the inventory difference, there was no additional dryout or heatup in the hot bundle. The worst time for the RIPs to trip in this case is coincident with the LOCA.

HPCF Break Scenario

The feedwater pumps are assumed to continue to operate for the HPCF break because the break location does not prohibit it. The reactor trips at the start of the LOCA, but all of the pumps continue normal operation. This case exhibits different clad temperature heatup from the MSLB case mainly because of the pressure difference. The MSLB has a much larger break area, and consequently allows the plant to depressurize to a much greater extent. In this case the higher pressure means that the water in the core will remain liquid to a much greater extent, and the voiding will be much lower. This causes a brief increase in reactivity, and therefore power. This short-lived effect is not sufficient to cause the PCT to equal the case presented in WCAP-17116-P.

Because the feedwater pumps supply more coolant than is being lost through the break, the total system inventory increases (see Figure 10-10). As shown in Figures 10-11 and 10-12, there is minimal change to break quality or flow as a function of assumed RIP trip time. In summary, for the HPCF break, assuming that the RIPs trip after the LOCA results in higher coolant inventory and lower PCT compared with a RIP trip coincident with the LOCA. Consequently, the worst time for the RIPs to trip is coincident with the LOCA.

Summary

As shown in the previously referenced figures, in all cases examined, extending the time of RIP trip past the time of LOCA does not have a negative impact on PCT. In all cases, the additional flow through the core in the first 5 seconds reduces the PCT, and there is no subsequent increase in clad temperature due to reduced inventory. For the HPCF break and MSLB cases, because the feedwater pumps continue to operate until the RIPs are tripped, the overall system inventory is greater for the delayed RIP trip cases. In the FWLB case, the total system mass is slightly lower, but it has no effect on PCT.

In all scenarios considered, the worst time for the RIPs to trip is coincident with the LOCA.

b) As stated above, the worst time for the RIPs to trip is at the time of initiation of LOCA.

c) The 10 RIPs are separated into three groups on different buses (Reference 10-1). The first 4 RIPs trip immediately when water level reaches LWL-3. When LWL-2 is reached, 3 more RIPs trip immediately, and the last 3 RIPs trip 6 seconds later. In a FWLB, because the break location prevents the flow of additional feedwater, functioning RIPs would hasten the arrival of LWL-3 and LWL-2. In this scenario, all RIPs trip by 13 seconds. For other cases in which the RIPs can continue to circulate coolant through the core, there will be a longer delay in tripping the pumps, but because the PCT occurs so early, any additional time pumping water will lessen the severity of an accident.

d) Any decrease in total system inventory is more than compensated for by additional flow. Any decrease in total inventory is not sufficient to cause a second heat up, and the extra initial flow lowers the initial PCT. The original assumption of RIP trip coincident with LOCA is limiting.

e) As RIPs trip, they do so in symmetric groupings, meaning that asymmetries in flow to the lower plenum should be minimal. (Reference 10-2) Additionally, the cases considered in WCAP-17116-P had no flow coming from the RIPs, and achieved acceptable results. Any additional flow would be beneficial. For these reasons, no additional noding or analysis is needed.

References

10-1 STP Drawing U3-ARSD-J-DWG-IBD-0001

10-2 Toshiba Drawing NT-5103053 Rev. 4.

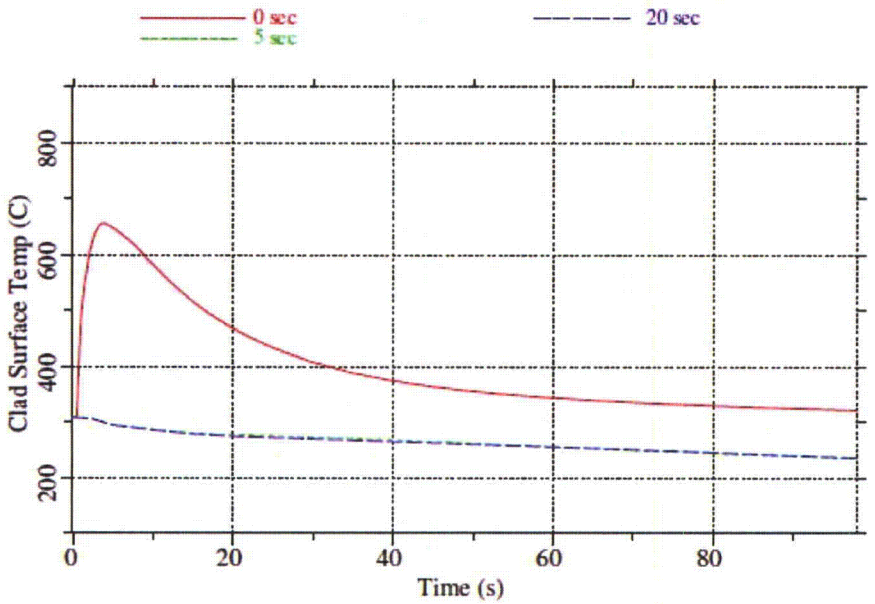

Figure 10-1 – Clad Surface Temp for Different RIP Trip Times, MSLB*

* The 5 second and 20 second curves lie on top of each other

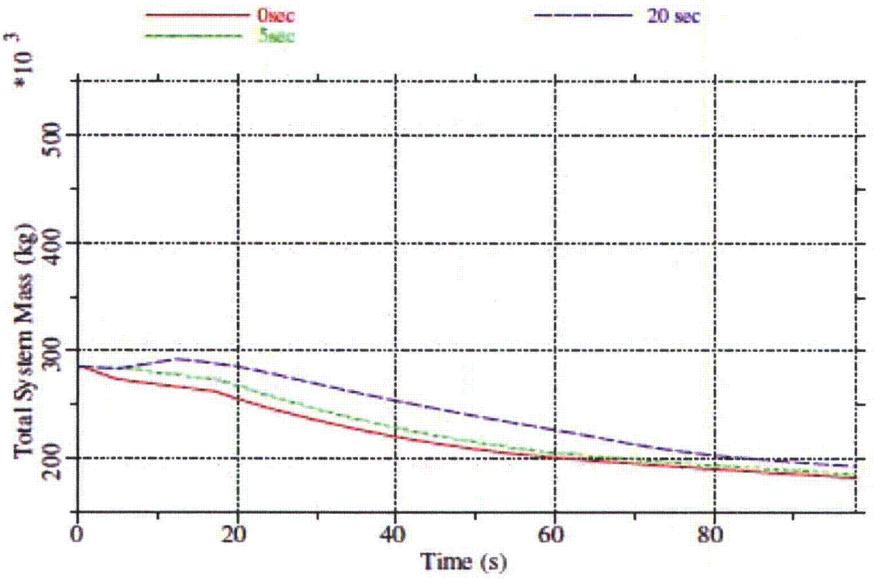

Figure 10-2 – Total System Mass for Different RIP Trip Times, MSLB

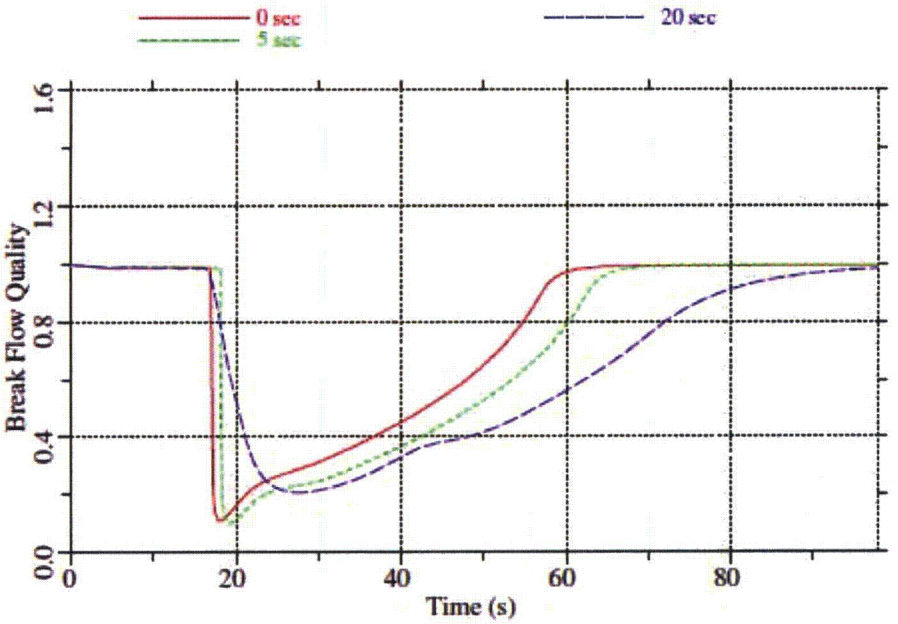

Figure 10-3 – Break Flow Quality for Different RIP Trip Times, MSLB

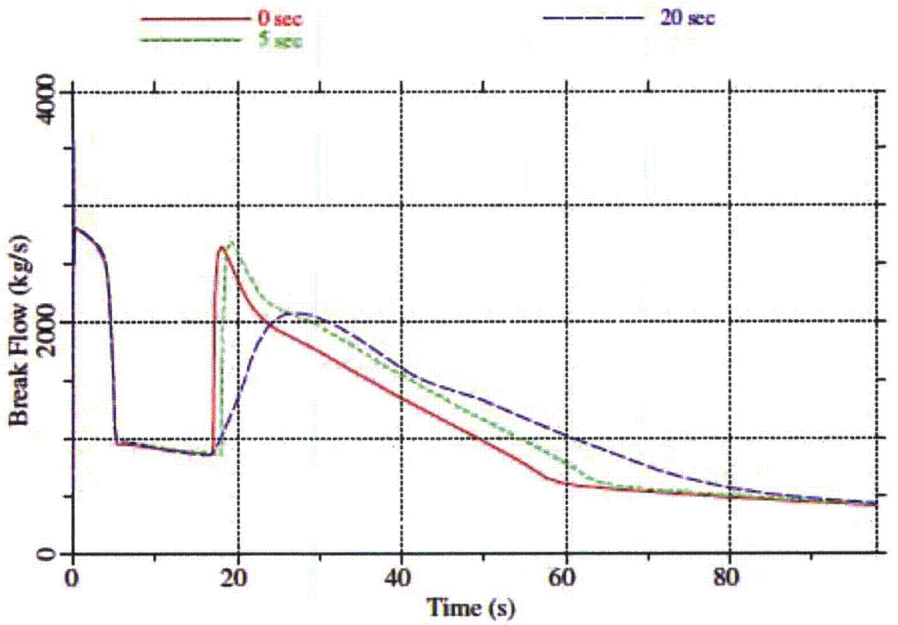

Figure 10-4 – Break Flow Rate for Different RIP Trip Times, MSLB

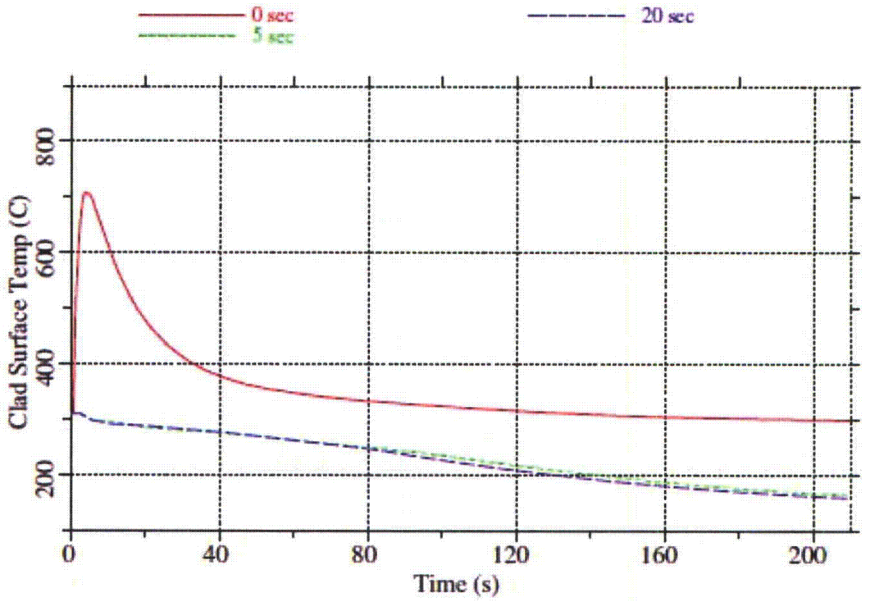

Figure 10-5 – Clad Surface Temperature for Different RIP Trip Times, FWLB*

* The 5 and 20 second curves lie on top of each other.

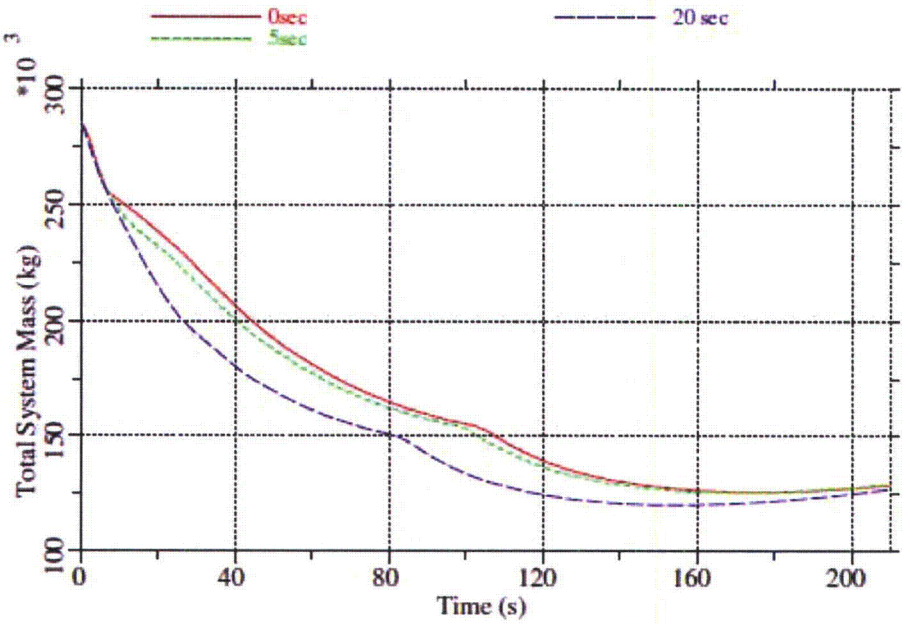

Figure 10-6 – Total System Mass for Different RIP Trip Times, FWLB

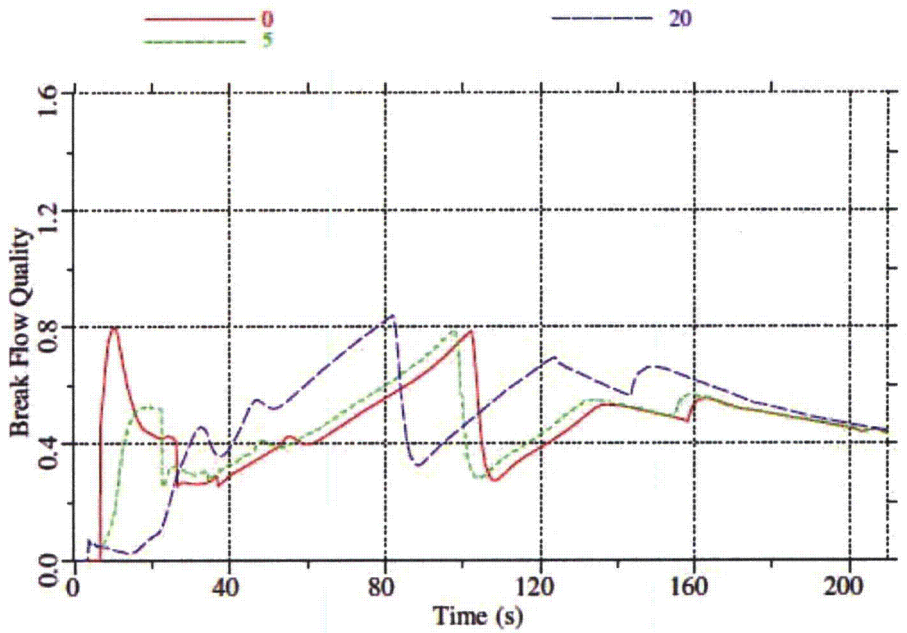

Figure 10-7 – Break Flow Quality for Different RIP Trip Times, FWLB

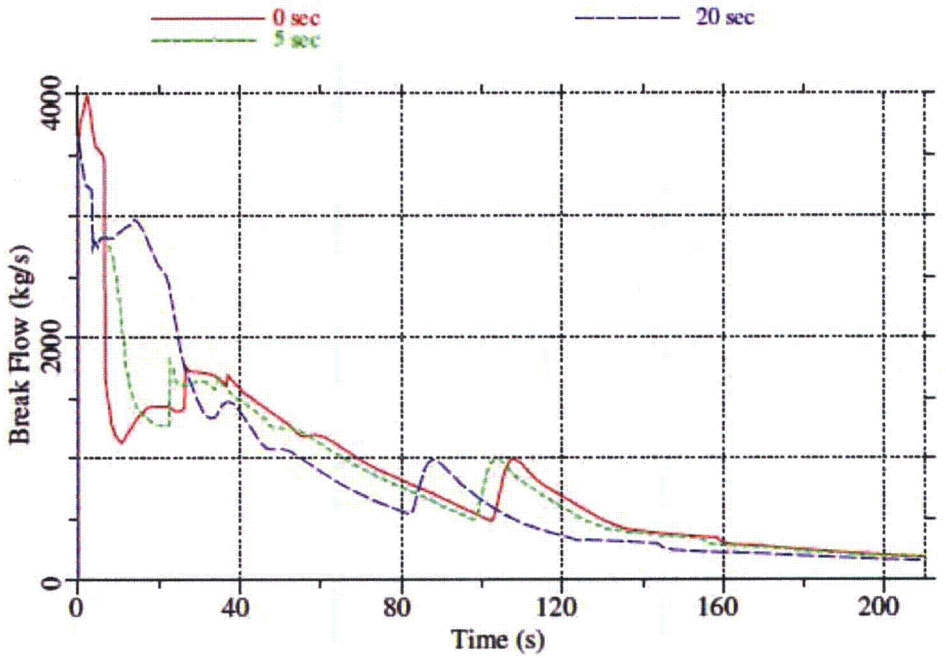

Figure 10-8 – Break Flow Rate (kg/s) for Different RIP Trip Times, FWLB

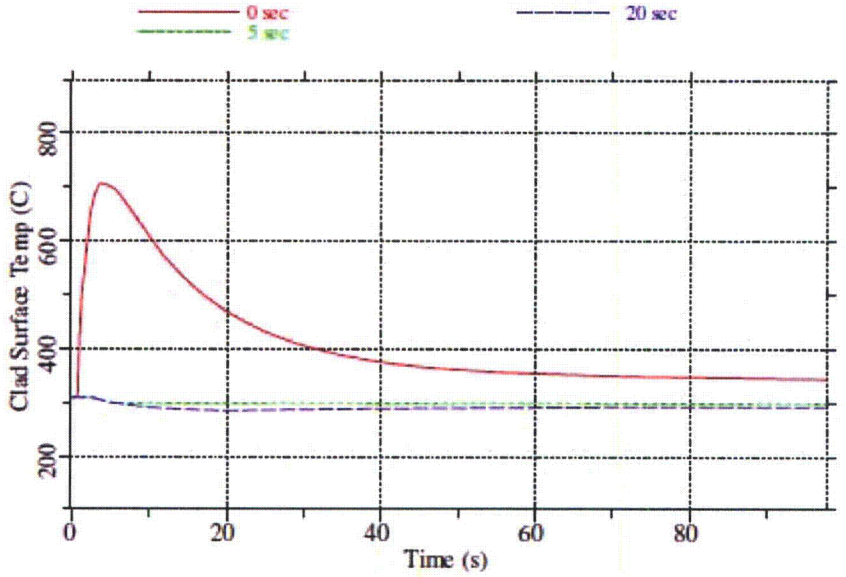

Figure 10-9 – Clad Surface Temp for Different RIP Trip Times, HPCF

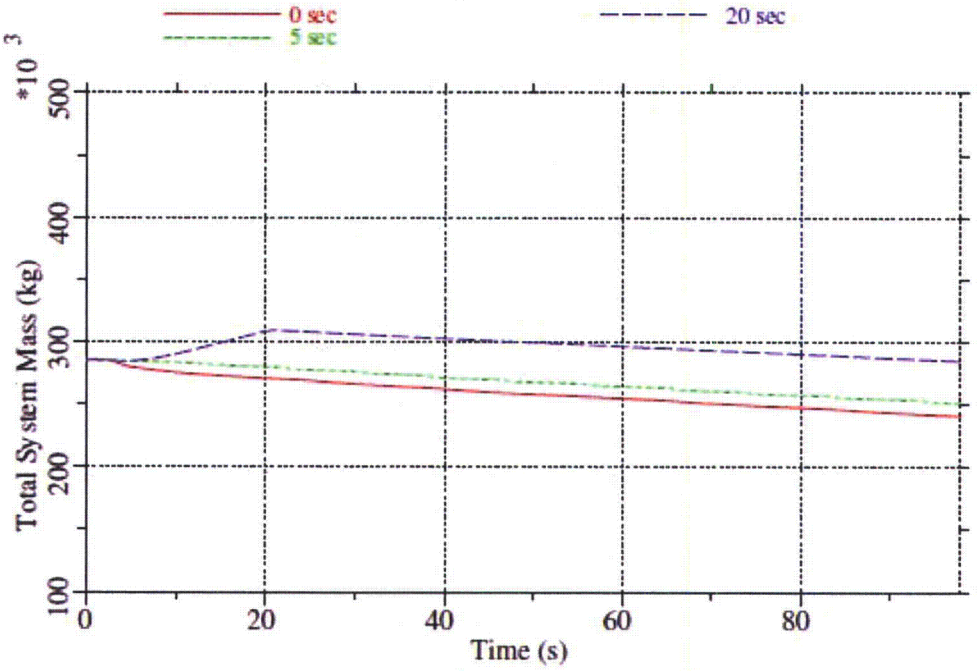

Figure 10-10 – Total System Mass for Different RIP Trip Times, HPCF

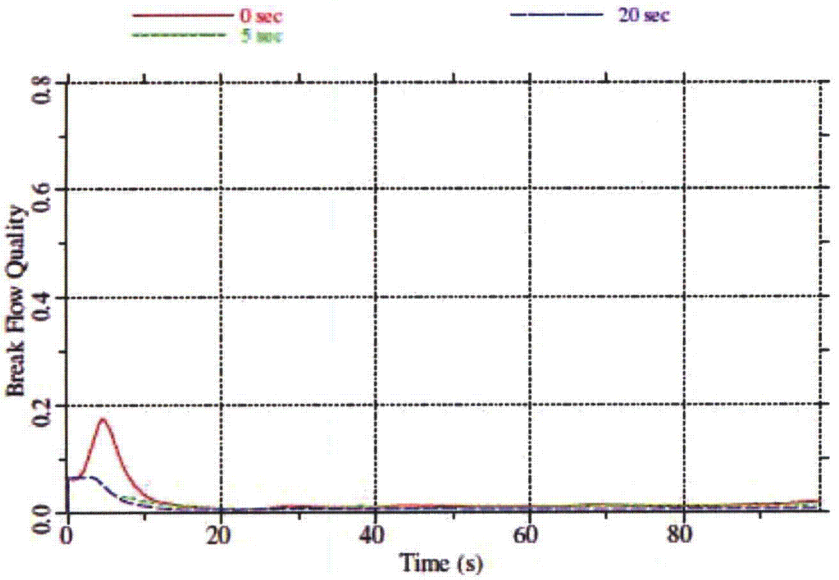

Figure 10-11 – Break Flow Quality for Different RIP Trip Times, HPCF

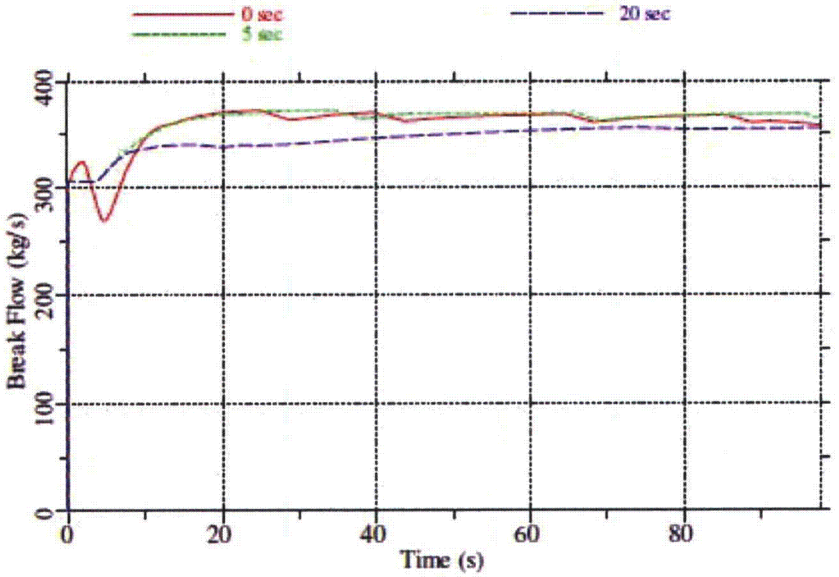

Figure 10-12 – Break Flow Rate for Different RIP Trip Times, HPCF

RAI-11

QUESTION:

10CFR50.46 requires that "ECCS cooling performance must be calculated in accordance with an acceptable evaluation model and must be calculated for a number of postulated loss of coolant accidents of different sizes, locations, and other properties sufficient to provide assurance that the most severe postulated loss-of-coolant accidents are calculated." A failure of the RIP vertical restraints can result in the loss of reactor coolant from the bottom of the RPV. ABWR DCD states that the break flow due to RIP failure would be bounded by the break flow in BDLB accident scenario. However, neither ABWR DCD nor WCAP-17116-P provides any justification to support the above statement.

a) Discuss the transient response to a RIP failure LOCA.

OR

b) Provide justification to support the ABWR DCD assumption that the break flow due to the RIP failure would be bounded by the break flow in BDLB accident scenario. What is the equivalent break flow area for the RIP failure?

RESPONSE:

A detailed justification, which supports the assumption that the break flow due to Reactor Internal Pump (RIP) failure is bounded by the design basis Bottom Drain Line Break (BDLB), is provided in ABWR DCD Tier 2 Subsection 15B.3.4.

The break area for the RIP failure, which is equivalent to a gap between the stretch tube and the RIP nozzle (See Figure 11-1), is less than the design basis BDLB area (20 cm^2).

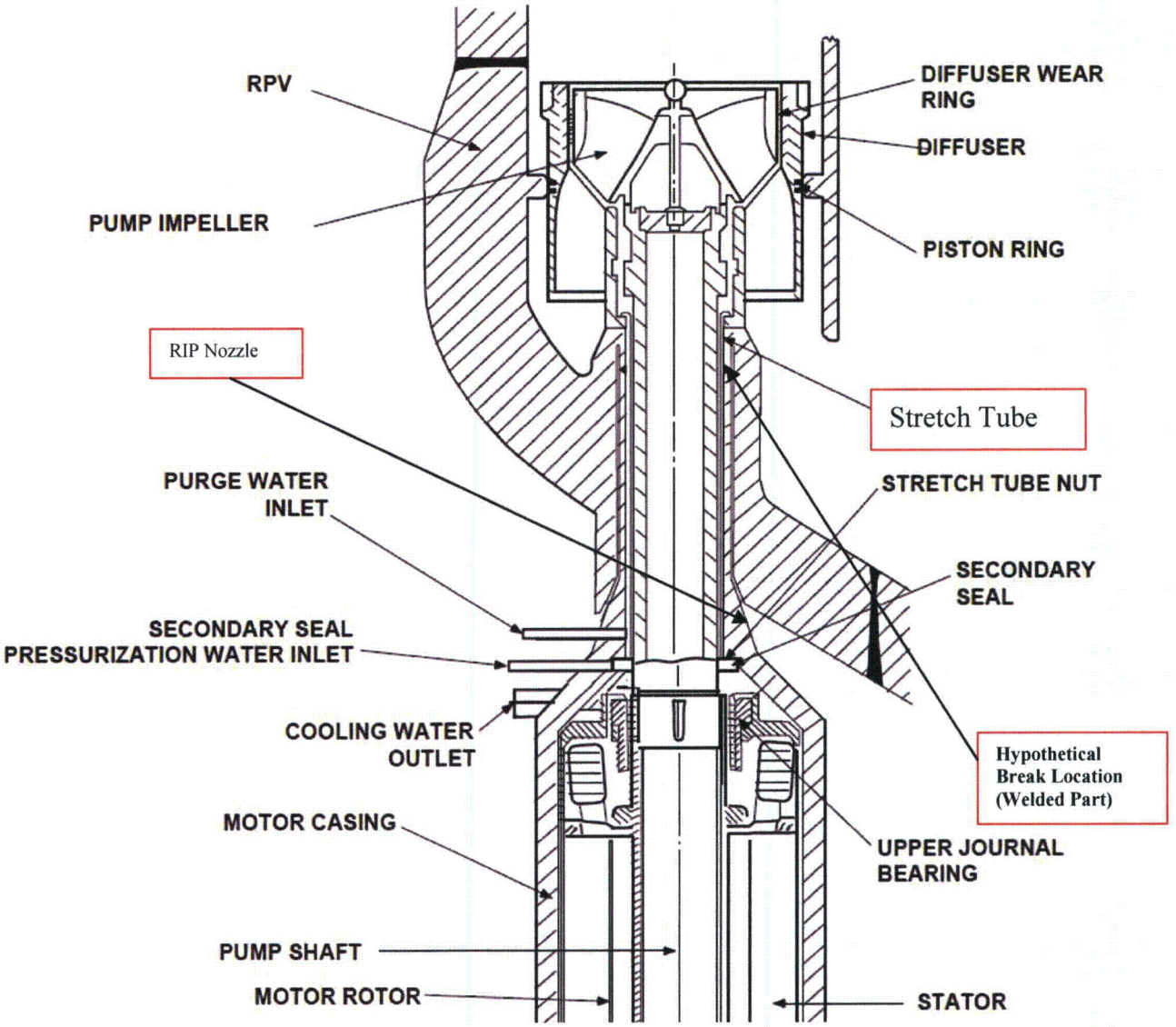

Figure 11-1 Break area for the RIP failure

RAI-12

QUESTION:

As noted in ABWR DCD, "Recirculation Motor Cooling (RMC) is continuously provided by purge water supplied to the motor internals from the Control Rod Drive System (CRDS). A motor internal auxiliary impeller drives the purge water upward through the stator and rotor windings then exits the motor housing or leaks into the reactor vessel along the pump shaft."

Is there potential for a LOCA from the bottom of the Reactor Pressure Vessel (RPV) through the RIPs due to the loss of Recirculation Motor Cooling? If yes, please describe the magnitude of leakage and the resulting LOCA response for ABWR.

RESPONSE:

As noted in ABWR DCD Tier 2 Subsection 5.4.1.3, the reactor recirculation system includes, among other support subsystems, the following two separate support subsystems: (1) the Recirculation Motor Cooling (RMC) subsystem and (2) the Recirculation Motor Purge (RMP) subsystem.

The purpose of the RMC subsystem is to remove heat from the recirculation pump motor (RM), which is generated by the RM internals and is also conducted from the reactor pressure vessel (RPV) to the RM. The Reactor Internal Pump (RIP) motor casing and its heat exchanger, which is part of the RMC subsystem, are filled by the Makeup Water (Purified) System (MUWP) water before operation. Cooling for the heat exchanger is provided by the Reactor Building Cooling Water System. The potential for a LOCA as a result of rupture of the motor cooling piping, including a description of the magnitude of leakage and the resulting response, is discussed in ABWR DCD Tier 2, Subsection 15B.3.4.7. In the event of a loss of RIP motor cooling due to a small size LOCA, the RIPs trip on high temperature of primary cooling water.

The purpose of the RMP subsystem is to prevent the buildup of primary coolant impurities on RM components. The RMP supplies a flow of clean water from the CRD system to the RM shaft stretch tube annular region, which is located just above the RM upper journal bearing. This is intended to minimize radiation dose for RIP maintenance activities. The potential for a small size LOCA as a result of rupture of the purge line, including a description of the magnitude of leakage and the resulting response, is discussed in ABWR DCD Tier 2, Subsection 15B.3.4.5.

RAI-13

QUESTION

As shown in Figure 4.3, the upper plenum appears to be modeled as a single node. As a result of this, the mass inflow to this node from the HPCF would be automatically distributed uniformly throughout its volume. The HPCF mass flow would also immediately reach thermally equilibrium condition. This uniformity does not seem realistic. The temperature and density could have large non-uniformity in this region. Furthermore, if there is a mixture level in the upper plenum, the modeling of where and how the HPCF flow is injected is important. If injected into the steam volume, immediate condensation results. If injected into the two phase mixture region, a one dimensional model will condense steam voids first and then decrease the enthalpy of the fluid. Condensation can result in local pressure depressions which will increase flow into the affected volume. Condensation effects in the upper plenum can increase flow through the core, artificially increasing the mixture level or decreasing the steam void volume in the core.

Section 11.3 of Appendix K to 10 CFR 50 requires that "appropriate sensitivity studies shall be performed for each evaluation model, to evaluate the effect on the calculated results of variations in noding, phenomena assumed in the calculation to predominate, including pump operation or locking, and values of parameters over their applicable ranges. For items to which results are shown to be sensitive, the choices made shall be justified."

a) Justify the use of a single control volume for the entire upper plenum and explain how the use of such nodalization leads to conservative results. It appears that the upper plenum should be refined with enough nodes to enable an accurate determination of fluid condition as delivered to the hottest fuel channel for subsequent cooling analysis.

b) At various pressures, how far does the ECCS flow penetrate from the nozzle to the center of the core?

c) Section 3.3.5 "Injection Flow - Fluid Interaction" of WCAP-11284-P-A, "Westinghouse Boiling Water Reactor Emergency Core Cooling System Evaluation Model: Code Description and Qualification" describes how external water can be added as core spray, feedwater and flooding injection water. Describe how the ECCS flow from the HPCF is assumed to mix with fluid in the upper plenum for the ABWR application.

d) Provide values used for the following model parameters (see Eq. 3.3-56 in WCAP-11284-PA):

F,s = maximum condensation
parameter $zc_{o,d}$ = falling distance

Provide justification for the selected values.

e) If the HPCF flow is available from only one sparger, discuss the asymmetric effects on core cooling and how this is conservatively accounted for in the ABWR analysis.

RESPONSE

a) [

]^{a,c}

For the LOCA transients with HPCF operating, the inventory in the reactor core is replenished via HPCF injection into the upper plenum. Figures 13-1 and 13-2 show the GOBLIN predicted results of two ABWR LOCA transients resulting in minimum amount of inventory in the reactor pressure vessel, namely the Feedwater Line break and the Residual Heat Removal (RHR) suction line break, respectively.

The first plot in each figure shows the dome pressure. The second plot shows the rate of HPCF flow that injects into the upper plenum region, and the sum of the Reactor Core Isolation Cooling (RCIC) flow and the Lower Pressure Flooder (LPFL) flow that deliver ECC water into the annular downcomer region.

The third plot shows the core liquid flow rate at the upper tie plate location, the flow rate from the downcomer into the lower plenum region, and the liquid flow rate at the steam separator exit. It shows that ECCS flow injected into the downcomer region circulates into the lower plenum, flows through the core, mixes with the HPCF in the upper plenum, and spills into the upper downcomer region, completing the recirculation path.

While HPCF adds inventory to the upper plenum, the details of how HPCF flow distributes in the upper plenum region is not important because HPCF water mixes with the upward flow from the reactor core and overflows into the downcomer via the steam separators, thus not requiring finer nodalization.

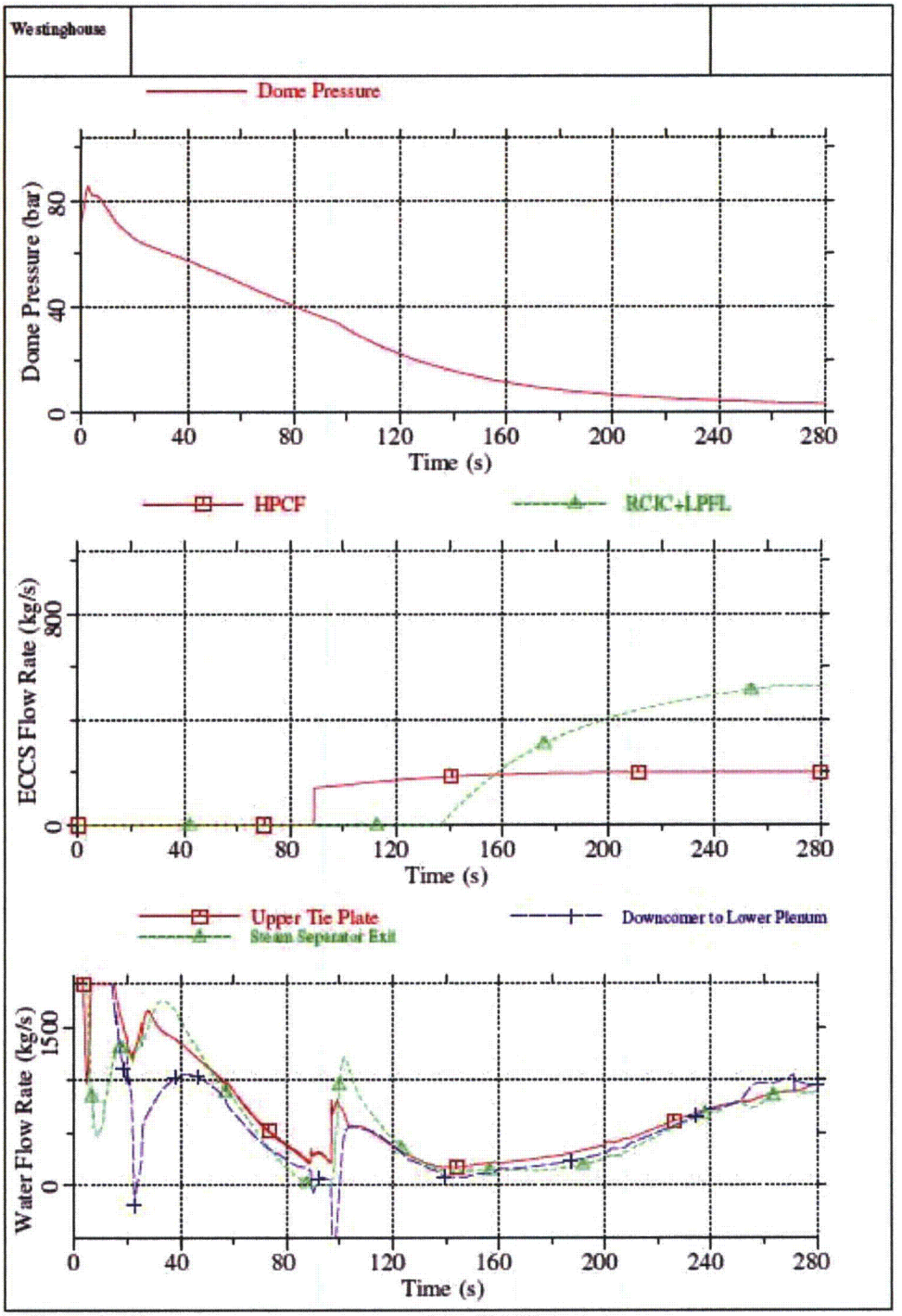

Figure 13-1 - Dome Pressure, ECC Flow and Flows
Between RPV Regions For Feedwater Line Break

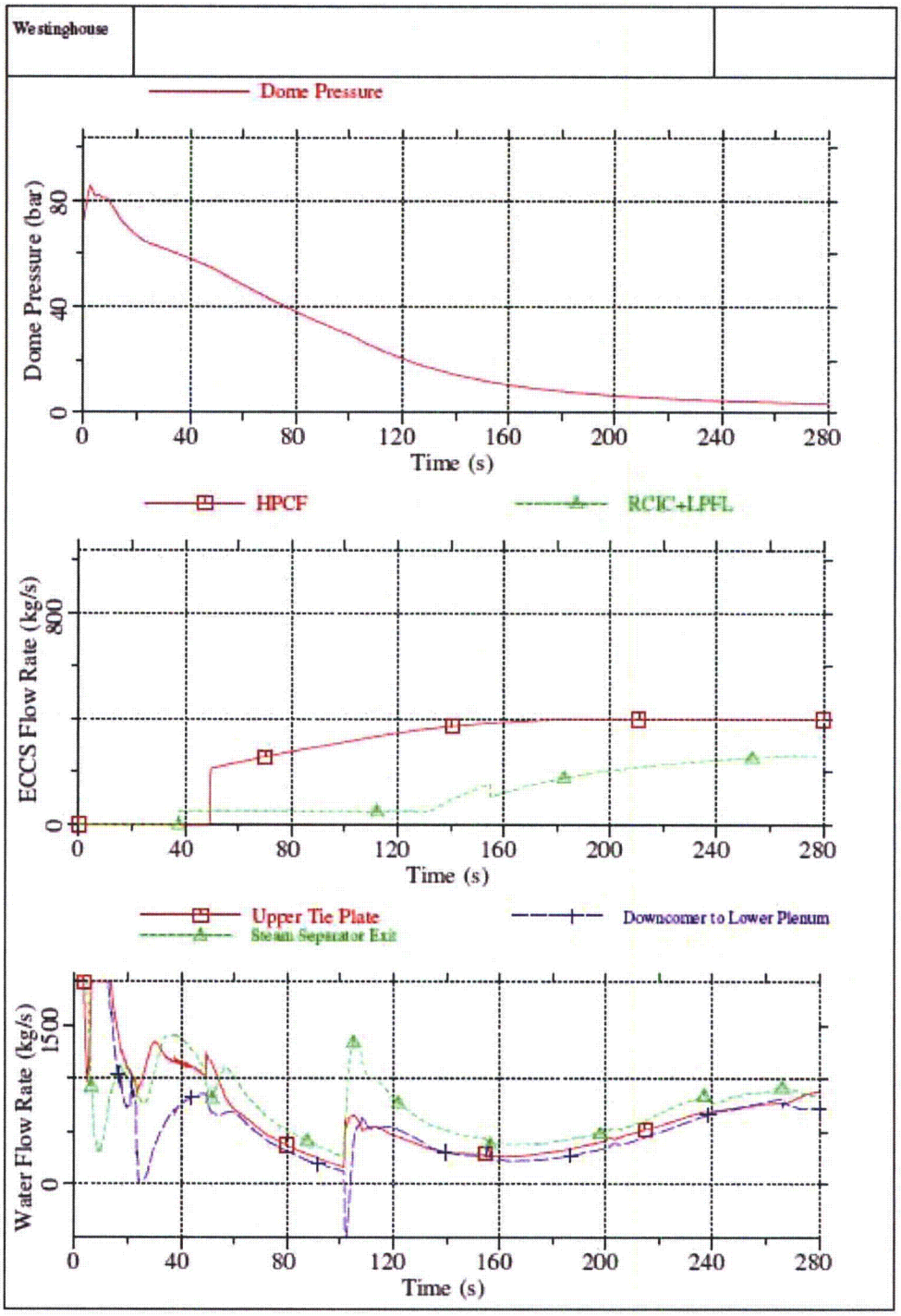

Figure 13-2 - Dome Pressure, ECC Flow and Flows Between RPV For RHR Suction Line Break

b) The High Pressure Core Flooder (HPCF) is designed to replenish Reactor Pressure Vessel (RPV) inventory in the event of a Loss of Coolant Accident (LOCA) and is not a core spray system. Therefore, the radial distribution of HPCF flow in the upper plenum is not important for safety analysis.

c) The two-phase tracking model is not activated in the GOBLIN ABWR upper plenum region. Therefore, the model described in Section 3.3.5 "Injection Flow – Fluid Interaction" of WCAP-11284-P-A does not apply to the HPCF flow. [

]^{a,c}

d) Because the two-phase level tracking model is not activated in the upper plenum region, the condensation effectiveness parameters are not used for the HPCF flow.

e) As explained in the response to item (a) of this RAI, the HPCF is mixed with the upward flow from the core region and spills over into the upper annular downcomer region via the steam separators. The HPCF is not a spray system, and consequently, the detail of how it is radially distributed in the upper plenum is not important for safety analysis.

WCAP-17116-P RAI-13 Supplement 1

QUESTION

As shown in Figure 4.3, the upper plenum appears to be modeled as a single node. As a result of this, the mass inflow to this node from the HPCF would be automatically distributed uniformly throughout its volume. The HPCF mass flow would also immediately reach thermally equilibrium condition. This uniformity does not seem realistic. The temperature and density could have large non-uniformity in this region. Furthermore, if there is a mixture level in the upper plenum, the modeling of where and how the HPCF flow is injected is important. If injected into the steam volume, immediate condensation results. If injected into the two phase mixture region, a one dimensional model will condense steam voids first and then decrease the enthalpy of the fluid. Condensation can result in local pressure depressions which will increase flow into the affected volume. Condensation effects in the upper plenum can increase flow through the core, artificially increasing the mixture level or decreasing the steam void volume in the core.

Section 11.3 of Appendix K to 10 CFR 50 requires that "appropriate sensitivity studies shall be performed for each evaluation model, to evaluate the effect on the calculated results of variations in noding, phenomena assumed in the calculation to predominate, including pump operation or locking, and values of parameters over their applicable ranges. For items to which results are shown to be sensitive, the choices made shall be justified."

a) Justify the use of a single control volume for the entire upper plenum and explain how the use of such nodalization leads to conservative results. It appears that the upper plenum should be refined with enough nodes to enable an accurate determination of fluid condition as delivered to the hottest fuel channel for subsequent cooling analysis.

b) At various pressures, how far does the ECCS flow penetrate from the nozzle to the center of the core?

c) Section 3.3.5 "Injection Flow - Fluid Interaction" of WCAP-11284-P-A, "Westinghouse Boiling Water Reactor Emergency Core Cooling System Evaluation Model: Code Description and Qualification" describes how external water can be added as core spray, feedwater and flooding injection water. Describe how the ECCS flow from the HPCF is assumed to mix with fluid in the upper plenum for the ABWR application.

d) Provide values used for the following model parameters (see Eq. 3.3-56 in WCAP-11284-PA):

F,s = maximum condensation
parameter $zc_{o,d}$ = falling distance

Provide justification for the selected values.

e) If the HPCF flow is available from only one sparger, discuss the asymmetric effects on core cooling and how this is conservatively accounted for in the ABWR analysis.

RESPONSE SUPPLEMENT 1

STPNOC provided a response to RAI-13 on October 14, 2010 in letter U7-C-STP-NRC-100227 regarding Topical Report WCAP-17116-P Revision 0, Supplement 5. In its review of the Westinghouse Licensing Topical Reports (LTRs), the NRC identified a discrepancy in the description for the reactivity coefficients between the LTR supporting the use of GOBLIN for ECCS evaluation (WCAP-11284-P-A) and the LTR supplement specific to the ECCS evaluation for the ABWR (WCAP-17116-P). The discussion in WCAP-11284-P-A indicates that GOBLIN uses a point kinetics model that incorporates reactivity feedback through coefficients that describe the effect of Doppler broadening (fuel temperature changes), moderator temperature changes, and void fraction. However, Table B-1 in WCAP-17116-P, on page B-9, shows a list of reactivity coefficients for fuel temperature and moderator density (not moderator temperature or void fraction). Furthermore, the moderator density reactivity coefficients appear to have units equivalent to moderator temperature reactivity coefficients.

This supplemental response provides clarification on how the reactivity coefficients in WCAP-17116-P, Table B-1 are interpreted for use with GOBLIN for the ABWR LOCA analyses.

GOBLIN has inputs for either void or moderator density reactivity coefficients. When void reactivity coefficients are used, there is an additional model that is activated to account for moderator temperature changes. However, the GOBLIN user manual [

]^{a,c}. Moderator density coefficients shown in Table B-1 of WCAP-17116-P are used in the following equation for the change in reactivity (r) due to changes in moderator density (ρ):

[ ]^{a,c}

As noted above, the units for the moderator density reactivity coefficients C_1, C_2, and C_3, shown in Table B-1 of the current revision of WCAP-17116-P, are incorrect. It was also found that Table B-1 shows an error message instead of the correlations used by GOBLIN to account for reactivity changes due to moderator density changes and fuel temperature changes. A markup of Table B-1 that corrects these errors is attached to this response with changes highlighted in gray shading. These changes will be reflected in Revision 1 to WCAP-17116-P to be issued with the approved version of the report.

Table B-1 (cont.) ABWR LOCA Analysis Model Input Parameters		
Parameter		Toshiba/W Values
Reactivity Inputs		
Moderator density reactivity coefficients*		
Linear coefficient ~~(C1)~~ (C_1)	[ ]a,c	~~1/°C~~ m^3/kg
Quadratic coefficient ~~(C2)~~ (C_2)		~~1/°C²~~ m^6/kg^2
Cubic coefficient ~~(C3)~~ (C_3)		~~1/°C³~~ m^9/kg^3
~~**Error! Objects cannot be created from editing field codes.**~~ [ ]a,c		
Fuel temperature reactivity coefficients		
Square root coefficient (B_3)	[ ]a,c	$1/°C^{1/2}$
~~**Error! Objects cannot be created from editing field codes.**~~ [ ]a,c		

RAI-14

QUESTION

Low Pressure Flooder (LPFL) injects water into the RPV outside of the core shroud via one of the feedwater lines on one loop and via the core cooling subsystem discharge return line on two loops. Since the LPFL mode of RHR is initiated automatically when a LWL-1 signal is generated, the LPFL flow will be injected into what should be a steam environment. Since the LPFL ECCS flow can affect the transient response depending upon how it is modeled, describe:

a) How the ECCS flow from the LPFL is assumed to mix with fluid in the upper downcomer.

b) Is the same "Injection Flow - Fluid Interaction" model described in Section 3.3.5 of WCAP-11284-P-A used in the downcomer region for the LPFL injection?

c) If the same model is used, provide the values used for the model parameters F_{MS} and $_{zcond}$ in the core shroud region. Provide justification for the selected values.

d) Similar to the potential for multi-dimensional effects of HPCF ECCS flow in the upper plenum, there is the potential for non-uniform delivery of LPFL ECCS flow in the downcomer. Provide justification for using a 1-D model to represent the mixing of the LPFL fluid in the downcomer and lower plenum. If there is a potential for imperfect mixing which could result in higher or lower enthalpy fluid feeding the hot assembly, justify the adequacy of the present ABWR modeling. If perfect mixing is assumed, provide a justification, including results of any scoping calculations to support the validity of this assumption.

e) As noted above, the LPFL flow is delivered to the upper portion of the reactor vessel annulus or downcomer. Consequently, there is potential that the LPFL injection flow could bypass the core and be carried out of the break in case of FWLB or RHR (injection and suction) line break LOCAs. Please discuss the adequacy of the GOBLIN 1-D model to simulate this phenomenon.

RESPONSE

a) The LPFL pumps inject water into the upper annular region outside of the core shroud. There are three LPFL pumps, each delivering ECCS water via a sparger. One LPFL pump uses one of the feedwater spargers, which has 54 nozzles. The two remaining LPFL pumps each uses a separate LPFL sparger with 18 nozzles. As a result of this configuration, the LPFL water is distributed circumferentially around the annulus and provides a large surface area to the fluid that exists within the downcomer. As a result, it is expected that the subcooled water will condense steam rapidly as it enters the region.

[

]^{a,c} A normal flowpath is used to deliver the subcooled water from the LPFL pumps to the downcomer. Because the code is a thermal equilibrium model, complete mixing is assumed in the sub-volume. One of the conditions for activating LPFL is low reactor vessel pressure. As shown in Figure 14-1, depressurization of the vessel continues when the LPFL delivers ECCS water to the downcomer region. The case shown is a feedwater line break (case fwlb4 in Table 4-9 of WCAP-17116-P), which is a representative case with LPFL functioning and is selected because it has the least inventory for the cases studied in WCAP-17116-P.

b) The model described in Section 3.3.5 of WCAP-11284-P-A is not used.

c) As noted in b) above, the model described in Section 3.3.5 of WCAP-11284-P-A is not used.

d) One of the conditions for activating the LPFL is low reactor vessel pressure. As shown in Figure 14-1 for the limiting feedwater line break case, the vessel pressure continues to decrease following the injection of LPFL. The continuous depressurization produces spontaneous flashing of water in the lower plenum and downcomer. Figure 14-2 compares the two-phase mixture level and wide range level to the LPFL injection elevation. This figure shows the existence of a two-phase mixture as the two-phase mixture level exceeds the 'collapsed' wide range measured level. The figure also shows that the LPFL coolant must fall a considerable distance through a steam environment where there is an upward vapor flow. Because the LPFL water is distributed in the downcomer via nozzles on the LPFL sparger, there is a large surface area between the water jets / droplets and the vapor in the upper downcomer. Although the code forces the liquid to be in thermal-equilibrium with the vapor, this is also expected to occur in a best-estimate calculation. Furthermore, the flashing of water to steam in the lower plenum and downcomer produces vigorous mixing of any water that remains subcooled, ensuring a uniform thermal condition at the core entrance.

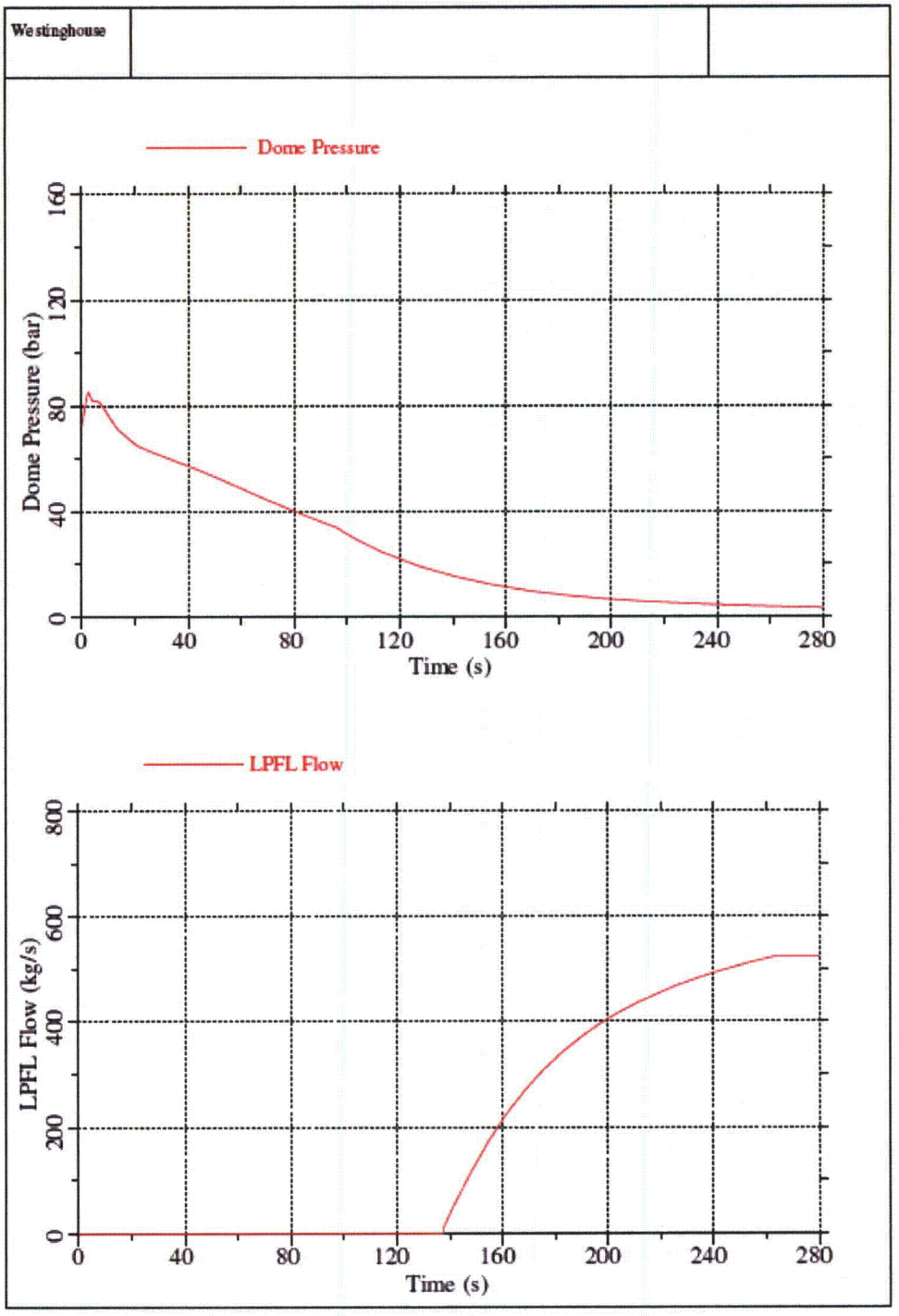

Figure 14-1 - Dome Pressure and LPFL Flow for Feedwater Line Break

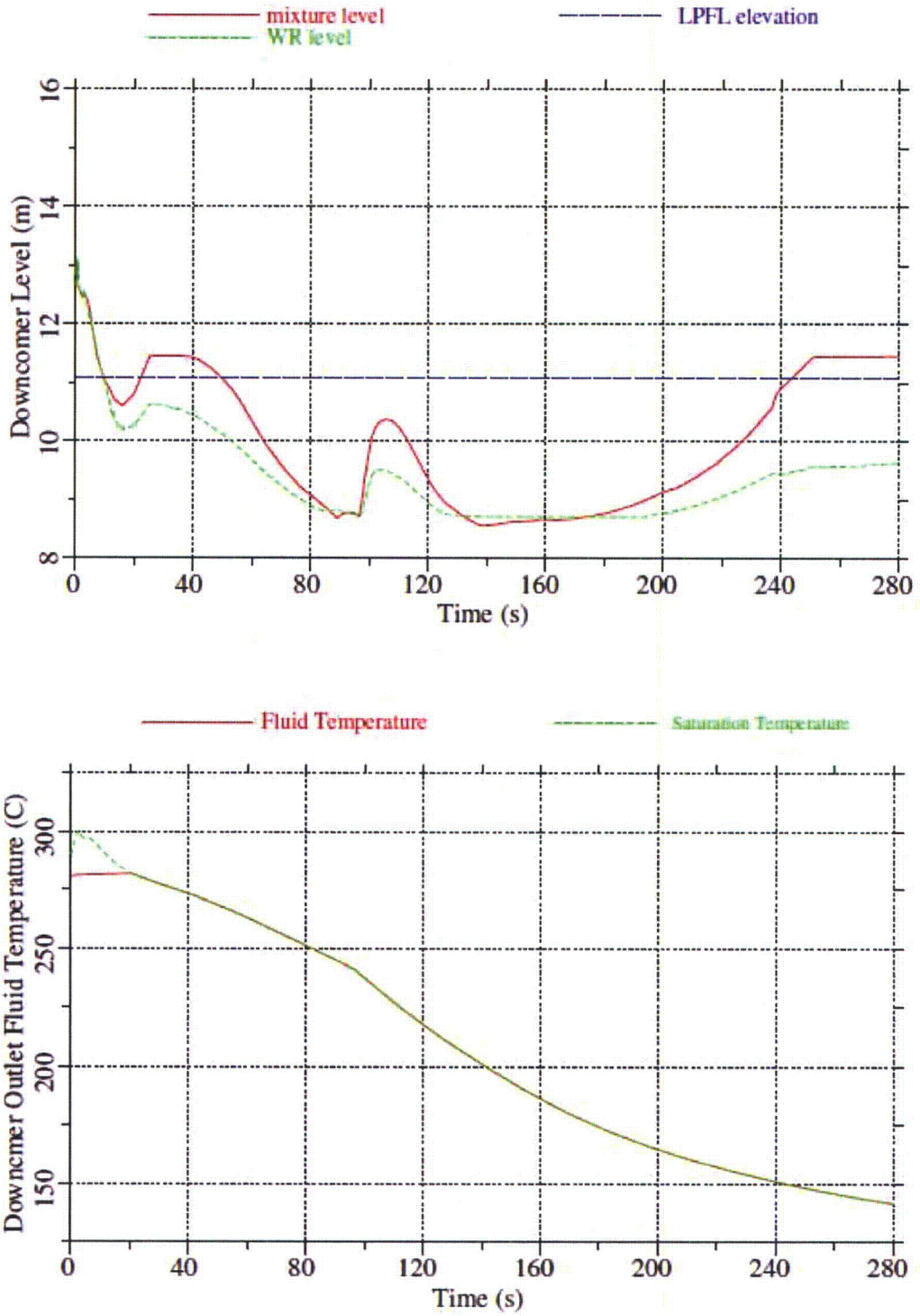

Figure 14-2 - Downcomer Two-phase Mixture Level and Fluid Temperature*

* For the second plot of Figure 14-2, after 20 seconds the two curves lie on top of each other.

e) Table 14-1 shows the time of LPFL initiation for both a RHR suction line break as well as a feedwater line break. The maximum steam flow rate during the period following LPFL injection was then determined, as well as the corresponding specific volume of the steam.

Table 14-1 – Steam Flow data

	RHR suction line break	Feedwater line break
Time of LPFL initiation (s)	130.804	137.476
Time of maximum steam flow (s)	131.504	138.376
Steam flow rate in downcomer (kg/s)	105.202	106.672
Steam specific volume in downcomer (m^3/kg)	0.1226	0.1235
Saturation Temperature in the downcomer (°C)	201.859	201.497

The Steam velocity was then calculated utilizing the following formula:

$V = W * \upsilon / A$

Where:

V = steam velocity (m/s)
W = mass flow rate of steam (kg/s)
υ = steam specific volume (m^3/kg)
A = flow area of the downcomer (m^2)

[

]^{a,c}

As shown above, the feedwater line break has a greater steam velocity, and as such bounds the RHR suction line break with respect to entrainment risk.

The drag force imposed on a droplet of subcooled LPFL water by the steam is calculated by the following equation, per Reference 14-4:

$$F_D = \frac{1}{2}\rho_g v^2 \cdot \left(\pi \frac{D^2}{4}\right) \cdot C_D = 0.173 \rho_g v^2 D^2$$

Where:

ρ_g = steam density (kg/ m^3)
v = steam velocity (m/s)
D = droplet diameter (m)
C_D = drag coefficient of a water droplet (~ 0.44)

$F_D = 0.173 * (1/0.1235) * 1.121^2 * D^2 = 1.760 * D^2$

The gravitational force on a droplet of subcooled LPFL water is calculated by the following equation, per Reference 14-4:

$$m \cdot g = \rho_f \frac{4}{3}\pi\left(\frac{D}{2}\right)^3 \cdot g = \frac{\pi}{6} g \rho_f D^3$$

$F_g = (pi / 6) * 9.81 * 1000 * D^3 = 5136\ D^3$

In order for entrainment to occur the drag force must overcome the gravitational force.

$F_D > F_g$

$1.760\ D^2 > 5136\ D^3$

$D < 0.343$ mm

The feedwater sparger has a diameter of ~45 mm so initial droplet size far surpasses the maximum droplet size that permits entrainment. The initial droplet dispersing into smaller droplets is addressed below:

The stability of a single droplet traveling through gas is determined by its Weber number. The Weber number is defined by the following equation, per Reference 14-3:

$We = [\rho_g (v_g - v_f)^2 * D] / \sigma$

Where:

ρ_g = steam density (kg/ m^3)
v_g = steam velocity (m/s)
v_f = droplet velocitry (m/s)
D = droplet diameter (m)
σ = droplet surface tension (N/m)

The density and velocity of the steam is determined from Table 14-1. The droplet velocity is assumed to be zero. In order for entrainment to occur, LPFL water droplets must first reverse flow direction from downwards through the downcomer to upwards. By nature of this flow reversal, the droplet experiences a moment of zero velocity. The droplet surface tension is directly correlated to the temperature of the water. As such the droplet temperature is conservatively assumed to be the saturation temperature at the top of the downcomer, documented by Table 14-1. The surface tension is then determined per Reference 14-2. Provided the droplet's Weber number remains below 12, the droplet will remain stable per Reference 14-3.

$12 > [\rho_g (v_g - v_f)^2 * D] / \sigma$

$12 > [(1/0.1235) * (1.1242-0)^2 * D] / 0.0373$

$D < (12*0.0373*0.1235)/1.1242^2$

$D < 43.739$ mm

Since a droplet size of less than 0.343 mm is required for entrainment to occur, and the equation above shows that droplets with a diameter of less than 43.739 mm will remain stable and not disperse into smaller droplets, there is no risk of LPFL water becoming entrained by steam flow and then being carried out of the break for RHR or FWLB scenarios.

References

14-1 APED-5458 "Effectiveness of Core Standby Cooling Systems for General Electric Boiling Water Reactors," March 1968.

14-2 NIST/ASME Steam Properties - NIST Standard Reference Database 10 - Version 2.11.

14-3 Wallis, Graham B. (1969). *One-dimensional Two-phase Flow*. McGraw-Hill.

14-4 Batchelor, G.K. (1967). *An Introduction to Fluid Dynamics*. Cambridge University Press.

RAI-15

QUESTION:

The ADS is comprised of eight safety relief valves (SRVs) with a rated flow capacity of 220 lbs/sec at a rated pressure of 1140 psid. Actuation of the ADS will remove mass and energy from the system. To ensure a correct understanding of the analysis calculation framework for the input parameters, the following information would be useful:

a) When ADS is assumed to be activated, is it correct to assume that flow is removed from the Steam Dome (node volume 1, 1) at the node enthalpy?

b) Is it correct to assume that the flow through the ADS is a linear function of differential pressure; 0 flow at 0 psid, and 1,763.7 lbs/second at 1140 psid?

RESPONSE:

a) The Automatic Depressurization System (ADS) valves are not connected to the steam dome. The ADS valves are located in the steam line upstream of the first MSIV. As shown in Figure 4-3, the four steam lines are represented by two lines in the ABWR evaluation model. One line represents a single steam line, which would contain a break (sub-volumes 9,2 and 9,3). The other line represents the 3 steam lines (sub-volumes 13,2 and 13,3). Six of the eight ADS valves are connected to sub-volume 13,2 and two are connected to sub-volume 9,2.

b) It is not correct to assume the flow through the ADS depends on differential pressure. The flow through the ADS valves is determined by a critical flow model, which is dependent on upstream stagnation conditions.

RAI-15S01

QUESTION

The response to item (b) of the RAI-15 states that the flow through the ADS valves is determined by a critical flow model. In order to better understand the modeling of the flow through the ADS, provide the specific critical flow model (e.g., Moody's) used in the LTR analyses. Further, clarify the effect on the stagnation pressure in sub-volumes 9,2 and 13,2 relative to form and friction losses which would reduce the stagnation pressure below the "dome" or "system" pressures shown in WCAP-17116-P. In addition, provide the throat (critical flow) area and any discharge coefficient assumptions that are used in the analyses.

SUPPLEMENT RESPONSE

To determine the flow through the ADS valves in support of the WCAP-17116-P analyses, it was not necessary to perform a hydraulic calculation, which would have required the model description and input parameters being requested in this RAI. Instead, the ADS capacity used in the LOCA analyses in WCAP-17116-P is the total minimum flow capacity for the ADS as defined in ABWR DCD Table 6.3-1.

RAI-15 Supplement 2:

QUESTION:

The response to item (b) of the RAI-15 states that the flow through the ADS valves is determined by a critical flow model. In order to better understand the modeling of the flow through the ADS, provide the specific critical flow model (e.g., Moody's) used in the LTR analyses. Further, clarify the effect on the stagnation pressure in sub-volumes 9,2 and 13,2 relative to form and friction losses which would reduce the stagnation pressure below the "dome" or "system" pressures shown in WCAP-17116-P. In addition, provide the throat (critical flow) area and any discharge coefficient assumptions that are used in the analyses.

SUPPLEMENT 2 RESPONSE:

The original response to RAI 15, which addressed the calculated flow through the ADS valves, was provided to the NRC in STPNOC Letter No. U7-C-STP-NRC-100155 dated July 7, 2010. A supplemental response, which indicated that the ADS capacity used was a design requirement for reactor depressurization and therefore accounts for any form and friction losses, was provided in STPNOC Letter No. U7-C-STP-NRC-100242 dated October 25, 2010. At the NRC audit of WCAP-17116-P held in Windsor, CT the week of February 14, 2011 and as documented in the Audit Plan, the NRC requested additional detail on how the ADS flow is calculated as a function of system pressure and inlet enthalpy. This second supplemental response provides that additional detail.

The design specification for the ADS provides required capacity as a flow rate of saturated steam at a specified reactor pressure, which is 2.903×10^6 kg/hr at 78.61 bar (absolute). The actual installed ADS valves are required to meet this specification independent of any form or friction losses between the steam dome and the actual location of the ADS valves. The evaluation model simulates the four steam lines with

[

]^{a,c}. The eight ADS valves are modeled as [ ]^{a,c} critical flow paths, with [ ]^{a,c}. The valve areas are controlled by signals that open the valves to a specified flow area after the ADS time delay has expired. The combined area of the two flow paths (0.0714 m^2) was sized to provide the specified flow rate at the design specification reactor vessel pressure. Figure 15-1 compares the valve capacity as modeled to the specification. As shown, the model is slightly conservative relative to the specification.

When the ADS valves are opened, the flow rate through the valves is determined by the upstream conditions, similar to any other critical flow path. Note that the ADS capacity specification is not intended to be the minimum flow that is passed by the ADS valves for all conditions, because it is defined as the flow rate of saturated steam at a specified reactor pressure. As described above, the specification is used to determine the combined flow area of the valves. A comparison of the actual ADS flow for a typical case (hpcf3) to the homogeneous equilibrium model (HEM) for saturated steam is shown in Figure 15-2. As shown, there is good agreement.

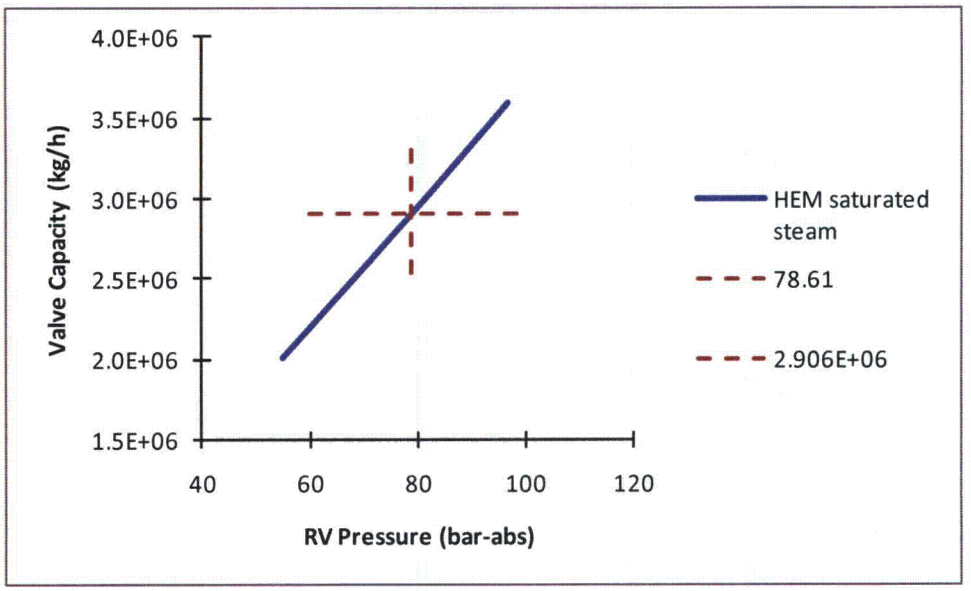

Figure 15-1 Comparison of Modeled Capacity to Specification

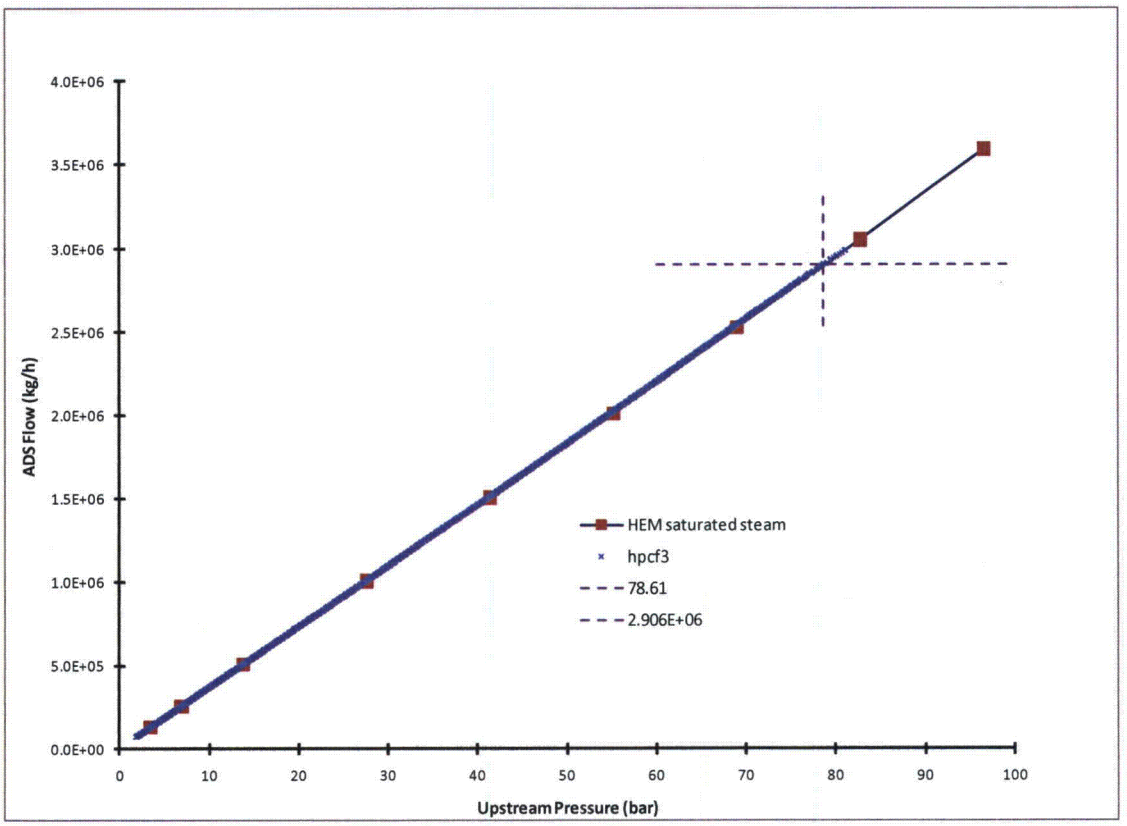

Figure 15-2 Comparison of Predicted ADS Flow for Typical Case to HEM at Saturated Steam

RAI-15S03

QUESTION:

RAI-15 requested additional information pertaining to the ADS flow model in GOBLIN code for the ABWR application. The response to RAI-15 and supplemented information presented by the applicant during the audit clarified that in USA7, the ADS flow area is based upon the safety valve design flow capacity and calculated using a homogeneous equilibrium model (HEM) for critical flow. During the simulation, the calculated flow through the ADS valve is based on the upstream (steam line) stagnation pressure, stagnation enthalpy, ADS flow area, and the HEM critical flow model. A figure was presented during the audit showing linear HEM saturated steam critical flow for the determined ADS flow area from a pressure of approximately 55 bar to approximately 95 bar. This figure also showed the safety valve design flow conditions to be lower than the flow based on the HEM predictions, which was considered to be conservative.

However, the reviewers noted that the safety valve design flow sizing in the ABWR DCD for over-pressure protection was based upon the Moody critical flow model. Furthermore, the reviewers also noted that the flow through the ADS valves is expected to be choked similar to that of flow through a postulated break under LOCA conditions. Appendix K requires the use of the Moody model after the discharging fluid has been calculated to be two-phase. Therefore, the ADS flow calculated using the HEM critical flow model would be different than the flow calculated using the Moody critical flow model.

In view of this, a comparison of the HEM model against the experimental data on critical flow that is representative of full range of expected ABWR LOCA pressure conditions is essential. The applicant should demonstrate by comparing the model predictions [against] test data (e.g., MARVIKEN critical flow steam data) that the HEM model as implemented in USA7 conservatively predicts the RPV depressurization over full range of ABWR LOCA pressure conditions.

SUPPLEMENT 3 RESPONSE:

As indicated in the RAI, 10 CFR 50 Appendix K I.C.1.b requires the use of the Moody critical flow model for the break flow. Westinghouse interprets this to mean that the Moody critical flow model must be applied to the flow from postulated breaks. For other designed features or internal critical flow checks, the use of a more mechanistic critical flow model is permitted and may be more appropriate.

The ADS, as part of the Emergency Core Cooling System (ECCS), is designed to automatically depressurize the system such that the low pressure ECCS can be actuated. Although the flow through the ADS valves represents a loss of inventory when the system is operational, its primary function is to depressurize the reactor vessel. There is a tradeoff between inventory loss and depressurization rate. If the depressurization rate is too fast, the low pressure ECCS equipment would be actuated too soon. In situations like this, it is more appropriate to use a better estimate model, such as HEM.

Figure 1 is a plot of the time-dependent nodal quality upstream of the ADS valves. The plot is based on case hpcf4, a high pressure core flooder (HPCF) line break, which requires ADS

actuation for recovery that is described in WCAP-17116. The figure shows that the condition upstream of the ADS valve is high quality or single phase steam. There are two curves shown in Figure 1, because the ADS valve flows are split between the two steamlines represented in the GOBLIN model. As shown, there is a time interval immediately after the ADS valves open when the mixture in the downcomer swells to the elevation of the steam lines, which causes the quality upstream of the ADS valves to decrease to ~ 0.98. Similar upstream conditions are expected for other scenarios that rely on ADS for system recovery.

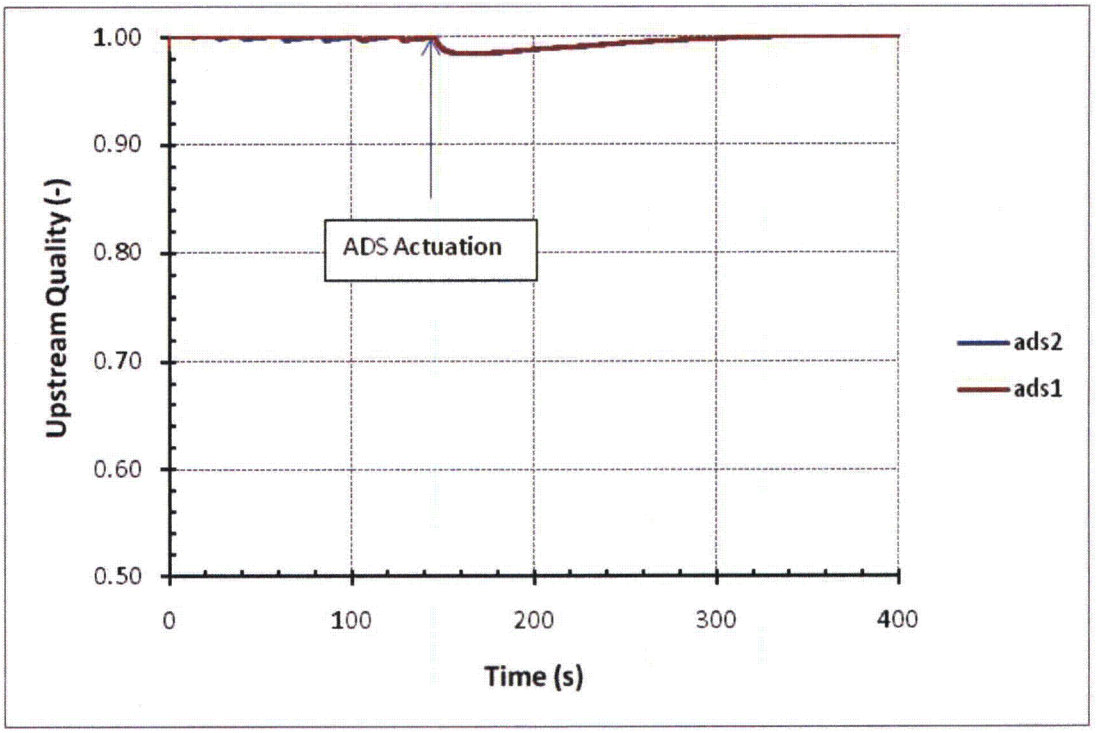

Figure 1 – Nodal Quality Upstream of ADS Valves

Figure 2 compares the two critical flow models for single phase steam. As shown, the predicted flow rates are nearly identical. Therefore, very little difference is expected in the system response if the ADS flow model were changed from HEM to Moody.

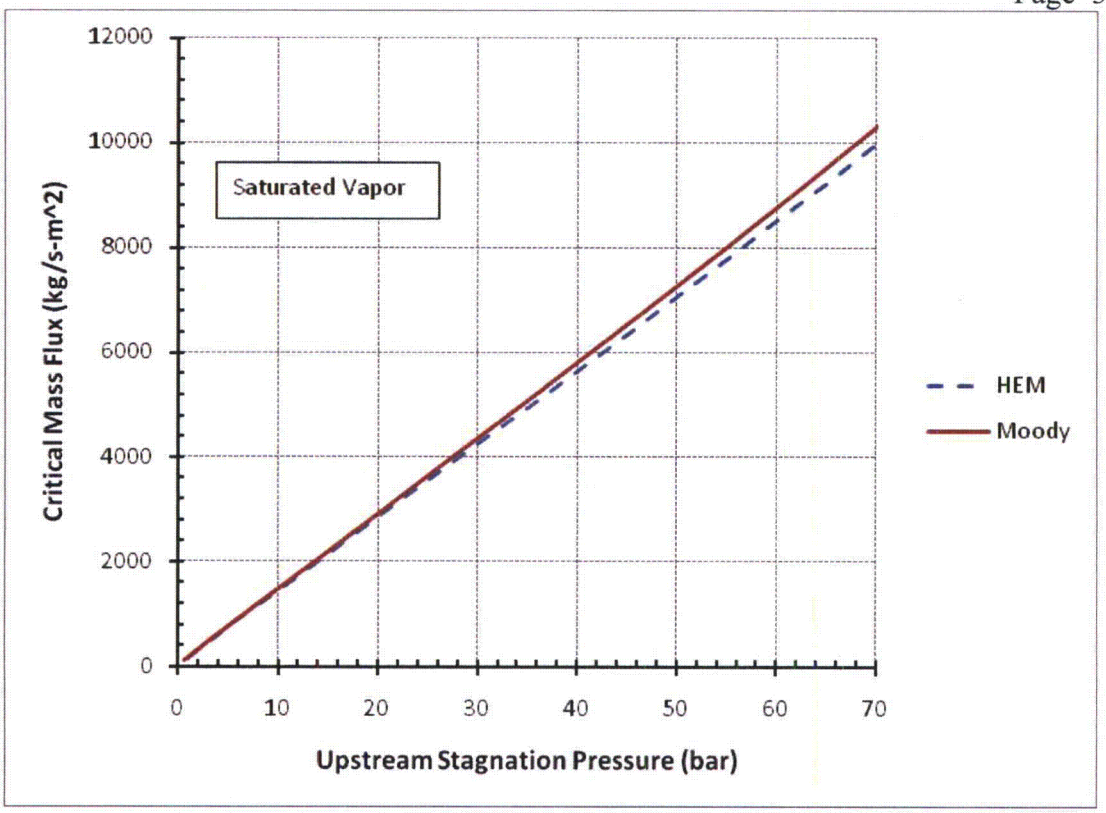

Figure 2 – Comparison of Moody and HEM for Single Phase Vapor

A sensitivity study was performed to demonstrate that the predicted system responses using the HEM and Moody models are nearly identical. Because the Moody model predicts slightly higher steam flow than HEM at ADS capacity reference pressure, the effective ADS flow area is reduced slightly so that the ADS flow capacities are identical at the reference pressure. The HPCF line break hpcf4 was used for this study, because it relies on ADS to actuate injection from the low pressure flooder (LPFL) pumps. A comparison of the predicted system inventories is presented in Figure 3. As shown, the system inventories are essentially identical. The results show that the difference in minimum system inventories is only 213 kg. The minimum system inventory occurs when the HEM model is used. Because core uncovery is limited to partial uncovery of lower powered assemblies, minimum system inventory rather than peak cladding temperature is used as an indicator for this study.

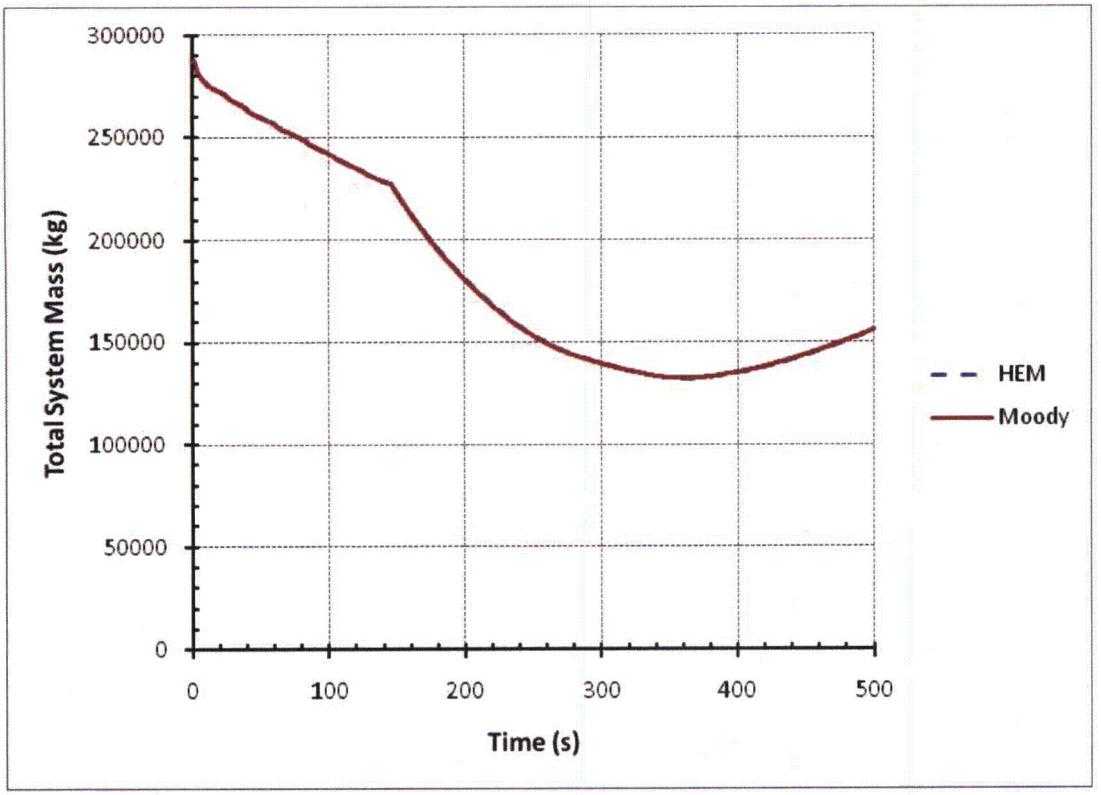

Figure 3 – Comparison of Total System Mass (hpcf4)

This sensitivity study shows that the particular critical flow model used to represent the flow from the ADS has very little effect on the system response, because the flow passing through the ADS is very high quality steam. It is also shown that the HEM is more conservative than the Moody model with regard to minimum system inventory.

The description of the GOBLIN code qualification is presented in Section 6 of Reference 1, which was reviewed by the NRC in a Safety Evaluation in August 1989. The qualification includes comparisons to both separate effects and integral tests. Included in these studies are comparisons to the FIX-II LOCA Blowdown and Pump Trip Heat Transfer Experiments. The FIX-II facility was an integral facility, because it was designed to simulate LOCA transients in an ASEA-ATOM external recirculation pump plant, similar in design to a BWR/2. The tests included a spectrum of split and double-ended guillotine breaks ranging from 10% – 150% of the full recirculation line flow area. The core was simulated by 36 electrically heated rods. The facility simulated all important features of the reference plant, including a steam separator, recirculation pumps, the ADS, and breaks in the recirculation loop. The HEM was used to represent critical two-phase flow through the ADS and the simulated break. Reference 1 presents comparisons between predicted results and experimental data for the 100% line break indicating that the comparisons were in excellent agreement with the data (See Figure 6 below for an example.) It also stated that similar agreement was obtained for other break sizes as described in Reference 2. Although break flow rate was not measured, comparison of the predicted system pressure response provides an excellent measure of the break flow modeling by the HEM as shown by the comparisons presented in Figure

4 through Figure 7. As shown, these data cover the full range of pressures expected for ABWR ADS operation.

a,c

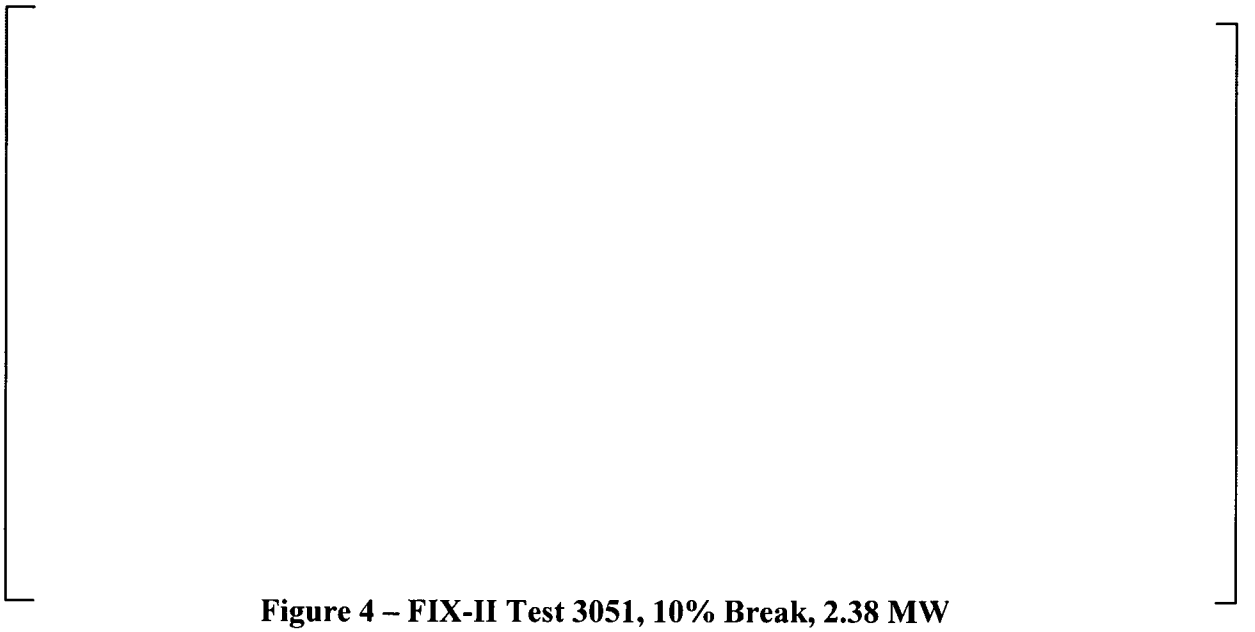

Figure 4 – FIX-II Test 3051, 10% Break, 2.38 MW

a,c

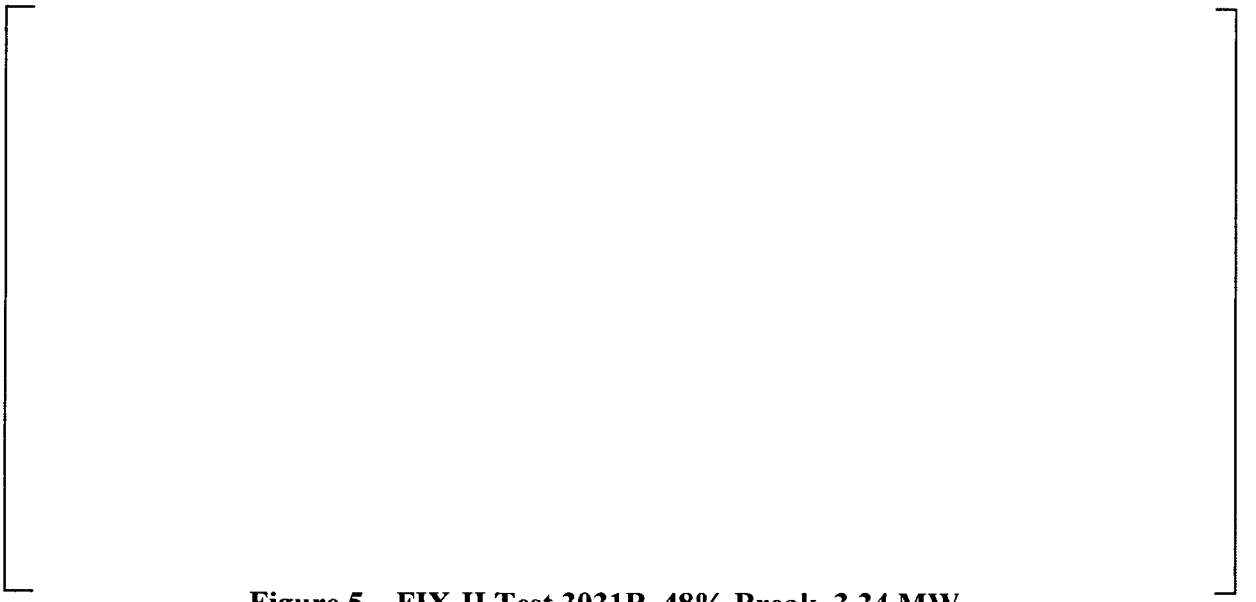

Figure 5 – FIX-II Test 3031B, 48% Break, 3.34 MW

a,c

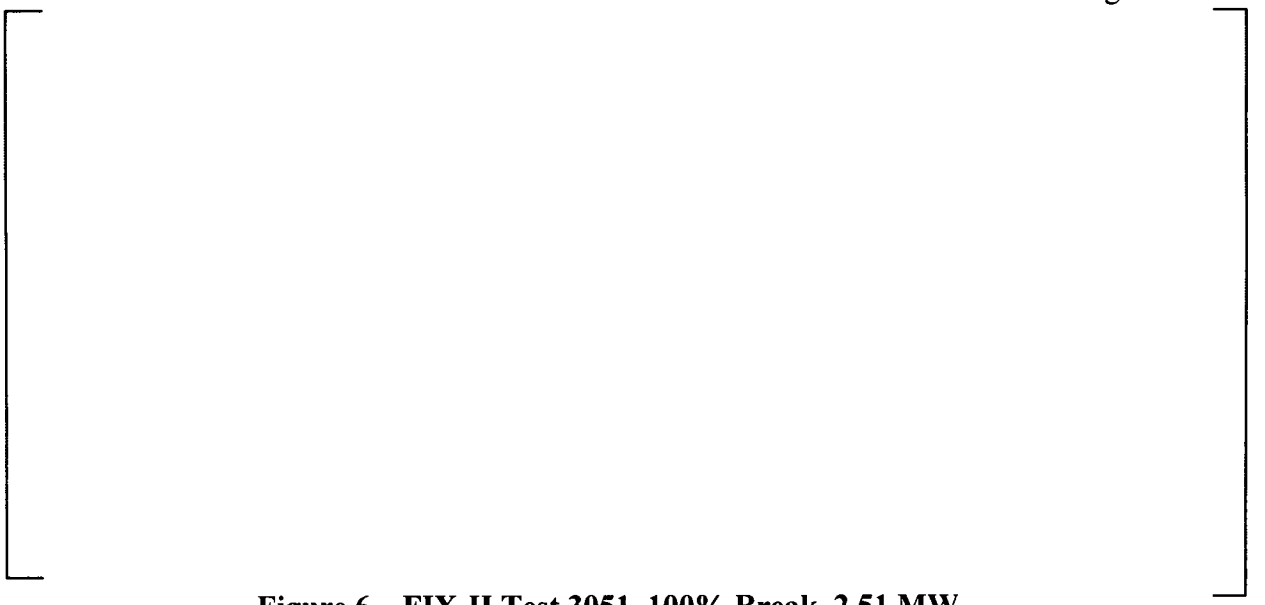

Figure 6 – FIX-II Test 3051, 100% Break, 2.51 MW

a,c

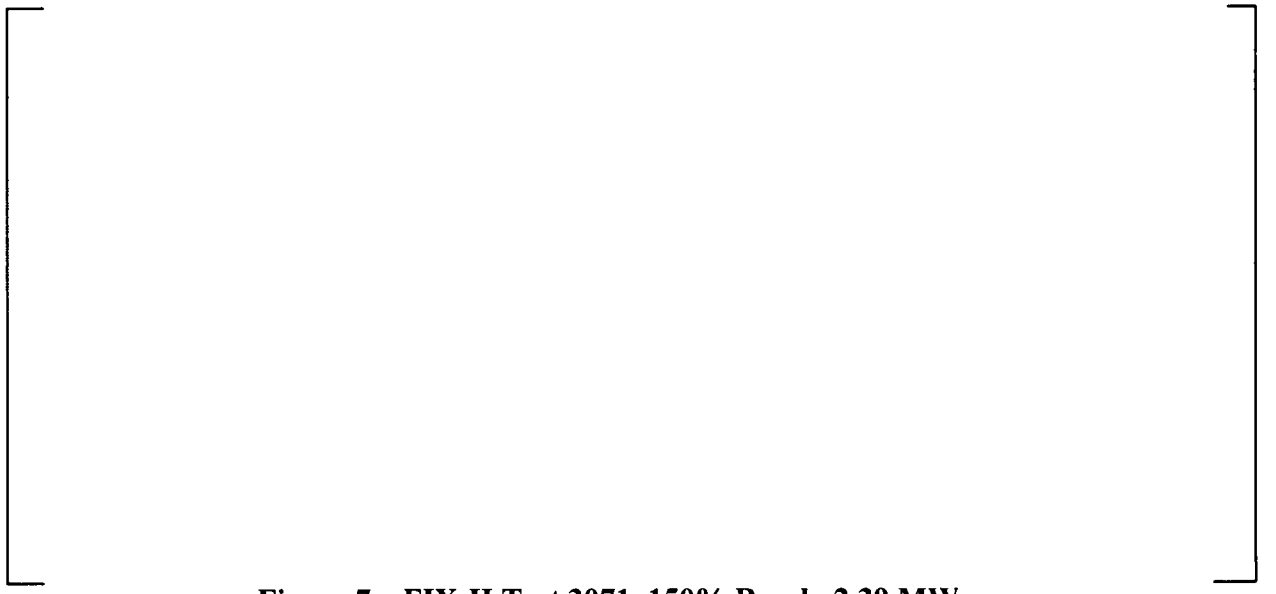

Figure 7 – FIX-II Test 3071, 150% Break, 2.39 MW

References

1. RPB 90-93-P-A, "Boiling Water Reactor Emergency Core Cooling System Evaluation Model: Code Description and Qualification", October 1989.
2. KPA 85-71, "GOBLIN – Comparison with FIX-II Break Spectrum Tests", May 1985.

RAI-16

QUESTION:

Section I.A.6 of Appendix K to 10 CFR50 requires that "heat transfer from piping, vessel walls, and non-fuel internal hardware shall be taken into account."

a) Since the steam dome volume acts as a dead volume prior to ADS actuation, metal heat release to steam could increase the steam enthalpy above saturation. When ADS activates, the rate of system depressurization could be affected by the amount of energy removal. Describe the metal heat release to the dead volume and estimate the amount of heat released to steam prior to ADS actuation and the potential for superheated steam to be vented through the ADS.

b) Is the volume and metal heat of the piping to the point where it is isolated from the reactor coolant system accounted in the ABWR ECCS Evaluation Model?

RESPONSE:

a) Table 16-1 shows the heat transfer between the metal of the steam dome and the steam immediately before the Automatic Depressurization System (ADS) actuates for each of three breaks. Figures 16-1 through 16-3 include the same data, along with the time when the ADS valves open. The steam flowing to the ADS valves becomes superheated in all cases described below except for the feedwater line break.

The ADS most affects the high pressure core flooder (HPCF) line break (HPCF3) transient because the system recovery is delayed until the low pressure core flooder (LPFL) pumps start. In this case, note in Table 16-1 that the heat transferred to the coolant in the steam dome is in the negative direction (from the steam to the metal) prior to ADS actuation. The initial temperature of the structures in the steam dome is based on normal operating conditions. After the break occurs, the steam line is isolated by fast closure of the turbine control valves. This results in a pressurization of the system, and the system pressure is controlled by the opening and closing of the safety / relief valves (SRVs). Because the steam dome pressure is higher than the initial operating pressure during this time, the steam temperature will be higher than the temperature of the metal structures. As a result, heat is transferred from the steam in the steam dome to the structures (e.g., the vessel dome and the steam dryer) as shown in Figure 16-3. After ADS actuates, the system pressure (and temperature) decreases and the direction of heat transfer reverses.

Table 16-1 – Integrated Heat Transfer From Metal Components in the Steam Dome Prior to ADS Actuation

	Steam Dome (MJ)	Dryers (MJ)	Total (MJ)
FWLB3	1.8	12.3	14.1
MSLB6	37.6	21.8	59.4
HPCF3	-190.8	-3.9	-194.7

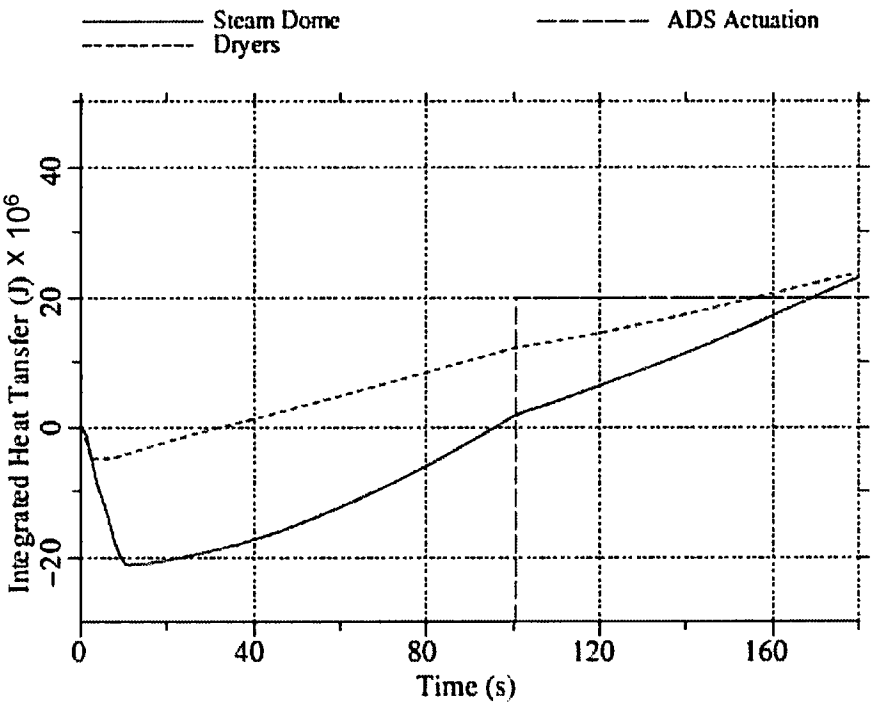

Figure 16-1 Integrated Heat Transfer from Steam Dome Structures to Coolant for FWLB3 case

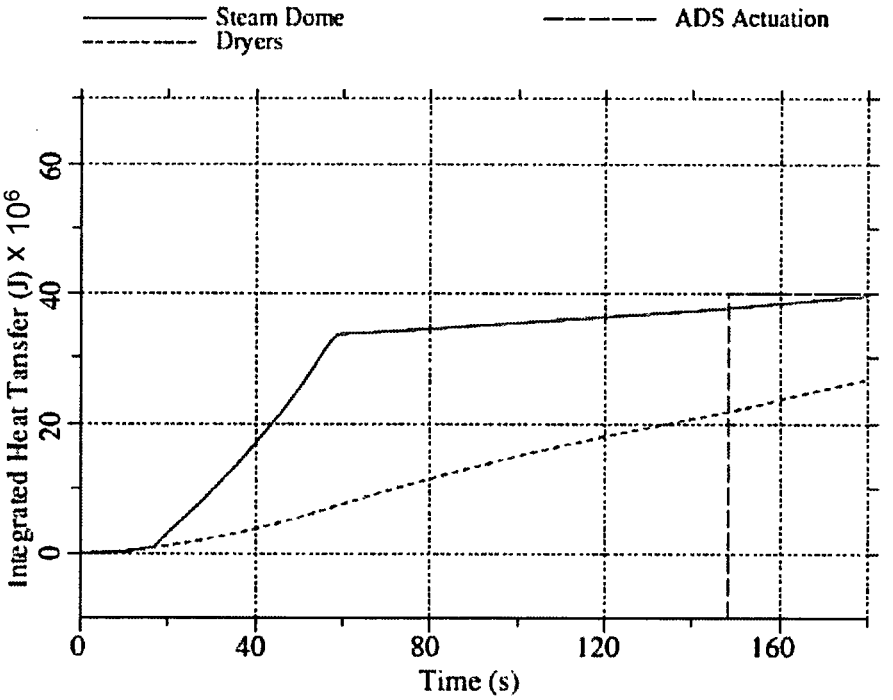

Figure 16-2 Integrated Heat Transfer from Steam Dome Structures to Coolant for MSLB6 case

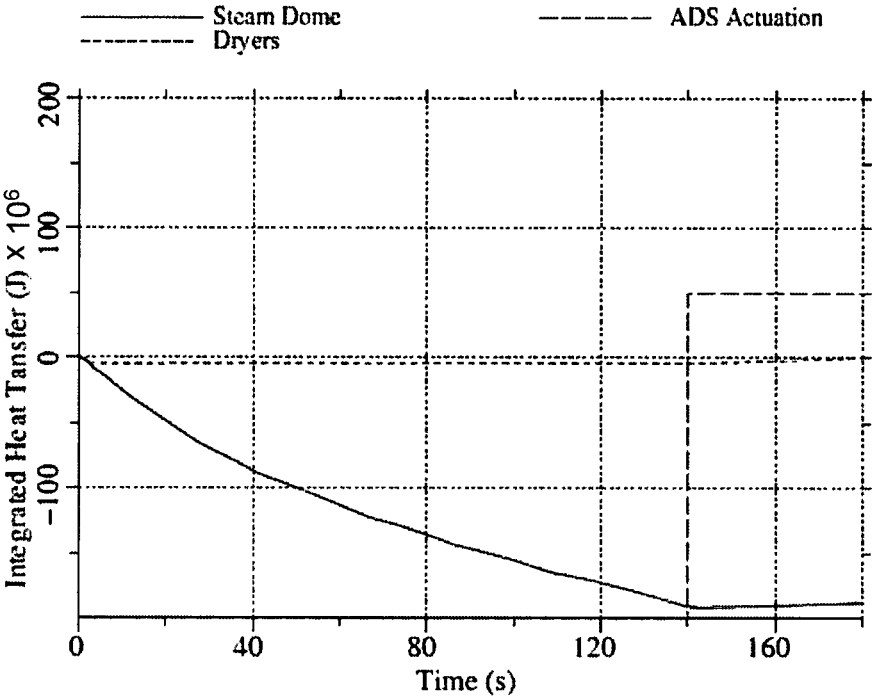

Figure 16-3 Integrated Heat Transfer from Steam Dome Structures to Coolant for HPCF3 case

b) All metal structures in the reactor pressure vessel are included in the GOBLIN heat structure model. The heat contained in the metal of the piping outside the reactor pressure vessel (i.e., the steam lines) is not modeled in GOBLIN. Because the section of the steam lines upstream of the Main Steam Isolation Valves (MSIVs) is quite short, it is assumed that the heat contained in the reactor internals would be far greater than any contained in the steam lines.

RAI-17

QUESTION

WCAP-17116-P states that "[t]he GOBLIN code has the capability to specify a series of control volumes in which a two-phase level is to be calculated and tracked with time. The model can be used when it is important to know the location of the two-phase mixture level."

a) Justify the two-phase level tracking model option (active or inactive) used for each RPV control volume including downcomer, lower plenum, core, upper plenum, and steam dome.

b) WCAP-17116-P states that the objective of the ECCS analysis for the ABWR is to "simply show that either the core does not uncover or it uncovers minimally..." The calculation of two-phase (or mixture) level in core is necessary to determine whether the core is covered or uncovered. Since the two-phase level in core is an integrated effect of void fraction distribution in lower plenum and core fluid control volumes, describe how the activation or deactivation of the two-phase level tracking model in lower plenum and core control volumes affect the core mixture level and determination of the core uncovery.

c) WCAP-17116-P states that "[t]he upper and lower downcomer regions are made up of nine sub-volumes. Feedwater as well as RCIC and LPCF injection are directed into the upper portion of the lower downcomer. Two-phase mixture level tracking is calculated throughout the entire downcomer." Section 3.3.2 of WCAP-11284-P-A, "Westinghouse Boiling Water Reactor Emergency Core Cooling System Evaluation Model: Code Description and Qualification" discusses the Two-Phase Level Tracking model. This model appears to assume saturated conditions below the two-phase mixture level interface. Prior to the initiation of the LOCA, and for some period after the initiation of the transient, the downcomer fluid below the mixture level is subcooled.

i. Describe how the mixture level and the interfacial mass and energy exchange are calculated for such a case.

ii. Is there an enthalpy gradient that exists in various nodes of the downcomer? If so, please justify the assumptions. If not, please justify the assumption of perfect mixing throughout the downcomer.

iii. Does the fluid in the downcomer become two-phase? Under what conditions and during what time periods for the various line breaks?

iv. If the downcomer fluid becomes two-phase, please describe any differences in the bubble rise model used in the downcomer as compared to that provided in WCAP-11284-P-A.

v. If the downcomer fluid becomes two-phase, and the same bubble rise model is used, please justify the adequacy of the concentration coefficient because the ABWR

pressure may be higher than that typically calculated for existing BWRs.

d) The two-phase level swell inside the core, upper plenum, steam dome and downcomer affects the break flow quality and the intervals of single and two-phase blowdown. As shown in Section 4.5.2 of WCAP-17116-P for MSLB LOCA (see Figure 4-15), rapid depressurization following the break in MSL results in significant void generation inside the RPV causing the two-phase level to reach the main steam line nozzle and initiation of two phase blowdown. Eventually, the reduction of RPV inventory leads to the break uncovery and initiation of single phase vapor blowdown again. Similarly, during the initial phase of a FWLB accident, the break flow is liquid only flow which is followed by the two-phase blowdown. Eventually, the two-phase level drops below the level of feedwater spargers resulting in break uncovery and initiation of single phase vapor blowdown. The two-phase level swell in core and upper plenum affects the break flow in HPCF line break analysis. Therefore.-

i. Discuss the effects of activation or deactivation of the two-phase level tracking model option in the RPV control volumes on calculations of break flow, flow quality, and RPV depressurization rates in MSLB, FWLB, and HPCF line break LOCA analyses.

ii. Provide the results of any sensitivity analysis performed to address the above issue.

RESPONSE

a) In the ABWR evaluation model, the two-phase level tracking model option, which is described in Section 3.3.2 of Reference 17-1, is used to track the two-phase mixture level in the annular space outside the core shroud and dryer skirt. The use of the two-phase mixture modeling in the downcomer is necessary as it provides a means to establish the initial water level. Two-phase level tracking is not used in the lower plenum, core or upper plenum. The response to part b) of this question discusses the use of level tracking in the core and the response to part d) discusses the use of level tracking in the upper plenum. With regard to the justification for not using level tracking in the lower plenum, there is never a time in any of the ABWR LOCA transients wherein the two-phase mixture level reaches the lower plenum. Thus, there is no need to track the mixture level in the lower plenum.

b) As stated in the response to item (a) of this RAI, the level tracking model is not used in the core or lower plenum of the ABWR evaluation model. The reason that the GOBLIN two-phase mixture model is not used in the core is that it is not designed to work in the active core region. The determination of whether the core is covered or uncovered is based on the calculated nodal void fractions in the core.

c) Use of the two-phase level tracking feature in the downcomer does not presume that the entire downcomer is at saturated conditions. See detailed responses below:

i. Section 3.3.2 of Reference 17-1 describes how the mixture level and the interfacial mass and energy exchange are calculated. The mixture level replaces the fixed control volume boundary that contains the mixture level with a moving boundary. The flow rate through the boundary is determined by maintaining continuity of phasic flow rates through the two-phase level for a given level velocity. The phasic flow rates are calculated for the volume above and below the mixture level by the drift flux correlation. When the water in the downcomer is subcooled, the use of the moving nodal boundary to track the water level eliminates issues related to subcooled water passing through a node containing saturated steam.

ii. There is an enthalpy gradient that is determined by the solution of the conservation equations. The enthalpy gradient is shown in Figure 17-1 for a HPCF line break (hpcf3) as the difference between saturated liquid enthalpy and nodal enthalpy. The enthalpy in any node is determined by solving the conservation equations, including the effects of heat transfer from interfacing structures. Similar to all computer codes of this type, there is an assumption that the fluid is uniformly mixed in the control cell. Figure 17-1 also compares the two-phase mixture level in the downcomer to the calculated wide-range level (collapsed level). As shown the two are equal until approximately 140 seconds when the ADS actuates and the system pressure starts to decrease. At that time, the liquid in the downcomer starts to flash and all the liquid in the downcomer becomes saturated. As a result, the two-phase mixture elevation exceeds the calculated wide-range water level. Refer to Figure 4-4 of WCAP-17116-P for the system pressure response.

iii. The limiting break scenario, from the standpoint of core uncovery, is the HPCF break. As shown in Figure 4-4 of WCAP 17116-P, the HPCF line break is not large enough to depressurize the system. The system pressure is maintained initially by the opening and closing of the SRVs. The fluid in the water-filled portions of the downcomer is sub-cooled during this period. As also shown in Figure 17-1, the two-phase mixture level and the measured (collapsed) wide range level are the same during this period. During the system depressurization following ADS actuation, voids are created in the downcomer mixture due to flashing. The effect of this can be seen by the departure of the two-phase mixture level from the measured (collapsed) water level. The hydraulic behavior in the downcomer nodes for the different line breaks depends on the location of the break and the size of the break.

iv. The GOBLIN code does not use a bubble rise model. The void fraction in each volume cell depends on the drift flux formulation, which is described in Section 3.3.1 of Reference 17-1.

v. The concentration coefficient correlation used in the drift flux formulation, which is defined in Section 3.3.1 of Reference 17-1, is pressure dependent and based on data taken in the FRIGG loop. The highest pressure used to obtain the data was ~68 bar, which is slightly below normal operating pressures.

d) As discussed above, the two-phase level tracking model is used only in the downcomer region. See the following responses:

i. The two-phase level tracking model is only used in the downcomer region, and the level tracking feature is always active. The position of the two-phase level in the downcomer affects the break flow, which affects the system depressurization for both the MSLB and the FWLB. The effect of the two-phase swell in the upper plenum following a HPCF line break is less distinct due to the lack of a two-phase level tracking in the upper plenum. If two-phase level tracking were used in the upper plenum, the effect of the level dropping below the sparger nozzles would lead to a significant reduction in the break flow and perhaps less loss of inventory. A sensitivity study wherein level tracking was added to the upper plenum is discussed in the next section.

ii. The HPCF line break analysis (hpcf3) was modified to include application of the two-phase level tracking in the upper plenum. The modified case was designated as hpcf3b. Figure 17-2 compares the system pressure responses with and without level tracking as well as the predicted mixture level in the upper plenum when the tracking model was used. As shown, the system pressure transient is nearly the same except that the actuation of ADS was delayed slightly when the level tracking model was used. The figure also shows that the mixture level decreases to the break elevation and remains at that location for a period of time. This is due to a reduction in break flow when the mixture level drops below the break as shown in Figure 17-3, which compares the break flows for the two cases. As shown, when the two-phase mixture level drops below the elevation of the break, the break flow decreases because it transitions from a two-phase mixture to single-phase vapor. The reduced break flow results in a short delay in reaching the LWL-1 setpoint for ADS actuation. The figure also compares the system masses for the two cases. As shown, the overall effect of including level tracking in the upper plenum is a reduction in the amount of mass lost before the ECCS can replenish the inventory. Figure 17-4 compares the peak cladding temperature (PCT) and the void fractions at the top of the average core channel. As shown, there is no impact on the PCT, and the average channel does not experience any partial core uncovery when level tracking is modeled in the upper plenum.

In conclusion, this evaluation shows that including level tracking in the upper plenum would not impact the calculated PCT, although it does reduce the overall loss of inventory and the extent of partial uncover of the low power bundles. Therefore, it is conservative to not include level tracking in the upper plenum.

References

17-1 RPB 90-93-P-A, "Boiling Water Reactor Emergency Core Cooling System Evaluation Model: Code Description and Qualification," October 1991.

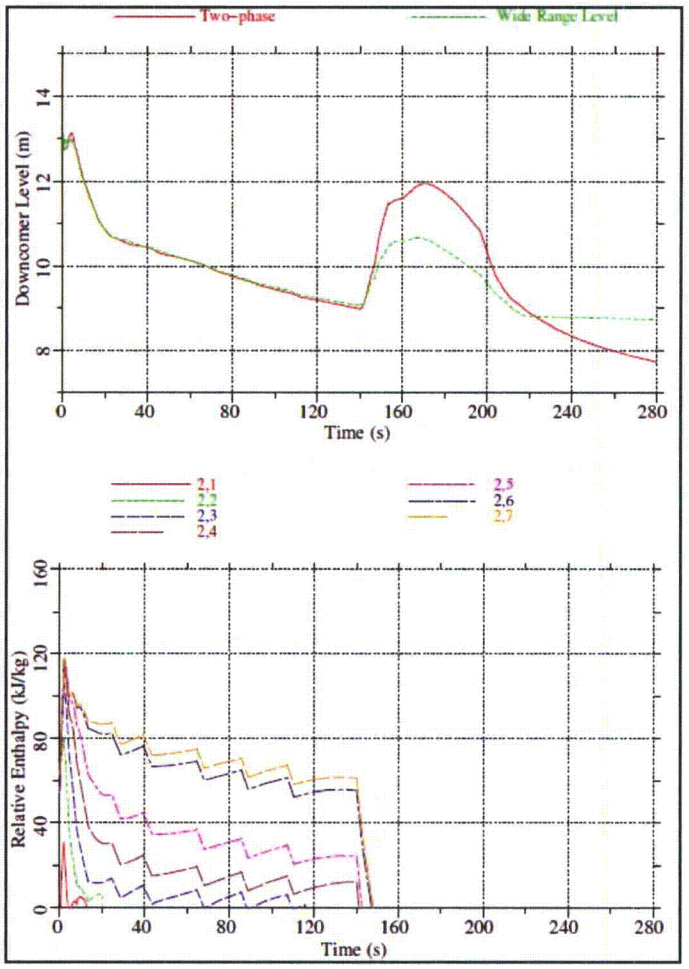

Figure 17-1 Downcomer Subcooling for HPCF Line Break (hpcf3)

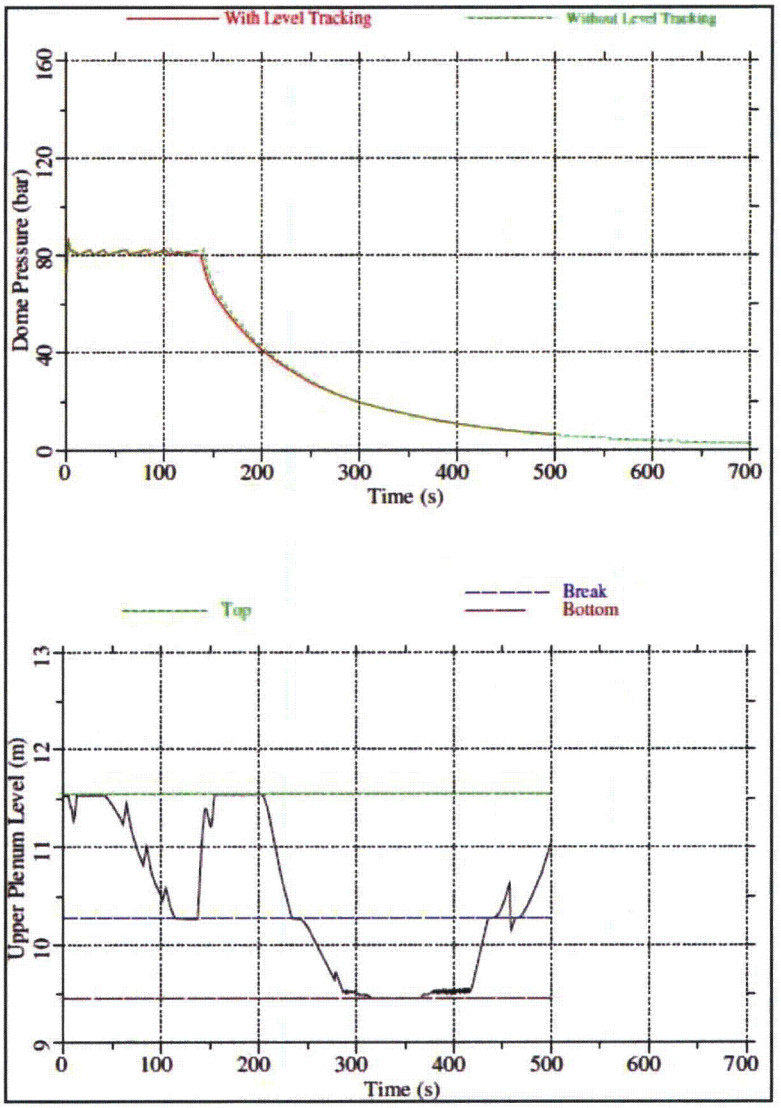

Figure 17-2 Dome Pressure and Upper Plenum Two-Phase Mixture Level*

* For dome pressure plot, the two curves lie on top of each other.

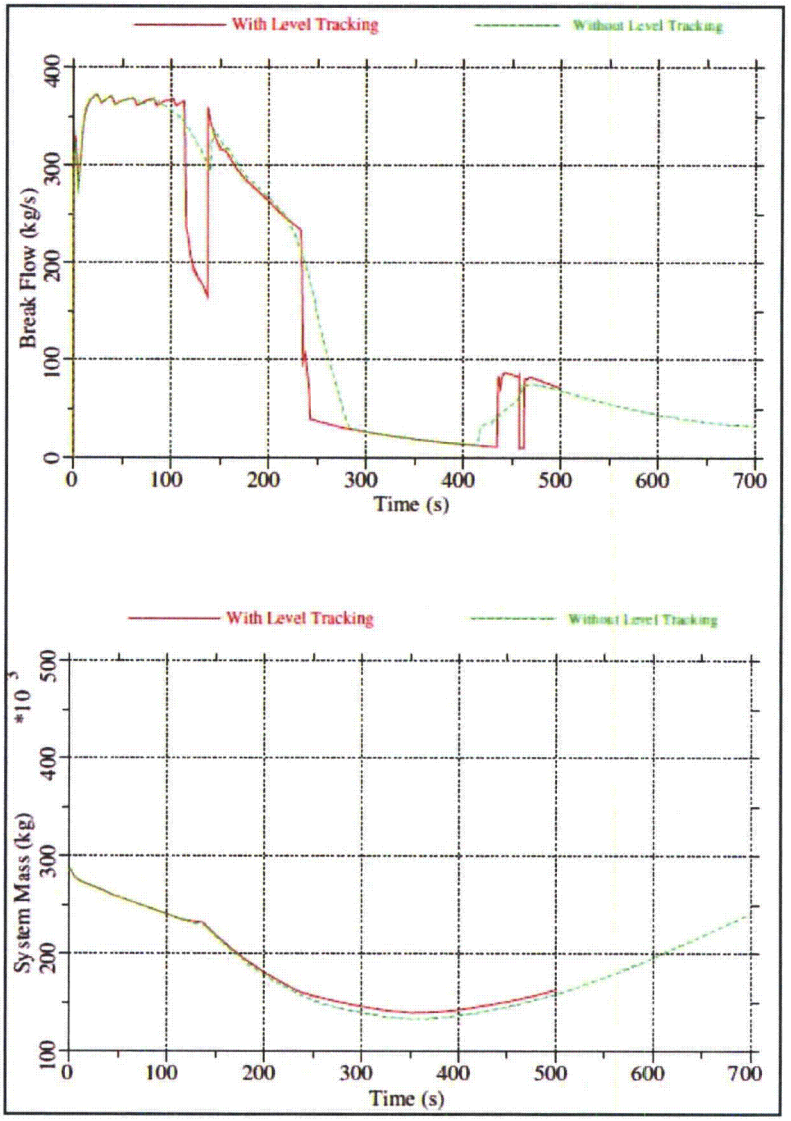

Figure 17-3 Effect of Level Tracking in Upper Plenum on Break Flow**

** For system mass plot, the two curves lie on top of each other.

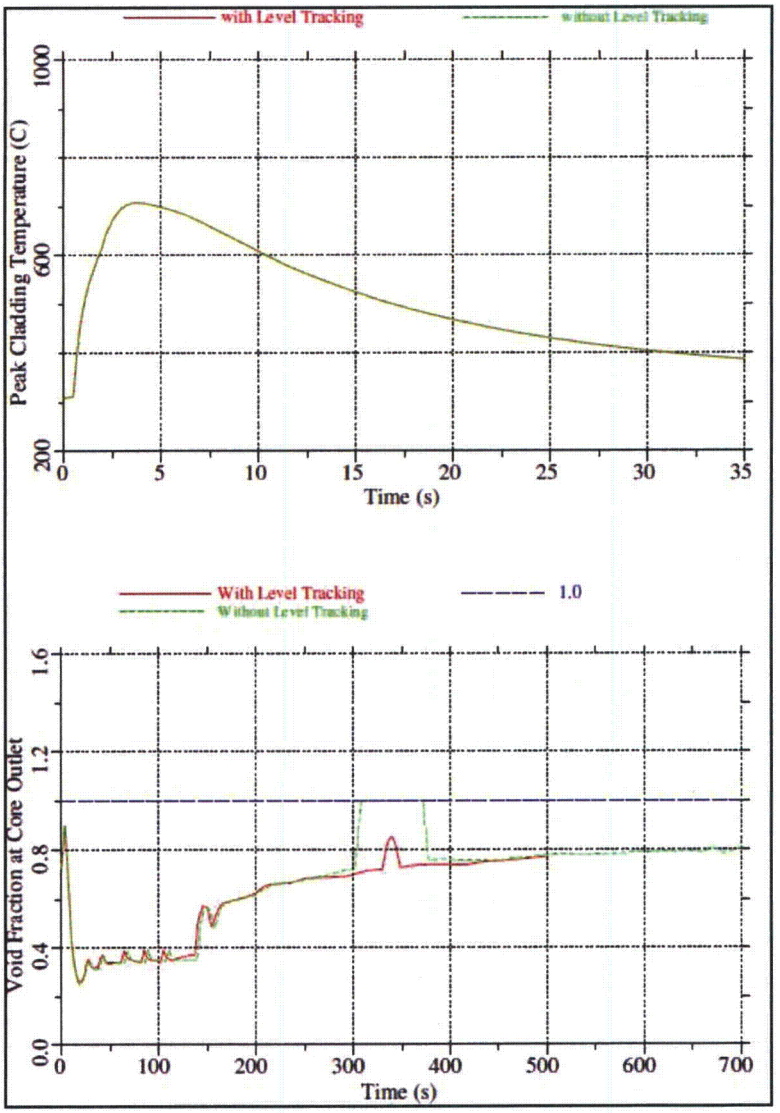

Figure 17-4 Comparison of PCT and Void Fraction at Outlet of Average Core†

† For clad temperature plot, the two curves lie on top of each other. For void fraction plot, curves with and without level tracking lie on top of each other except between 300-400 sec as noted.

RAI-17 Supplement 1:

QUESTION:

WCAP-17116-P states that "[t]he GOBLIN code has the capability to specify a series of control volumes in which a two-phase level is to be calculated and tracked with time. The model can be used when it is important to know the location of the two-phase mixture level."

a) Justify the two-phase level tracking model option (active or inactive) used for each RPV control volume including downcomer, lower plenum, core, upper plenum, and steam dome.

b) WCAP-17116-P states that the objective of the ECCS analysis for the ABWR is to "simply show that either the core does not uncover or it uncovers minimally..." The calculation of two-phase (or mixture) level in core is necessary to determine whether the core is covered or uncovered. Since the two-phase level in core is an integrated effect of void fraction distribution in lower plenum and core fluid control volumes, describe how the activation or deactivation of the two-phase level tracking model in lower plenum and core control volumes affect the core mixture level and determination of the core uncovery.

c) WCAP-17116-P states that "[t]he upper and lower downcomer regions are made up of nine sub-volumes. Feedwater as well as RCIC and LPCF injection are directed into the upper portion of the lower downcomer. Two-phase mixture level tracking is calculated throughout the entire downcomer." Section 3.3.2 of WCAP-11284-P-A, "Westinghouse Boiling Water Reactor Emergency Core Cooling System Evaluation Model: Code Description and Qualification" discusses the Two-Phase Level Tracking model. This model appears to assume saturated conditions below the two-phase mixture level interface. Prior to the initiation of the LOCA, and for some period after the initiation of the transient, the downcomer fluid below the mixture level is subcooled.

i. Describe how the mixture level and the interfacial mass and energy exchange are calculated for such a case.

ii. Is there an enthalpy gradient that exists in various nodes of the downcomer? If so, please justify the assumptions. If not, please justify the assumption of perfect mixing throughout the downcomer.

iii. Does the fluid in the downcomer become two-phase? Under what conditions and during what time periods for the various line breaks?

iv. If the downcomer fluid becomes two-phase, please describe any differences in the bubble rise model used in the downcomer as compared to that provided in WCAP-11284-P-A.

v. If the downcomer fluid becomes two-phase, and the same bubble rise model is used, please justify the adequacy of the concentration coefficient because the ABWR pressure may be higher than that typically calculated for existing BWRs.

d) The two-phase level swell inside the core, upper plenum, steam dome and downcomer affects the break flow quality and the intervals of single and two-phase blowdown. As shown in Section 4.5.2 of WCAP-17116-P for MSLB LOCA (see Figure 4-15), rapid depressurization following the break in MSL results in significant void generation inside the RPV causing the two-phase level to reach the main steam line nozzle and initiation of two phase blowdown. Eventually, the reduction of RPV inventory leads to the break uncovery and initiation of single phase vapor blowdown again. Similarly, during the initial phase of a FWLB accident, the break flow is liquid only flow which is followed by the two-phase blowdown. Eventually, the two-phase level drops below the level of feedwater spargers resulting in break uncovery and initiation of single phase vapor blowdown. The two-phase level swell in core and upper plenum affects the break flow in HPCF line break analysis. Therefore.-

i. Discuss the effects of activation or deactivation of the two-phase level tracking model option in the RPV control volumes on calculations of break flow, flow quality, and RPV depressurization rates in MSLB, FWLB, and HPCF line break LOCA analyses.

ii. Provide the results of any sensitivity analysis performed to address the above issue.

SUPPLEMENT 1 RESPONSE:

The original response to RAI 17 was provided to the NRC in STPNOC Letter No. U7-C-STP-NRC-100227 dated October 14, 2010. At the NRC audit of WCAP-17116-P held in Windsor, CT the week of February 14, 2011, the NRC requested additional information concerning this response, which is identified in the Audit Plan. The purpose of this supplemental response is to provide that additional information. The specific information requests and the response to those requests are provided below.

For Item 17b:

Information Request

Since the mixture level tracking model cannot be used when there is uncovering of the reactor core, please describe the criteria used to determine when there is uncovering of the reactor core.

Response to Information Request

For the ABWR ECCS evaluation model, level tracking is only used in the downcomer. The level tracking feature cannot be used in the core region. The determination of whether the core is covered or uncovered is based on the calculated nodal void fractions in the core.

The criterion used to determine when there is uncovering of the reactor core is when the nodal void fraction in the first unheated node above the core (i.e., [ ]^{a,c}) increases to [ ]^{a,c}.

Only the HPCF breaks show partial uncovery of the lower-power assemblies. The core and hot assembly are modeled using [ ]^{a,c} axial nodes (nodes [ ]^{a,c} through [ ]^{a,c}). Figure 17-1 shows the nodal void fractions for nodes [ ]^{a,c} through [ ]^{a,c}, where node [ ]^{a,c} is the unheated node at the end of the heated channel. As shown, there is partial uncovery of the average assembly starting at approximately 300 seconds. This is shown when the nodal void fraction abruptly increases from approximately 0.7 to 1.0. As also shown in Figure 17-1, the hot assembly does not uncover. However, the average void of the hot assembly is higher than the average core.

a,c

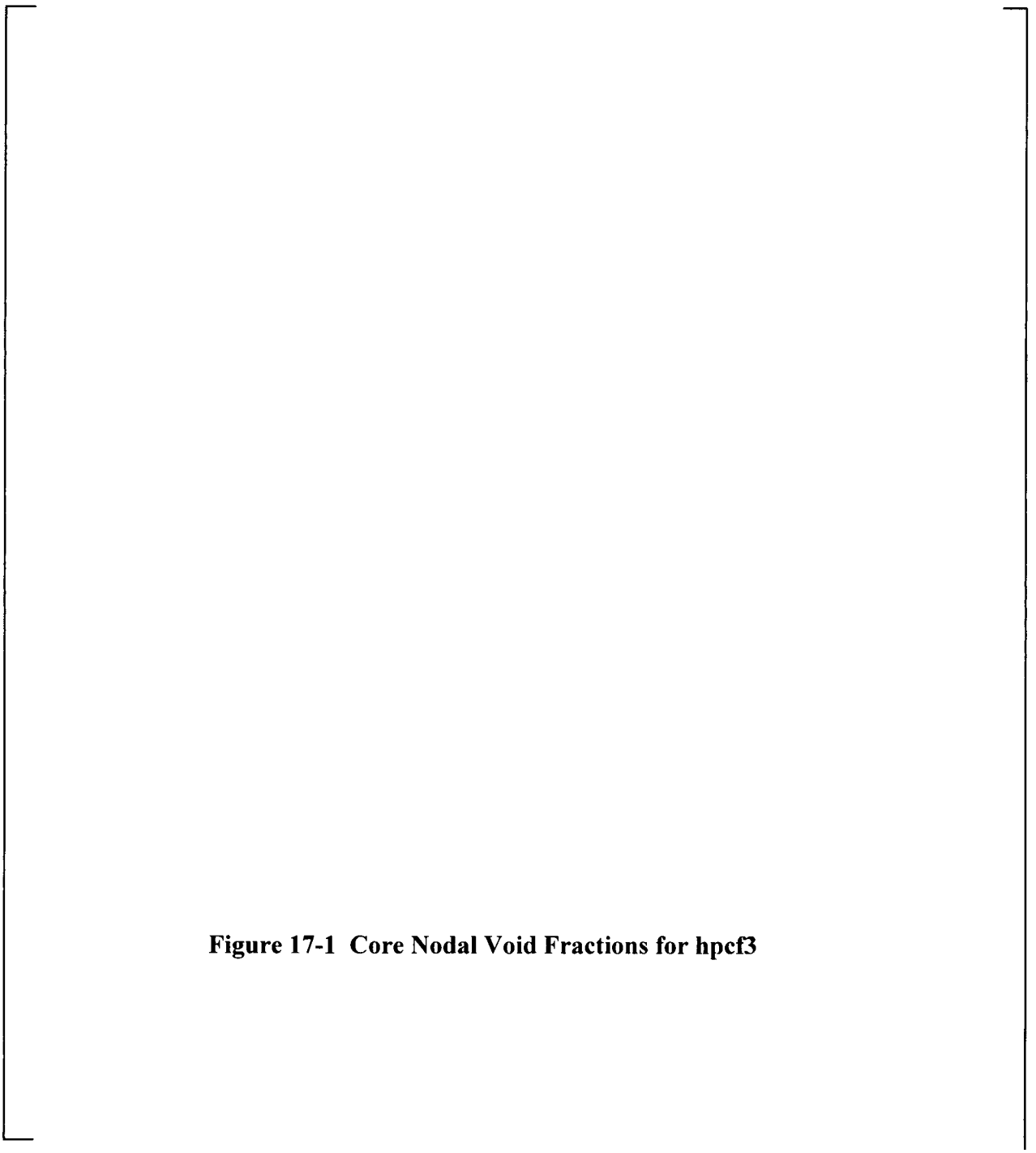

Figure 17-1 Core Nodal Void Fractions for hpcf3

For Item 17c:

Information Request

Please describe the calculation process used to determine the amount of mass and energy exchange at the mixture level interface when the fluid below the mixture level is subcooled, or provide a reference to the model description for the ABWR ECCS Evaluation Model.

Response to Information Request

This aspect of the evaluation model is the same as the previously approved evaluation model that is used for BWR/2 through BWR/6 analyses.

When a level is defined in a region, the node division follows the level. The level then becomes the border between two cells. The cells surrounding the level have variable size. Restructuring occurs if one of these cells becomes too small.

In the situation where the water is subcooled, there is no energy exchange between the steam above the interface and the subcooled water below the interface. In the event there is water injected into the node above the water level, the water will fall down into the 'mixture', where it will mix with it. There is energy exchange with the liquid due to metal structures in contact with the water.

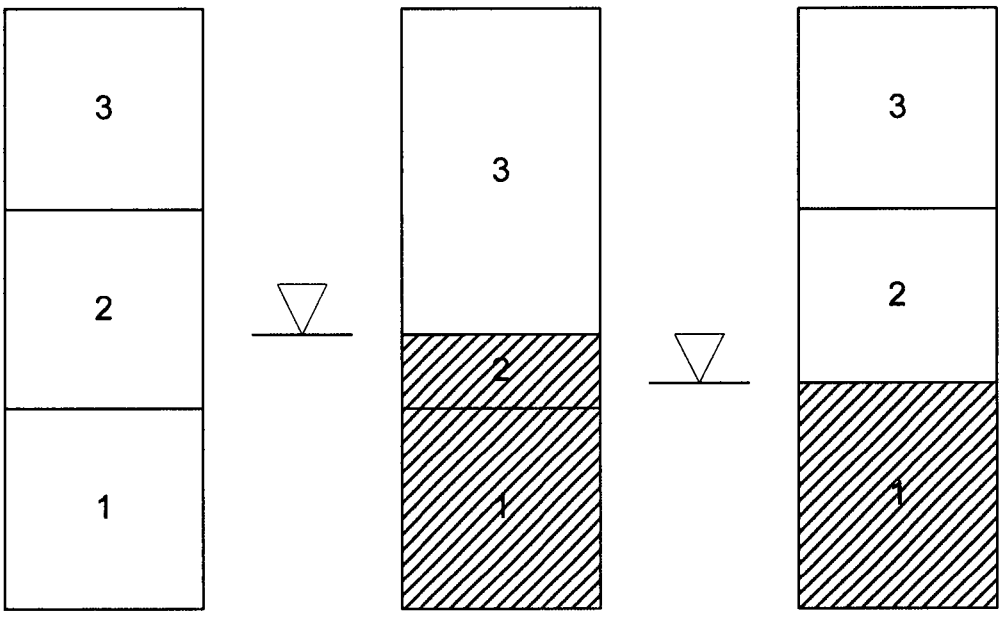

Figure 17-2 Schematic of Mixture Level at Different Times

RAI-18

QUESTION:

As noted in Section 4.2 of WCAP-17116-P, the ECCS system activation signals are initiated based on the RPV water level.

a) Describe how the water level used for the generation of ECCS system activation signal is calculated. Which water level is used for the ECCS activation (i.e., two-phase mixture level or the collapsed water level)?

b) Which RPV control volume water level is used for the generation of ECCS actuation signals?

c) Discuss the effects of activation or deactivation of the two-phase level tracking model in the RPV control volumes on initiation of ECCS system.

RESPONSE:

a) The ECCS is activated by indications from the wide-range water level instrumentation, which measures the pressure drop between two elevations. As such, a collapsed water level is used to actuate the ECCS.

b) The pressure taps for the wide range level instrumentation are located at 16.342 m and 8.978 m. The higher tap is located in sub-volume 1,1; the lower tap is located in sub-volume 2.4 as described in Figure 4-3.

c) The two-phase level tracking model has no effect on initiation of the ECCS system.

RAI-19

QUESTION

Section K LA of Appendix K to 10 CFR 50 states that "[a] range of power distribution shapes and peaking factors representing power distributions that may occur over the core lifetime must be studied. The selected combination of power distribution shape and peaking factor should be the one that results in the most severe calculated consequences for the spectrum of postulated breaks and single failures that are analyzed."

Section 6.2 of WCAP-11427-P-A, ""Westinghouse Boiling Water Reactor Emergency Core Cooling System Evaluation Model: Code Sensitivity" discusses the effect of power distributions for a BWR. However, for the ABWR LOCA analysis presented in WCAP-17116-P a symmetrical axial power shape (chopped cosine) with a 1.5 axial peaking factor is assumed as a conservative power shape. The potential for cladding heat-up in ABWR LOCA following the initial cladding temperature excursion depends upon the potential for uncovering of the core due to the imbalance between mass depletion and ECC flow delivery and is a function of the flow between the lower plenum and the core, the void generation within the core, and the drift velocities within the two-phase mixture. Considering the fact that the level swell is an integrated effect of power along the axial length of the rod; if the total power of the rod is the same, there will be substantially less level swell in a top peaked power shape than a chopped cosine for the same amount of fluid mass. Therefore, in ABWR where the mixture level is calculated to remain above the top of the core in the hot assembly, it is important to assure that power distribution assumptions are not unrealistically contributing to the conclusion that the core remains covered by a two-phase mixture.

a) As required by Appendix K Section K.I.A, provide justification that the selected power profile (i.e., chopped cosine) and peaking factor results in the most severe calculated consequences for the spectrum of postulated breaks and single failures that are analyzed in WCAP-17116-P.

b) Discuss the effect of top skewed power distributions on core two-phase level and PCT in the ABWR LOCA.

RESPONSE

a) Various normalized axial power shapes with associated axial power peaking factors (APPF) for a typical cycle depletion are shown in Figure 19-1 below for multiple burnup steps from 0 to 17.79 MWd/kg.

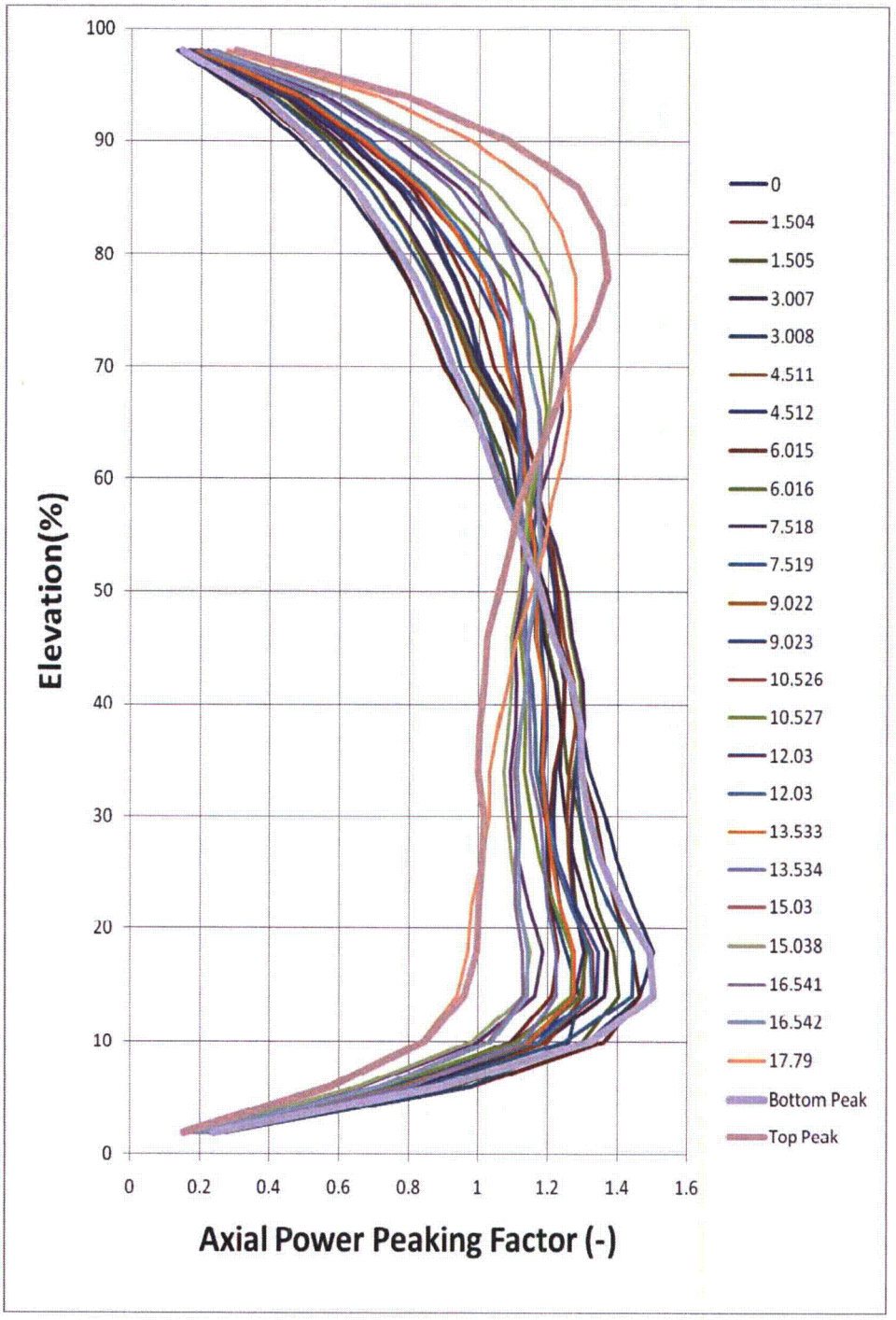

Figure 19-1 – Axial Power Peaking Factors for Different Burnups**

** Burnups in Mwd/kg are shown in the legend.

Two limiting APPFs are selected to make representative cases for the bottom and top peak APPFs. These two selected cases are at the burnup of 9.022 and 15.03 MWd/kg. The 25 node APPF values are then input to the GOBLIN LOCA system response computer code. Table 19-1 shows the resulting peak cladding temperatures (PCTs) from the fuel heatup code for bottom, top peaked and the limiting chopped cosine axial power shapes.

Table 19-1 PCT Results for Different AXIAL Power Shapes

Axial Power Peaking Factor Shape	PCT (^{o}C)	Node ID*
Bottom Peak	851.1	15
Chopped Cosine	879.0	17
Top Peak	851.8	22

* Noding diagram is given in Figure 4-3 of Reference 19-1

Table 19-1 demonstrates that the limiting axial power profile is still the chopped cosine profile based on PCT results.

b) Figure 19-2 shows the void fraction in the hot assembly for each of the axial power shapes at various axial elevations. This indicates that the void distribution is different for each power shape, but the outlet void fractions are nearly the same. This is to be expected since the integrated power up to the outlet is the same in all cases. The previous section concludes that the maximum PCT still occurs for the chopped cosine axial power shape. WCAP-11427-P-A discusses earlier dryout and uncovery times for a top-peaked shape but this is for a BWR design with external recirculation piping and jet pumps. The ABWR design with rapid coastdown of the RIPs produces an early boiling transition before the reactor scram occurs. The increased voiding results in a reduction in core power, and along with reactor scram, further results in a rapid decrease in cladding temperature. Additionally, since the elevation of potential large pipe breaks is above the core, along with a robust ECCS, there is not an extended core uncovery in the ABWR.

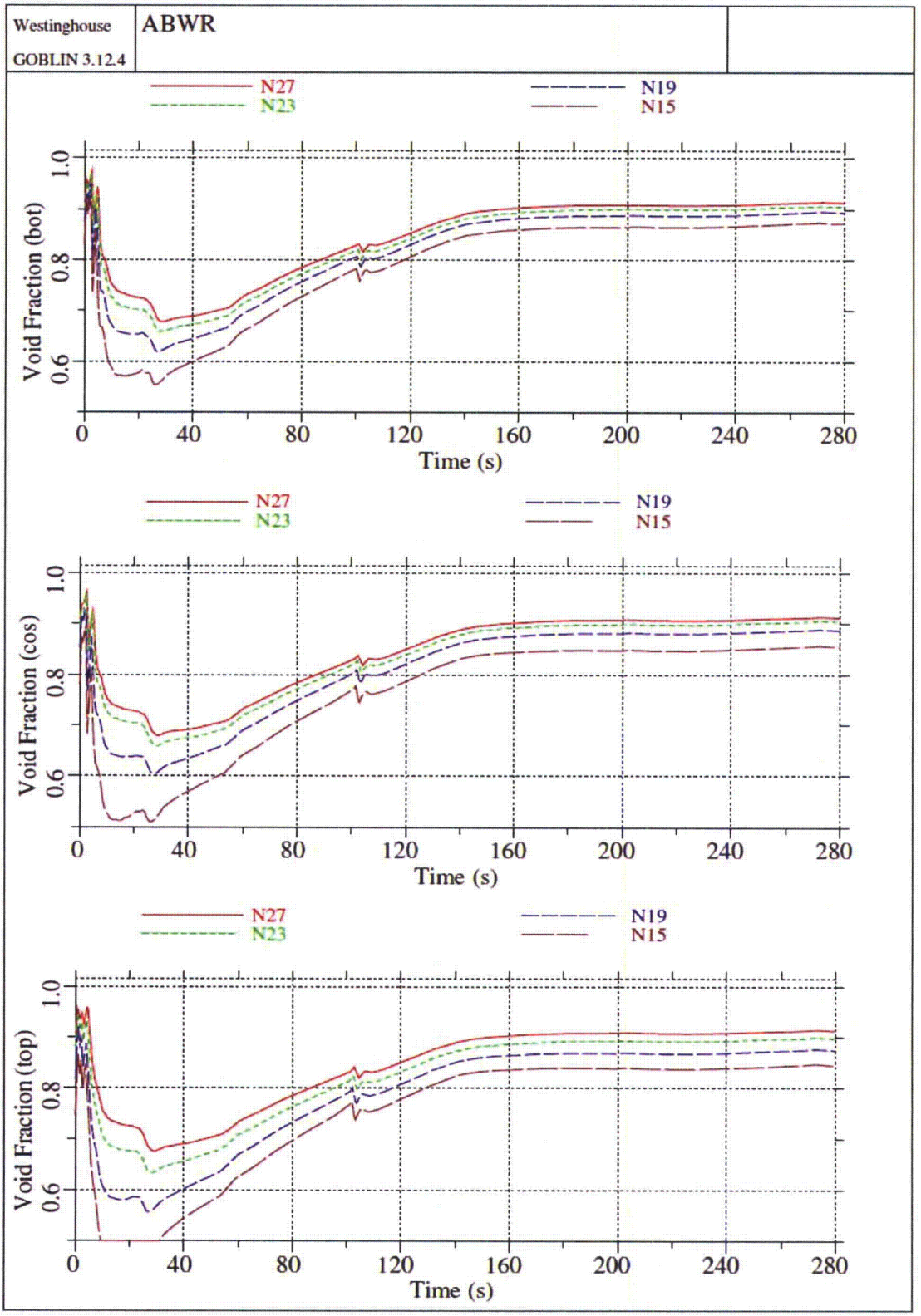

Figure 19-2 – Comparison of Void Fractions at Various Nodal Elevations for Three Axial Power Shapes

References

19-1 WCAP-17116-P "Westinghouse BWR ECCS Evaluation Model: Supplement 5 – Application to the ABWR," September 2009.

RAI-19 Supplement 1:

QUESTION:

Section K LA of Appendix K to 10 CFR 50 states that "[a] range of power distribution shapes and peaking factors representing power distributions that may occur over the core lifetime must be studied. The selected combination of power distribution shape and peaking factor should be the one that results in the most severe calculated consequences for the spectrum of postulated breaks and single failures that are analyzed."

Section 6.2 of WCAP-11427-P-A, ""Westinghouse Boiling Water Reactor Emergency Core Cooling System Evaluation Model: Code Sensitivity" discusses the effect of power distributions for a BWR. However, for the ABWR LOCA analysis presented in WCAP-17116-P a symmetrical axial power shape (chopped cosine) with a 1.5 axial peaking factor is assumed as a conservative power shape. The potential for cladding heat-up in ABWR LOCA following the initial cladding temperature excursion depends upon the potential for uncovering of the core due to the imbalance between mass depletion and ECC flow delivery and is a function of the flow between the lower plenum and the core, the void generation within the core, and the drift velocities within the two-phase mixture. Considering the fact that the level swell is an integrated effect of power along the axial length of the rod; if the total power of the rod is the same, there will be substantially less level swell in a top peaked power shape than a chopped cosine for the same amount of fluid mass. Therefore, in ABWR where the mixture level is calculated to remain above the top of the core in the hot assembly, it is important to assure that power distribution assumptions are not unrealistically contributing to the conclusion that the core remains covered by a two-phase mixture.

a) As required by Appendix K Section K.I.A, provide justification that the selected power profile (i.e., chopped cosine) and peaking factor results in the most severe calculated consequences for the spectrum of postulated breaks and single failures that are analyzed in WCAP-17116-P.

b) Discuss the effect of top skewed power distributions on core two-phase level and PCT in the ABWR LOCA.

SUPPLEMENT 1 RESPONSE:

The original response to RAI 19 was provided to the NRC in STPNOC Letter No. U7-C-STP-NRC-100227 dated October 14, 2010. At the NRC audit of WCAP-17116-P held in Windsor, CT the week of February 14, 2011, the NRC requested additional information concerning this response, which is identified in the Audit Plan. The NRC requested additional details regarding the effect of a top skewed power distribution on the High Pressure Core Flooder (HPCF) analyses for which there is an uncovering of the reactor and whether the chopped cosine power

distribution bounds the top skewed power distribution and the bottom skewed power distribution. The purpose of this supplemental response is to provide this additional information.

While Subsection 6.3.3.7.6 of the ABWR DCD documents that the HPCF line break is the most limiting break for minimum transient water level in the downcomer, Section 4.7.1 of WCAP-17116-P, which documents the Westinghouse analysis, concludes that the full size feedwater line break (FWLB) is the most limiting break for minimum inventory.

a) Because Westinghouse analysis established the FWLB case to be most limiting for minimum inventory, the FWLB case was chosen for the axial power shape sensitivity study. The analysis transmitted in the original RAI-19 response confirms that, for this case, the chopped cosine case remains limiting.

b) Section 4.5.1.2 of WCAP-17116-P documents that the hot assembly does not uncover for the HPCF line break. The response to RAI-3 (Reference STPNOC Letter No. U7-C-STP-NRC-100199 dated September 7, 2010) discusses the consequences of the lower power assemblies experiencing a partial core uncovery. As illustrated in Figure 3-1 of that response (duplicated as figure 19-1 below) the secondary heat up for the low-power assemblies does not reach within 400°C of the initial peak.

   The HPCF line break case was re-analyzed utilizing the same axial power shape described in detail in the original RAI-19 response, which included a sensitivity study utilizing a FWLB case. Figures 19-2 and 19-3 below illustrate the effects of a top-peaked power shape. As predicted, a top-peaked power shape causes the secondary heat up of the lower-powered bundles to be more significant. However, the secondary heatup results in clad temperatures which are well below the peak clad temperature during the initial heatup caused by RIP coastdown. In addition, the effect of the increased secondary heatup of the lower-powered nodes is insignificant, because the clad temperature of the higher-powered nodes remains above the clad temperature of the lower-powered nodes.

The Westinghouse analysis concludes that, for the case resulting in minimum inventory, which is the FWLB, the chopped cosine power shape bounds the top peaked power shape. In addition, the effect of a top-peaked power shape on the secondary heatup due to partial core uncovery during the HPCF case is not expected to be significant enough to surpass the initial peak in clad temperature. These two conclusions combine to support the continued use of a chopped cosine axial power shape.

As a result of this RAI response, Section 4.7 of WCAP-17116-P will be revised as shown in the markup attached to the response to RAI 32 Supplement 2. Changes from Revision 0 are highlighted with gray shading.

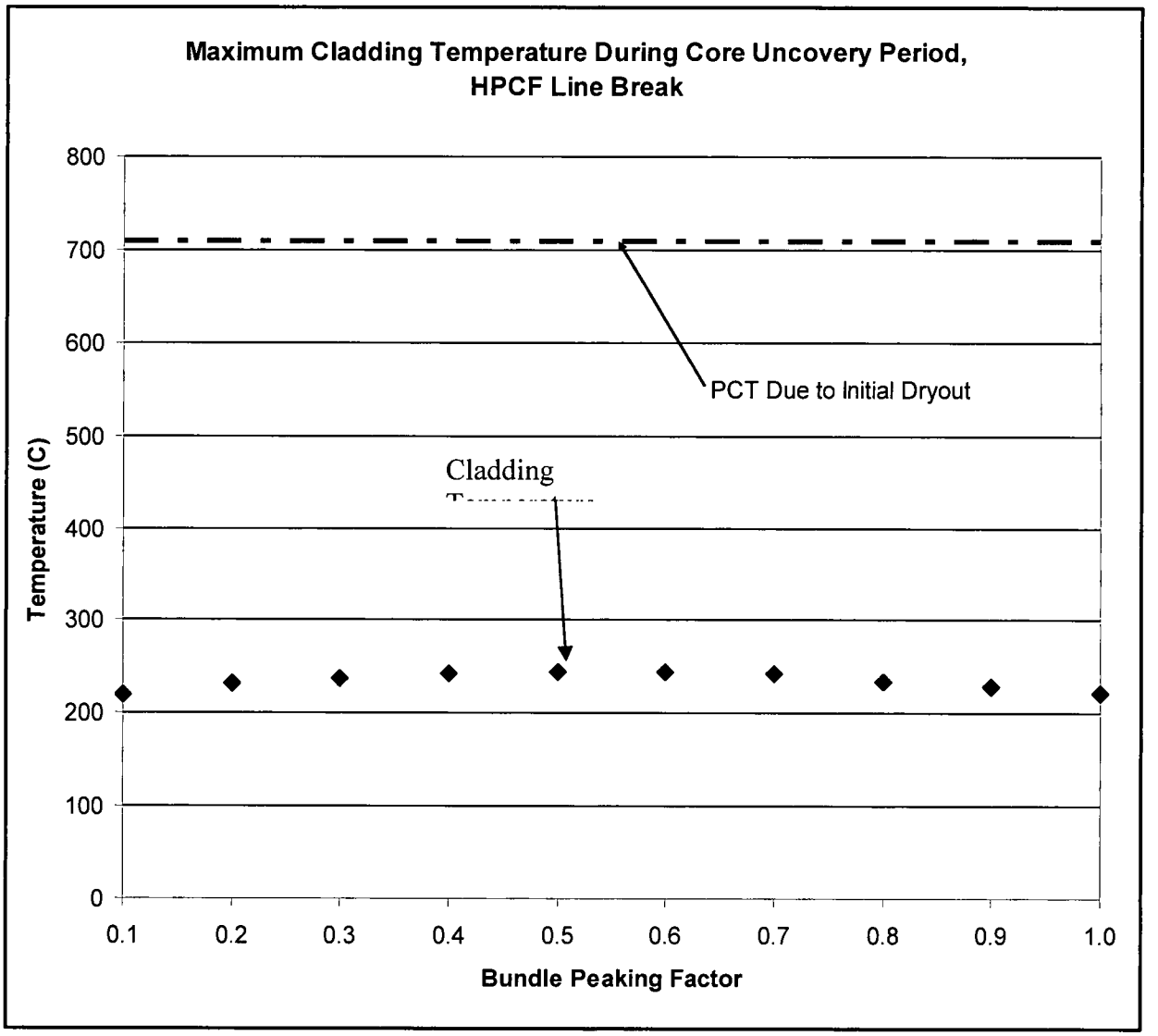

Figure 19-1 – Variation of Maximum Cladding Temperature During Partial Core Uncovery with Respect to Bundle Peaking Factor

a,c

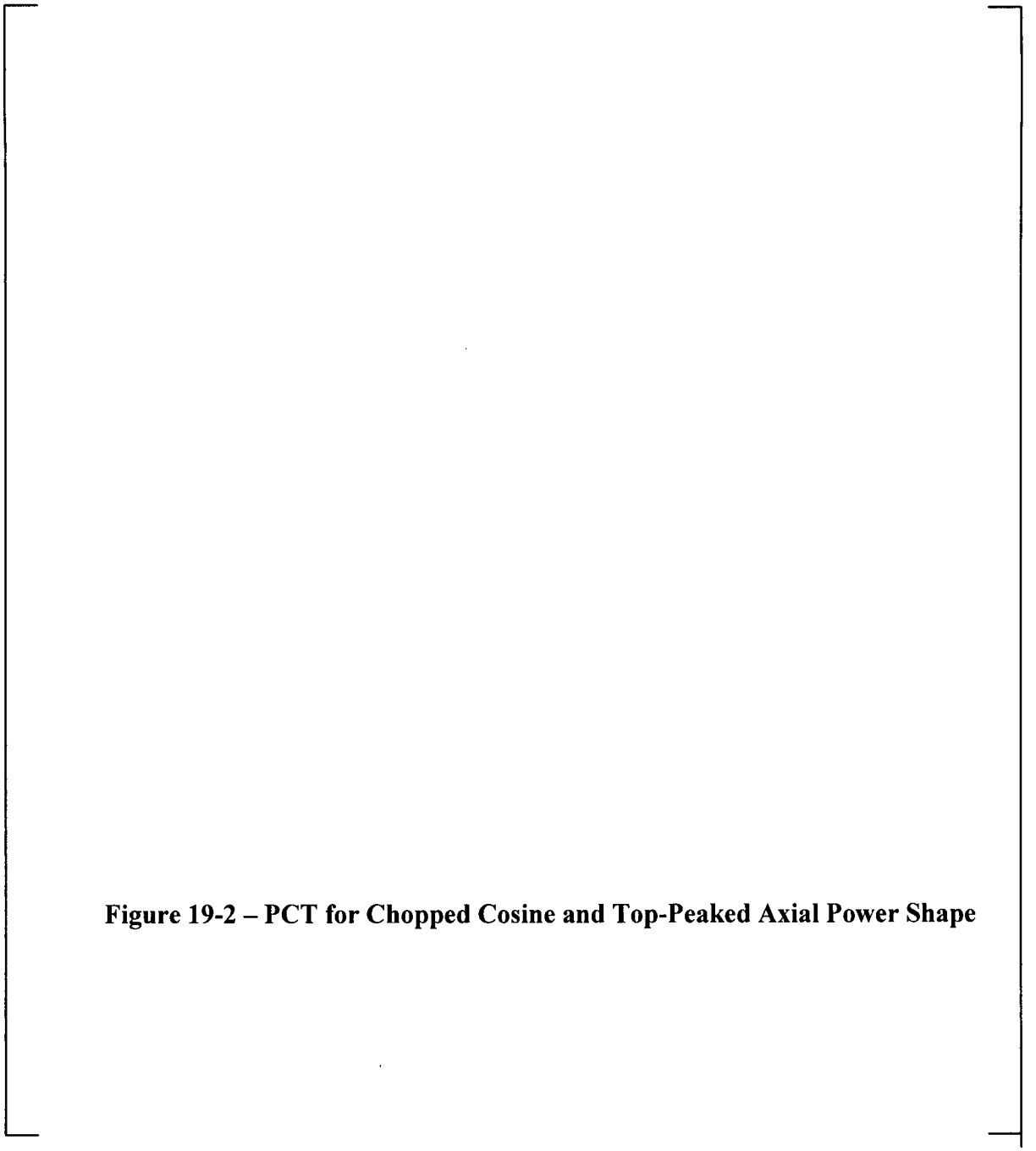

Figure 19-2 – PCT for Chopped Cosine and Top-Peaked Axial Power Shape

a,c

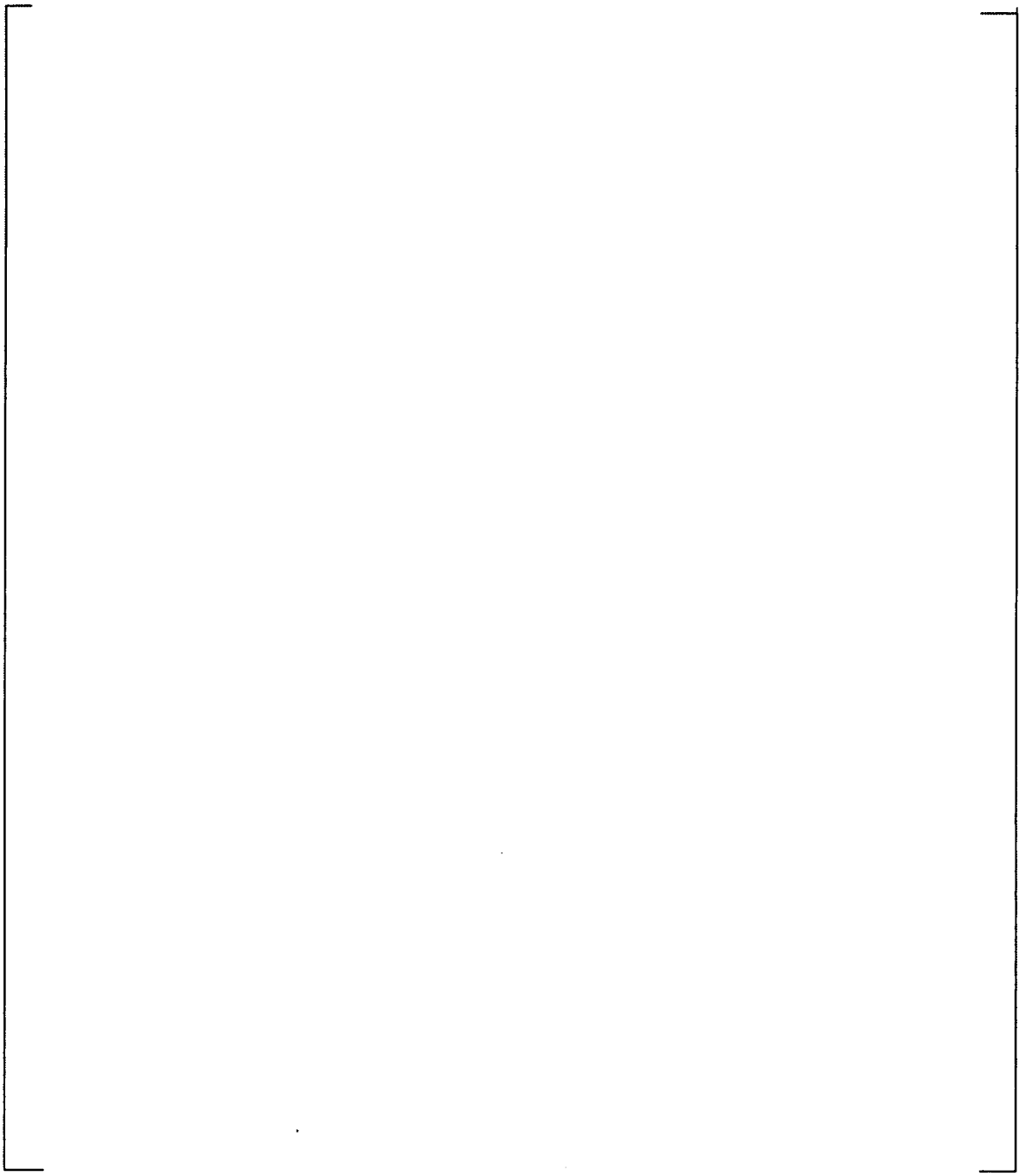

Figure 19-3 – Void Coefficients for Chopped Cosine and Top-Peaked Axial Power Shape

RAI-20

QUESTION:

As indicated in Section 5.3 of WCAP-17116, the CPR correlation D4.1.2 (developed for the SVEA-96 Optima2 fuel) is implemented in the GOBLIN code for the ABWR application. It has been stated that the correlation is described in detail in Section 5.0 of WCAP-16081-PA. However, WCAP-16081-P-A provides discussion on CPR correlation D4.1.1.

a) Provide explanation of any changes/modifications made to the D4.1.1 CPR correlation to arrive at the D4.1.2 correlation.

b) The NRC SER documented in WCAP-16081-P-A recommends using different uncertainties for the CPR correlation based on the system pressure (3.15% below 45 bars and 2.32% above 45 bars). Please explain whether and how these uncertainties have been incorporated into the D4.1.2 correlation. Also provide an explanation as to whether the use of system pressure based sensitivities is carried over to the GOBLIN analysis. If not, please provide a justification for not doing so.

RESPONSE:

a) The GOBLIN code currently uses the D4.1.2 CPR correlation. An earlier version of GOBLIN used the D4.1.1 CPR correlation. The D4.1.2 includes correction factors due to the sub-bundle to full-bundle effect, the double-peaked axial power profile correction, and the R-factor correction. These three items are described in Section 5 of WCAP-16081-P-A. Otherwise, the D.4.1.1 correlation described in WCAP-16081-P-A is the same as the D4.1.2 correlation.

b) The GOBLIN code does not specifically account for variations in uncertainty. However, as described in Reference 20.1 below, the GOBLIN code uses two correlations for determining the critical power ratio: one for the flow boiling regime and one for the pool boiling regime. The code computes the critical heat flux using both correlations and uses the maximum of the two to determine the onset of dryout.

   System pressure-based sensitivities are not carried over to the GOBLIN analysis, nor are they required. As described in WCAP-17116, the ABWR LOCA transients are characterized by early dryout due to rapid loss of flow before the system pressure has changed significantly. Figure 5-4 of WCAP-17116-P shows that GOBLIN is consistently conservative in its prediction of dryout for loss of flow transients. Therefore, there is no need to perform pressure-based sensitivity analyses.

Reference

20.1 RPB 90-93-P-A, "Boiling Water Reactor Emergency Core Cooling System Evaluation Model: Code Description and Qualification," October 1991.

RAI-20S01

QUESTION

10 CFR Part 50, Appendix K.C.4.c requires that, "Correlations of appropriate transient CHF data may be accepted for use in LOCA transient analyses if comparisons between the data and the correlations are provided to demonstrate that the correlations predict values of CHF which allow for uncertainty in the experimental data throughout the range of parameters for which the correlations are to be used. Where appropriate, the comparisons shall use statistical uncertainty analysis of the data to demonstrate the conservatism of the transient correlation."

Confirm that the CPR correlation (D4.1.2) allows for uncertainty in the experimental data throughout the range of parameters encountered in the experiments that are used to develop the correlation. If the CPR correlation (D4.1.2) is to be considered conservative, confirm the conservatism for all situations, including transient power tests (see also outstanding RAI-21).

SUPPLEMENTAL RESPONSE

The D4.1.2 CPR correlation is derived from the same data as the D4.1.1 correlation, described in detail in Section 5 of WCAP-16081-P-A, with additional updates addressing the sub-bundle to full-bundle effect, the double-peaked axial power profile correction and the R-factor correction. The D4.1.2 correlation remains based on the same steady-state CHF data as for the D4.1.1 correlation. Since the Westinghouse CPR correlation is based on steady-state data, the requirements of Section I.C.4 item (c) of 10 CFR 50, Appendix K do not apply.

Section 5.3.1 of WCAP 17116-P discusses the conservatism of predicting the transient CHF test data from the FRIGG loop tests, through the application of the steady-state D4.1.2 CPR correlation. During an ABWR LOCA the peak clad temperature (PCT) is driven by the boiling transition phase, specifically the time of dryout. The conservatism of the evaluation model is established through comparison of predicted dryout times to measured dryout times for various transient test cases, addressing the range of parameters encountered during an ABWR LOCA. As discussed in the response to RAI-21, the results documented in Section 5.3.1 of WCAP-17116-P for the D4.1.2 CPR correlation are more conservative than those for the D4.1.1 CPR correlation, which was previously approved in WCAP-16081-P-A.

RAI-21

QUESTION

Figure 5-4 of WCAP-17116-P shows that the CPR correlation predicts the flow transient experiment data conservatively. However, some of the data obtained in the power transient experiments are predicted non-conservatively by the correlation. Section 5.3.1 of WCAP-17116-P states that "[a] typical ABWR LOCA transient is characterized by a rapid decrease in flow and a slow decrease in reactor power in the first 3 seconds of the event. Therefore, the slight non-conservatism shown in the power transient tests does not impact the overall conclusion that GOBLIN predicts boiling transition time conservatively."

a) Unlike the justification given in WCAP-17116 that a typical ABWR LOCA is characterized by a rapid decrease in flow and a slow decrease in reactor power in the first 3 seconds; during some LOCA immediately following the isolation of main steam line or closure of TCV, reactor power may rise due to reactivity feedback effect (as a result void collapse). Provide justification that the selected CPR correlation is conservative under such conditions.

b) The comparison of the predictions from the BISON-SLAVE code incorporating the D4.1.1 CPR correlation against the transient test data collected in the FRIGG facility, shown in Figure 7.10 of WCAP-16081-P resulted in less than 3% of the data being nonconservatively predicted. However, the comparison of the GOBLIN code incorporating the D4.1.2 correlation against the same test data, shown in Figure 5-4 of WCAP-17116, shows that more than 11% of the data are predicted non-conservatively. Please provide a discussion of the impact of non-conservatism in the CPR correlation on the uncertainties in the GOBLIN prediction of peak cladding temperature under transient accident conditions.

c) Please provide a detailed description of the treatment of CPR correlation uncertainties as they impact the GOBLIN application to ABWR LOCA analyses.

RESPONSE

a) As shown by the sequence of events tables in the response to RAI-32, the TCVs or MSIVs close early in each of the events in WCAP-17116-P. As shown by the figures in the response to RAI-32, the core power decreases for all of these events. As such, any reactor feedback from a result of void collapse, which is accounted for in these figures, is not significant enough to overcome the overall slow decrease in power characteristic of the first 3 seconds.

b) WCAP-16081-P-A Figure 7.10 compares the FRIGG facility measured dryout times to the BISON-SLAVE predicted times. WCAP-16081-P-A Tables 7.4, 7.5, and 7.6 show the results. The non-conservative predictions (last) column of Tables 7.4, 7.5, and 7.6 are based on CPR criteria, not the predicted time. Using the CPR criteria, the number of non-conservative predictions is less than 3%. Using the measured time, the non-conservative predictions using

the BISON-SLAVE code are higher than those in WCAP-17116-P Figure 5-4, which compares the FRIGG facility measured dryout times to the GOBLIN predicted times.

c) See the response to RAI- 20 for a discussion of the GOBLIN CPR correlation D4.1.2 treatment of uncertainties.

RAI-22

QUESTION:

In WCAP-17116-P Section 6.1.1, Westinghouse states that "calculated cladding temperatures are determined with the highest initial calculated stored energy."

a) Describe typically at what time and life the power distribution corresponds to the highest initial calculated stored energy. Does this represent the period of maximum densification?

b) What typical power distributions characterize this time in life? (Full power, ARO).

RESPONSE:

b) The initial stored energy in the LOCA heat-up calculation is established by the use of conservative gap heat transfer coefficients and fuel pellet conductivity. The methodology for providing initial stored energy to LOCA analysis is described in the Westinghouse fuel mechanical design methodology topical report (Reference 22.1). The calculated initial stored energy depends on many factors (e.g., rod power history, cladding creep, fuel densification, thermal conductivity, etc). The initial conditions for LOCA analysis at a given time/burnup are conservatively generated at the peak nodal power at the Linear Heat Generation Rate (LHGR). Figure 22-1, below, shows a typical LHGR limit for Westinghouse BWR fuel. The highest initial stored energy typically occurs just before the power fall-off at the LHGR limit, and is mainly a result of fuel thermal conductivity degradation from burnup. At that point the fuel has fully densified.

b) The axial power distribution for initial stored energy is an envelope of all possible axial power distributions for a given bundle at full power. In general this envelope axial power distribution is conservative because the peak node power is scaled up to the LHGR limit.

This power distribution results in a very conservative rod average power.

Reference

22.1 - WCAP-15942-P-A, "Fuel Assembly Mechanical Design Methodology for Boiling Water Reactors Supplement 1 to CENP-287," March 2006.

[ ] a,c

Figure 22-1 Typical LHGR Limit for Westinghouse BWR Fuel

RAI-23

QUESTION

In WCAP-17116-P Section 6.1.6, Westinghouse indicates that heat transfer from piping, vessel walls, and non-fuel internal hardware is accounted for according to the method described in Sections 3.5 and 3.6 of WCAP-11284-P-A. This is in compliance with the requirement of Section I.A.6 of Appendix K, "Heat transfer from piping, vessel walls, and non-fuel internal hardware shall be taken into account."

Section II.1.a of Appendix K also requires sufficiently complete description of the evaluation model to permit a technical review of the values of all parameters or the procedure for their selection. Appendix B of WCAP-17116-P only provides information regarding the surface areas and thicknesses of the metal heat structures. However, it is not completely clear how the metal heat structures are modeled; single and doubly exposed slabs, lumped parameter models, or more correct fin models for some of the internals structures. Furthermore, detailed information on heat structure nodalization is not available. Therefore, describe the heat structure model input in detail.

RESPONSE

GOBLIN can model any number of heat-transferring plates simulating different parts of the vessel or its internals that are in contact with the coolant. The plates may be insulated on either side or in contact with two different volume cells. The one-dimensional heat conduction equation is solved using a finite difference technique and a user-specified nodal subdivision of each plate. Table B-1 and Figures B-1 through B-4 of WCAP-17116-P document the dimensions and geometry of the core structures. These core structures are then broken down into many individual heat slabs. There are over 160 such heat slabs in the ABWR model that are used to represent the reactor vessel and its internals. The volume nodes that border the left and right side of each slab are defined, as well as the heat transfer area of each side, based upon the dimensions and geometry of the structure modeled by each heat slab. This modeling could include the same volume on both sides of the heat slab as is the case of the steam dryer, which as Figure B-1 illustrates, borders volume WV-P on both sides. A heat slab can also be defined as insulated on one side such as is the case for the reactor pressure vessel (RPV) wall, which as Figure B-1 illustrates, borders volume WV-Q on one side without bordering another volume node on the other. No heat slab is modeled in such a way that multiple volume nodes border a single side of the heat slab. For example the RPV wall is broken down into 5 heat slabs for the region where it borders volume nodes WV-S1 through WV-S5 as illustrated by Figure B-1, with one heat slab corresponding to each individual volume node. The top and bottom elevations of each individual heat slab are then input such that the heat slabs stack on top of one another to provide the overall model of each core structure. The material type(s) and number of mesh points for each heat slab are also defined.